The Thesis Committee for Yorguo El Hachem
Certifies that this is the approved version of the following Thesis:

The UTexas Seal Coat Design Method Using 3D Laser Technology

APPROVED BY
SUPERVISING COMMITTEE:

Jorge A. Prozzi, Supervisor

Magdy Mikhail

The UTexas Seal Coat Design Method Using 3D Laser Technology

by

Yorguo El Hachem

Thesis

Presented to the Faculty of the Graduate School of

The University of Texas at Austin

in Partial Fulfillment

of the Requirements

for the Degree of

Master of Science in Engineering

The University of Texas at Austin

August 2019

Dedication

I am dedicating this thesis to my beloved family and my dearest friends who have meant and continue to mean the world to me. Their love and support helped me achieve my goals.

Acknowledgements

From Lebanon to the United states, there were many people who helped me make this journey possible. First, I am extremely thankful to my advisor and mentor Professor Jorge A. Prozzi for his valuable support, advice, and guidance throughout my two-year graduate studies with the research group. His encouragement was essential for the development of this work. He has been an excellent mentor, guide, and role model for me throughout the program.

I would also like to thank Dr. Magdy Mikhail for his time reviewing this work. His support and contribution are greatly appreciated. I also want to thank Professor Robert Gilbert, the Chair of the Civil, Architectural and Environmental Engineering department, for his excellent life lessons in addition to his professional teaching. I am also very thankful to all the other faculty members for sharing their knowledge and expertise. Overall, I am proud to have been part of a wonderful transportation engineering program studying among the pioneers of the industry.

I am also very grateful to have been part of an amazing research group that provided room for fruitful discussions with fellow researchers, enriched my study with bright ideas, and helped me learn from their diverse experiences.

Having travelled more than 11,000 km to pursue this degree, many challenges were awaiting. I am extremely thankful to my alma mater, the Lebanese American University, and my undergraduate advisor Dr. Gabriel Bazi, for providing me the right guidance and support that made my endeavor smoother.

I am also indebted to my wonderful family in Lebanon whom without their love and support this journey would not have been possible. They provided the perfect balance

that was needed to move forward. The continuous support of my brother and best friend Anthony could never go unnoticed. He was always there for me since day one, the 14th of August 2017. Additionally, my dearest friends always remined me to remain independent and fearless in pursuing my dreams.

Finally, the biggest thanks are to God who continuously showers me with numerous blessings and abundant graces. His accompany throughout these two years made the glorious moments sweeter and the stressful times easier. Lastly, the University Catholic Center provided me with the appropriate shelter during emotional and spiritual distresses. "*Close to campus close to Christ*", this center provided me with a transformative formation for lifelong discipleship, leadership, and service.

Abstract

The UTexas Seal Coat Design Method Using 3D Laser Technology

Yorguo El Hachem, M.S.E.

The University of Texas at Austin, 2019

Supervisor: Jorge Prozzi

The size of the highway network has grown beyond the manageable capabilities of transportation agencies and stakeholders who are concerned with maintaining their assets using limited funding abilities. For that reason, pavement preservation programs have become very popular because they offer cost-effective spending schemes that maximize the service life of roads. Seal coats are one of the most popular pavement preventative treatments used around the world due to their high durability and low cost compared to other surface treatments. Their performance depends on the adequate computation of the aggregate and binder application rates. Misestimating these rates leads to raveling, bleeding, or other distresses. Accordingly, numerous design methods have been developed and are being implemented worldwide. This research assesses the different design philosophies and considers the assumptions adopted by each. It is challenging to design a seal coat when several design methods recommend different and inconsistent application rates. For the first time, the three-dimensional laser is incorporated in the design of seal coats in order to provide a fast, objective, and reliable approach. A predictive model is

developed to determine the adequate aggregate application rate based on the size of the aggregates, i.e. the average least dimension, and their density. This study also assesses the contemporary texture characterization techniques and analyzes the variance of the sand patch test. The findings indicate that the sand patch test is not a reliable estimator of the volume of voids in the surface texture, which negatively affects the calculation of the binder application rate. The study recommends an algorithm that accurately measures the volume of voids in the existing surface texture using 3D surface scans. The outcome enhances the estimation of the binder application rate, and the findings can be applied to the existing design methods to improve the performance of the seal coat. Finally, highway agencies could incorporate the 3D laser within the binder sprayer to measure the surface texture during construction and automatically adjust the rate.

Keywords: Aggregate Application Rate, Average Least Dimension, Binder Application Rate, Chip Seal, Pavement Preventative Treatment, Sand Patch Test, Seal Coat, Surface Dressing, Surface Treatment, Texture, 3D Laser.

Table of Contents

List of Tables

List of Figures

Chapter 1: Introduction

MOTIVATION AND RESEARCH SIGNIFICANCE

Over the centuries, roads have served humanity communicate and travel long distances enabling economy and other aspects of daily life to thrive. The Illustrated Glossary for Transport Statistics defines the roadway as a "*line of communication (travelled way) open to public traffic, primarily for the use of road motor vehicles, using a stabilized base other than rails or air strips. Included are paved roads and other roads with a stabilized base, e.g. gravel roads. Roads also cover streets, toll roads, bridges, tunnels, supporting structures, junctions, crossings and interchanges; excluding dedicated bicycle lanes*" (Khou Sid'Ahmed, Barreto, & Strelow, 2009). The highway and pavement infrastructure play a critical role in transporting humans, facilitating business and commerce, and supporting the nation's economy. High-quality transportation systems and services are signs of well-developed and industrialized societies. Studies have shown that there is a significant relationship between the road infrastructure and the economic development. In addition, time-series analyses of several decades show that there is a positive correlation between per capita gross national product and the density of the paved road network (Queiroz & Gautam, 1992; Larsen, 1968; Rodrigue & Notteboom, 2017). Road condition is also a factor that impacts economy. This crucial contribution to economic growth and social prosperity makes roads valuable assets for both the people and the governments. The United States of America "*advanced a national unity of effort to strengthen and maintain secure, functioning, and resilient critical infrastructure*" whereby the Presidential Policy Directive 21 (PPD-21, Critical Infrastructure Security and Resilience) identified transportation systems including highways as one of the sixteen critical infrastructure sectors (CISA, 2013; Ravi, 2018; US DHS, 2015). More than two

trillion dollars have been invested in the United States' highway transportation system. As identified by the co-sector-specific agencies for the transportation system sector, the Department of Homeland Security and the Department of Transportation, the highway and motor carrier consist of more than 4,000,000 roadway miles with more than 600,000 bridges and 350 tunnels (CISA, 2013). In its latest infrastructure report card, the American Society of Civil Engineers (ASCE) rated the US roads as "D" stating that: "*America's roads are often crowded, frequently in poor condition, chronically underfunded, and are becoming more dangerous.*" Additionally, one out of five highway miles are in poor pavement condition while the roads are facing a significantly increasing backlog of rehabilitation needs. The highway system has been underfunded for several years with an $836 billion capital-need backlog (ASCE, 2017.1; TRIP, 2016; USDOT, 2016). The roadway infrastructure is a multifaceted asset that requires attention by all the budget-managing authorities and users.

Cooperation between pavement management officials and legislatures is important for understanding the role pavement infrastructure has on both the society and the economy. In the last decade, major state departments of transportation focused their research on pavement preservation techniques and opportunities to improve the existing pavement infrastructure (Kim & Adams, 2012; Mahoney, et al., 2014; Wood, Janisch, & Gaillard, 2006; TxDOT, 2017.2; Ali & Mohammadafzali, 2014). The goal of pavement preservation is to extend the overall life of pavements while decreasing the life cycle cost incurred. Over the years, insufficient funding motivated state departments of transportation and highway agencies to explore, research, and adopt pavement preservation programs. This expanded the overall research efforts in the field, and the adoption of various low-cost pavement preservation techniques emerged.

Previously, maintenance and rehabilitation were only performed when the pavement was severely cracked and structurally inadequate (Beatty, et al., 2002). As the network grew bigger and as the funding needs increased, this philosophy changed, and new strategies emerged. Rather than waiting for the pavement to completely deteriorate and reach a failing stage, a scheme of preventative maintenance is adopted to preserve the condition at an acceptable level. These preservation treatments are placed on four-to-20-year cycles (TxDOT, 2017.2; Wu, Groeger, Simpson, & Hicks, 2010). Among the prevailing pavement preservation treatments, seal coat is the most commonly used. It is widely agreed on and well-recognized for being a cost-effective and durable preventative pavement preservation treatment worldwide (Prozzi & Serigos, 2016; Rahman, Islam, Musty, & Hossain, 2012; Serigos, Smit, & Prozzi, 2017; Martinez, Garcia, Smit, & Prozzi, 2017). Seal coats consist of spraying a binder seal on the existing pavement surface followed immediately by spreading the aggregates. Afterwards, the whole layer is rolled, and the chip-sealed section is opened to traffic (Einarsson, 2009; Gransberg & James, 2005; Ambarish, 2012; Banerjee, Smit, & Prozzi, 2012). The effectiveness of this dual system, the chips and the seals, is directly related to the adequate estimation of both the binder application rate (BAR) and the aggregate application rate (AAR). The amount of binder needed is directly proportional to the volume of voids in the covering aggregates and the texture of the existing pavement surface. The amount of aggregates needed is related to the shape and volumetric properties of aggregates such that it fully covers the road with a one aggregate thick layer. A poorly designed seal coat compromises the safety of the users due to distresses such as raveling or bleeding that are thoroughly discussed in Chapter 2. Ever since the first seal coat design method was published by Hanson in 1935, several agencies and researchers have been trying to come up with new design methods in order to account for unforeseen site conditions that former designs did not consider. The aim of all the

design methods is to adequately estimate the aggregate application rate and the binder application rate that can successfully seal coat the existing pavement surface.

Meanwhile, the light amplification by stimulated emission of radiation technology, also known as the laser technology which was first studied by Albert Einstein in the early 1900's, has since greatly advanced. Lasers have become a key component in many tools that people use in their everyday life. They are used to scan barcodes at grocery-store checkouts, to read information stored on compact disks, in surgery procedures, in manufacturing processes that involved cutting, engraving, drilling, or marking, and recently by pavement management programs (Universal Laser Systems Inc., 2018). A wide-range of laser-based products for professional field measurement applications is commercially available. These field measurement applications, which are of interest to the pavement engineering sub-discipline, include measuring distances, heights, or elevations (Laser Technology Inc., 2019). Traditionally, contact measurement devices have been used for various pavement engineering measurement applications ranging from surveying topography to alignment layout to thickness verification to roadway texture assessment and even aggregate texture measurement. In recent years, the use of laser-scanning techniques has gained an increasingly popular interest in engineering surveys. The adoption of lasers in engineering applications provides tremendous benefits including: simple and straightforward use, speedy data collection and processing, high-speed scanning processes, very high accuracy, non-contact measurement technique, absence of operator bias, lower operating cost, 3D modelling, and many more (Wang, Yan, Huang, Chu, & Abdel, 2011; Serigos, Smit, & Prozzi, 2014).

With the aim of adequately estimating the appropriate aggregate application rate and binder application rate, several agencies typically adopt a base seal coat design for generic pavement surface and modify the application rates to meet the local site conditions

that are highly non-homogeneous. However, most of the on site characterization techniques remain empirical approximations as well as biased estimations that are mostly based on the judgment and experience of the site engineer. In contrast to these techniques, the incorporation of lasers in the design and construction of seal coats has the potential to limit the bias from the data collection process and could provide precise and accurate estimates relevant for the site-specific conditions.

The research presented in this thesis aims at studying the incorporation of a 3D laser scanner prototype to improve the design and construction of the most commonly used preventative treatment: seal coats. The findings of this research can be applied to existing design methods allowing agencies to continue using their current design philosophies with minor corrective modifications. In order to achieve the goal of this study, compulsory field data was collected on pavement sections within Texas, and laboratory experiments were conducted on aggregates at The University of Texas at Austin.

OBJECTIVES

The goal of this research is to improve the design and construction of the most popular pavement preventative maintenance and preservative treatment in Texas, i.e. seal coats. The proposed improvement incorporates the use of 3D laser scanners to measure site properties in a fast, controlled, accurate, and unbiased manner. In order to achieve this goal, the following objectives were fulfilled:

1. Conducting a thorough and extended literature review of the existing seal coat design methods across the globe,
2. Assessing the variability of traditional contact methods for evaluating pavement texture with focus on the Sand Patch Test (ASTM, 2015.1),

3. Measuring the volume of voids in the existing surface texture using the 3D laser scanner prototype,
4. Modeling the aggregate surface coverage based on volumetric and shape parameters of seal-coat graded aggregates, and
5. Developing the UTexas Seal Coat Design Method that incorporates 3D laser scanners in both the design and construction processes.

SCOPE AND METHODOLOGY

Several design methods have been developed by highway agencies and adopted by transportation officials in order to cost-effectively preserve the existing pavement surface and extend its life. This thesis offers a new seal coat design method that integrates a high-resolution 3D laser scanner in both the design and the construction processes. There is no consensus on which of the previously developed design methods is the best. Interestingly, as shown in Chapter 3 and Appendix of this thesis, different design methods suggest different seal coat aggregate and binder application rates for the same pavement section. The Texas Department of Transportation (TxDOT) relies on three different seal coat design methods for material dosing with (1) the Modified Kearby Design Method being the most commonly used method, (2) the McLeod Design Method being proposed for emulsified binders, and (3) the Transversely Varying Asphalt Rates being adapted to tailor for the site-specific needs, especially varying surface texture. In practice, the design methods are used as initial dosages suggestions, and good engineering judgement is needed to adjust accordingly as field conditions dictate (TxDOT, 2017.2).

The research performed as part of this thesis aimed at developing a method that reduces the reliance on engineering judgment by automatically evaluating the surface conditions using an accurate, fast, and reliable method. Field and laboratory tests were

conducted in order to integrate the laser in the design method. A series of five different algorithms (i.e. ALD, shape properties, volume of voids in texture, aggregate coverage, and predictive modelling) were created in order to process the data and generate the relevant information that was used to develop the knowledge behind the application of laser technology in seal coats. The philosophy behind these algorithms is discussed accordingly upon their appearance within the thesis body chapters. The results of these field and laboratory tests are analyzed, and the findings are discussed. It should be noted that the analyses and findings within this thesis are limited to the scope of the field tests and laboratory experiments conducted within the study. It is also important to note that future field implementation of the design method with adequate laser-retrofitted construction equipment is needed to validate the findings. This implementation remains beyond the scope of this thesis.

DESCRIPTION OF CONTENTS

This work is divided into six comprehensive chapters: (1) Introduction, (2) Literature Review, (3) Summary of Existing Seal Coat Design Methods, (4) UTexas AAR Improvement using 3D Laser Technology, (5) UTexas BAR Improvement using 3D Laser Technology, and (6) Conclusion and Recommendations. The Appendix compares the application rates recommended by the popular seal coat design methods used worldwide.

The current chapter provides a brief statement of the problem with the motivation and significance of the research carried out in the master's thesis. In addition, the objective is clearly identified and discussed followed by the scope and the methodology.

Following the introduction, chapter two provides background information and a broad literature review of pavement deterioration, preservation programs, as well as an overview of seal coats.

Afterwards, chapter three goes in depth into the contemporary seal coat design methods around the world discussing the design philosophies, assumptions, and recommendations of each. The authors decided to focus on eleven exclusive methods commonly used, each having its own approach.

Subsequently, chapter four introduces the 3D laser scanner prototype adopted within the study. In addition, a predictive model for determining the aggregate application rate from basic aggregate features is advanced.

Meanwhile, chapter five discusses the concept of pavement texture and existing characterization techniques. The chapter proves that the prominent methods are variable in nature and fail in providing an accurate estimate of the volume of voids in the existing surface texture. Accordingly, an algorithm is developed to accurately and objectively measure the volume of voids in the surface texture using the 3D laser scanners. Lastly, recommendations for retrofitting existing design methods in order to incorporate the 3D laser scanner for texture assessment and binder application rate improvement are recommended.

Finally, chapter six summarizes the research work conducted, discusses the important findings within this thesis, and provides some recommendations and insights for future work.

Consequently, the Appendix discusses the problematic nature of having different design methods adopted by various agencies. After considering a specific highway section and designing the seal coat using the numerous considered methods, it is made evident that the outcomes of these methods are inconsistent.

Chapter 2: Literature Review

PAVEMENT DETERIORATION AND FUNDING NEED

Infrastructure is a multifaceted asset that requires attention by all budget managing authorities and users. Specifically, the highway pavement infrastructure is critical for the transportation of people, the marketplace, and the nation's economy. Most developed and industrialized societies are noted for high-quality transportation systems and services. There is a very strong association between economic development (in terms of per capita GNP) and road infrastructure. Thus, it is essential for pavement management officials and legislatures to understand the role that pavement infrastructure has on society and the economy as well as the importance of maintaining or improving the condition of the current pavement infrastructure. However, the components of the pavement infrastructure require a great deal of maintenance and rehabilitation in order to prosper. Pavements require an enormous investment upfront to build them, they deteriorate with time and usage, and they require continuous maintenance to make best use of their value. There are several factors leading to pavement deterioration including but not limited to the following:

- Environmental effects: rain, snow, abrupt temperature changes, etc.
- Traffic: lower volume traffic, higher volume traffic, overloading, etc.
- Material degradation: oxidation, fatigue, pH incompatibility, low quality, etc.
- Natural disasters: earthquakes, hurricanes, floods, tornadoes, landslides, etc.
- Construction: unprepared surface, low temperatures, underestimating, etc.
- and many more (Jones, 2015; Adlinge & Gupta, 2012)

It goes without saying that the owner of the road is responsible for maintaining the surface in a good condition or at least in an acceptable condition for its users. At a first glimpse, one might think that roads are owned by public agencies, but there is a significant portion

of roads privately owned, managed, and/or operated. Texas Department of Transportation (TxDOT) divides the roads in two categories based on jurisdiction: on-system if the road is under the jurisdiction of TxDOT (IH Highways, US Highways, State Highways, Spurs, Loops, Business Routes, Farm or Ranch to Market Roads and Spurs, Pass, Park and Recreation Roads, and Frontage Roads) and off-system otherwise (City Streets, Certified County Roads, Toll Road Authority Roads, and Federal Roads). The state manages 28.87% of the lane miles in Texas while the remaining portion of the roads are owned, operated, and managed by cities, certified counties, toll road authorities, and the federal government (TxDOT, 2017.1). Traditionally federal and state gas tax revenues were enough to meet funding needs. Lately, funding has been a major challenge for operating agencies as the infrastructure magnitude has grown bigger than what can be feasibly managed. Transportation project funding include multiple revenue sources with different uses of these sources (TxDOT, 2019). Being one of the largest and dynamically growing states in the United States of America, many Texas' roads have exceeded their design life. The latest American Society of Civil Engineers (ASCE) infrastructure report card for the state of Texas evaluated the state roads and highways with a grade of D. The report defines this grade as poor and at risk with the following description: "*The infrastructure is in poor to fair condition and mostly below standard, with many elements approaching the end of their service life. A large portion of the system exhibits significant deterioration. Condition and capacity are of serious concern with strong risk of failure*." Experts state that TxDOT's budget for routine maintenance is around $1 billion per year of which 40 to 50% is allocated for pavements, and yet the budget falls short behind the total pavement maintenance needs (ASCE, 2017.2; TxDOT, 2017.2). This problem is not specific to the state of Texas alone as the overall roadway infrastructure level in the US is also D. The report states that

"*America's roads are often crowded, frequently in poor condition, chronically underfunded, and are becoming more dangerous*" (ASCE, 2017.1).

The issue of underfunding the highway system has been a chronical issue for the past years with a huge backlog resulting in $836 billion of highway and bridge capital needs (ASCE, 2017.1; ASCE, 2017.2). Over the years, state departments of transportation and highway agencies have shown interest in pavement preservation programs because such practices deem to extend the life span of the pavements with a lower life-cycle cost (Beatty, et al., 2002). The motivation is that a proactive maintenance scheme provides a cost-effective means for making best use of the pavement infrastructure that requires a continuous allocation of money and resources.

Most pavement management authorities use performance models to characterize the condition of the pavement asset over time. These models help pavements managers in assessing the urgency and the impact of maintaining the pavement infrastructure and in explaining it to stakeholders using laypeople's terms of time and money. The performance models take into consideration multiple aspects about the infrastructure design, life and usage. In order to measure the condition of the asset over time, i.e. performance, it is beneficial to understand the deterioration of the pavement infrastructure over time as well. Figure 2.1, illustrates an example of a performance model using pavement condition index, which is a common performance indicator for the pavement infrastructure with respect to time (Radhakrishnan, 2016). The pavement condition index (PCI) was developed by the US. Army Corps of Engineers to quantify the pavement condition of roads and parking lots through visual surveys (ASTM, 2018; US Corps of Engineers, 1997).

Figure 2.1 (Tomkins, Horner, Lampley, & Shields, 2018) conveys the degradation of pavement condition as the age of pavement increases. It is shown that as the pavement ages, its condition drops, but this drop is steady and low at early life of the pavement and

increases as the pavement ages. Additionally, the figure shows the cost of preventative maintenance and rehabilitation action at various conditions and times for the pavement asset. A proactive preventative maintenance intervention upfront will cost less than a reactive reconstruction afterwards while providing an adequate condition. The effects of preventative and reactive maintenance are unquestionably different. Since preventative maintenance is exercised at an early age of the pavement life and more frequently than reactive maintenance, the effect is different. A pavement receiving adequate preventive maintenance tends to experience smaller fluctuations in its condition and provide a comparable service. With reactive maintenance, the pavement condition drops to unacceptable and unserviceable levels and would be more expensive to restore.

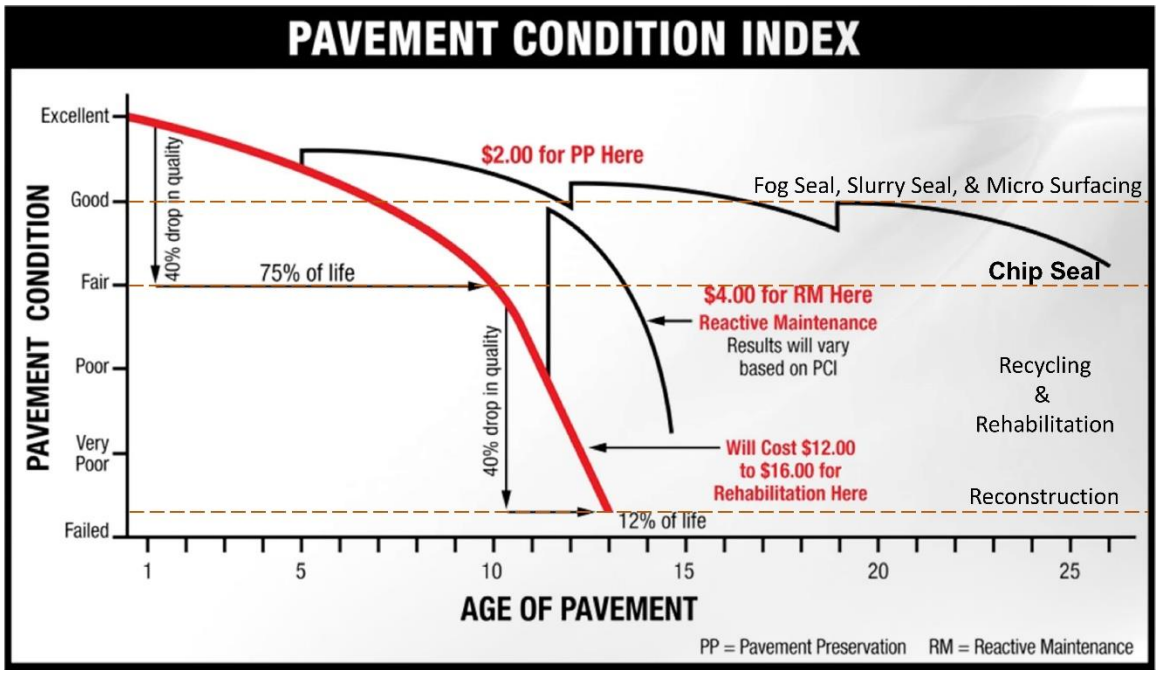

Figure 2.1: Variation of the Pavement Condition with Age

In his master's research at The University of Texas at Austin, Wilfrido Martinez-Alonso conducted a life-cycle cost analysis on pavement preservation techniques in Texas. He concluded that "*the timely application of preventive maintenance (PM) treatments has proved to be a cost-effective way to maintain paved roads.*" The effectiveness of preventative maintenance lies in the treatment's ability to offset the pavement's deterioration at an early age or even reduce the rate at which the pavement is deteriorating. Their application is most effective when the roadway is still in a good condition, i.e. structurally sound, with minimal distresses (Martinez-Alonso, Prozzi, & Smit, 2017). The study also concluded that seal coats are the most effective pavement preservation with the lowest cost to benefit ratio over a 25-year-analysis window. In Texas, seal coats are the most cost-effective alternative for different highway classifications, traffic volumes, traffic loads, environmental conditions (Martinez-Alonso, Prozzi, & Smit, 2017).

PAVEMENT PRESERVATION PROGRAMS

Pavement preservation as defined by the Federal Highway Administration (FHWA) is "*a program employing a network-level, long-term strategy that enhances pavement performance by using an integrated, cost-effective set of practices that extend pavement life, improve safety, and meet motorist expectations. These practices in general do not increase pavement capacity or strength but reduce the effects of aging (environmental and traffic loading) and restore serviceability*" (USDOT, 2017; Zheng, Groeger, Simpson, & Hicks, 2010; Geiger, 2005). A combination of periodic and preventive maintenance is what values pavement preservation over pavement rehabilitation. On the long term, it is easier and cost-effective to maintain a roadway in good condition than rehabilitating or reconstructing a heavily damaged section that requires immediate repair. By retaining a good pavement condition, preventative maintenance enhances the utmost important

component that interests transportation agencies: safety. The challenge with pavement preservation is the idea of performing work on roads in good condition while bad roads remain untouched, which challenges the habit of prioritizing work for worst-first (Zheng, Groeger, Simpson, & Hicks, 2010). This proactive approach intends to apply a cost-effective treatment in a timely manner allowing the pavement to restore its original condition. The essence of pavement preservation is applying the right treatment to the right road at the right time using the right material and construction practices. This then becomes the combination of minor rehabilitation, preventive maintenance, and routine maintenance activities to reduce the effects the environment and traffic loading have on the road, to preserve the pavement condition, and to extend its life. Previous research has identified several benefits of pavement preservation including (1) Economy: planned work dictates the long-term performance expectation, which overall provides more spending stability and better network condition; (2) Performance: network-level strategies optimize the performance period and reduce the need for urgent and frequent reconstruction while maintaining safer roads; (3) Sustainability: well-defined preservation policies can insure achieving sustainable targets; (4) Safety: shorter work zones and faster treatments reduce the likelihood of on-site work incidents in addition to achieving higher skid resistant surfaces that improve the road safety; (5) Flexibility: a variety of surface treatments and alternatives in a flexible toolbox of implementation that caters to the available budget (Van, Gaj, Cawley, & Gray, 2017). To correct for minor distresses, pavement preservation is an essential practice during the pavement life (Scott, 1986). On the other hand, pavement preservation cannot correct pavement failures such as heavy rutting, load-associated cracking, poor ride-quality surface, or replace insufficient reconstruction budget issues.

Continuous research and advancements in construction practices led to a series of effective treatments proposed for highway preservation. Following is a brief description of the commonly used asphalt-surfaced treatments (Cawley & Gray, 2017):

- Micro-surfacing is a mix of crushed well-grade aggregates, Portland cement (or any other mineral filler), polymer-modified asphalt emulsion, water, and emulsifying aggregates. Asphalt emulsion is composed of liquid asphalt cement emulsified in water using an emulsifying agent. Using a spreader box, the mix is laid over the width of the surface in order to minimize raveling and oxidation. Micro-surfacing improves the surface friction and fills minor irregularities and rutting up to 1.5 inch deep. Nevertheless, it does not significantly enhance the structural capacity of the pavement structure (Peshkin, et al., 2011; Smith & Beatty, 1999; Gransberg D. , 2010; Merritt, Lyon, & Persaud, 2015; Wu, Groeger, Simpson, & Hicks, 2010).
- Slurry Seals are also a mixture of well-graded fine aggregates, emulsified asphalt, water, and a mineral filler. It is applied on the pavement surface in thin layers using squeegees. They intend to seal the underlying surface from water infiltration, fill cracks and voids, and improve the friction of the surface. Similarly, slurry seals do not provide any additional structural capacity yet tend to improve road functionality (Merritt, Lyon, & Persaud, 2015; Wu, Groeger, Simpson, & Hicks, 2010).
- Ultrathin Bonded Wearing Course (UTBWC) is a thin overlay that aims to improve the ride quality of the asphalt pavement surface as well as seal and protect it. It delays an early fatigue cracking problem and offsets shallow ruts. Similar to other preventative treatments, the UTBWC does not add structural capacity and serves as a pavement life extender (Merritt, Lyon, & Persaud, 2015).
- Seal coat is an asphalt pavement preservation treatment that seals fine cracks in the pavement surface preventing water intrusion and improving the surface friction. It is

made of an asphalt binding membrane that is sprayed on the existing surface and a uniformly-graded aggregate layer. Although it does not improve the structural capacity of the pavement surface, seal coat remains a very durable wearing surface (Merritt, Lyon, & Persaud, 2015; Wu, Groeger, Simpson, & Hicks, 2010).

SEAL COAT

Highway agencies around the world have researched, investigated, and pursued various pavement preservation techniques. When it comes to cost and durability, seal coats take the lead. Generally speaking, seal coating encompasses multiple pavement-surface treatments including crack seal, fog seal, slurry seal, seal coat, sand seal, cape seal, geotextile seal, and many more. One main difference between the various treatments is the aggregate component (Mouaket, Sinha, & White, 1992). For instance, when applying a fog seal, a light diluted asphalt emulsion is sprayed onto a pavement surface without spreading aggregates at all. Slurry seals utilize the mixture of emulsified asphalt along with fine aggregates. Meanwhile, seal coats are made of a layer of asphalt covered with aggregates like crushed stone, gravel, or slag. While in a sand seal, natural sand is used to cover the layer of asphalt instead of coarse aggregates (Mouaket, Sinha, & White, 1992). Many studies were conducted on the cost effectiveness of different treatment methods, and there seems to be a consensus that seal coats offer the highest benefit to cost ratio. A study in the 2000's compared the cost and expected life of maintenance treatments. The study concluded that seal coat is the best surface treatment technique because of its low cost and high durability (Hicks, Seeds, & Peshkin, 2000). Similar propositions have been made by Chen et al., Daleiden, and Martinez et al. stating that seal coat outperforms other preventative treatment methods in terms of cost and performance life (Chen, Lin, & Luo, 2003; Daleiden & Chen, 2005; Martinez-Alonso, Prozzi, & Smit, 2017).

This preventive method is called differently in various countries, such as *seal coat* in the United States (Gransberg & James, 2005; Yazgan & Senadheera, 2003; Lee, Shields, & Jun Ahn, 2011); *chip seal* in New Zealand (Transit NZ, RCA, & Roading NZ, 2005), *sprayed seal* in Australia (Holtrop, 2008), *surface dressing* in the United Kingdom (Roberts & Nicholls, 2008) and *bituminous asphalt surface treatment* under ASTM D 1369-84. Back in the 1920s and 1930s, seal coat started and was initially applied only on low-traffic volume US roads intuitively without a particular design method (TxDOT, 1997). Meanwhile in New Zealand, F.M. Hanson, a researcher and scientist, proposed the first chip design method in his paper "*Bituminous Surface Treatment of Rural Highways*" at the conference of the New Zealand Society of Civil Engineers in 1935. This method was later adjusted and employed by different countries around the world. Countries like Australia, France, New Zealand, South Africa, United Kingdom, and the United States performed extensive research and developed their own design specifications. Over time, advances in seal coat design technology and knowledge of distresses have progressively allowed the use of this method on high-volume roads (Gransberg & James, 2005; Transit NZ, RCA, & Roading NZ, 2005; Shuler, 1990).

In addition, many different configurations of seal coats were developed including: (1) single seal coat, (2) double seal coat, (3) racked-in seal, (4) void-fill seal, (5) sandwich seal, (6) wet lock seal, (7) dry lock seal, (8) stress absorbing membrane seal, (9) slurry seal, (10) cape seal, (11) open graded porous asphalt seal, (12) stress absorbing membrane interlayer seal, (13) geotextile seal, etc. (Gransberg & James, 2005; Transit NZ, RCA, & Roading NZ, 2005). Different specification developed by countries around the globe vary from design to execution based on the underlying philosophy, construction steps, number of layers sealed, variations in aggregate size and gradation, diversity in the asphalt binder application rates, disparities in asphalt types, and therefore assign a different design

approach to each of them. In reference to "*Chipsealing in New Zealand*", Table 2.1 illustrates these different seal coat types (Transit NZ, RCA, & Roading NZ, 2005):

Seal Coat Type	Illustration
(1) Conventional Seal Coat	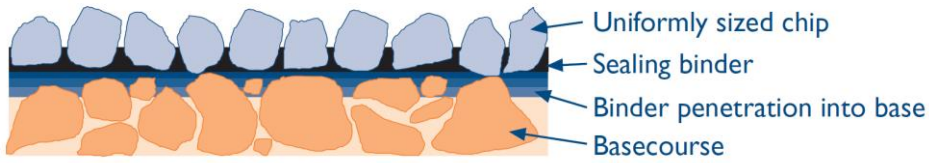
(2) Two Coat Seal Coat	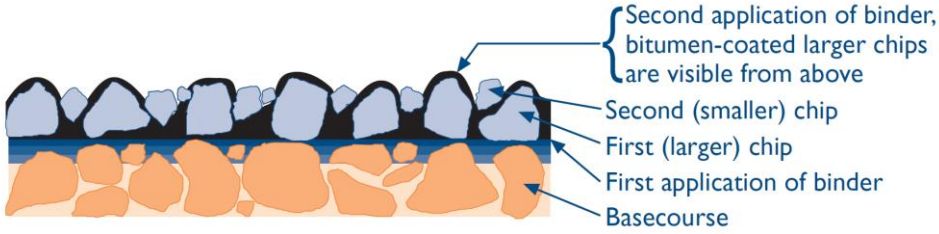
(3) Racked-in Seal Coat	
(4) Void-fill Seal	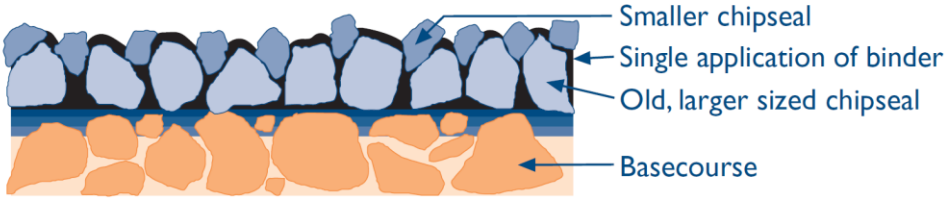
(5) Sandwich Seal	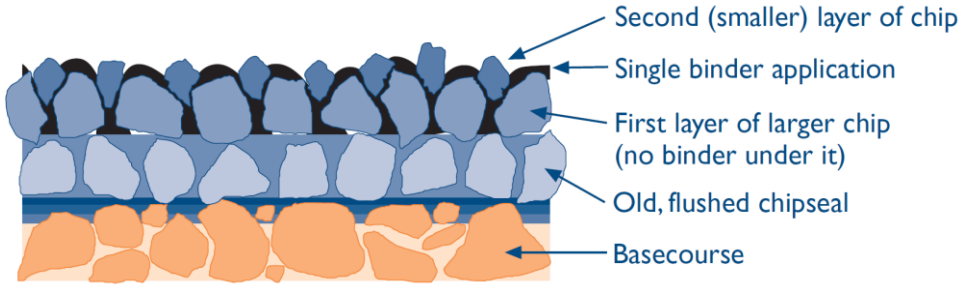

Table 2.1: Different Seal Coat Surface Configurations

(6) Wet Lock Seal	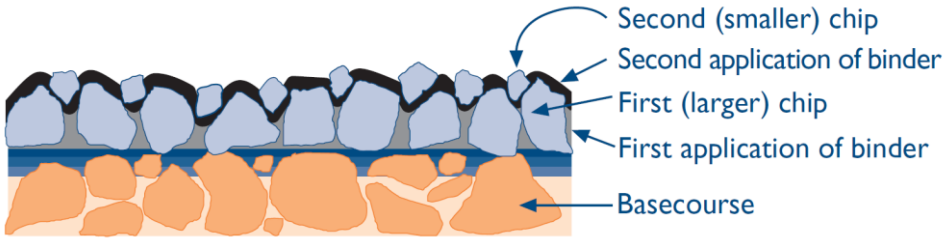
(7) Dry Lock Seal	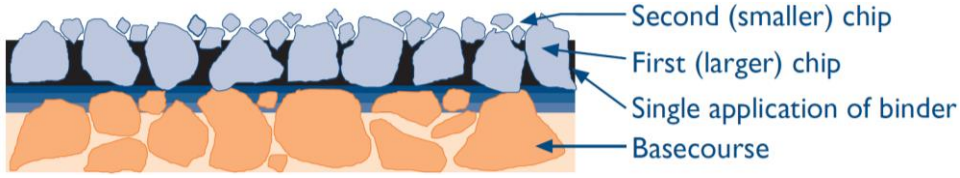
(8) Stress Absorbing Membrane	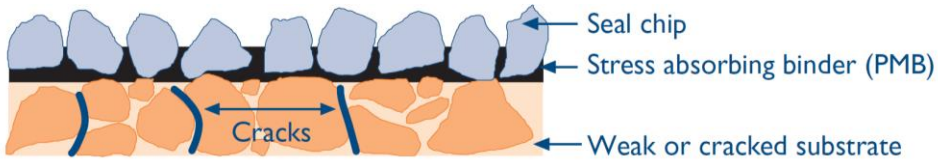
(9) Slurry Seal	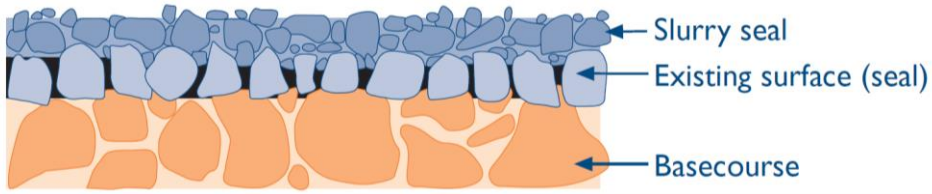
(10) Cape Seal	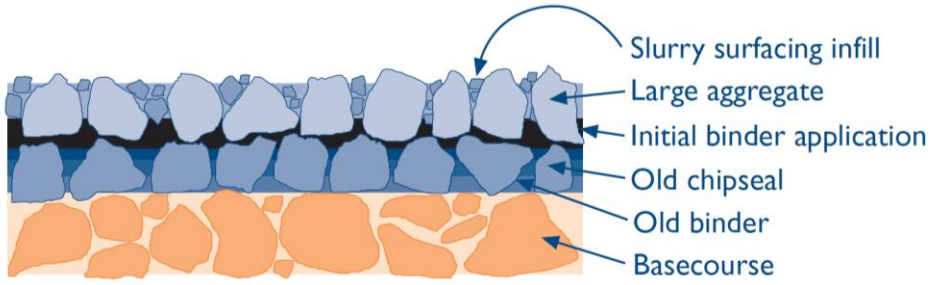
(11) Open-Graded Porous Asphalt (OGPA) Seal	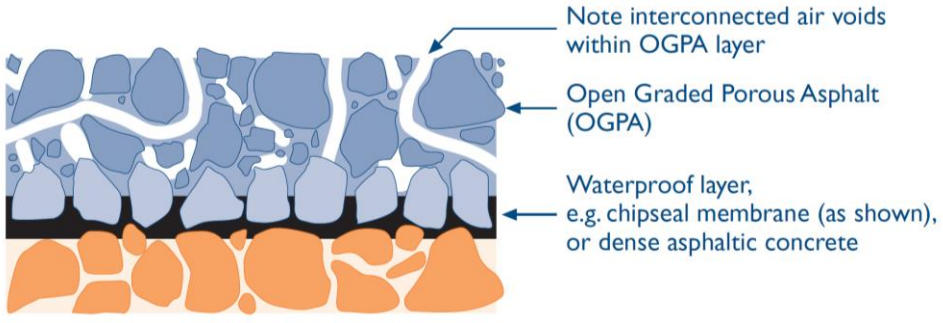

Table 2.1 continued

(12) Stress Absorbing Membrane Interlayer (SAMI) Seal	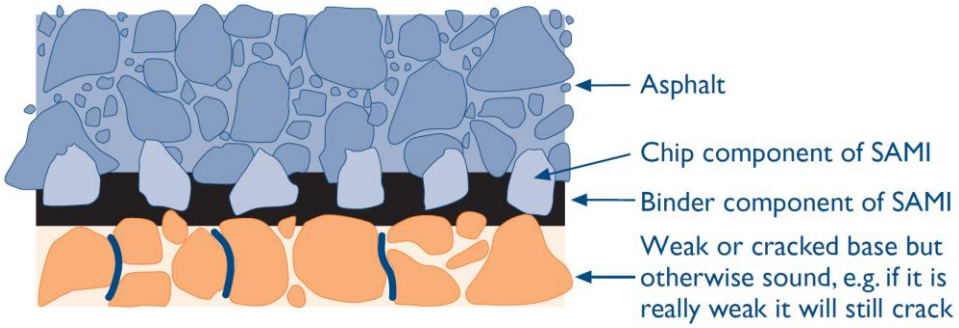
(13) Geotextile Seal	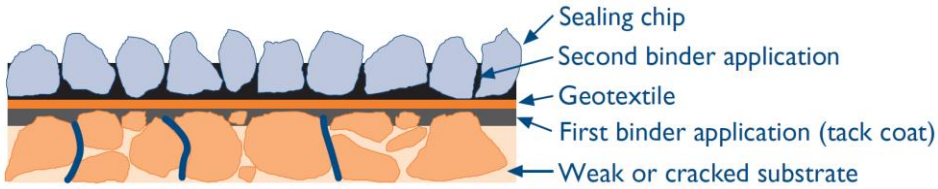

Table 2.1 continued

The basis for designing any of the aforementioned seal coat configurations is derived from the conventional seal coat design with distinct modifications or additions that tailor this differentiation and emphasize the need for it.

The conventional seal coat, single seal coat shown as illustration (1) in Table 2.1, consists of two materials: asphalt bitumen binder and aggregate chips. The design philosophies revolve around determining the appropriate asphalt application rate (AAR) and binder application rate given compatible material types and good bitumen and chip qualities. When designed and constructed properly, seal coats improve the overall condition of the roadway infrastructure whereby the sprayed binder (Shuler, 1990; Einarsson, 2009; Kutay, Ozdemir, Hibner, Kumbargeri, & Lanotte, 2016; Elmore, Solaimanian, McGennis, Phromson, & Kennedy, 1995; McLeod, 1969; Gransberg & James, 2005):

- Seals non-structural cracks to block water penetration and waterproof the surface,
- Maintains the integrity of a cracked pavement, and

- Glues the composite system to the underlying.

In addition, the spread aggregates:

- Transfer the load to the underlying layers,
- Enrich the surface macrotexture,
- Enhance the skid resistance and surface drainage,
- Provide a new wearing surface,
- Insure an abrasion resistant layer against traffic and environmental impacts,
- Improve light reflection of pavements during the night,
- Offer visual delineation between the mainline and the shoulder,
- Retard pavement aging and weathering, and
- Increase the load bearing structural capacity of the pavement to a certain extent.

On the other hand, poorly designed seal coats can cause additional distresses and worsen the roadway condition. One of the serious distresses witnessed with poor jobs is raveling or aggregate loss shown in Figure 2.2 (Pierce & Kebede, 2015; TxDOT, 2017.2). This phenomenon involves the loss of chips from the composite treatment which poses a great danger on the cars following an aggregate chip and fly off. Excessive amounts of aggregates, dirty aggregates, wet aggregates, insufficient binder application rates, inadequate embedment of aggregates in the asphalt binder layer, oversized aggregates, delayed aggregate spreading i.e. binder hardening and chilling, late season sealing, aggregate-asphalt binder incompatibility, and fast traffic before significant adhesion are main reasons behind seal coat failures manifested by raveling (Gransberg & James, 2005; Lee, Shields, & Jun Ahn, 2011; Transit NZ, RCA, & Roading NZ, 2005; Lawson & Senadheera, 2009; SANRAL, 2007; McLeod, 1969).

Figure 2.2: Failed Seal Coat Job due to Raveling (TxDOT, 2017.2)

The counter effect is known as bleeding, shown in Figure 2.3, where the aggregates are totally covered by the overestimated amount of binder, or the amount of aggregates spread is not sufficiently covering the surface. This poses a serious threat to the drivers' safety because the asphalt binder would cover the surface of aggregates and result in a very slick and smooth surface which, in return, has a very low skid resistance that increases the likelihood of crashes (Kearby, 1953; Transit NZ, RCA, & Roading NZ, 2005). Poor asphalt binder selection, overestimated asphalt application rate, flaky and elongated aggregates, excessive curing, aggregate loss, undersized aggregates and immediate rainfall after construction are the main reasons for bleeding and failing seal coat treatments (Gransberg & James, 2005; Lee, Shields, & Jun Ahn, 2011; Transit NZ, RCA, & Roading NZ, 2005; Lawson & Senadheera, 2009; SANRAL, 2007; McLeod, 1969). These two distresses tend to be the most crucial distresses that can be controlled from a design perspective.

Figure 2.3: Failed Seal Coat Job due to Bleeding (TxDOT, 2017.2)

On the other hand, poor construction practices lead to additional distresses including streaking and bond failure shown in Figure 2.4. Streaking takes place when an unintentional non-uniform asphalt spraying is applied across the road due to misaligned nozzles. This unevenness is manifested by black and grey streaks that represent excess and deficient binder contents respectively. In addition to misalignment, streaking is caused by clogged nozzles, different nozzle sizes, inconsistent asphalt discharge rate, incorrect height, or very low air temperature. Bond failure between the existing pavement and the new treatment surface treatment takes place when certain considerations are not catered for. These instances include dirty aggregates, very dusty existing surface, wet pavement, very viscous binder, and extremely cold weather (McLeod, 1969; TxDOT, 2017.2). A viscous binder is desired to prevent the binder from simply flowing off the road, yet a fluid binder is also desired to allow the aggregates to compact. This balance of viscosity and fluidity is a key factor in the binder application process.

Figure 2.4: Failed Seal Coat Job due to Bond Failure (TxDOT, 2017.2)

Chapter 3: Summary of Existing Seal Coat Design Methods

When it comes to designing the seal coat, the aggregate application rate (AAR) and the binder application rate (BAR) dominate the design process as they directly affect the overall product performance and the resulting distresses, if any. Most of the design approaches calculate the application rates and recommend material specifications taking into account local conditions, weather, and other specific needs. Early on, there was no rationale behind determining the exact amounts of asphalt binder and aggregate chips, and hence no design method. Instead, on site trial-and-error valuations were employed to estimate the approximate amounts of those materials needed.

In 1934, F.M Hanson pioneered the development of an analytical-empirical seal coat design method leading the way in determining the proportions of aggregate and asphalt binder (Hanson, 1935; Transit NZ, RCA, & Roading NZ, 2005). Later in 1953, another design method was developed in Texas by J. P. Kearby and refined by Benson and Gallaway two years later (Kearby, 1953). About two decades later, Epps et al. modified the original Kearby method incorporating some adjustments based on their findings (Epps, Gallaway, & Hughes, 1981). In the meantime, another design method was established by N.W. McLeod in 1969 in Canada (McLeod, 1969). Currently, the Modified Kearby and the McLeod design methods are two commonly used methods by State Departments of Transportation in the United States and Canada in addition to several highway agencies around the world (Gransberg & James, 2005; TxDOT, 2017.2; Beatty, et al., 2002; Lord & Shuler, 2008). These methods evaluate the binder and aggregate application rates (BAR & AAR) using quantitative laboratory tests that assess the volumetric and shape properties of the aggregates. In addition, estimates of the embedment depth of the aggregate in the binder are obtained from traffic volume and texture evaluations. On the other hand, many

countries have adopted various design methods under the philosophy of considering basic aggregate and binder application rates that are readjusted to cater for the available material limitations and differing site conditions. The base rates either have roots from Hanson's original design philosophy or are tied to local empirical experiments. Some U.S. state DOT's still do not rely on the traditional seal coat design methods, but they rather use preliminary formulas based on previous experiences in local seal coat constructions (Zoghi, Ebrahimpour, & Pothukutchi, 2010).

Although most of the design methods are based on similar principles and philosophies, they often do not provide the same aggregate or binder application rates. In Chapter 3 and the Appendix of this thesis, a highway section is considered for seal coat design using different methods in order to determine the inconsistencies in design and to highlight the need for an objective, reliable, and universal approach that reaches consensus. The realm of this literature review considers the following design methods:

- Hanson Design Method (Hanson, 1935),
- Kearby Design Method (Kearby, 1953),
- McLeod Design Method (McLeod, 1969),
- Modified Kearby Design Method (Epps, Gallaway, & Hughes, 1981),
- Spanish Design Method (Bardesi & Tomas, 2004),
- New Zealand Design Method (Transit NZ, RCA, & Roading NZ, 2005),
- Australian Design Method (Alderson, 2006),
- South African Design Method (SANRAL, 2007),
- British Design Method (Bateman, 2016),
- French Design Method (AFNOR, 2007), and
- TxDOT Chip seal manual (TxDOT, 2017.2).

HANSON DESIGN METHOD (HANSON, 1935)

F.M. Hanson developed the earliest seal coat design method in New Zealand in 1935. This development led to an era of research and improvement on what is now known to be one of the most durable and cost-effective pavement preventative surface treatment. This proactive treatment is adopted by more than fifty highway agencies across the globe. In this section, the 1935 Hanson design method is discussed in detail based mainly on Hanson's original paper (Hanson, 1935).

The two main components in the seal coat design are the aggregates and the bitumen. The design method is focused on the determination of two important parameters: (1) the Binder Application Rate (BAR) and (2) the Aggregate Application Rate (AAR). The amount of binder needed is a function of the percent of voids in the layer of covering aggregates. The binder should not fill all the voids between the aggregates, but at the same time should fill a significant portion of them to hold the aggregates in place. A series of tests were conducted on a wide selection of commercially available aggregates of nominal sizes ranging between 0.5 and 1.5 inches. To quantify the amounts of voids in the loose aggregate layer, the aggregates were spread randomly on a leveled smooth platform. Water was poured in traceable amounts up to the level that reached the average height of the aggregates. The volume of poured water was equivalent to the volume of voids, and the depth of water was taken as the average depth of the surface. These tests indicated that "*for practical purposes, the voids in a loose layer of chips on the road could be taken as 50% of the average depth of the aggregate*." It should be noted that the volume of voids in a pavement surface layer represents the air spaces within the asphalt mixture mass. On the other hand, the volume of voids in a layer of aggregates (in seal coat structure) is the air space between the aggregates, that is the voids within the seal coat aggregate mass plus the bitumen content as shown in the following equation:

$$V_{\text{Voids in Seal Coat Aggregate Layer}} = V_{\text{air}} + V_{\text{Binder}}$$

Similarly, it was found that, when aggregates are compacted by a roller, the volume of voids drops to approximately 30% of the total volume. In other words, the space occupied by the voids amounts to approximately 30% of the compacted seal coat depth. Likewise, after the seal coat layer undergoes continuous compaction with time, the volume of voids continues to decrease to ultimately occupy 20% of the compacted depth. Figure 3.1 depicts the change in volume of voids at several stages of the seal coat life (Transit NZ, RCA, & Roading NZ, 2005).

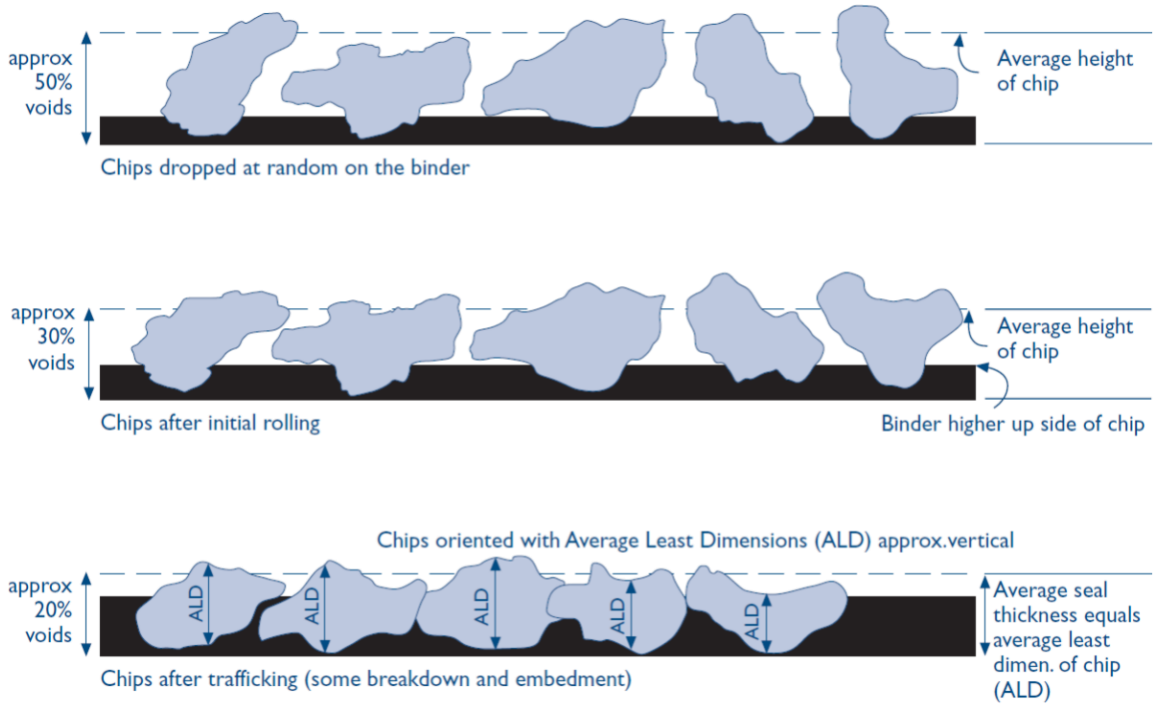

Figure 3.1: Reduction of Volume of Voids in a Seal Coat with Time

Hence, if the binder occupies 20% of the average layer depth, it will rise to the average height of the chips after adequate trafficking, and all the voids will be filled with binder. This phenomenon represents the minimum requirement for bleeding surfaces. It should be

noted that for a given area, the depth and the volume can be used interchangeably whereby the volume is the product of the area and the depth.

In Hanson's theory: "*If the bitumen fills half the voids, or in other words, rises to half the height of the layer of stone, then a strong waterproof mat of stone and bitumen will cover the road bed, and at the same time the top half of the stone will present a mosaic, non-skid surface*." The bitumen is said to cover the bottom portion of the aggregates except when the aggregates are so small and immerse into the bitumen layer. With roller compaction and trafficking, the bottom portion of the aggregates adhere to the existing surface and the extra aggregates will be brushed aside forming a one-stone thick matrix. Accordingly, the binder application rates, the aggregates application rate, and size of the aggregates play a crucial role in the seal coat design and performance. The main factors in the calculation of the aggregate and binder spreading rates are the following:

- Volume of voids,
- Estimated whip-off, and
- Average Least Dimension (ALD) of chip aggregates, which is the arithmetic average of the least dimension of each aggregate particle in a seal coat.

Hanson measured the least dimension manually using a caliper. The least dimension helps estimate the volume of voids in the aggregates covering the asphalt binder. Based on his research findings, Hanson concluded that the binder application rate (BAR) would be determined such that 20% of the total seal coat volume after traffic compaction, i.e. ultimate volume of voids, is filled with binder up to 60 to 75% depending on the type of aggregate used and the volume of traffic (Gransberg & James, 2005). The design philosophy follows these steps:

1. Identify the area to be seal coated.

2. Determine the aggregate application rate such that aggregates would form a mat of one aggregate thick and account for a whip off ratio.
3. Determine experimentally the net loose volume.
4. Solids occupy 50% of net loose aggregate volume, compacted voids represent 20% of the compacted seal coat volume, which is 62.5% of net loose volume.
5. Determine the volume of the voids.
6. Determine the volume of the binder such that 70% of the voids are filled, and the height covered with binder can be determined as:

$$\text{Height covered with binder} = \frac{V_{Binder}}{V_{Voids}} \times \text{compacted height}$$

To determine the compacted depth of the seal coat layer, the aggregate application rate, and the binder application rate, Hanson suggests the following two approaches.

Hanson's Loose Depth Approach

The loose depth is given by:

$$H = \frac{V}{A}$$

Where V is the volume of the loose aggregate layer, and A is the area covered by it. For a loose aggregate layer, the volume of loose aggregates represents 50% of the total seal coat volume, and the volume of voids represent the other 50% which can be designated by:

$$V_{Aggregates} = V_{Voids\ in\ Loose\ Aggregate\ Layer} = 0.5 \times V_T$$

Where V_T is the total layer volume. Since the volume and the depth can be used interchangeably for a given area, the depth occupied by voids represents half the total depth of the loose aggregate layer. Assuming that the compacted layer volume (depth) is given by "X", the volume of voids in the compacted seal coat layer can be expressed as:

$$V_{Voids\ in\ Compacted\ Seal\ Coat\ Layer} = X - \frac{V_T}{2}$$

Yet as aforementioned, *"… the volume of voids continues to decrease to ultimately occupy 20% of the compacted seal coat depth…"* This leaves the volume of voids as:

$$V_{\text{Voids in Compacted Seal Coat Layer}} = 0.2(X)$$

Equating the two previous expressions of the volume of voids in a compacted layer gives:

$$X - \frac{V_T}{2} = 0.2(X) \qquad \rightarrow \qquad \mathbf{X = 0.625\ V_T}$$

This implies that the compacted layer depth is 37.5% less than the loose layer depth, i.e. a drop by a factor of 1.6.

Hanson's Average Least Dimension (ALD) Approach

The philosophy behind this approach is that the average compacted depth of the seal coat layer can be estimated as the average least dimension of the chips because most of the chips after compaction and trafficking tend to lie on their flattest side. Hanson suggested measuring the average least dimension using the caliper for a representative sample of 200 to 300 aggregate particles of the prospective batch. The ALD is determined as

$$\text{ALD} = \frac{\sum_{i=1}^{n} \text{Least Dimension}}{n}$$

The compacted depth is estimated as the ALD and represents 62.5% of the loose aggregate depth, i.e. the loose depth = 1.6 (ALD). It should be noted that there is a tolerance limit for aggregate flakiness: it is recommended that no more than 10% of aggregates have their largest dimension greater than four times the least. Furthermore, Hanson's experience with seal coats revealed that chips were held in position if the bitumen occupied 50 to 70% of the void volume. Accordingly, the AAR was derived as follows, where the compacted depth is equal to the ALD (mm). For an area of 1 m^2, the compacted volume is given by:

$$\text{Compacted Volume } V_T(m^3/m^2) = \frac{\text{ALD (mm)}}{1000}$$

After significant compaction (rolling and trafficking), the volume of voids drops to 20% of the total compacted volume:

$$V_V(m^3/m^2) = 0.2 \times \text{Compacted Volume} = 0.2 \times \frac{\text{ALD (mm)}}{1000}$$

The volume of aggregates in a compacted seal coat layer is:

$$V_{aggregate}(m^3/m^2) = V_T - V_V = 0.8 \times \frac{\text{ALD (mm)}}{1000}$$

The voids in a loose layer of chips represents 50% of the average depth of the aggregates:

$$AAR(m^3/m^2) = 2 \times V_{aggregate} = 0.0016\ \text{ALD (mm)}$$

Hanson recommended designers to allow for aggregate whip-off by increasing the aggregate application rate by 10% or as deemed necessary. Consequently, the binder application rate is calculated based on the aggregate application rate. Experience had shown that if 70% of the total voids were filled with binder, the aggregates would be held in place. Hence, the binder application rate is given by:

$$BAR\ (L/m^2) = 0.7 \times V_V = 0.14 \times \text{ALD(mm)}$$

The determination of the final application rate depends also on different site-specific conditions. Adjustments to existing surfaces, traffic, or the use of emulsions should be considered to determine the final binder application rate.

KEARBY DESIGN METHOD (KEARBY, 1953)

J. P. Kearby, a senior resident engineer with the Texas Highway Department, developed the first practice for determining the application rates in the US. The main approach uses coarse graded aggregates of a uniform size with a spread ratio that covers the experimented surface one stone in depth. The method also limits the quantity of asphalt to sufficiently embed a portion of the thickness of the loose mat of aggregates. The factors considered are the volume and weight of traffic, the characteristics of available mineral aggregates and asphaltic materials, the available construction equipment, and the cost. Kearby claimed that the asphalt treatment's success depended on the subgrade and flexible base rather than the treatment itself.

He developed test methods to estimate the appropriate binder and aggregate content with a minimum dependence on visual approximation and judgment. However, computations alone do not guarantee satisfactory results, and specific conditions require visual inspection and judgment to alter the quantities accordingly.

The aggregate application rate is a function of the aggregate's unit weight, specific gravity, percent of voids, shape, size, and screen analysis in the aim of obtaining a blanket of aggregates one stone in depth. Kearby introduced the notion of "*effective mat thickness*" that represents the average thickness of the aggregate when forming a blanket of one aggregate in depth. A board test is employed to measure the quantity of aggregates required to cover an area of one square yard. In this test, the aggregates are spread as to fully cover the area one stone in depth. The required weight is recorded in units of mass per square area, i.e. lb/yd^2. The spread ratio is another aggregate feature metric that represents the number of square yards covered by one cubic yard of aggregates. The spread ratio, i.e. aggregate application rate (AAR), is obtained using the tray test results and the unit weight of the aggregate as follows:

$$\text{Spread Ratio, SR or AAR} = \frac{\text{Unit Weight}}{\text{Board Test}} = \frac{\text{lb/yd}^3}{\text{lb/yd}^2} = \text{yd}^2/\text{yd}^3$$

The critical aggregate quantity requires that the seal coat thickness to be one aggregate deep. The average mat thickness can then be estimated from the spread ratio as:

$$\text{Average Mat Thickness} = \frac{36}{\text{SR}} = \text{(in)}$$

Where 36 is a conversion factor from yards to inches. Additionally, Kearby recommends a set of eight different grades of aggregates for seal coats and are presented in Table 3.1.

Grade	Sieve Size	Percent Retained
I	1-1/8 inch	0%
	1 inch	40% - 60%
	7/8 inch	95% - 100%
II	1 inch	0%
	7/8 inch	40% - 60%
	3/4 inch	95% - 100%
III	7/8 inch	0%
	3/4 inch	40% - 60%
	5/8 inch	95% - 100%
IV	3/4 inch	0%
	5/8 inch	40% - 60%
	1/2 inch	95% - 100%
V	5/8 inch	0%
	1/2 inch	40% - 60%
	3/8 inch	95% - 100%
VI	1/2 inch	0%
	3/8 inch	40% - 60%
	1/4 inch	95% - 100%
VII	3/8 inch	0%
	1/4 inch	40% - 60%
	# 10	95% - 100%
VIII	1/4 inch	0%
	# 10	40% - 60%
	#20	95% - 100%

Table 3.1: Recommended Aggregate Grades for Asphalt Surface Treatments

The quantity of fines in the aggregate mix is critical because the fines tend to settle at the bottom of the seal coat layer, prevent the proper aggregate embedment, and increase the whip-off likelihood, i.e. raveling.

When it comes to binder quantification, the amount of asphalt per square yard of surface, which is required to embed a desired portion of the effective aggregate mat thickness, is key. This quantity depends on the percentage of voids in the aggregate, the condition of the surface or base on which the treatment is to be placed, the hardness of the aggregates, and the type, kind, and amount of traffic. The BAR is given as:

$$\text{BAR } (\text{in}^3/\text{yd}^2) = \text{Desired Embedment Depth}(\text{in}) \times 1296\ (\text{in}^2/\text{yd}^2) \times \%\ \text{of Voids}$$

To capture the design factors, Kearby developed a nomograph that uses as inputs the average size of aggregates, the percent embedment depth, and the percentage of voids between aggregates (as shown in Figure 3.2).

Kearby noted important design considerations highlighted as follows:

- If an emulsion-based binder is used, the BAR should be increased accordingly to account to the emulsion-residual binder ratio;
- If the existing surface is bleeding or soft, the BAR should be decreased to prevent a bleeding seal coat job;
- If soft aggregates are used, they are expected to be crushed by trafficking, and hence the BAR should be decreased to account for a smaller effective mat thickness;
- If high traffic volumes are expected, the BAR should be decreased and larger size aggregates should be used because an over-compaction is anticipated;
- If light traffic volumes are likely, the BAR should be increased because an under-compaction is expected and more binder is needed to hold aggregates in place;
- If a high proportion of heavy vehicles is projected, the BAR should be decreased and larger aggregates should be used under the same reasoning as earlier;

- Gap graded aggregates are problematic and not recommended because they lead to surface raveling for areas with aggregates in the upper gradation range and bleeding for areas with aggregates in the lower gradation range; and
- The use of flat and elongated aggregates is not recommended and should be limited to a maximum of 10%.

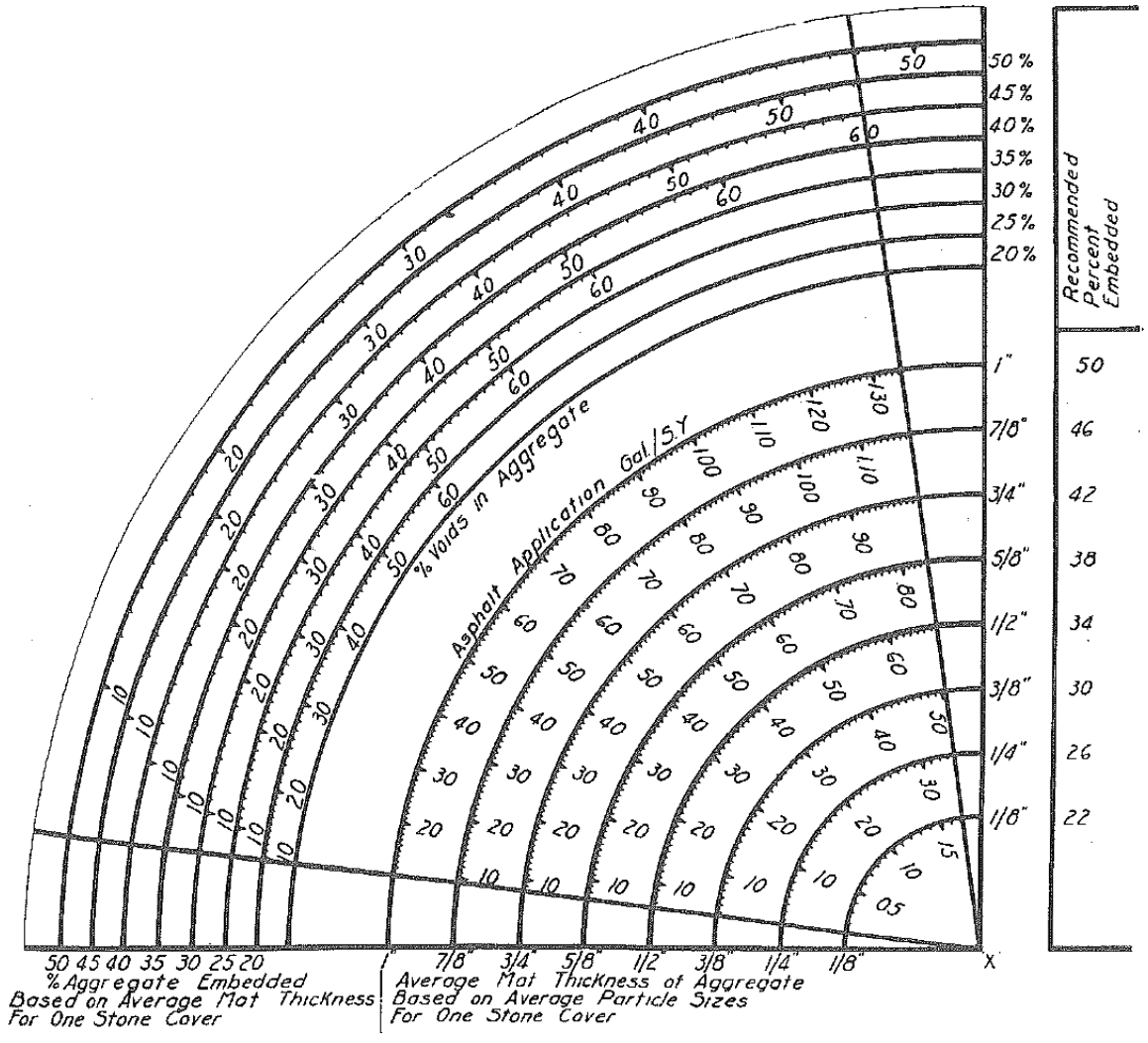

Figure 3.2: Kearby's BAR Nomograph (Kearby, 1953)

Unfortunately, Kearby did not address these situations in the nomograph. Additionally, the nomograph offers a limited range for the void percentage and the percentage embedment depth. Finally, the aggregate size range only varies between 1/8 inch and 1 inch.

MCLEOD DESIGN METHOD (MCLEOD, 1969)

N.W. McLeod, a Canadian asphalt consultant at Imperial Oil Ltd., published "*A General Method of Design for Seal Coats and Surface Treatments*" in his 1969 synopsis. This design method reviews the ideal binder and aggregate application rates that are needed during construction aimed at limiting the dependency on the engineering judgement on site. McLeod emphasized the fact that a strong foundation was needed before considering applying a seal coat; otherwise, the treatment would fail.

McLeod highlighted the importance of aggregates and their effect on the long-term performance of seal coats. Chip shape, gradation, average least dimension, spread modulus, void fraction, resistance to abrasion and weathering, resistance to crushing, and aggregate-binder adhesion are key factors that need to be addressed. The amount of aggregates spread should be sufficient to form a blanket of one stone in depth and ultimately placed such that the least dimension is in an upward direction. This amount is a function of the size, shape, and unit weight; in addition, the rate is incremented by a five to 20 percent for whip-off. It is undesired to have a high whip-off ratio because loose aggregates damage the vehicles, weaken the structure, and waste money. The gradation of the aggregates is one-sized which is strictly defined as "*60 to 70 percent by weight of the aggregate passing the specified sieve and retained on a sieve having an opening that is seven tenths of the specified size.*" As for the size of these aggregates, it was assumed that large aggregates provided a rougher-textured surface, enhanced grip, were easier for constructions and the determination of the BAR, but remained noisier. Smaller aggregates, on the other hand, provided a quieter surface, but were meticulous when it came to BAR and increased the chances of surface bleeding. The average least dimension (ALD) is a key component in this design. The ALD, if not measured, could be estimated using the following equation:

$$\mathrm{ALD} = \frac{\mathrm{M}}{1.139285 + 0.011506\ \mathrm{FI}}$$

Where M is the median particle size, which is a theoretical sieve size through which 50 percent of the material passes, and FI is the flakiness index, which is measured using a slotted plate in compliance with Tex 224-F (TxDOT, 2004).

In order to insure sufficient interlocking and treatment stability, the aggregates are required to be angular with no more than 10% by weight of flat or elongated particles. Specific aggregate gradations are required as per this design and are shown in the Table 3.2.

Size Number	Nominal Size, Square Openings	Amounts Finer than Each Laboratory Sieve (Square Openings), mass percent														
		100-mm (4-in.)	90-mm (3½-in.)	75-mm (3-in.)	63-mm (2½-in.)	50-mm (2-in.)	37.5-mm (1½-in.)	25.0-mm (1-in.)	19.0-mm (¾-in.)	12.5-mm (½-in.)	9.5-mm (⅜-in.)	4.75-mm (No. 4)	2.36-mm (No. 8)	1.18-mm (No. 16)	300-µm (No. 50)	150-µm (No. 100)
1	90 to 37.5-mm (3½ to 1½-in.)	100	90 to 100	...	25 to 60	...	0 to 15	...	0 to 5	...	...	...	...	...	...	...
2	63 to 37.5-mm (2½ to 1½-in.)	...	...	100	90 to 100	35 to 70	0 to 15	...	0 to 5	...	...	...	...	...	...	...
24	63 to 19.0-mm (2½ to ¾-in.)	...	...	100	90 to 100	...	25 to 60	...	0 to 10	0 to 5	...	...	...	...	...	...
3	50 to 25.0-mm (2 to 1-in.)	...	...	...	100	90 to 100	35 to 70	0 to 15	...	0 to 5	...	...	...	...	...	...
357	50 to 4.75-mm (2-in. to No. 4)	...	...	...	100	95 to 100	...	35 to 70	...	10 to 30	...	0 to 5	...	...	...	...
4	37.5 to 19.0-mm (1½ to ¾-in.)	...	...	...	...	100	90 to 100	20 to 55	0 to 15	...	0 to 5	...	...	...	...	...
467	37.5 to 4.75-mm (1½-in. to No. 4)	...	...	...	...	100	95 to 100	...	35 to 70	...	10 to 30	0 to 5	...	...	...	...
5	25.0 to 12.5-mm. (1 to ½-in.)	...	...	...	...	...	100	90 to 100	20 to 55	0 to 10	0 to 5	...	...	...	...	...
56	25.0 to 9.5-mm (1 to ⅜-in.)	...	...	...	...	...	100	90 to 100	40 to 85	10 to 40	0 to 15	0 to 5	...	...	...	...
57	25.0 to 4.75-mm (1-in. to No. 4)	...	...	...	...	...	100	95 to 100	...	25 to 60	...	0 to 10	0 to 5	...	...	...
6	19.0 to 9.5-mm (¾ to ⅜-in.)	...	...	...	...	...	...	100	90 to 100	20 to 55	0 to 15	0 to 5	...	...	...	...
67	19.0 to 4.75-mm (¾-in. to No. 4)	...	...	...	...	...	...	100	90 to 100	...	20 to 55	0 to 10	0 to 5	...	...	...
68	19.0 to 2.36-mm (¾-in. to No. 8)	...	...	...	...	...	...	100	90 to 100	...	30 to 65	5 to 25	0 to 10	0 to 5	...	...
7	12.5 to 4.75-mm (½-in. to No. 4)	...	...	...	...	...	...	...	100	90 to 100	40 to 70	0 to 15	0 to 5	...	...	...
78	12.5 to 2.36-mm (½-in. to No. 8)	...	...	...	...	...	...	...	100	90 to 100	40 to 75	5 to 25	0 to 10	0 to 5	...	...
8	9.5 to 2.36-mm (⅜-in. to No. 8)	...	...	...	...	...	...	...	...	100	85 to 100	10 to 30	0 to 10	0 to 5	...	...
89	9.5 to 1.18-mm (⅜-in. to No. 16)	...	...	...	...	...	...	...	...	100	90 to 100	20 to 55	5 to 30	0 to 10	0 to 5	...
9	4.75 to 1.18-mm (No. 4 to No. 16)	...	...	...	...	...	...	...	...	...	100	85 to 100	10 to 40	0 to 10	0 to 5	...
10	4.75-mm (No. 4 to 0[A])	...	...	...	...	...	...	...	...	...	100	85 to 100	...	...	...	10 to 30

[A] Screenings.

Table 3.2: Standard Aggregate Sizes and Gradation (McLeod, 1969)

McLeod introduced the concept of spread modulus to determine the average thickness of the seal coat using the gradation of the aggregates. It is the weighted average of the mean particle size of the largest 20%, the middle 60%, and the smallest 20% of a one-size graded cover aggregate and calculated using the following formula:

$$\text{Spread Modulus, M} = 0.2\left(\frac{a+b}{2}\right) + 0.6\left(\frac{b+c}{2}\right) + 0.2\left(\frac{c+d}{2}\right)$$

Where, a is the sieve smallest opening in inches with 100% of the aggregates passing, b is that with 80% passing, c with 20% passing, and d with 0% passing.

Figure 3.3 provides a visual demonstration of the spread modulus distribution.

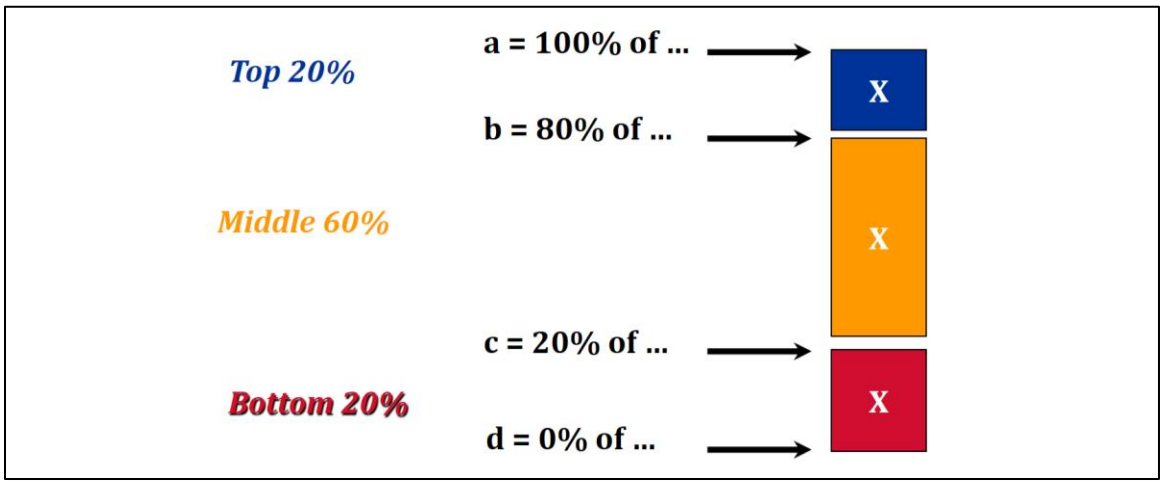

Figure 3.3: Spread Modulus Distribution

McLeod also incorporated the concept of average least dimension (ALD) of the aggregates in order to determine the average size of the seal coat layer. A series of tests were conducted on different aggregate types to determine the correlation between the spread ratio and the ALD. McLeod concluded that a ratio of 1.33 was needed for M/ALD to be able to adequately design the chip and employ sufficient amounts of binder. The recommended aggregate application rate, in lb/yd^2, is determined as:

$$\text{AAR}(\text{lb/yd}^2) = \left(\frac{36 \times 36 \times 0.8 \times \text{ALD(in)}}{1728}\right) \times 62.4(\text{lb/ft}^3) \times \text{G} \times \text{E}$$

Where 0.8 is the proportion of aggregates by volume in the seal coat structure (based on Hanson's theory that the volume of voids in aggregates after significant compaction is

20%), ALD is the average least dimension of the aggregates in inches, 62.4 is the unit weight of water in lb/ft^3, G is the dry bulk specific gravity of the aggregates, E is the wastage factor calculated as $\left(1+\frac{\%}{100}\right)$, and $\left(\frac{36\times36}{1728}\right)$ is a unit conversion factor from inches to ft^3/yd^2 as shown below:

$$1\text{ in} = 1\frac{\text{in}^3}{\text{in}^2} = 1\frac{\text{in}^3 \times \frac{1}{12^3}\text{ft}^3/\text{in}^3}{\text{in}^2 \times \frac{1}{36^2}\text{yd}^2/\text{in}^2} = \frac{36^2}{12^3} = \frac{36\times36}{1728}(\text{ft}^3/\text{yd}^2)$$

McLeod also defined specific properties for the asphalt binder for the surface treatment to perform adequately. Binder-surface adhesion, net residuals, application temperature, traffic, surface texture, aggregate absorption are key factors to consider when designing a seal coat. In compliance with Hanson's initial assumption, the binder should cover 70% of the aggregate depth to ensure appropriate embedment. Percentages lower than 50% increase the likelihood of raveling. McLeod explicitly stated that: "*When enough asphalt binder is applied to embed the median particle size to 70% of its thickness, only 15 per cent of the aggregates (the smallest sizes) would be completely submerged in asphalt binder while just 3% of the particles (the largest sizes) would be embedded to less than 50 per cent of their depth*." This consideration addresses the effects the aggregate gradation and binder content have on raveling (loose aggregates) and bleeding (submerged aggregates). The appropriate binder application rate, in gal/yd^2, is determined as:

$$\text{BAR}(\text{gal/yd}^2) = \left(\frac{36\times36\times0.2\ \text{ALD(in)}}{231}\right)\left(\frac{\text{T}}{\text{R}}\right)+\frac{\text{S}+\text{A}}{\text{R}}$$

Where 0.2 is the proportion of voids by volume in the seal coat layer. It should be noted that not all the voids are filled with binder to prevent bleeding, and that is accounted for by the traffic factor. T is the traffic factor (shown in Table 3.3), S is the existing surface texture correction factor (shown in Table 3.4), R is the proportion of residual asphalt content in

the binder used, A is an aggregate absorption factor which accounts for the binder loss, and $\left(\frac{36\times36}{231}\right)$ is a conversion factor from inch to gal/yd^2 as follows:

$$1\text{ in} = 1\frac{\text{in}^3}{\text{in}^2} = 1\frac{\text{in}^3 \times \frac{1}{12^3}\text{ft}^3/\text{in}^3}{\text{in}^2 \times \frac{1}{36^2}\text{yd}^2/\text{in}^2} = \frac{36^2}{12^3}\text{ft}^3/\text{yd}^2 \times 7.48\text{ gal/ft}^3 = \frac{36\times36}{231}\text{gal/yd}^2$$

Asphalt Application Rate – Correction Due to Traffic, T					
Vehicles per day per lane	< 100	100 – 500	500 – 1000	1000-2000	> 2000
Traffic Correction Factor	0.85	0.75	0.70	0.65	0.60

Table 3.3: McLeod BAR Traffic Correction Factor

Existing Surface Texture Rating	**(US) gal/yd^2**	**(SI) L/m^2**
Black	- 0.06	- 0.272
Smooth	nil	nil
Hungry 1h	+ 0.03	+ 0.136
Hungry 2h	+ 0.06	+ 0.272
Hungry 3h	+ 0.09	+ 0.408

Table 3.4: McLeod BAR Surface Correction Factor

It is recommended that the asphalt binder ultimately occupies 70% of the total volume of voids in the seal coat structure. This allows the consideration of margins of safety for bleeding determined as the difference between 100% content and 70%. Similarly, the margin of safety for raveling can be determined as the difference between 50% asphalt content and 70%.

MODIFIED KEARBY DESIGN METHOD (EPPS, GALLAWAY, & HUGHES, 1981)

J. A. Epps and B. M. Gallaway first attempted to modify the original Kearby design method in 1972 and 1974. To determine the binder application rate, the existing method recommended a nomograph that did not incorporate high porosity aggregates, and the study initially focused on modifying the Kearby seal coat design method to do so (Epps & Gallaway, 1972; Epps, Gallaway, & Brown, 1974). Few years later, they introduced the modified Kearby design method that corrected the recommended dosages for site-specific conditions. Their study showed that seal coats were still good for high traffic volumes of 4,000 vehicles per lane per day with an average life of six to ten years. They intended to provide a guideline that improved the chance of constructing a successful seal coat. Their considerations highlighted the fact that seal coats are site specific and a "*one-design-that-fits-all*" is not appropriate; nevertheless, this method ends up providing unique rates.

In this method, specific aggregate types and gradations, which are 85% by weight passing a specific size and retained on half this size, are specified. It is highlighted that one-size or uniform gradation improves the seal coat performance as it reduces the likelihood of raveling or bleeding when properly designed. The aggregate application rate is determined using the dry loose unit weight in accordance with TEX 404A standard (TxDOT, 2014) and the quantity of aggregates, which is determined using the board test. The board test determines the weight of aggregates needed to cover one-yard squared tray. The aggregate application rate is determined from laboratory tests as follows:

$$\text{AAR } (\text{yd}^2/\text{yd}^3) = \frac{\text{W}\left(\frac{\text{lb}}{\text{ft}^3}\right)}{\text{Q}\left(\frac{\text{lb}}{\text{yd}^2}\right)} \times 27\frac{\text{ft}^3}{\text{yd}^3} = 27\left(\frac{\text{W}}{\text{Q}}\right)$$

Where W is the dry loose unit weight and Q is the Board Test aggregate weight.

The asphalt binder is required to be fluid enough when uniformly sprayed to allow rapid wetting yet viscous enough to retain the aggregates and prevent distortion when opened to traffic. Many other considerations should be catered for including temperature, sunlight, wind, dust, moisture, traffic, aggregate compatibility, and many more. The binder application rate is determined using the following equation:

$$\mathrm{BAR(gal/yd^2)} = 5.61\mathrm{E\ (in)}\left(1 - \frac{\mathrm{W}}{62.4\mathrm{G}}\right)(\mathrm{T}) + \mathrm{V(gal/yd^2)}$$

Where E is the embedment depth shown in Figure 3.4 and obtained in inches as follows:

$$\mathrm{E} = \mathrm{e} \times \mathrm{d}$$

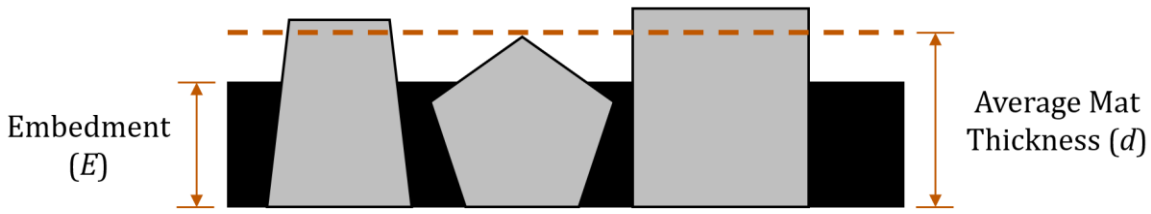

Figure 3.4: Illustration of the Asphalt Embedment Depth and Average Mat Thickness

Accordingly, d is the average mat depth, also known as the average least dimension, determined in inches from laboratory tests as follows:

$$\mathrm{d\ (in)} = \frac{4}{3} \times \frac{\mathrm{Q\ (lb/yd^2)}}{\mathrm{W\ (lb/ft^3)}}$$

Where W is the dry loose unit weight and Q is the board test aggregate weight. In addition, e is the percent embedment shown in Figure 3.5. The proportion of voids in the binder dosage equation is represented by $\left(1 - \frac{\mathrm{W}}{62.4\mathrm{G}}\right)$ where G is the dry bulk specific gravity and 62.4 is the unit weight of water in lb/ft^3. The traffic correction factor in the equation is represented by T and is adopted from field experiences and tests as presented in Table 3.5.

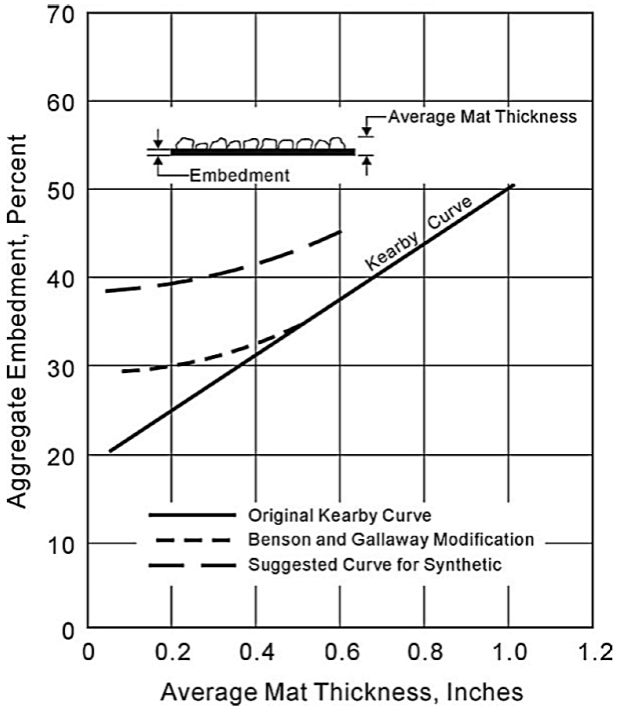

Figure 3.5: Percent Embedment Graphs (Epps, Gallaway, & Hughes, 1981)

Asphalt Application Rate – Correction Due to Traffic, T					
Vehicles per day per lane	>1000	500-1000	250-500	100-250	<100
Traffic Correction Factor	1	1.05	1.1	1.15	1.2

Table 3.5: Traffic Correction Factor

As shown in Table 3.5, if the traffic volume is not sufficient to ensure a good compaction, a higher binder application rate is needed to retain the aggregates and prevent raveling. The correction factor for surface texture in the equation is represented in Table 3.6. The evaluation of surface condition requires engineering judgement and expert assessment. It is recommended to decrease the binder application rate if the surface is bleeding and

increase the dosage if the surface is porous in order to compensate for the volume of voids in the existing surface texture.

Asphalt Application Rate Correction due to Existing Pavement Surface Condition	
Description of Existing Surface	**Correction (V), gal/SY**
Flushing, slightly bleeding surface	-0.06
Smooth, nonporous surface	-0.03
Slightly porous, slightly oxidized surface	0
Slightly pocked, porous, oxidized surface	0.03
Badly pocked, porous, oxidized surface	0.06

Table 3.6: BAR Correction for Existing Surface Texture

The last BAR term is 5.61, which is a unit conversion factor from inch to gal/yd^2 as follows:

$$1\text{ in} = 1\frac{\text{in}^3}{\text{in}^2} = 1\frac{\text{in}^3 \times \frac{1}{12^3}\text{ft}^3/\text{in}^3}{\text{in}^2 \times \frac{1}{36^2}\text{yd}^2/\text{in}^2} = \frac{36^2}{12^3}\text{ft}^3/\text{yd}^2 = \frac{3}{4}\text{ft}^3/\text{yd}^2$$

$$1\text{ ft}^3 = 7.48\text{ US gallon}$$

$$1\text{ in} = \frac{3}{4}\text{ft}^3/\text{yd}^2 \times 7.48\text{gal}/\text{ft}^3 = 5.61\text{gal}/\text{yd}^2$$

Asphalt emulsions and cutbacks offer lower power consumption and easier transportation and handling (Roberts, Kandhal, Brown, Lee, & Kennedy, 1996). When cutback or emulsions are used, the residual binder should be considered. Hence, the binder application rate is adjusted when an emulsion or a cutback are used as the binder component of the seal coat as follows:

$$\text{BAR}_{(\text{emulsion})} = \frac{\text{BAR}_{\text{required}}}{\text{Residual Asphalt}}$$

The modified Kearby design method provides a guide for certain grades of cutbacks and the approximate quantity of cutter stock in those cutbacks that are typically used for seal coat operations. The recommended emulsion application rate can be obtained by dividing the theoretical binder application rate by the amount of residual asphalt present in them, but experience over time suggests that flushing is likely to occur as a result of such correction and the recommended binder application rate is the following:

$$\mathrm{BAR}_{\mathrm{Recommended}} = \mathrm{BAR} + \mathrm{K}(\mathrm{BAR}_{\mathrm{Corrected}} - \mathrm{BAR})$$

Where $\mathrm{BAR}_{\mathrm{recommended}}$ is the recommended binder application rate, BAR is the uncorrected binder application rate obtained by the design method, $\mathrm{BAR}_{\mathrm{corrected}}$ is the corrected binder application rate for cutbacks or emulsions using the previous approach, and K is the correction factor based on field experience as tabulated in Table 3.7.

K for Asphalt	Spring	Summer	Fall	Winter
Emulsion	0.6	0.4	0.7	0.9
Cutback	0.7	0.6	0.8	0.9

Table 3.7: Field experience Correction Factors for Emulsions and Cutbacks

The researchers also provide tables for volume-temperature correction factor as the quantity of asphalt that needs to be sprayed should be proportional to the quantity retained on the road at 60°F. Hence the binder application rate at the spray temperature is:

$$\mathrm{BAR}_{\mathrm{Spray\ Temp}} = \frac{\mathrm{BAR}_{60}}{\mathrm{Correction\ Factor}}$$

The authors also allude to other environmental logistical considerations that need to be catered for when constructing the seal coat. The main environmental factors that need to be pondered are moisture, wind, and surface temperature. It should also be highlighted that

the aggregates used on site should not be neither wet nor dirty. Failure to comply with such considerations would compromise the performance of the surface treatment and would lead to premature failure and safety-compromising distresses.

Holmgreen conducted some studies later in 1985 and realized that the binder application rate recommended by Epps et al back in 1981 was not sufficient to hold the aggregates in place (Holmgreen, Epps, Hughes, & Gallaway, 1985; Kutay, Ozdemir, Hibner, Kumbargeri, & Lanotte, 2016).

SPANISH DESIGN METHOD (BARDESI & TOMAS, 2004)

Spain has been applying seal coats to their roads since the 19th century, however it was until Article 533 of the PG-3, published in 1988, that seal coat design procedures were standardized. Due to numerous advances in technology and improved techniques that minimize waste and maximize efficiency of the surface treatment, 95% of all the roads in Spain use emulsions. When designing seal coats, the Spanish method takes into account the type of treatment needed, the aggregate size and gradation, and the type of binder to be used. Given these considerations, the Spanish method uses six main types of seal coats: single seal coat, sandwich seal, sandwich double seal, racked-in seal, double seal coat, and triple seal coat.

Regarding the aggregates, this method categorizes them by means of the gradation fraction D/d, where D is the smallest sieve opening (in mm) that has a percent passing higher or equal to 90% and d is the largest sieve opening (in mm) with a percent passing of less than 10%. They also classify the aggregates as normal (A) and special (AE). Normal aggregates are those extracted from natural sources such as quarries or alluvial deposits. Special aggregates are artificially made, usually by sintering or autoclaving. For example, AE 20/12 stands for a special aggregate where the smallest sieve opening that had a percent passing higher than or equal to 90% is 20 mm and the largest sieve with a percent passing of less than 10% is 12 mm.

Spain is one of the countries that have drastically switched from using asphalt cement (AC) in their paving operations to mostly asphalt emulsions. This binder is classified by penetration (in tenths of millimeters) at 25° C of a 100 grams calibrated indenter (Caminos y Aeropuertos, 2011). For instance, B 150/200 stands for an unmodified binder that at a temperature of 25° C, allows a 100 g calibrated indenter to penetrate 150 to 200 tenths of a millimeter.

A good estimate for the application rate of aggregate can only be obtained if the contractor knows the type of aggregates that will be used beforehand. Accordingly, the coverage potential of each aggregate type is determined (in liters per meter square). Coverage potential is the minimum amount of aggregate needed to saturate the surface. For single seal coat, the aggregate application rate ranges between 1.1×C and 1.2×C where C is the aggregate coverage potential. However, when project proposals are being drafted, it is highly likely that the type of aggregates used is unknown. Hence, empirical methods and rules of thumb are used to estimate the amount of aggregate and binder expected to be used. The two main Spanish empirical methods to determine an adequate aggregate application rate (AAR) are discussed below.

Spanish's C.R.R. (Centre de Recherches Routiers) Approach for AAR

This method was first developed in Belgium and suggests that the aggregate application rate is dependent on the average aggregate size and the amount of aggregates lost during construction. The aggregate application rate is determined in L/m^2 b as follows:

$$AAR = \Delta - 0.01\Delta^2 + R$$

$$\Delta = \frac{(D + d)}{2}$$

Where Δ is the average aggregate size (mm), d is the minimum aggregate size (mm), D is the maximum aggregate size (mm), and R is a correction factor for aggregate losses (L/m^2). In this method, the correction factor, R, is dependent on Δ, and its value ranges linearly from 1.0 L/m^2 for Δ = 5 mm and 1.5 L/m^2 for Δ = 20 mm.

Spanish's Linckenheyl Approach or the Decimal Rule for AAR

This method is one of the most commonly applied rules of thumb throughout Spain. Under normal conditions the following aggregate application rates apply:

$$AAR = 0.9 \times \Delta \text{ for } \Delta \geq 10 \text{ mm}$$

$$AAR = 3 + 0.7 \times \Delta \text{ for } \Delta < 10 \text{ mm}$$

Similarly, the binder application rate is dependent on the size and shape of the aggregates used. In the case of single coat seal coat, the binder should reach a height of about 60% to 70% the size of the aggregates used. Any amount lower than that range will result in raveling due to poor adhesion between binder and aggregates, while any amount higher will result in bleeding pavement. The two main empirical methods of determining the adequate binder application rate are discussed below.

Spanish's C.R.R. Approach for BAR

This method was first developed in Belgium and is the complement of the aggregate application rate whereas the binder application rate is determined in kg/m^2 as:

$$BAR = a + b \times AAR$$

Where a is a road texture factor, b is an aggregate type correction factor, and AAR is the aggregate application rate (L/m^2)

The typical values for factors (a) and (b) can be found in Table 3.8.

Factor	Description	Correction Factor
Road Surface Texture (a)	Bleeding	a = 0.00
	Normal	a = 0.34
	Porous, dry, or cracked	a = 0.59
Aggregate Type (b)	Pre-Coated	b = 0.06
	Artificial	b = 0.07
	Natural	b = 0.09

Table 3.8: BAR Correction Factors for Texture and Aggregate Type

Spanish's Linckenheyl Approach or the Decimal Rule for BAR

The Decimal Rule's major assumption is that the binder application rate is completely dependent on aggregate size. The total amount of binder should cover two-thirds of the aggregate height as shown in the Figure 3.6. It is estimated as:

$$\text{BAR} = 0.1 \times \text{AAR}$$

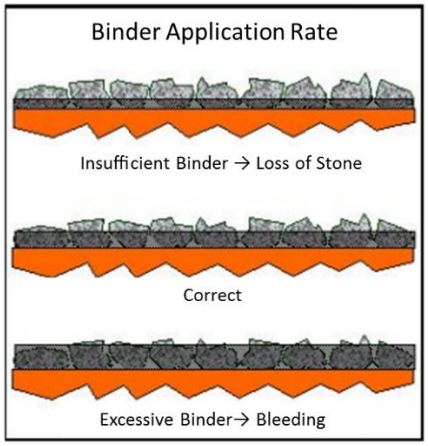

Figure 3.6: Adequate Binder Depth (Bardesi & Tomas, 2004)

In both methods, the binder application rate refers specifically to the residual bitumen. Since Spain uses mostly emulsions, the emulsion application rate is obtained after dividing the BAR by the percentage of residual bitumen in the emulsion. In general, both methods will tend to overestimate the binder application rate for fine aggregates and underestimate it for coarse aggregates when multiple layer seal coat is applied.

As shown in Table 3.9, Spain developed tables of basic binder and aggregate application rates for the main seal coats that are applied throughout the country.

Single Chip Seal				
Aggregate		**Binder Type**		
Type	**Application Rate (l/m^2)**	*B 150/200 BM- 5*	*ECR-3 ECR-3m*	*ECR-2 ECR-2m*
		Application Rate (kg/m^2)		
AE 16/8	10 - 13	1.3	~	~
A 12/6; AE 12/6	7 - 10	1.0	1.0	~
A 8/4; AE 8/4	5 -8	~	0.8	0.8
A 6/4; AE 6/4	4 -7	~	0.6	0.6

Table 3.9: Basic Binder and Aggregate Application Rates (Bardesi & Tomas, 2004)

NEW ZEALAND DESIGN METHOD (TRANSIT NZ, RCA, & ROADING NZ, 2005)

The New Zealanders were the first to develop seal coat design methods (Hanson, 1935) as described in the first section of Chapter 3. Hanson's conclusion was that, for a seal on a smooth surface to be successful, the rate of binder application should fill 70% of the voids after trafficking, 20% of seal volume, with binder as follows:

$$\text{BAR} = 0.7 \times 0.2 \times \text{ALD} = 0.14\,\text{ALD} \qquad (\text{L/m}^2)$$

Where, ALD is the average least dimension in mm.

Later in 1969, the New Zealanders investigated the effect of traffic and existing surface texture on Hanson's basic application rates by applying a set of three different rates for each site: the design rate, a higher rate, and a lower rate. Consequently, experienced practitioners predicted the future performance of these surface treatments. The combination of the subjective observations, measured traffic volumes, pre-seal surface texture, aggregate ALD, and application rates enabled the development of a spray rate chart that led to the development of the Transit New Zealand Design Algorithm known as RD286 (NRB 1971), which recommended the following binder application rate:

$$\text{BAR} = (0.138\,\text{ALD} + \text{e})\text{T}_\text{f} \qquad (\text{L/m}^2)$$

Where ALD is the average least dimension in mm, e is the surface texture correction factor in L/m^2, and T_f is an adjustment factor for traffic.

The surface correction factor, e, is determined such that an existing surface with high macrotexture needs to be filled with enough binder to form a layer that secures the chips. Hence, the binder application rate is increased. The texture is assessed using the mean texture depth (MTD) that is obtained from the sand patch test (SPT). This test method is thoroughly discussed in the first section of Chapter 5. Empirically, the texture correction factor for the BAR is obtained after conducting some sealing tests as:

$$\text{e} = 0.21 \times \text{MTD} - 0.05$$

Where e is the surface texture correction factor in L/m^2, and MTD is the Mean Texture Depth from the SPT in mm.

On the other hand, the traffic factor, T_f, takes into account the differences in chip orientation that occur under different traffic volumes and that some embedment into the substrate will occur under high traffic loadings. The basic assumption that Hanson made about chips lying on their flattest side was found not to occur, especially under light traffic. Therefore, as the chip layer is thicker, it requires more binder to fill the larger volume of voids. Under light traffic conditions, insufficient compaction of the seal coat requires an increase in the binder content to maintain the aggregates in place.

Further development took place in the late 80's and 90's whereby the traffic factor was thoroughly investigated. The objective was to minimize the binder application rate in order to save money conditioned upon being able to hold the aggregates in place. A series of tests were conducted whereby different seal coats were designed, traffic was monitored, and the adequate traffic correction factor that should have been adopted was back-calculated for as follows:

$$T_f = \frac{BAR}{0.138 \times ALD + e}$$

The experimental results revealed that the binder application rate needed to be increased at lower traffic volumes (lower than 1,000 vehicles/lane/day) and even more for very low traffic volumes (lower than 100 vehicles/lane/day). Nevertheless, the rate should be maintained as is for higher traffic volumes (greater than 1,000 vehicles/lane/day). Additionally, the concept of equivalent light vehicles (elv) was introduced whereby heavy commercial vehicles (HCV) were considered equivalent to ten light vehicles or cars in agreement with South African recommendations.

Later additional investigations indicated that the total volume of voids was significantly higher than 20% in a compacted seal, and that the voids continued to decrease with further compaction under traffic (Patrick, 1999). The research focused on monitoring the volume of voids – ALD ratio against traffic as follows:

$$\frac{V_V}{ALD} = A + B \times \log(\text{cumulative traffic in elv})$$

Where A is a measure of the initial state of voids in a seal, and B is the rate of change in voids with traffic. The study estimated A at 0.83 and B at -0.07 such that traffic is measured in cumulative equivalent light. Figure 3.7 is an illustration of the obtained results.

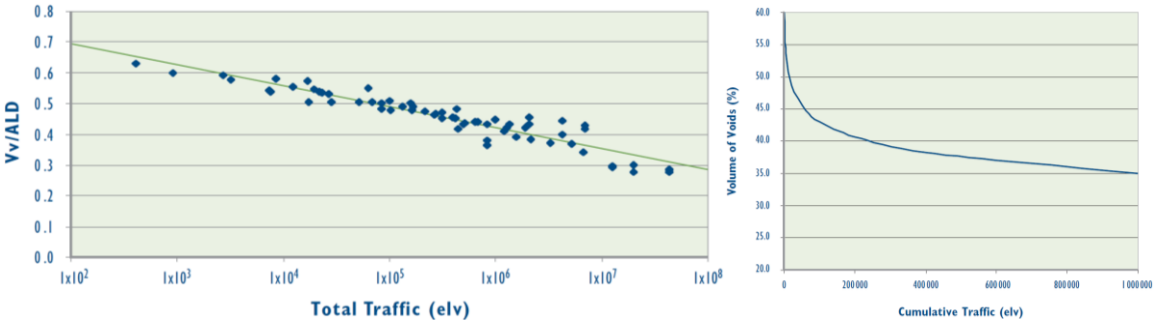

Figure 3.7: Seal Coat Void Ratio as a Function of Cumulative Traffic

These developments led to the onset of New Zealand seal coating design in 2004 when a relatively comprehensive approach was recommended. This design method complies with the fact that durable seals have 60% to 70% of their voids filled with binder. After monitoring many seal coating jobs, it was determined that the binder should fill 35% of the volume of voids before the first winter to prevent premature chip loss. Figure 3.8 shows the variation of the proportion of binder as the volume of voids in a seal coat layer decrease with time and significant compaction.

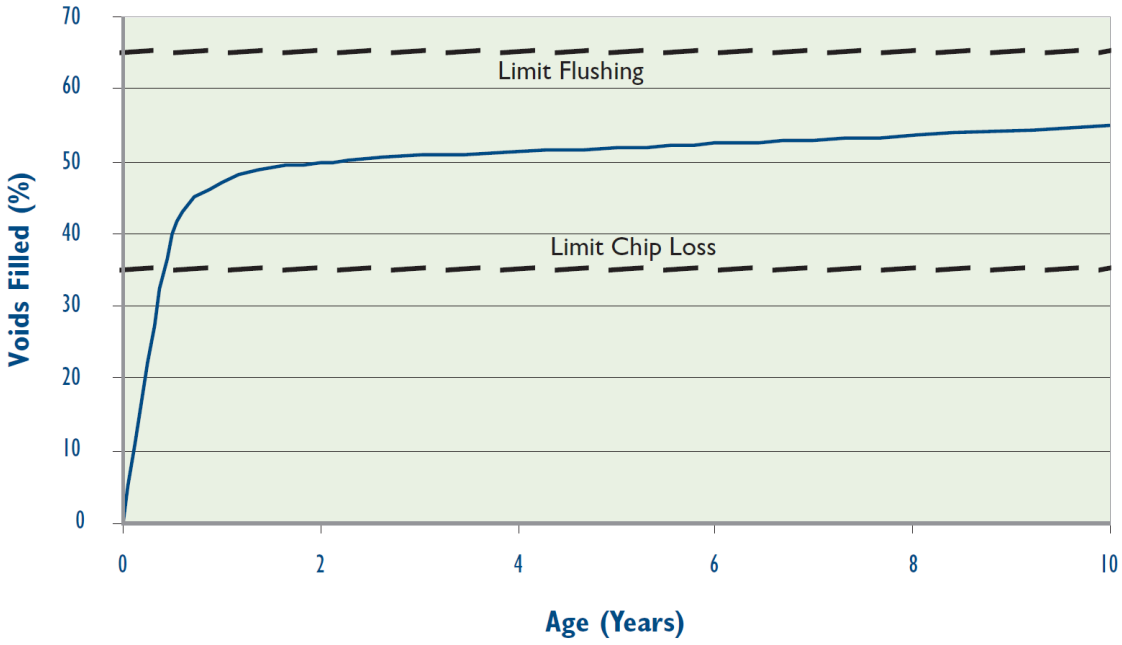

Figure 3.8: Proportion of Voids Filled with Binder with Respect to Time

This design philosophy requires the binder to fill at least 35% of the total volume of voids before the first cold. It is required to construct the surface treatments in the middle of the seal coating season with at least 100 days to spare until the first major frost happens.

The previous derivation of the volume of voids was adopted as shown below:

$$\frac{V_V}{ALD} = 0.83 - 0.07 \times \log(elv)$$

The total volume of voids in the seal structure shown in Figure 3.9 is given by:

$$V_V = V_B + V_A + V_E$$

Where V_V is the total volume of voids, V_B is the volume of binder, V_A is the volume of air, and V_E is the volume of aggregate embedment. Accordingly, the volume of voids and the volume of binder can be expressed as:

$$V_V = ALD \times (0.83 - 0.07 \times \log(elv))$$

$$V_B = 0.35 \times V_V = 0.35 \times ALD\big(0.83 - 0.07 \times \log(T \times 100)\big)$$

$$V_B = ALD\left(0.291 - 0.025 \times \log(T \times 100)\right)$$

Where T is the equivalent light vehicles per lane per day.

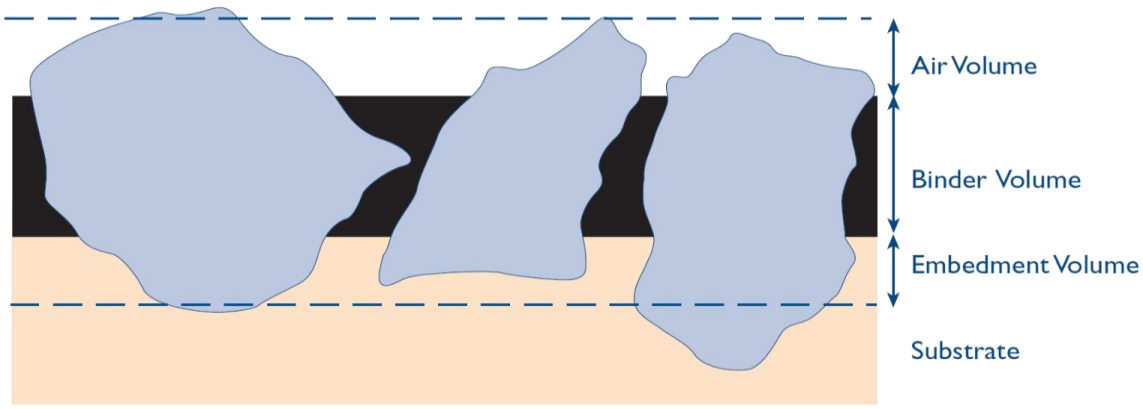

Figure 3.9: Components of the Volume of Void in Aggregates

The impact of HCVs on binder application rate is considered in determining T as follows:

$$T = elv = ADT \times (1 + 0.09 \times p)$$

Where p is the percentage of heavy commercial vehicles (HCV) and ADT is the average daily traffic in vehicle per day per lane.

At 11% heavy commercial vehicles, $T = 2 \times ADT$

The volume of binder then becomes:

$$V_B = ALD\left(0.291 - 0.025 \times \log(2 \times ADT \times 100)\right)$$

This represents the basic volume of binder needed for a generic pavement section. A set of adjustments is needed to cater for differing site-specific conditions. The amount of binder should take into account additional allowance for the existing surface texture that increases the estimate of the ALD. On the other hand, the aggregate chips might not lie on the existing surface but embeds the existing texture. Hence, the assumption of chip embedment being almost 30% of the texture depth comes into place. Thus 70% of the mean texture

depth (MTD) is added to the average least dimension of the aggregate to increase the BAR when accounting for texture. Hence the BAR becomes:

$$V_B = (ALD + 0.7MTD)\left(0.291 - 0.025 \times \log(2 \times ADT \times 100)\right)$$

Additionally, a series of five site-specific adjustments are considered. First, soft substrates, i.e. existing pavement surface, affect the binder content. The ball penetration test is used to assess the hardness of the pavement by measuring the penetration into the road under a standard impact load. This test simulates the embedment of aggregate chips into the existing pavement after trafficking. Based on the South African seal design method, an adjustment for substrate hardness can be made by changing the ALD of the chip in the algorithm as tabulated in Table 3.10.

Soft Substrate Adjustment (Ball Penetration Test)				
Ball Penetration	$\leq$ 1mm	1 – 3 mm	3 – 4 mm	> 5mm
ALD adjustment	+ 1 mm	-	- 1 mm	Not suitable

Table 3.10: Soft Substrate Adjustment for Different Ball Penetration Values

Second, absorptive surfaces are considered. As no method is available for assessing the degree of absorption, the preferred procedure is to seal the surface first with a small chip. If this is not possible, the basic binder application rate could be increased in the order of 0.1 to 0.2 L/m^2 upon the discretion of the engineer. Third, steep grades are evaluated suggesting that on steep uphill grades slow-moving heavy vehicles can cause premature flushing. Accordingly, a reduction of 0.1 to 0.15 L/m^2 in binder application rate for these areas is commonly used to minimize the chance of binder pick-up from the truck tires, which causes tracking and potential flushing of the surface. The impact the chip shape has on the volume of voids, and thereby the BAR, is studied. Chip shape is controlled by a

minimum ratio of ALD-to-AGD of 1:2¼; where, AGD is the average greatest dimension of the aggregate. Some aggregate crushing systems can result in more cubical chip with ratios less than 1:2. Consequently, the binder application rate needs to be increased accounting for the higher volume of voids. Typically, the application requires up to 10% extra binder for chips with more cubical shapes. Finally, urban and low traffic volume reseals are considered. According to expert experience, these seals suffer from chip loss along centerlines. Chip loss can be solved by increasing binder application rates by 10% and up to 20%. In areas with higher traffic volumes, the addition of binder reduces the seal life because flushing may occur along the wheel-paths. Different application rates are recommended if logistically possible. Hence, the final binder application rate adds up to:

$$\mathrm{BAR} = (\mathrm{ALD} + 0.7 \times \mathrm{MTD}) \times \left(0.291 - 0.025 \times \log(2 \times \mathrm{ADT} \times 100)\right) + \mathrm{As} + \mathrm{Ss} + \mathrm{Gs} + \mathrm{Cs} + \mathrm{Us}$$

Where As is the allowance for an absorptive surface, Ss is that for a soft substrate, Gs for steep grade, Cs for chip shape, and Us for urban and/or low traffic volumes.

On the other hand, the aggregate application rate is expressed in m^2/m^3 that is relevant to the area covered with a truck load of aggregates of a certain capacity in m^3. The voids on a lightly-trafficked road are likely to be around 40% after two years. This equates to a chip application rate of approximately $\frac{830}{\mathrm{ALD}}$ m^2/m^3. If the thickness of a seal is equal to ALD, then the volume required to seal one m^2.

$$\mathrm{V_T} = \frac{\mathrm{ALD}}{1000} \quad (\mathrm{m^3/m^2})$$

The total seal volume consists of the volume of solids and the volume of voids. Hence, the volume of solids can be determined as follows:

$$\mathrm{V_S} = (1 - \mathrm{V_V}) \times \frac{\mathrm{ALD}}{1000} \quad (\mathrm{m^3/m^2})$$

Where (1 – Vv) is the proportion of solids in the seal coat system.

Hanson has proven that chips in their bulk loose nature have a void content of approximately 50%. Since this is the state in which the aggregates get delivered to the jobsite in trucks, the loose volume of chips needed is:

$$V_{L(\text{Loose Chips})} = 2 \times (1 - V_V) \times \frac{\text{ALD}}{1000} \quad (m^3/m^2)$$

The AAR is determined as the reciprocal of V_L as follows:

$$\text{AAR} = \frac{1000}{2 \times \text{ALD} \times (1 - V_V)} \quad (m^2/m^3)$$

Hanson's research indicated that the voids in a compacted seal are approximately 20%. This allows replacing the V_V in the previous equation by 0.2 as follows:

$$\text{AAR} = \frac{1000}{2 \times \text{ALD} \times 0.8} = \frac{1000}{1.6\ \text{ALD}} = \frac{625}{\text{ALD}} \quad (m^2/m^3)$$

It is recommended to allow for up to 10% additional aggregates for whip-off leaving the previous AAR estimate at $\frac{625}{\text{ALD}}$. Unfortunately, there is no consensus on the appropriate aggregate application rate that needs to be applied. In 2001, Alderson indicated that an application rate of $\frac{900}{\text{ALD}}$ appears to be appropriate for most seal coats ensuring that the excess chips applied quickly disappears by whip off (Alderson A. , 2001). The sealing manual published in 1993 also recommends using a rate of $\frac{900}{\text{ALD}}$ (Major, 1993). Other professionals suggest using a rate of $\frac{750}{\text{ALD}}$ for single seal coats using aggregates between Grades 2 and 4 allowing for 10% whip-off and providing a uniformity of spread. The recommended aggregate grades are presented in Table 3.11.

The aggregate chips used for surface treatment are required to be derived from high quality natural rock or stone. Near single-sized crushed aggregate meeting the criteria for sealing chips are required per the TNZ M/6 specification (Transit NZ, 2002).

Grade	ALD (mm)	% of LD within 2.5 mm of ALD	AGD/ALD Ratio	% passing Sieve #4	% with at least two broken faces
2	9.5 – 12	Min 65%	Max 2.25	1.1	Min 98%
3	7.5 – 10	Min 70%	Max 2.25	1.1	Min 98%
4	5.5 – 8	Min 75%	Max 2.25	1.1	Min 98%

Table 3.11: Aggregate Gradation for New Zealand Seal Coat

AUSTRALIAN DESIGN METHOD (ALDERSON A. , 2006)

The Australian design philosophy is based on the concept originally proposed by Hanson in 1935, which states that achieving a satisfactory sprayed seal, the voids within the sealing aggregate mosaic should be filled to about one-half to two-thirds with binder. Adjustments for differing aggregate shape and traffic are applied to develop a basic binder application rate. To this rate, further allowances are applied to cater for the surface texture of the underlying substrate, embedment of the seal into it, and any binder absorbed by either the sealing aggregate or the underlying substrate.

Traffic data is crucial for this design method as it is one of the main components that affect the embedment of the aggregate in the seal coat layer. Traffic counts from the site or areas near the site are used to represent the traffic distribution that would be experienced when the seal coat is open to traffic. Traffic volume is collected as annual average daily traffic (AADT) which considers carriageway (divided or undivided), direction of traffic, number of lanes, and percentages of traffic within each lane. Separate designs are required for lanes with different traffic volumes or different load distributions. Following general guidelines, typical traffic volumes are characterized as follows:

- Very Low ≤ 200 v/l/d
- 201 v/l/d ≤ Low ≤ 750 v/l/d
- 751 v/l/d ≤ Medium ≤ 2000v/l/d
- High ≥ 2000 v/l/d

Traffic needs to be proportioned to each lane for single carriageway, i.e. when no physical separation between opposite bounds exists, and for each carriageway for dual carriageways as indicated in Table 3.12 (Alderson A. , 2006).

Width of seal (m)	Estimated Design Traffic (v/l/d)	Comment	
3.7 - 5.6	AADT	Seal width is considered too narrow for 2 lanes	
6.2 - 7.4	½ × AADT	Traffic is considered to predominantly travel in distinct lanes on seals of this width, especially if the centre line and/or lanes are line marked	
Sealed shoulders, parking lanes, identified by edge line marking to be separate from the traffic lanes	adopt < 50	If not line marked, some of the traffic may wander onto the shoulder and < 50 v/l/d may not be appropriate. If in doubt, a traffic count should be conducted.	
Overtaking lanes (in one direction)			
left hand lane (3.7m)	60–80% of ½ × AADT	Determine % of HV for each lane as a proportion of the total traffic volume in that lane.	If in doubt, arrange a traffic count for each lane
right hand lane (3.7 m)	20–40% of ½ × AADT		
Single lane in opposite direction	½ × AADT	%HV same as in AADT	
On and off ramps on freeways or urban road systems	Traffic volumes (AADT) before and past the ramp, may provide a good indication of AADT on ramp. Otherwise, arrange a traffic count. Traffic volume on the road connected to the ramp may also provide additional useful information to determine AADT on the ramp.		
Service roads to major roads	For one-way traffic, the Design Traffic is equal to the AADT For two way traffic use ½ AADT	AADT refers to traffic using the service road only. If not available arrange a traffic count..	

Lane (assumed 3.7m wide)	Estimated Design Traffic (v/l/d)	Comments	
Multi lane, heavily trafficked	½ AADT divided by the number of lanes in the carriageway OR ½ AADT x % traffic in each lane	These roads are usually in urban areas or linking major centres. Traffic volume is often > 2000 v/l/d in all lanes but the % heavy vehicles may vary between lanes.	
2 lane carriageway			
left hand (outer) lane	60 to 80% of ½ AADT	60% for urban / 80% for rural	Each carriageway = ½ AADT
right hand (inner) lane	40 to 20% of ½ AADT	40% for urban / 20% for rural	
Sealed shoulders, Parking lanes identified by edge line marking to be separate from the traffic lanes	adopt < 50	On some busy roads, trucks may tend to travel partially on the shoulder, and this must be taken into account. A traffic count should be conducted, and/or traffic pattern determined.	
Where two lanes merge into one (at end of a duplicated section)	½ AADT	Merged traffic is ½ AADT, but design of binder application rates and layout of sprayer runs within the merge area require particular care.	
Off and on ramps	% of ½ x AADT	If actual traffic counts are not available for ramps, traffic on the side road, before and past the ramp, may provide an indication of the traffic volume using the ramp.	

Table 3.12: Estimation of Design Traffic for Single and Dual Carriageways

The data is divided between light and heavy vehicles where the heavy vehicles are those above 3.5 metric tons. The equivalent heavy vehicles (EHV) metric is used to determine the adjustment to the basic voids factor for traffic and is calculated as follows:

$$(\text{EHV})\% = \text{Heavy Vehicle } \% + \text{Large Heavy Vehicle}\% \times 3$$

$$\text{Equivalent Light Vehicles (ELV)} = \text{Light Vehicles} + 10 \times \text{EHV}$$

Surface treatment work should not be done shortly before special events such as: seasonal touristic peaks, holidays, grain harvest, specific events (such as marathons or sport games), construction, maintenance and rehabilitation work nearby because unprecedented traffic is likely to lead to premature surface treatment failure. When treating roads that provide access to quarries or mining locations, heavy and large heavy vehicles are expected to use these roads. Adjustments are need for the binder application rate as follows:

1. Determine the equivalent number of heavy vehicles (HV + 3.0 × LHV),
2. Factor the Equivalent Number of Heavy Vehicles by 10 then add the actual number of light vehicles to determine a nominal design traffic volume, and
3. Select a basic voids factor based on this nominal traffic volume.

When using this procedure, additional reductions in voids factor of up to 0.02 $L/m^2/mm$ should be made for channelized or slow-moving vehicles.

Unique to the Australian design method are the specifications for varying seal coat sizes. There are separate designs for seals 10 mm and larger and seals 7 mm and smaller. Further designs are provided for variations in the single design procedure using polymer modified binders and bitumen emulsion binders.

Design Philosophy for 10 mm seals

The 10 mm and larger seals require uniformly graded aggregates that need to be spread consistently in a one-stone thick layer. The average least dimension (ALD) becomes an important factor in this design method because it affects the calculation of the total voids. Aggregate particles will tend to lie on their flattest side with the least dimension being the vertical dimension. The extent of reorientation of the aggregates is less at low traffic volumes resulting in greater random orientation of aggregate particles and greater void volume. The ALD is used to calculate both the BAR and AAR. The design procedures

assume that, for seals 10 mm and larger, only a single layer of aggregate particles adheres to the binder film. The void space is obtained from the aggregate application rate (AAR) and dictates the binder application rate (BAR) as shown in Figure 3.10.

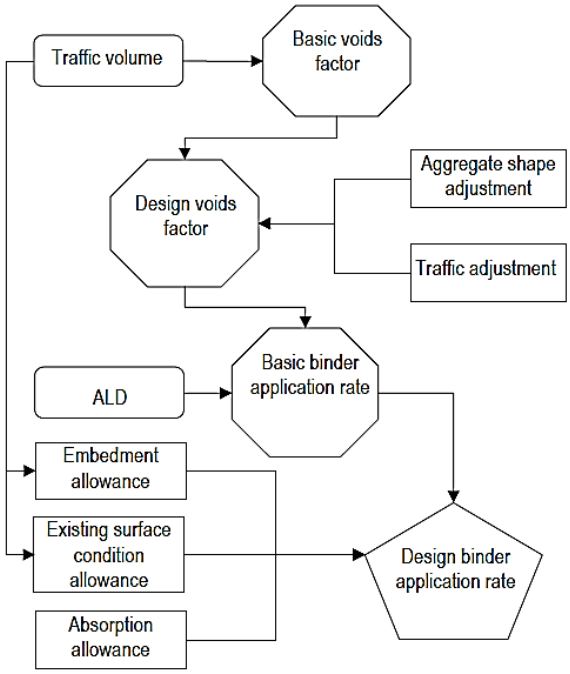

Figure 3.10: BAR Design Flow Chart (Alderson A. , 2001)

Some additional requirements are the considerations for traffic and whip-off. The average annual daily traffic indicates the traffic volume for which the seal coat will be designed. Regarding whip-off, there is no additional allowance in the AAR. After compaction by rolling and trafficking, an aggregate layer typically has 40 to 60% voids. The binder layer should reach at least 35% of the aggregate layer height after construction and opening to traffic and is expected to reach 50 to 65% after two years of trafficking. The proportion of voids to be filled with binder may vary to optimize requirements such as surface texture,

and maximum seal life. For specific applications such as non-traffic areas, a minimum texture is generally required for skid resistance.

The main design objective is that two years after construction, the binder should cover 50 to 65% of the seal coat mat layer, that is the height of the aggregate layer. The binder application rate (BAR) is a function of: (1) aggregate size, (2) aggregate shape, (3) orientation of the aggregate particles, (4) embedment of aggregate into the base, (5) texture of the existing surface onto which the seal is being applied, (6) absorption of binder into either the (6a) pavement or (6b) aggregate, the (7) traffic volume and (8) nature of the traffic. All application rates determined by this method are expressed in L/m^2 of residual binder at the standard reference temperature of 15°C [59°F].

The basic seal design requires one-sized aggregates with a flakiness of 15 to 25% for an area with traffic volume having less than 10% heavy vehicles. A design flowchart is presented in Figure 3.11 (Alderson A. , 2006) to outline a summary of the whole process. First, a range for the basic voids factor, V_f, is determined as function of traffic. This factor has been developed for an average mix of light and heavy vehicles in a free traffic flow situation. Figure 3.12 shows the charts that are used to determine the range. After determining the basic void factor, the design voids factor, V_F, is determined in $L/m^2/mm$ by adjusting the basic void factor, V_f, to account for abnormal aggregate shape, V_a, and the effect of traffic, V_t. The adjustment for aggregate shape, V_a, is presented in Table 3.13. When the initial traffic assumption is not correct, an adjustment, V_t, needs to be made to compensate for variations in the traffic composition, in particular for non-trafficked areas, overtaking lanes with few heavy vehicles or for large proportions of heavy vehicles, channelization or concentration of traffic, and slow-moving heavy vehicles in climbing lanes or stop/start conditions. Table 3.14 presents adjustment factors for traffic effects.

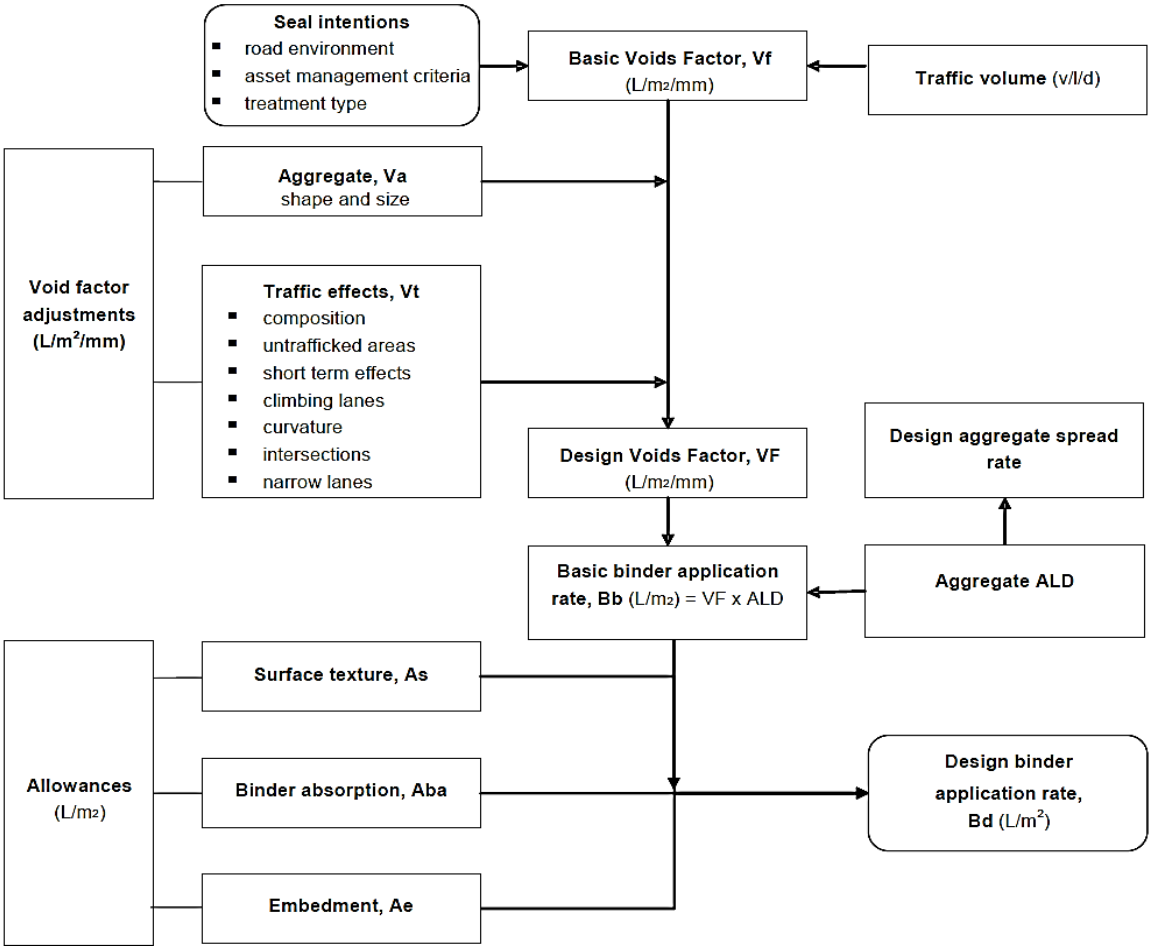

Figure 3.11: Design Process for Seal Coats with Aggregates Greater than 10 mm

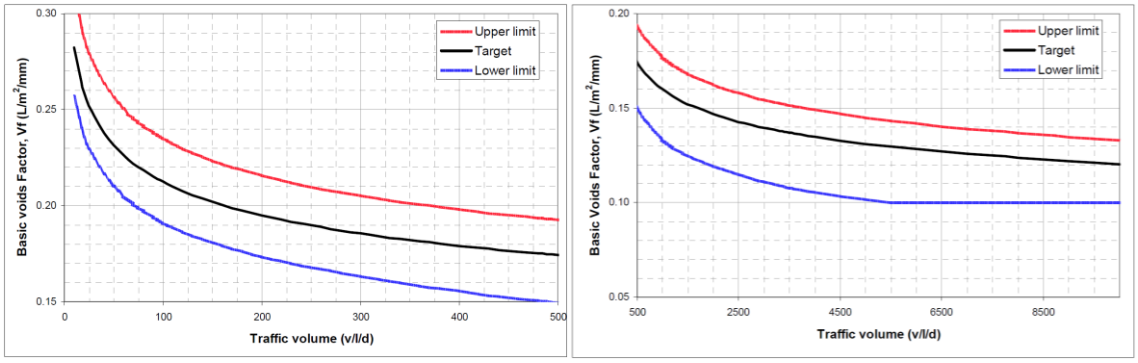

Figure 3.12: Basic Void Factor for Different Traffic Volumes

Aggregate type	Aggregate shape	Flakiness index (%)	Shape adjustment Va (L/m²/mm)
Crushed or partly crushed	Very flaky	> 35	Considered too flaky and not recommended for sealing
	Flaky	26 to 35	0 to - 0.01
	Angular	15 to 25	Nil
	Cubic	< 15	+ 0.01
	Rounded	n.a	0 to + 0.10
Not crushed	Rounded	n.a	+ 0.01

Table 3.13: Adjustment to Basic Voids Factor for Aggregate Shape, V_a

Traffic	Adjustment to Basic Voids Factor (L/m²/mm)			
	Flat or downhill		Slow moving – climbing lanes	
	Normal	Channelised*	Normal	Channelised*
On overtaking lanes of multi-lane rural roads where traffic is mainly cars with ≤10% of HV	+0.01	0.00	n.a.	n.a.
Non-trafficked areas such as shoulders, medians, parking areas	+0.02	n.a.	n.a.	n.a.
0 to 15% Equivalent Heavy Vehicles (EHV)	Nil	-0.01	-0.01	-0.02
16 to 25% Equivalent Heavy Vehicles (EHV)	-0.01	-0.02	-0.02	-0.03
26 to 45% Equivalent Heavy Vehicles (EHV)	- 0.02	- 0.03	- 0.03	- 0.04**
> 45% Equivalent Heavy Vehicles (EHV)	- 0.03	- 0.04**	- 0.04**	- 0.05**

N/A Not applicable

EHV Equivalent Heavy Vehicles, includes both Heavy Vehicles and Large Heavy Vehicles × 3 (See Section 1.5.4).

* Channelisation - a system of controlling traffic by the introduction of an island or islands, or markings on a carriageway to direct traffic into predetermined paths, usually at an intersection or junction. This also applies to approaches to bridges and narrow culverts.

** If adjustments for aggregate shape and traffic effects result in a reduction in Basic Voids Factor of 0.4 L/m2/mm or more, special consideration should be given to the suitability of the treatment and possible selection of alternative treatments.Note that the recommended MINIMUM Design Voids Factor is 0.10 L/m2/mm in all cases.

Table 3.14: Adjustment for Traffic Effects

The design void factor, V_F, rounded to the nearest 0.01 L/m^2/mm is calculated as:

$$V_F = V_f + V_a + V_t$$

Following, the basic binder application rate is calculated to the nearest 0.1 L/m^2 as:

$$BAR_{Basic} = V_F \times ALD$$

Where ALD is the average least dimension in mm. Afterwards, a set of allowances is applied to adjust the basic binder application rate (L/m^2). First, a surface texture allowance,

As, is determined after assessing the surface texture based on the sand patch test method as summarized in Table 3.15 (Alderson A. , 2006). It is recommended to sample the texture measurements every 400 to 500 m.

Aggregate size of proposed seal	Measured texture depth (mm)	Surface texture allowance (L/m²)	Aggregate size of proposed seal	Measured texture depth (mm)	Surface texture allowance (L/m²)
Existing: 14, 16 or 20 mm seal			**Existing: 5 or 7 mm seal**		
5 or 7 mm	0 to 0.3	**Note 1**	5 or 7 mm	0 to 0.3	**Note 1**
	0.4 to 0.6	**Note 2**		0.4 to 0.9	+0.1
	0.7 to 0.9	+0.1		1.0 to 1.5	+0.2
	1.0 to 1.3	+0.2		1.6 to 2.2	+0.3
	1.4 to 1.9	+0.3		2.3 to 3.2	+0.4
	2.0 to 2.9	+0.4		>3.2	+0.5
	>2.9	+0.5	10 mm	0 to 0.3	**Note 1**
10 mm	0 to 0.3	-0.1		0.4 to 0.7	+0.1
	0.4 to 0.5	0		0.8 to 1.1	+0.2
	0.6 to 0.7	+0.1		1.2 to 1.8	+0.3
	0.8 to 0.9	+0.2		>1.8	**Note 3**
	1.0 to 1.3	+0.3	14 mm	0 to 0.2	**Note 1**
	1.4 to 1.8	+0.4		0.3 to 0.6	+0.1
	>1.8	**Note 3**		0.7 to 0.9	+0.2
14 mm	0 to 0.3	-0.1		1.0 to 1.4	+0.3
	0.4 to 0.5	0		1.5 to 2.0	+0.4
	0.5 to 0.6	+0.1		>2.0	+0.5
	0.6 to 0.7	+0.2	**Existing: asphalt/slurry surfacing**		
	0.8 to 0.9	+0.3	All	0 to 0.1	0
	1.0 to 1.3	+0.4		0.2 to 0.4	+0.1
	1.4 to 1.8	+0.5		0.5 to 0.8	+0.2
	>1.8	**Note 3**		0.9 to 1.4	+0.3
Existing: 10 mm seal				>1.4	+0.4
5 or 7 mm	0 to 0.3	**Note 1**			
	0.4 to 0.9	+0.1			
	1.0 to 1.4	+0.2			
	1.5 to 2.0	+0.3			
	2.1 to 2.7	+0.4			
	>2.7	+0.5			
10 mm	0 to 0.3	**Note 1**			
	0.4 to 0.7	+0.1			
	0.8 to 1.1	+0.2			
	1.2 to 1.7	+0.3			
	>1.7	**Note 3**			
14 mm	0 to 0.2	**Note 1**			
	0.3 to 0.6	+0.1			
	0.7 to 0.9	+0.2			
	1.0 to 1.2	+0.3			
	1.3 to 1.7	+0.4			
	>1.7	**Note 3**			

Notes:

1. Embedment considerations dominant
2. Specialised treatments necessary
3. This treatment might not be advisable depending on the shape and interlock of aggregates so alternative treatments (surface enrichment, small size seal or others) should be considered
4. For application of aggregate sizes greater than 14 mm, adopt allowances applicable to 14 mm aggregate.

Table 3.15: Surface Texture Allowance for Existing Surface

The embedment allowance accounts for the voids lost due to the aggregate being forced into the existing surface. The depth of embedment depends on the hardness of the surface being sealed and nature of the passing traffic. Premature embedment problems are recognized when the wheel paths fill up with binder in a very short period of time after construction while the rest of the seal remains coarser textured. In order to test the hardness of the existing surface, a ball penetration test is conducted in accordance with Austroads Test Method AG:PT/T251 (Austroads, 2010). Figure 3.13 shows the recommended embedment adjustments as a function of traffic volume and the ball penetration values.

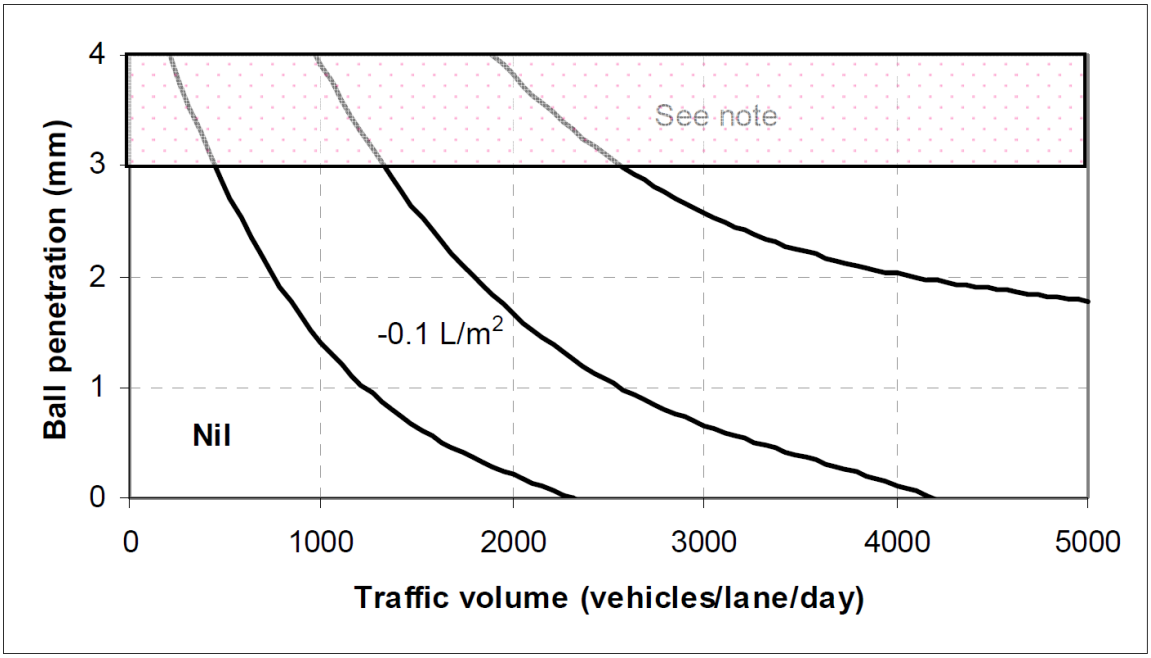

Figure 3.13: Embedment Allowance

If the ball penetration value exceeds 3 mm, it is recommended to either use a different surface treatment other than the seal coat or to take other precautions to treat the surface hardness beforehand. Detailed description of these remedies are provided in the original

Australian design manual (Alderson A. , 2006). For unusually absorptive pavement surfaces, long-term absorption of the binder into the base course can occur. The allowance for this generally ranges between +0.1 to +0.2 L/m^2. Where more than 0.2 L/m^2 is required, an alternative treatment should be considered. It is strongly recommended that all new pavement surfaces be primed or primer-sealed. However, in some areas a seal is applied directly to the prepared granular pavement and the following binder absorption allowances provide a guide for use in these situations:

- For granular unbound pavements allow +0.2 to +0.3 L/m^2
- For pavements using cementitious binders allow +0.1 to +0.2 L/m^2
- For bitumen stabilized pavements allow -0.2 to 0.0 L/m^2
- For the use of chemical binders, refer to Austroads publication Series Part 4D

Another issue that could arise is the absorption of the binder into particularly absorptive aggregates. These aggregates fall into two general categories:

- Porous, e.g. sandstone, rhyolite, etc.
- Vesicular or full of cavities, e.g. scoria, slags, etc.

In general, binder absorption into aggregate is not common, but if an allowance is required, it does not usually exceed 0.1 L/m^2. After determining the allowances that are required to cater to local site-specific conditions, the binder application rate is determined as:

$$\mathrm{BAR} = \mathrm{BAR}_{\mathrm{Basic}} + \mathrm{Allowances}$$

On the other hand, the amount of aggregate required in a seal coat for 10 mm or larger aggregates is determined based on the average least dimension (ALD) of these aggregates. Traffic usually impacts the compaction of the aggregates. Accordingly, the application rate is estimated as:

For Traffic > 200 v/l/d $\quad \mathrm{AAR} = 900/\mathrm{ALD}$

For Traffic < 200 v/l/d $\quad \mathrm{AAR} = 850/\mathrm{ALD}$

To achieve a satisfactory aggregate mosaic, the actual spread rates are varied in practice by as much as ±10 m^2/m^3 from the design spread rate. It is not required to add an additional allowance for whip-off. The Australian design method also allows for the use of emulsions and polymer modified binders that come with their own allowances.

Design Philosophy for 7 mm Seals

The 7 mm and smaller seals are popular for low to medium traffic. These seals have fewer requirements. The ALD is not determined because the aggregate layer can often be made of two or more aggregate particles in thickness. This treatment is an interim surfacing that is required to at least meet the existing texture until the placement of a more durable seal. A design flowchart is presented in Figure 3.14 to outline a summary of the process.

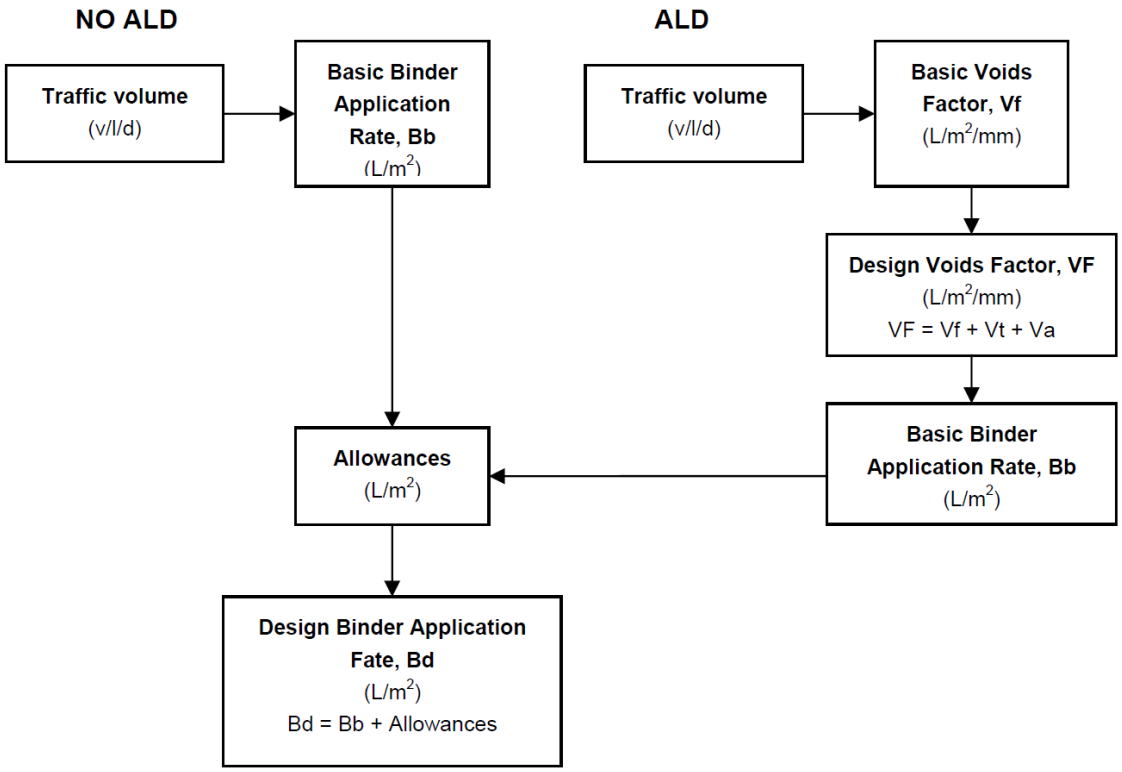

Figure 3.14: Design Process for Single Seal Coat with Aggregates Less than 7 mm

If the average least dimension is determined, the design procedure for aggregates 10 mm or larger is recommended. On the other hand, the basic binder application rate is determined relative to traffic as shown in the Table 3.16.

Traffic (v/l/d)	Basic Binder Application Rate, B_b (L/m^2)
< 100	1.0 – 0.8
100 – 600	0.9 – 0.7
601 – 1200	0.8 – 0.6
1201 – 2500	0.7 – 0.5
> 2500	0.5

Table 3.16: Basic Binder Application Rate for Aggregates 7 mm or smaller

It should be noted that the lower range of the basic BAR is selected for flaky aggregates (FI > 25%) or when traffic has 15% or more heavy vehicles. The higher basic binder application rates are used with more cubically shaped aggregates. If not certain of the site-specific conditions, the midpoint basic binder application rate is recommended.

Consequently, the AAR has a wide range depending on the seal objective as shown in Table 3.17. Lighter aggregate application rates are used in conjunction with light binder application rates to fill the spaces in a coarse-textured surface. Heavier aggregate application rates are applied where a completely interlocked aggregate layer is required.

Seal Aim	# aggregate thicknesses	Rate (m^2/m$^{3)}$
Normal ALD based design, small aggregate mosaic	1	900/ALD
Correction seal to fill a coarse-textured surface	2	260 – 290
Normal, small aggregate mosaic, no ALD	1 to 2	200 – 250

Table 3.17: Aggregate Application Rates with 7 mm or Smaller Aggregates

SOUTH AFRICAN DESIGN METHOD (SANRAL, 2007)

The South African National Roads Agency published the Design and Construction of Surfacing Seals (SANRAL, 2007). The manual provides guidelines for selecting the appropriate surface treatment based on the existing surface conditions. Following is a list of conditions that are deemed suitable for single seal coat layers:

- Traffic volume: It is expressed as equivalent light vehicle (elv) and determined as:

  $$\mathrm{ELV} = \mathrm{L} + 40\mathrm{H}$$

  Where L is the number of light vehicles and H is the number of heavy vehicles. Good-performing single seal coats are recommended for traffic volumes not exceeding 5,000 elv/lane/day.
- Turning action: Seal coats are deemed suitable for rural areas with occasional heavy vehicles and residentially developed areas.
- Gradient: Seal coats are recommended for roads with gradients up to 8%. Otherwise, climbing-vehicle's low speed and descending-vehicle braking actions would lead to premature distresses that affect the seal performance.
- Maintenance capability: Seal coats are deemed appropriate when road authorities have medium to high maintenance capabilities. High maintenance capability is defined as being able to perform any type of maintenance whenever needed; while, medium maintenance capability is when routine maintenance, patching, and crack sealing on regular basis are feasible.
- Surface texture requirement: High rough-textured surfaces are needed for rural high-speed roads and smooth-textured surfaces are desired in cities to facilitate road cleaning and minimize noise generation. There is a limit to the texture level that can be achieved with seal coats; the largest size of aggregate recommended is 13 mm.

- Availability of aggregate: Good quality aggregates are highly recommended. Such aggregates should be resistant to impact, abrasion, acid attack, etc.
- Construction techniques: The availability of adequate equipment and an experienced construction team has a crucial effect on the performance of the seal coat as the tolerance levels are very narrow.
- Environmental conditions: The prevailing temperature and moisture levels affect the binder grade choice and sealing window. Single seals are not recommended for roads that are subject to storm water due to high erosion and raveling risks.
- Quality of base: The condition and structural adequacy of the existing road dictates the performance of the surface treatment. Single seals are not recommended to be applied before fixing noticeable imperfections and distresses.
- Cost-benefit analysis & feasibility
- Other special conditions

In the South African design process, many different factors are considered including material properties, existing pavement and surface condition, road geometry, traffic, and climate. The performance of the seal coat is affected by the condition of the layers underneath the surface treatment. These layers serve as a support and provide the structural capacity to withstand loads. The base type provides the resistance of the seal coat embedment into the base, which is dependent on the type of material used and the degree of compaction. When a seal coat is laid over a weak base, the aggregates tend to embed into the existing layer, which, in turn, decreases the available voids and promotes bleeding. The cracks present within the old surface subject to treatment are expected to reflect upwards through the seal coat at a rate proportional to the traffic volume and loads. Hence, the condition of the existing surface dictates both the design and the expected performance of the seal coat treatment applied. This makes it vital to assess the condition of the existing

pavement before applying the preventative maintenance treatment. The assessment is required to account for specific conditions and correct the severe distresses that would tremendously affect the performance of the seal coat.

The aggregates used should conform to the recommendations of the COLTO (Committee of Land Transport Officials) specifications (COLTO, 1987) and comply with the requirements of SABS (South African Bureau of Standards) specification 1200 M (SABS, 1996). Such recommended factors include the grading, crushing strength, aggregate crushing value, 10% FACT Value, flakiness index, polished stone value, fines and dust content, adhesion and sand equivalent values. Table 3.18 provides grading requirements and properties of aggregates recommended to be used (SANRAL, 2007).

The ideal spread rates for aggregates vary in accordance with the seal type, shape of the aggregates, flakiness, and other specific consideration. It is recommended that the final aggregate application rate be determined by spreading a known volume of aggregates by hand on site. As shown in Figure 3.15, an approximate rate of spread for the aggregates is proposed based on the ALD and flakiness index.

Property	Grade of Aggregate	
	Grade 1	Grade 2 & 3
Flakiness Index [%] (max)		
19,0 mm nominal size	25	30
13,2 mm nominal size	25	30
9,5 mm nominal size	30	35
6,7 mm nominal size	30	35
10 % FACT [kN] (min)	210	210
Wet to Dry Ratio [%]	75	75
Aggregate Crushing Value (ACV) [%] (max)	21	21
Polished Stone Value (PSV) (min)	50	50

Sieve size (mm)	*Grade*	Percentage passing by mass						
		26,5 mm nominal size	*19,0 mm nominal size*	*13,2 mm nominal size*	*9,5 mm nominal size*	*6,7 mm nominal size*	*4,75 mm nominal size*	2,36 mm nominal size
37,50	Grades 1&2	100	-	-	-	-	-	-
26,50		85 - 100	100	-	-	-	-	-
19,00		0 - 30	85 - 100	100	-	-	-	-
13,20		0 - 5	0 - 30	85 - 100	100	-	-	-
9,50		-	0 - 5	0 - 30*	85 - 100	100	-	-
6,70		-	-	0 - 5**	0 - 30*	85 - 100	100	-
4,75		-	-	-	0 - 5**	0 - 30*	85 - 100	*100*
3,35		-	-	-	-	-	0 - 30	-
2,36		-	-	-	-	0 - 5**	0 - 5	*0 - 100*
	Grade 3	*Grading shall comply with the requirements for grades 1 and 2 with the following exceptions: * 0 – 50 ** 0 – 10*						
Fines content: Material passing a 0,425 mm sieve (max)	Grade 1	0,5	0,5	0,5	0,5	0,5	1,0	*15,0*
	Grade 2	1,5	1,5	1,5	1,5	2,0	2,5	*15,0*
	Grade 3	N/A	N/A	2,0	2,0	3,0	3,5	*15,0*
Dust content: Material passing a 0,075 mm sieve (max)	Grade 1	N/A	N/A	N/A	N/A	N/A	N/A	*2,0*
	Grade 2	0,5	0,5	0,5	0,5	1,0	1,0	*2,0*
	Grade 3	*N/A*	*N/A*	*1,5*	*1,5*	*1,5*	*1,5*	*2,0*

Table 3.18: Aggregate Gradation and Properties for Seal Coats

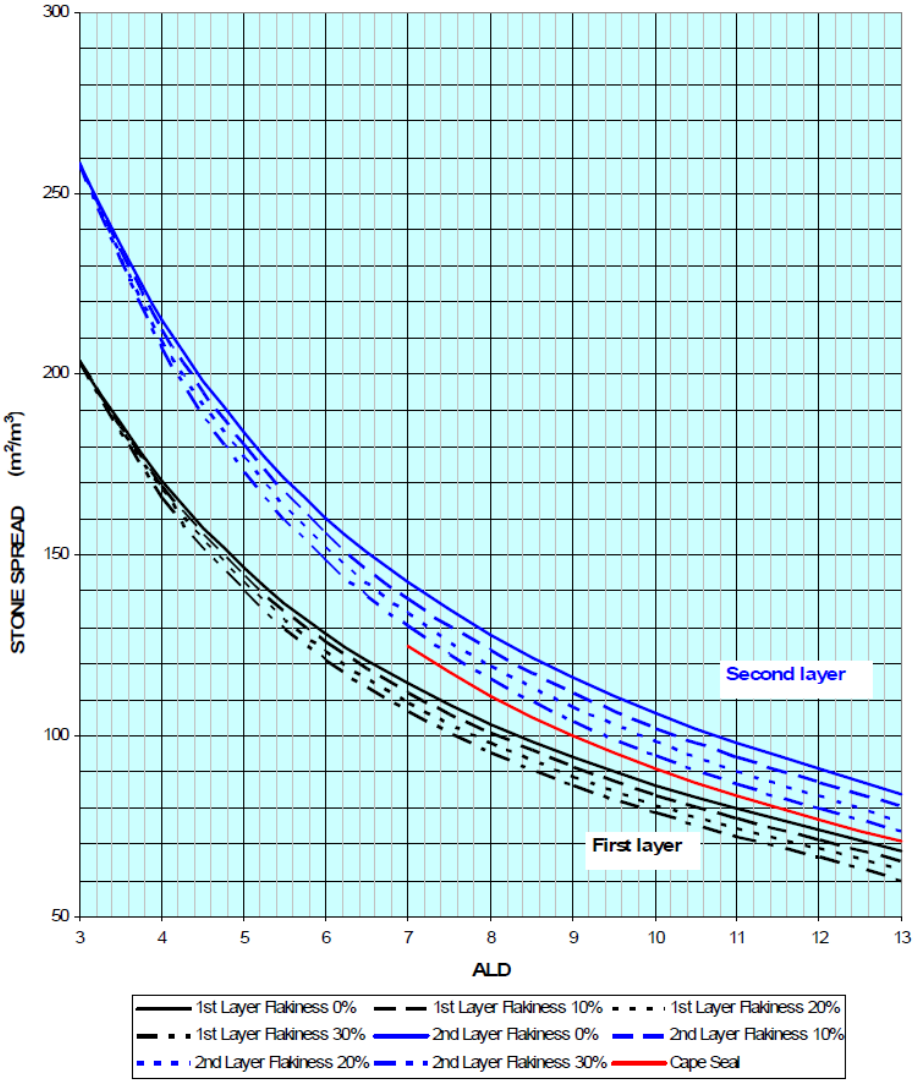

Figure 3.15: Approximate Spread Rates

The choice of the type of bituminous binder depends on the type and purpose of the seal, climatic conditions, durability of the binder and long-term performance, price of the binder at the time of application, convenience of application, compatibility with the aggregate, traffic, and road geometry. The South African single seal builds off Hanson's design method whereby the binder partially fills the voids in the aggregates. These voids are controlled by the average least dimension of the aggregates. The South African design

method further specifies that when there is no stone embedment into the existing surface, the minimum amount of voids to be filled with binder to prevent stone loss is 42%. It proposes a correlation between the voids, the hardness of the aggregates, and traffic where the amount of void loss due to traffic is dependent on the hardness of the aggregates and the traffic itself. It is specified that 0.7 mm of texture depth is required to provide adequate skid resistance. Hence, the effective layer thickness (ELT) is a function of the average least dimension.

$$\text{ELT} = 0.85679 \times \text{ALD} + 0.46715 \qquad \text{(mm)}$$

Where the percentage of void content in the aggregate layer is a function of the ELT

$$\text{Void \%} = 45.333 - 0.333 \times \text{ELT}$$

Figure 3.16 illustrates the principles for determining the void system in the seal coat aggregate matrix.

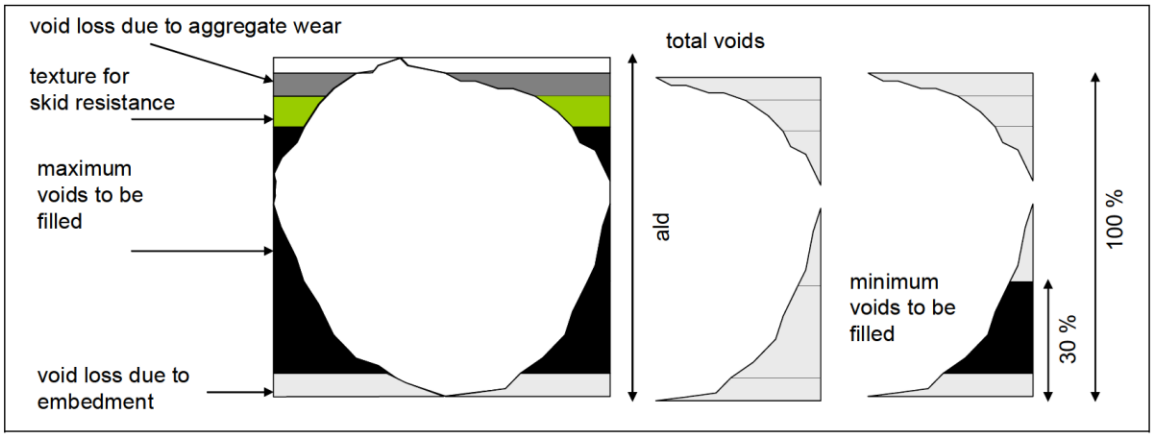

Figure 3.16: Void System (SANRAL, 2007)

After determining the size of aggregates to be used and the average least dimension, the traffic is assessed as equivalent light vehicle according to:

$$\text{ELV} = \text{L} + 40\text{H}$$

The embedment during construction is estimated as 50% of the ultimate embedment. The total aggregate embedment potential is obtained from the corrected ball-penetration test in accordance with TMH6 (Technical Methods for Highways) – Method ST4 (TMH, 1984).

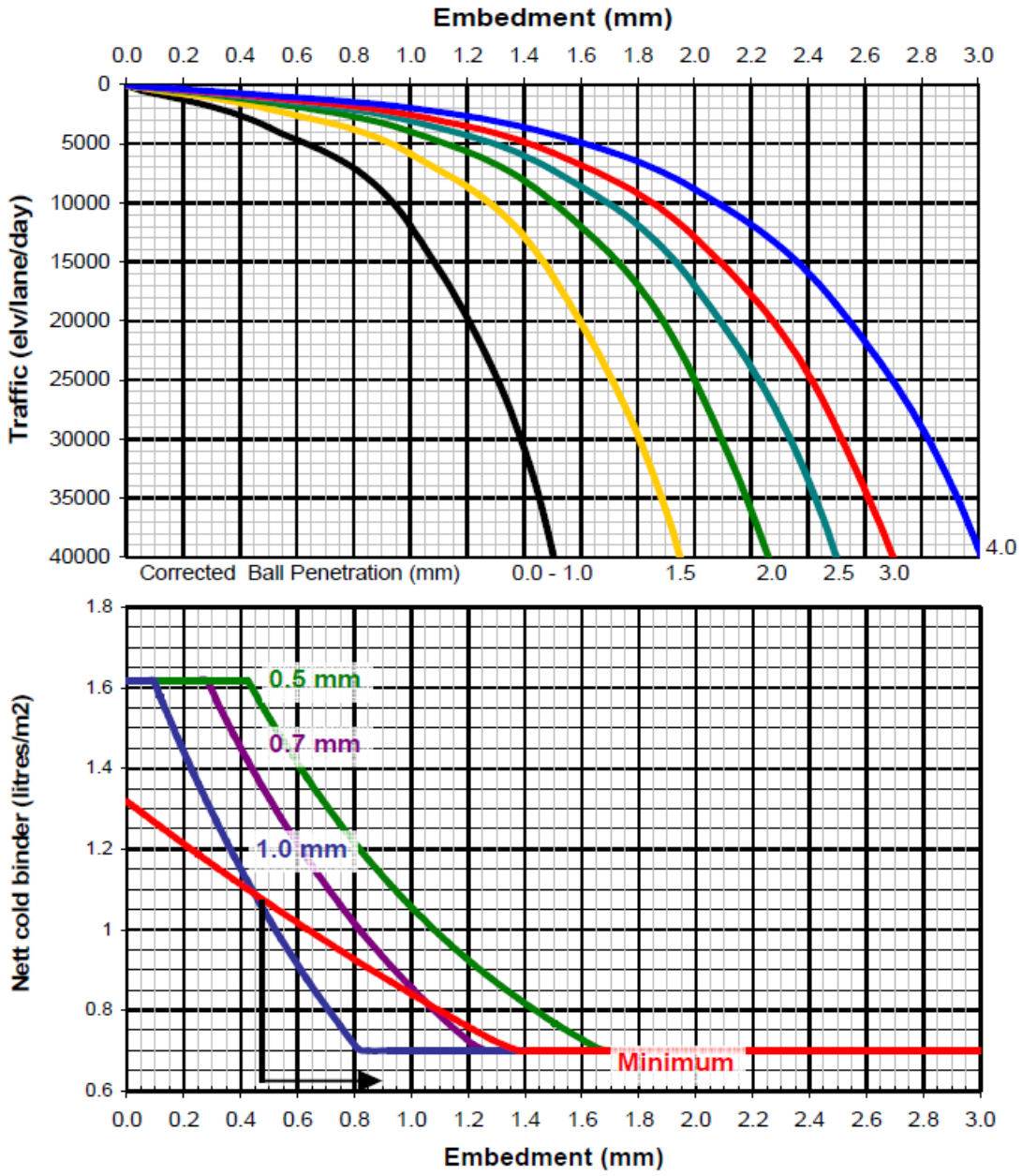

Figure 3.17: Design Chart for Aggregate with ALD of 8mm

Afterwards, a range for binder application rate is determined bestowing between to the minimum and the maximum tolerable dosages. The traffic estimation and surface penetration values allow the determination of an estimate for embedment which, in return, specifies the workable range for BAR for each specific ALD as shown Figure 3.17. Accordingly, the basic binder application rate is determined based on the required texture.

After determining the basic binder application rate, site-specific conditions should be identified in order to adjust the binder to meet the requirements. First when it comes to existing surface texture, three main factors are considered: (1) texture depth, (2) expected embedment of the chips, and (3) degree of cracking. As shown in Figure 3.18, the existing surface texture dictates the additional amount of binder required to fill the surface voids.

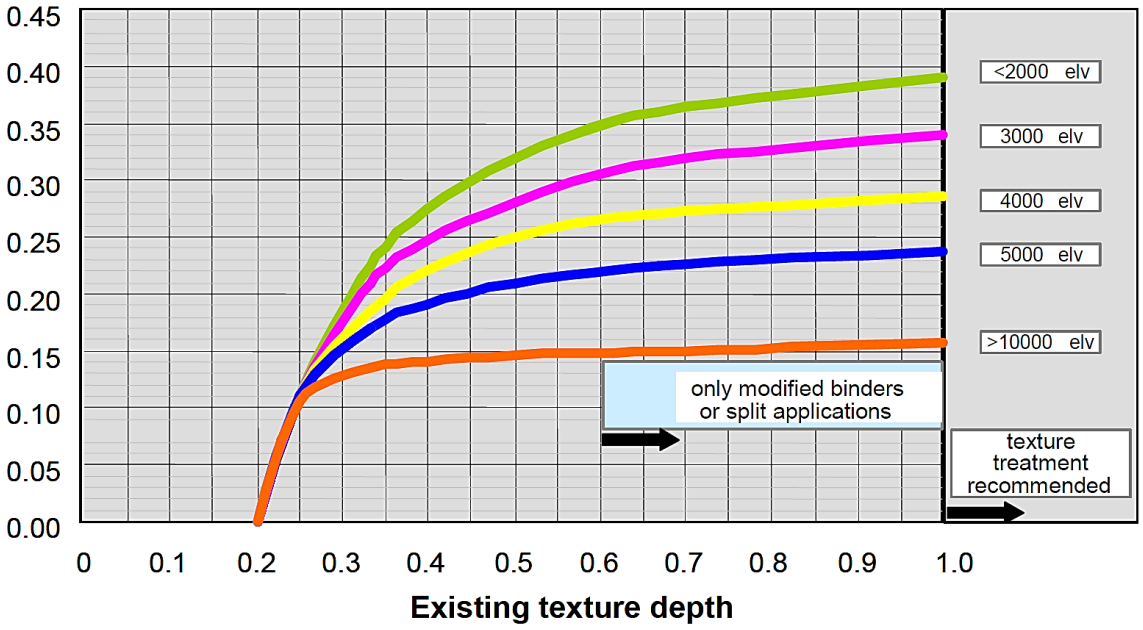

Figure 3.18: Binder Adjustment for Existing Surface Texture

Similarly, the embedment of the aggregates in the existing surface, which is assessed by the ball penetration test, provides an estimate of the total voids available after those lost

with aggregate embedment. Finally, cracking provides a better understanding of crack reflection into the new surface.

A main factor in the seal coat design for South Africa is the climate. The air and road temperatures are greatly affected by altitude, and there is a lot of variation in the duration of the sunshine in South Africa. Therefore, the country is divided into climatic regions for seal coat design defined by Weinert N-values:

$$N = 12 \times \frac{E_j}{Pa}$$

Where E_j is the evaporation during January and Pa is the total annual precipitation.
With conventional binder, the minimum application rates may be reduced by 10% in areas with N-values less than two and increased by 10% in areas with N-values greater than five.

When considering traffic, there are many related sub-factors to account for including the volume, loading, tire pressure, axles, speed, and traffic distribution. The volume of traffic affects the degree of compaction of the seal coat as well as contribute to the polishing of the aggregates. In terms of loading, heavy loads accelerate the process of embedment of the chips. The tire pressure also affects the degree of embedment and bleeding. The number and combinations of axles on large vehicles, such as tandem and tridem axles, can cause severe surface damage at intersections and curves and, therefore, must be accounted for in the seal coat design process. The speed of traffic on a particular road is an important factor in the design because slow moving traffic will compact the surface more than faster moving traffic due to the increased amount of time spent on a single location on the road. Finally, the traffic wandering distribution refers to the position of the vehicles on the road. Since cars tend to follow the wheel path, certain sections of the road are compacted more than others. The wandering effect also affects the compaction of the seal coat. In addition, heavy vehicles tend to select the slow-moving lane. Overall, the

binder application rate is reduced by 10% where heavy vehicles with low speeds are expected. Road geometry plays a major role in seal coat design because vehicles will interact differently with varying shapes and grades of pavement. Construction difficulties regarding steep grades could also affect the performance of the seal coat. In general, steep gradients, sharp bends, traffic circles, intersection, and areas with frequent stopping traffic impose a lot of stress and stress concentrations which cause damage in early seal coat life.

The aggregate application rate is another factor that could affect the binder application rate. For a medium-dense aggregate matrix shown in Figure 3.19, it is recommended to increase the BAR by 10% and by 20% for open shoulder to shoulder aggregate matrix.

Figure 3.19: Dense and Open Aggregate Matrices

When adjusting the basic BAR for site conditions, one should exercise caution with extreme cases that would lead to very low or very high rates. Very low rates are obtained from very high expected traffic, high ball penetration test, smooth texture, and low ALD. On the contrary high rates are obtained when the contrary cases align. In addition, practical measures should be considered regarding the feasibility of construction of the proposed design and the internal policies adopted by the agency.

BRITISH DESIGN METHOD (BATEMAN, 2016)

The British design method is described in the Design Guide for Road Surface Dressing (Bateman, 2016). Before designing the single seal coat system, it is important to identify whether the current roadway conditions are best suitable for a single seal coat or not. Figure 3.20 presents flow charts that provide different surface treatment recommendations for heavily and lightly trafficked road respectively (Bateman, 2016).

The primary design steps and principal variables include input data, surface dressing and binder types, polished stone value (PSV) of aggregates, aggregate size, rate of spread of binder, and adjustment to the rate of spread of binder for local conditions. The input data consists of surface temperature category, road hardness, traffic category, traffic speed, surface condition, and highway layout. The seal coat and binder types are a function of hardness category, traffic category, surface condition, highway layout, and season. PSV of aggregates entails the traffic category and highway layout. Aggregate size involves the hardness and traffic categories. The rate of spread of binder consists of hardness and traffic categories, traffic speed, surface condition, highway layout, and season. Finally, the adjustment to the rate of spread of binder for local conditions consists of traffic speed, season, surface condition, gradient, shade, local traffic, and change of chipping size. The design aims at achieving an acceptable texture depth after embedment and trafficking. At present, there is no definitive method to design for the macrotexture that will exist after embedment has taken place, but in-service texture depth requirements can be included in the job specifications. Another objective is to minimize tire/road noise by considering factors as the type of seal coat, selection of the type of component materials (binder and chippings), the rates of spread of binder and chippings, and local adjustments to those values along the site when conditions change.

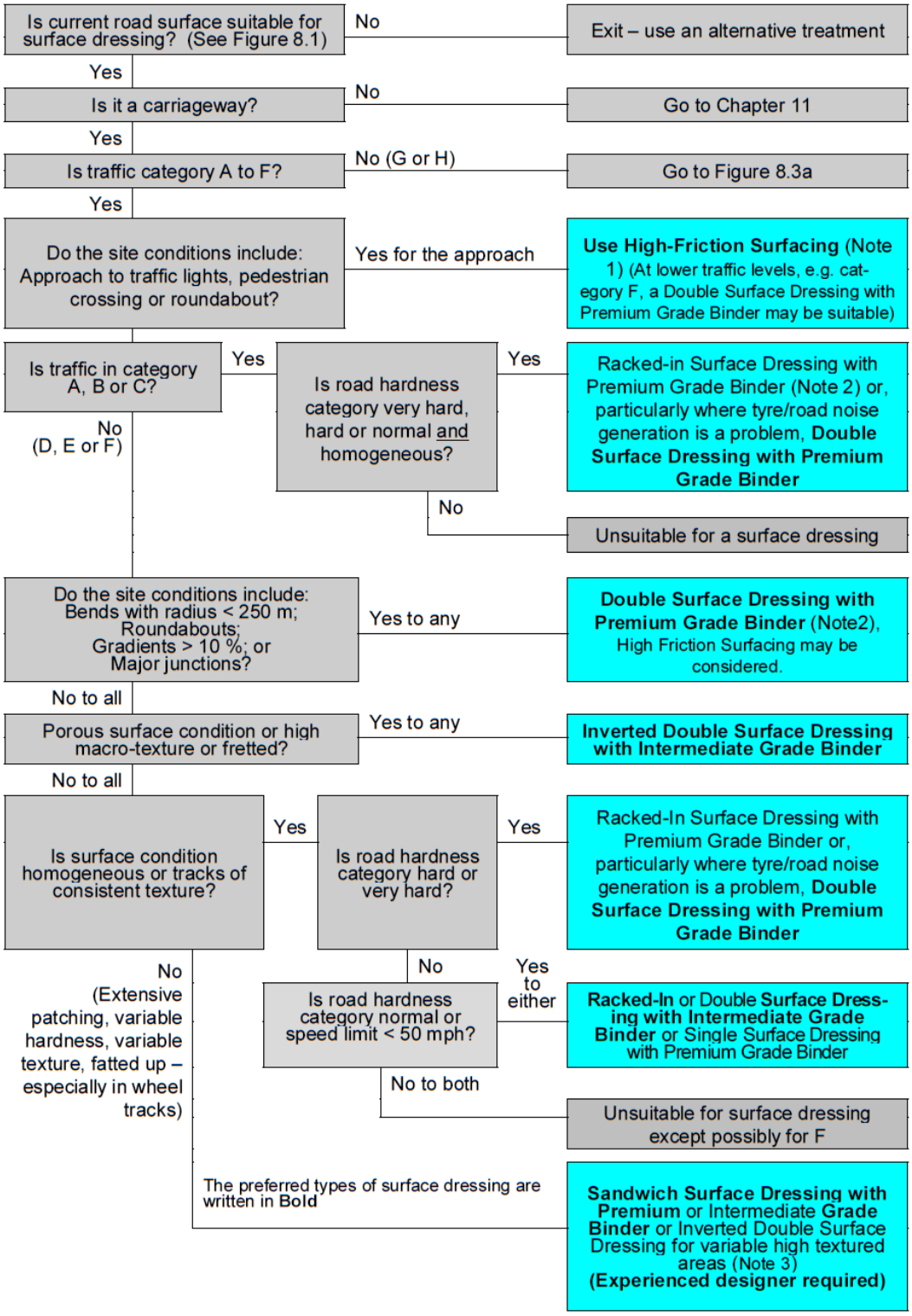

Figure 3.20: Surface Treatment Recommendations for Heavy and Light traffic

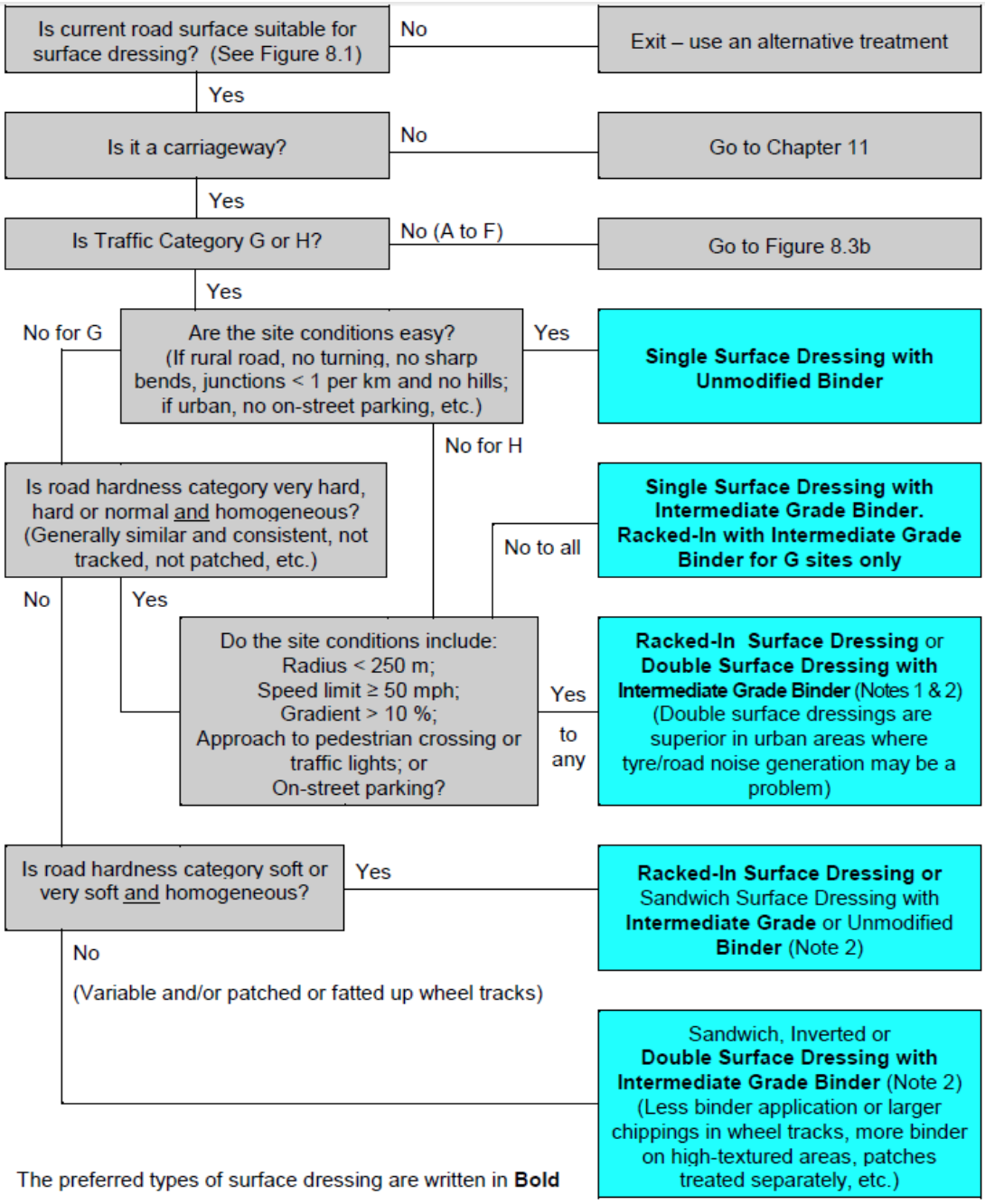

Figure 3.20 Continued

The aggregates should comply with the British Standard Institute BS EN 13043 (BSI, 2002.1) and the recommendations of PD 6682-2:2009+A1:2013 BSI National Guidance Document for surface treatments' aggregates (BSI, 2009). The use of uncrushed gravel should be avoided. On very hard substrates, particularly on roads in traffic categories A and B defined in Table 3.21, resistance to crushing is important and specifying a lower Los Angeles value should be considered. Seal coats with larger-size chippings should be carried out early in the season to ensure adequate embedment before the onset of cold weather. The size of substrate is a function of traffic and hardness of the substrate of the existing road. Other factors considered in the aggregate portion of the design include the size, cleanliness, crushed, minimum Polished Stone Value, limits on the maximum Los Angeles Value (normally 30) and Aggregate Abrasion Value (normally 12). The recommended aggregate sizes are the following:

- S14: Nominal Size → 14mm and BS EN 13043 Designation 8/14 mm (BSI, 2002.1)
- S10: Nominal Size → 10mm and BS EN 13043 Designation 6.3/10 mm (BSI, 2002.1)
- S6: Nominal Size → 6mm and BS EN 13043 Designation 2.8/6.3 mm (BSI, 2002.1)

As indicated in Table 3.19, the aggregate application rate is a function of size, shape, and relative density. A coverage rate between 100% and 105% shoulder to shoulder is determined by BS EN 12272-1 (BSI, 2002.2).

Aggregate Size	**Range of Spread Rates**	
	kg/m^2	$m^2/tonne$
2.8/6.3 mm	8 – 11	125 – 91
6.3/10 mm	10 – 14	100 – 71
8 / 14 mm	12 – 16	83 – 62

Table 3.19: British Design Recommended Aggregate Application Rate

The binder should be a cationic bituminous emulsion in accordance with BS EN 13808 (BSI, 2013). All lanes that carry different traffic levels should always be designed separately regarding the binder. Some of the binder will penetrate an open and negatively textured surface and, unless allowance is made for this loss, insufficient binder may be left on the surface to hold larger sizes of chippings. As shown in Table 3.20, a basic design for the binder application rate is provided based on a 67% binder content of bitumen.

Traffic Category	Hardness Category of Road Surface									
	Very Hard		Hard		Normal		Soft		Very Soft	
	Size of Chipping (mm)	Binder Rate (L/m²)	Size of Chipping (mm)	Binder Rate (L/m²)	Size of Chipping (mm)	Binder Rate (L/m²)	Size of Chipping (mm)	Binder Rate (L/m²)	Size of Chipping (mm)	Binder Rate (L/m²)
A	(a)		(a)		(a)		(b)		(b)	
B	S10	1.8 (c)	(a)		(a)		(a)		(b)	
C	S10	1.8 (c)	S10	1.6 (c)	(a)		(a)		(b)	
D	S6	1.5 (c)	S10	1.6 (c)	(a)		(a)		(a)	
E	S6	1.5 (c)	S10	1.6 (c)	S10	1.6 (c)	S10	1.6 (c)	(a)	
F	S6	1.5 (c)	S6	1.5 (c)	S10	1.6 (c)	S10	1.6 (c)	(a)	
G	S6	1.5	S6	1.5	S6	1.5	S10	1.6	(a)	
H	S6	1.5	S6	1.5	S6	1.5	S6	1.4	S6	1.4

Notes: (a) Multiple layer surface dressing preferred – see Figures 8.3a and 8.3b.
(b) Conditions not suitable for single surface dressings – see Figure 8.3b.
(c) Polymer-modified versions of this type of binder are preferred in those conditions – see Section 5.3.4 and Figure 8.3b.
(d) The surface dressing types are coded for convenience: S is for single and the chipping sizes are the maximums so S6 is a 2.8/6.3 chipping single surface dressing and S10 is a 6.3/10 chipping.

Table 3.20: British Design Method Basic Binder Application Rate

Corrections to accommodate to local conditions, type of aggregate used, and type of binder used are required to achieve an adequate seal coat surface including:

- Surface Temperature Categories: At lower temperatures, it is less likely for aggregates to embed the existing substrate; hence, more binder is needed to hold the chip. The altitude also affects the properties of the binder because of the change in temperature. Accordingly, UK is divided in to four surface temperature categories from A to D. The sections of the asphalt road surface shaded by trees, buildings, bridges, or tunnels, tend to be cooler and thus more resistant to chipping embedment when compared to areas in the sun. Hence, the rate of application should be increased in the shady areas.
- Traffic Category and Speed: Different traffic categories dictate the type of seal coat to be implemented. "*Because medium and heavy vehicles cause most of the embedment of chippings, the principal measure of traffic for design purposes is the number of medium and heavy vehicles per day*" (Bateman, 2016). Medium and heavy vehicles are defined as vehicles with a gross weight greater than 3.5 tons. The traffic speed also affects the seal coat type to be used. When the surface treatment is subjected to regular high speeds, stronger seal coat types should be considered. Table 3.21 presents the recommended traffic categories (Bateman, 2016).

Medium & Heavy Vehicles/lane/day	0 - 50	51 - 125	126 - 250	251 - 500	501 - 1250	1,251 - 2,000	2,001 - 2,500	2,501 - 3,250	> 3,250
Traffic Category	H	G	F	E	D	C	B	B	A
NRSWA Type	4	4	3	3	2	1	1	0	0

Table 3.21: British Traffic Categorization

The areas subject to less traffic than the rest including hard shoulders and edge strips experience a lower embedment than other trafficked areas. Hence, an increase in the asphalt application rate is needed to compensate for the lack of sufficient embedment.

- Road Hardness: Road hardness (reflects the ability of the existing pavement surface to tolerate the aggregate embedment) is measured with a hardness probe in accordance to BS 598-112 (BSI, 2004). Figure 3.21 illustrates the hardness category identification.

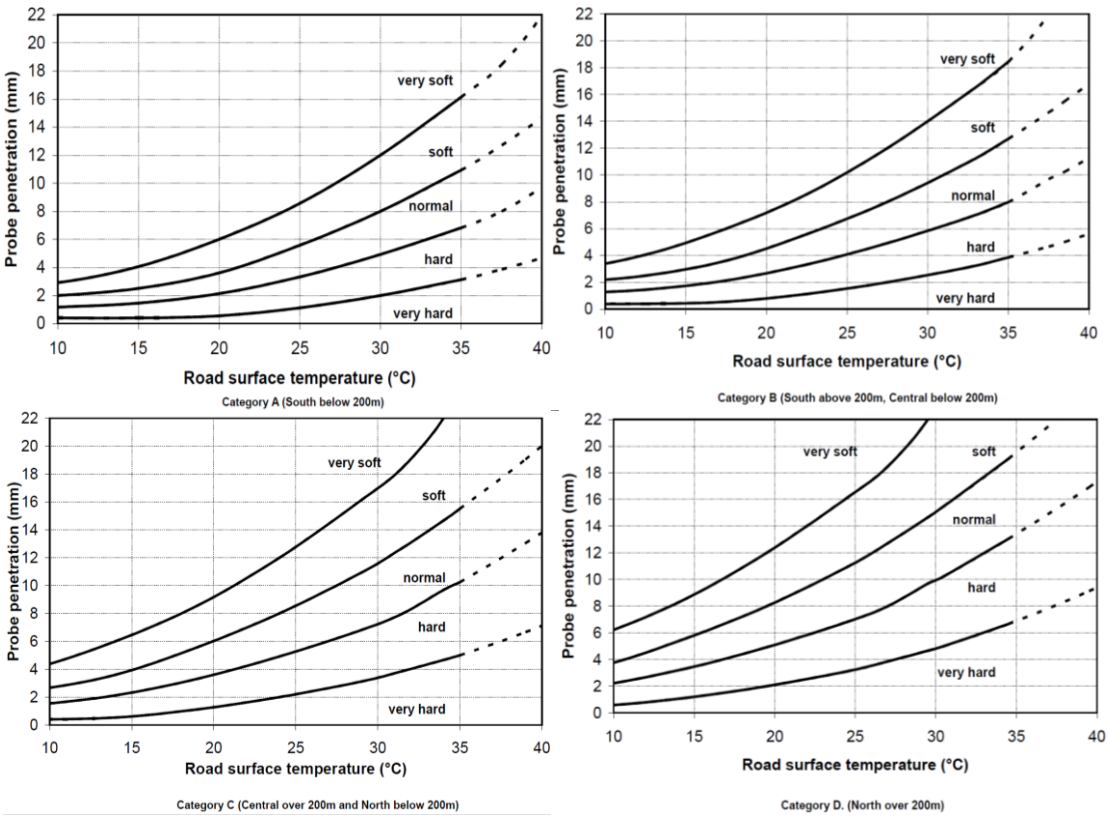

Figure 3.21: Road Hardness Based on Penetration Test and Temperature Category

- Highway Layout: The gradient, the sharpness of bends, high acceleration and deceleration rates, and the degree of super-elevation affect the stresses on the pavement surface. The following categories are used when selecting the seal coat type:
    - Gradient – up to 5 % gradient; 5 % to 10 % gradient; and over 10 % (1 in 10).
    - Radius of curvature – under 100 m radius; 100 – 250 m radius; and over 250 m
    - Junction or crossing – approach; and non-approach

- Surface Condition: After assessing the condition of the existing surface, the seal coat requires (1) having adequate binder content for the initial retention of the chip before long-term embedment, and (2) avoiding excess binder to minimize the risk of bleeding. As shown in Table 3.22, the surface condition affects the type of seal coat used.

Existing surface characteristic	Traffic Category H	G	F	E	D	C	B	A
Very Hard and homogeneous	Yes	Yes	Yes	Yes	Yes	Yes	Yes	Yes
Hard and homogeneous	Yes	Yes	Yes	Yes	Yes	Yes	Yes	Yes
Normal and homogeneous	Yes	Yes	Yes	Yes	Yes	Yes	Yes	Yes
Soft and homogeneous	Yes	Yes	Yes	Yes	Texture	Texture	E	
Very Soft and homogeneous	Yes	Yes	Yes	Texture	E	E		
Fatting up in wheel tracks	Yes	Yes	Texture	Texture	E	E		
High macro-texture or fretted	Yes	Yes	Yes	Yes	Defects	Defects	E	
Porous	Yes	Yes	Yes	Defects	Defects	E		
Very variable	Defects	Defects	Defects	Defects	Defects	E	E	
Extensive patching	E	E	E	E	E			
Severe bleeding & extensive blackening								

Yes	The surface dressing can be designed to meet the most onerous performance requirements in terms of macro-texture and levels of defects to BS EN 12272-2 (BSI).
Texture	It is difficult to maintain high macro-texture, especially in the wheel tracks and for high-speed roads. Texture requirements for low speed roads may be achievable.
Defects	It is difficult to design a surface dressing that will meet the most onerous requirements for the test method of visual assessment of defects to BS EN 12272-2 (BSI) and the requirements should not be specified.
E	In some circumstances, a suitable surface dressing may be designed by an expert to meet less onerous performance levels. Extra care in execution is required.
	Surface dressing is not an appropriate treatment.

Table 3.22: Suitability of Existing Surface

Table 3.23 summarizes the secondary factors influencing the BAR. The cumulative adjustment for the BAR should be within -0.2 and +0.4 L/m^2.

Influence	Property	Effect (L/m²)	Comments
Season	Early and mid-season Late season	0 +0.2	Late season work is very risky especially with S10, double surface dressing is recommended if the work has to be completed, see Fig 7.3.2.
Aggregate type	Crushed rock or slag Gravel	0 +0.1	Gravel is only appropriate for Traffic Categories G and H.
Shape	Flakiness category FI_{10} FI_{15} FI_{20} FI_{25} and above	 +0.1 0 -0.1 Consider design	Flakiness index should conform to PD 6882-2. Adjustment is only required for non-conforming aggregates. Very cubical chippings, FI_{10}, require more binder to hold them initially. Flaky chippings ($>FI_{20}$) may result in early loss of texture depending on traffic.
Shade	Un-shaded, open to sun Partially shaded Fully shaded	0 +0.1 +0.2	Shaded areas are cooler and, therefore, the road is effectively harder so more binder is required. Double surface dressing is recommended for fully shaded areas (see Table 9.2.3).
Surface condition (Consider suitability, see Figure 8.1 and type of surface dressing Figures 8.3a and 8.3b)	Very binder rich Binder rich Normal Texture in wheel tracks Binder lean / porous Very binder lean and porous, high macro-texture, or variable and hard.	-0.2 -0.1 0 +0.1 +0.2 Consider Design	For variable soft binder rich areas a sandwich surface dressing should be considered. Above F traffic category if there is tracking due to being binder rich, larger chippings should be considered for the wheel tracks as part of a double surface dressing. A pad coat is recommended to normalise and seal porous road surfaces (see Section 9.2.4). Double surface dressing with intermediate binder is recommended for variable hard and binder lean substrates (see Table 9.2.3).
Gradient	> 5 % uphill < 5 % > 5 % downhill > 10 % downhill	-0.2 0 +0.1 +0.2	The gradient affects the traffic stress on the surface dressing and, therefore, the rate of embedment. Racked-in or double surface dressings are recommended for hills and downhill high-speed sections (see Tables 9.2.2 and 9.2.3).
Traffic Speed	High speed (≥50 mph limit) Low speed (<50 mph limit)	+0.1 0	Roads subject to high-speed traffic induce greater surface stress. Racked-in or double surface dressings with premium binders are recommended.
Local traffic	Design range Effectively un-trafficked	0 +0.2	Un-trafficked areas, such as hatched sections, and also between the wheel tracks and edges of carriageways, require more binder. Hard shoulders, unless a contra flow is planned, and sizeable areas with hatched lines to exclude traffic are effectively untrafficked.

Table 3.23: British BAR Correction for Secondary Factors

FRENCH DESIGN METHOD (IDRRIM, 2017; AFNOR, 2007)

Seal coats are a very common surface treatment technique in France. Two of the main objectives for surface treatments are sealing the existing pavement and enhancing the skid resistance by improving the surface macrotexture. The limitation of usage is directly associated with the type of coat at hand. Fragility to tangential loads necessitates the use of polymer modified binder. Local defects should be treated prior to the sealing job that happens within the paving summer season. According to the French method, the major variables affecting the design are the following:

- The physical characteristics of the pavement to be coated
    - State of the support (existing substrate), and
    - Section geometry.
- The functional characteristics of the pavement to be coated
    - Traffic,
    - Site (agglomeration), and
    - Operating condition.
- The environmental characteristics of the pavement to be coated
    - Section exposure, and
    - Climatic region.
- The time of construction

The design methodology is based on: (1) a choice of structure recommended for typical site configurations; (2) a choice of gravel dosage based on the determination of covering potential; and (3) a choice of binder dosage established by a baseline on which patches are applied to incorporate the specificity of the site.

The type of the seal coat is a function of the traffic, the support, the environment, the extreme winter conditions, the time of realization, the extent of surface sealing, and the

desired texture. Preventative maintenance treatments are recommended for roads subject to traffic levels up to T1 defined in Table 3.26. Surface wearing coats such as seal coats can be applied to roadway sections of low and medium traffic up to T2. In particular, single seal coats are expected to perform well on roads with homogeneous supports of different surface textures and medium traffic up to T2.

The aggregates are selected such that they comply with:

- Fragmentation resistance determined by the Los Angeles (LA) test according to standard NF EN 1097-2 (AFNOR, 2010.2);
- Wear resistance determined by the Micro-Deval test (MDE) according to standard NF EN 1097-1 (AFNOR, 2011); and
- Polish Stone Value (PSV) according to standard NF EN 1097-8 (AFNOR, 2009).

The aggregate properties investigated include size, gradation, cleanliness, flakiness, angularity, moisture content, petrography, specific gravity, bulk density, sulfur content, Slag GGBFS (Ground Granulated Blast-Furnace Slag) content. The French recommend a specific aggregate gradation for definite aggregate sizes identified as D/d, where D is the smallest sieve opening, in mm, that has a percent passing greater than or equal to 85%, and d is the largest sieve opening (in mm) with a percent passing of less than 15%. Table 3.24 shows the recommended gradations.

Aggregate Size	Passing (% by mass)							Category		Fines Content
	2D	1.4D	D	D/1.4	d	d/2	0.5mm	G		F
Gravels with D/d < 2 (4/6.3; 6.3/10; 10/14)	100	98 – 100	85 – 99	–	0 – 15	0 – 5		Gc85/15	-	
	100	98 – 100	85 – 99	–	0 – 20	0 – 5		Gc85/20		
Gravels with D/d ≥ 2 (2/4)	100	98 – 100	85 – 99	25 – 80	0 – 15	0 – 5	≤ 1	Gc85/15	G 25/15	$f_{0.5}$ to f_1
	100	98 – 100	85 – 99		0 – 20	0 – 5		Gc85/20		
	100	98 – 100	85 – 99	20 – 70	0 – 15	0 – 5		Gc85/15	G 20/15	
	100	98 – 100	85 – 99		0 – 20	0 – 5		Gc85/120		

Table 3.24: Aggregate Gradation (IDRRIM, 2017)

After complying with the aggregate gradation and the necessary quality tests, Table 3.25 is used to determine the recommended application rate.

Gradation d/D	AAR (L/m^2)
4/6	6 - 7
6/10	8 – 9
10/14	11 - 13

Table 3.25: French Recommended AAR for Different Aggregate Sizes

Before the start of the project, it is necessary to determine the covering potential of the available aggregates. For a single seal coat, the dosage to be retained must be that corresponding to the covering potential + 5% maximum.

The binder characteristics investigated include viscosity and binder content, rupture index, passive adhesiveness, storage, density, pH, and many more. The use of emulsions to extend the seal coat season is common, but the risk of raveling increases if an anhydrous binder for single seal coat layers is not used. When traffic is important (T1 or T0), it is advisable to choose a modified binder that guarantees a rise in cohesion fast and a high viscosity that ensures optimum wetting of the gravel. Table 3.26 provides a description of the French traffic classes.

Traffic Class	Average Annual Daily Truck Traffic AADTT
T5	between 0 and 25
T4	between 25 and 50
T3-	between 50 and 100
T3+	between 100 and 150
T2	between 150 and 300
T1	between 300 and 750 PL
T0	between 750 and 2,000 PL
TS	between 2,000 and 5,000 PL
T exp	Greater than 5,000 PL **(PL = Poid Lourdes Heavy Weight)

Table 3.26: French Traffic Classes

In France, heavy commercial vehicles are defined by standard NF P 98-082 as vehicles with a total permissible gross weight greater than 3.5 tonnes (GVW ≥ 35 kN). The basic binder dosages are selected based on the structure of the seal coat, the nature of binder and the size of the aggregates. These dosages, given as an indication, correspond to a roadway

whose surface is homogeneous, smooth-textured, free from bleeding (traditional coated type, normally worn) and supporting traffic from 50 to 100 PL/d /direction (T3-). Table 3.27 presents recommendations for the basic BAR.

Base Design		
Gradation d/D	Cutback BAR (kg/m^2)	EAR (kg/m^2)
4/6	1.05	1.30
6/10	1.35	1.75
10/14	1.60	2.15

Table 3.27: Basic French Binder Application Rates for Different Aggregate Sizes

This basic rate is corrected to better meet the site-specific conditions enhancing the durability and efficiency of the surface treatment. The factors that are considered are:

- Traffic: On the slow lanes of high-volume sections (AADT ≥ T1), truck traffic tends to quickly embed the chips in the support the raise the binder level. On the corresponding routes, an under-dosing of the order of 10 to 15% is to be applied. On the fast lanes of 2x2 highways or on the central lane of the 3-lane roads, the low number of trucks on these must be considered and generally overdosing the binding. Finally, when the traffic is low, a good setting of the aggregates in the binder is realized by an overdose which can reach 10 to 15%. For more than 1,000 vehicles per direction per day, a reduction of the dosage of 3 to 5% per 1,000 vehicles per day and per direction.
- Surface Condition: An empirical classification of the existing pavements surface is done in accordance with three criteria:
    - Assessing the surface macrotexture in terms of MTD as per AFNOR standard NF EN 13036-1 (AFNOR, 2010.1),

    - Capturing the porosity / permeability empirically through a particular level of cracking of the support, and
    - Measuring the hardness empirically through the punching character of the support favoring the indentation of aggregates.
- Alignment: In the case of important ramps, or heavy channeled traffic, the dosage should be reduced. In cornering areas where significant tangential efforts are developing, an overdose compatible with traffic is to be expected.
- Region altitude and environment: Common sense suggests a lower dosing of the binder in hot regions than in cold regions, at low altitude than at high altitude. Varying the binder dosage is also to be predicted as a function of sunshine and especially in the case of shaded sections where the maturation of the dressing is slower.
- Size and shape of aggregates: In addition to delicately handling the supply of aggregates, it is necessary to check the size, the flakiness, the cleanliness, and even the moisture content in order to adjust accordingly the binder dosage.
- Binder category: Recent developments in the formulation of cutbacks with low volatile oils (vegetable or heavy mineral) minimize the correction needed. The non-volatile character and the lower density of the vegetable oils lead to negative dosage adjustments. For bitumen emulsions, it is always necessary to make the adjustment related to the residual binder content
- Time of realization: During the construction of seal coat in the late season, it is allowed to apply a thicker binder film with an additional dosage of up to 5%. This operation is more difficult to control with cutbacks with none or little volatile oils; the risk being to experience bleeding in the following spring.

- Accumulation of corrections: The accumulation of corrections may lead to large differences in extreme cases. Experience has shown that a difference of more than 35% or less than -20% requires road improvement prior to treatment application.

Table 3.28 provides a comprehensive summary of the correction factors that are adopted to meet the needs of site-specific conditions.

Parameter		Correction of Dosage (%)
Traffic (HV/ln/day)	T0…… > 750	-15
	T1…… 300 – 750	-12
	T2…… 150 – 300	-8
	T3+…… 100 – 150	-5
	T3-…… 50 – 100	0
	T4…… 25 – 50	+5
	T5……< 25	+10
	No HV	+12
Environment	Very Sunny	-5
	Sunny	-2
	Normal	0
	Shady	+5
	Very Shady	+10
Profile	Flat & Straight	0
	Sloping & Straight	-5
	Flat & curvy	+2
	Sloping & Curvy	-2
Existing Texture	Very rough ……... MTD > 1.7	+18
	Rough …….. MTD > 1.2	+12
	Not that rough …….. MTD > 0.8	+6
	Smooth not bleeding …….. MTD < 0.8	0
	Tendency to bleed …….. MTD < 0.8	-5
	Bleeding …….. MTD < 0.8	-10
Porosity and Permeability	Permeable	+5
	Impermeable	0
Hardness or rigidity	Not Punch-able	0
	Punch-able	+7

Table 3.28: French Binder Application Rate Correction

Construction Time	**April/May**	**0**
	June/July/August	**0**
	Starting September	**+5**
Binder Category	Cutback with Mineral Oil	+3
	Modified Cutback	+1
	Cutback with vegetable oil	-3
	Emulsion @65%	+6
	Emulsion @69%	0
	Modified emulsion @69%	0
Gradation	Normal (as guided)	0
	Finer	-5
	Coarser	+5
Flakiness	>15%	-4
	<10%	+4
	Normal Range	0
Region	Hot	-4
	Moderate	0
	Cold	+4
Altitude	< 500m	0
	500 – 1000m	+2
	> 1000 m	+4

Table 3.28 Continued

The French monitor the performance of the seal coat one year after construction in accordance to NF EN 12271 (AFNOR, 2007) to obtain the CE marking, i.e. European Conformity. The site investigation is an opportunity to validate the structure and dosage of the seal coat for each section of the route. The objective is to validate the adequacy between the design and the level of performance targeted by the client. The different classes proposed in the national foreword NF EN 12271 specification are:

- ESU Class A: High performance seal coat. The level of defects tolerated is low (Visual Assessment Level of Defects: VAD I).
- ESU Class B: Good performance seal coat. The level of defects tolerated is low to medium (Visual Assessment Level of Defects: VAD I or VAD II).

- ESU Class C: Average performance seal coat. The level of defects tolerated is low to high (Visual Assessment Level of Defects: VAD I or VAD II or VAD III).

These classes are based on traffic and the condition of the surface. The visual assessment of defects tests the levels of sweating (bleeding), peeling (raveling), plucking (bond failure), and streaking. Additionally, macrotexture MTD, noise, gravel quality, and binder quality are also assessed for conformance.

TXDOT CHIP SEAL MANUAL (TXDOT, 2017.2)

Texas Department of Transportation (TxDOT) invests up $180 million per year in seal coats to maintain 197,500 lane-miles of roadway. Seal coat is one of the main components of TxDOT's preventive maintenance program, which has been operational since 1987 and sealing 17,000 to 20,000 lane-miles per year (TxDOT, 2017.2). It is desirable in Texas to place seal coats on a six-to-eight-year cycle, but this is not always possible due to funding constraints. It is estimated that the average life of a seal coat surface treatment is between six and eight years, and some treatments have performed successfully for periods of up to 20 years. TxDOT differentiates between chips seals and surface treatment whereby the latter is an application of asphalt material covered by a single layer of aggregate to a prepared compacted base while the former is applied to a paved surface.

In designing seal coats, TxDOT relies on three different methods. First, the modified Kearby method as recommended by the Texas Transportation Institute in 1981. It serves to guide inexperienced personnel through the art of seal coat design and train personnel including inspectors, designers, and laboratory technicians. It is used to determine initial binder and aggregate application rates but does not replace good engineering judgment. Site-specific conditions are assessed to adjust both the binder and the aggregate application rates. Second, McLeod's design method is also considered bearing in mind that this method was developed primarily for use with emulsion binders and has not been verified in Texas. Lastly, the transversely varying asphalt rates (TVAR) remains the main seal coat design method adopted by Texas. It entails varying the amount of asphalt being poured along the width of the pavement with the objective of meeting the requirements of both the existing pavement and the new seal coat layer. The motivation behind this method is the fact that the texture of the existing pavement varies along the width of the pavement as shown in Figure 3.22. Since trafficking is one of the main

contributors to the compaction of the seal coat, less binder is needed for along the wheel path to hold on to the aggregates in comparison to the rest of the section. This would mitigate the problem of either having asphalt in excess along the wheel path resulting in bleeding or having asphalt in deficit elsewhere resulting in raveling. The viability of this design method depends on the adequate assessment of the texture. One dosage may still be effective on surfaces with existing flushing in the wheel path. This allows the variation of the application rate transversely and accommodation for the difference in texture in the wheel path and between the paths.

Figure 3.22: Varying Texture Pavement (TxDOT, 2017.2)

Guidance for relating sand patch test results to desirable asphalt rate is presented in Table 3.29. It is suggested to increase the BAR outside the wheel paths. It is recommended that a minimum of four randomly spaced locations be tested and the results averaged.

Difference in Sand Patch Average Diameters, mm	Asphalt Rate Increase Outside of Wheel Paths
Less than 20	None
21 to 50	15%
Greater than 50	30%

Table 3.29: Guidance for Interpreting Sand Patch Test Results to Vary the BAR

In essence, the existing texture between the wheel paths is usually coarser and subjected to less trafficking. Both factors lead to needing more binder in this area. On the other hand, the existing texture of the wheel path is smoother and subjected to more trafficking. Those two factors dictate the need for less binder compared to other areas across the pavement. This justifies the need for varying binder application rates as one-dosage-fits-all will not be suitable for any pavement surface as it is widely variable.

COMPARING THE POPULAR DESIGN METHODS

The Appendix compares the aggregate application rates and the binder application rates obtained by the different seal coat design methods discussed in Chapter 3. A case study is considered in which the seal coat of a specific highway section is designed according to all the reviewed design methods. Table 3.30 shows the aggregate application rates and the binder application rates along the road obtained by different design methods.

Slow Lane				
Design Method	**AAR**		**BAR**	
Hanson	66 m^2/m^3		1.20 L/m^2	
Kearby	116 m^2/m^3		1.04 L/m^2	
McLeod	78 m^2/m^3		1.13 L/m^2	
Modified Kearby	116 m^2/m^3		0.87 L/m^2	
Spanish	11.8 L/m^2	85 m^2/m^3	1.4 kg/m^2	[3]1.4 L/m^2
New Zealand	87 m^2/m^3		1.22 L/m^2	
Australian	105 m^2/m^3		1.00 L/m^2	
South African	91 m^2/m^3		1.08 L/m^2	
British	14 kg/m^2	[2]**114 m^2/m^3**	1.20 L/m^2	
French	12 L/m^2	83 m^2/m^3	[1,3]1.70 kg/m^2	1.17 L/m^2
Fast/Passing Lane				
Design Method	**AAR**		**BAR**	
Hanson	66 m^2/m^3		1.20 L/m^2	
Kearby	116 m^2/m^3		1.04 L/m^2	
McLeod	78 m^2/m^3		1.48 L/m^2	
Modified Kearby	116 m^2/m^3		1.19 L/m^2	
Spanish	11.8 L/m^2	85 m^2/m^3	1.4 kg/m^2	[3]1.4 L/m^2
New Zealand	87 m^2/m^3		1.47 L/m^2	
Australian	105 m^2/m^3		1.86 L/m^2	
South African	91 m^2/m^3		1.70 L/m^2	
British	14 kg/m^2	[2]**114 m^2/m^3**	1.40 L/m^2	
French	12 L/m^2	83 m^2/m^3	[1,3]2.32 kg/m^2	1.60 L/m^2
Shoulder				
Design Method	**AAR**		**BAR**	
Hanson	66 m^2/m^3		1.20 L/m^2	

Table 3.30: Case Study AAR and BAR Results

Kearby	116 m^2/m^3		1.04 L/m^2	
McLeod	78 m^2/m^3		1.87 L/m^2	
Modified Kearby	116 m^2/m^3		1.47 L/m^2	
Spanish	11.8 L/m^2	85 m^2/m^3	1.4 kg/m^2	[3]1.4 L/m^2
New Zealand	87 m^2/m^3		1.87 L/m^2	
Australian	105 m^2/m^3		2.55 L/m^2	
South African	91 m^2/m^3		1.77 L/m^2	
British	14 kg/m^2	[2]**114 m^2/m^3**	1.5 L/m^2	
French	12 L/m^2	83 m^2/m^3	[1,3]2.60kg/m^2	1.79 L/m^2

[1] 69% Emulsion **[2] 1600 kg/m^3 as a bulk unit weight** **[3] $\rho = 1.0$ tonne$/m^3$**

Table 3.30 Continued

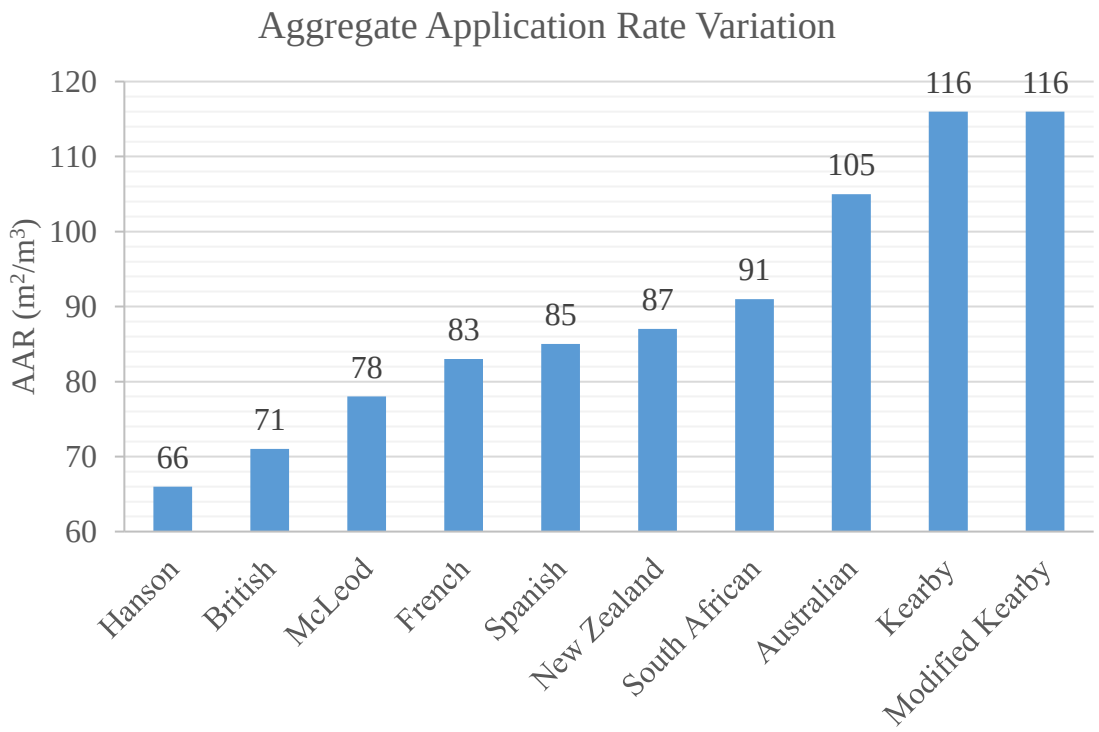

Figure 3.23: Comparison of Different Design Method Dosages

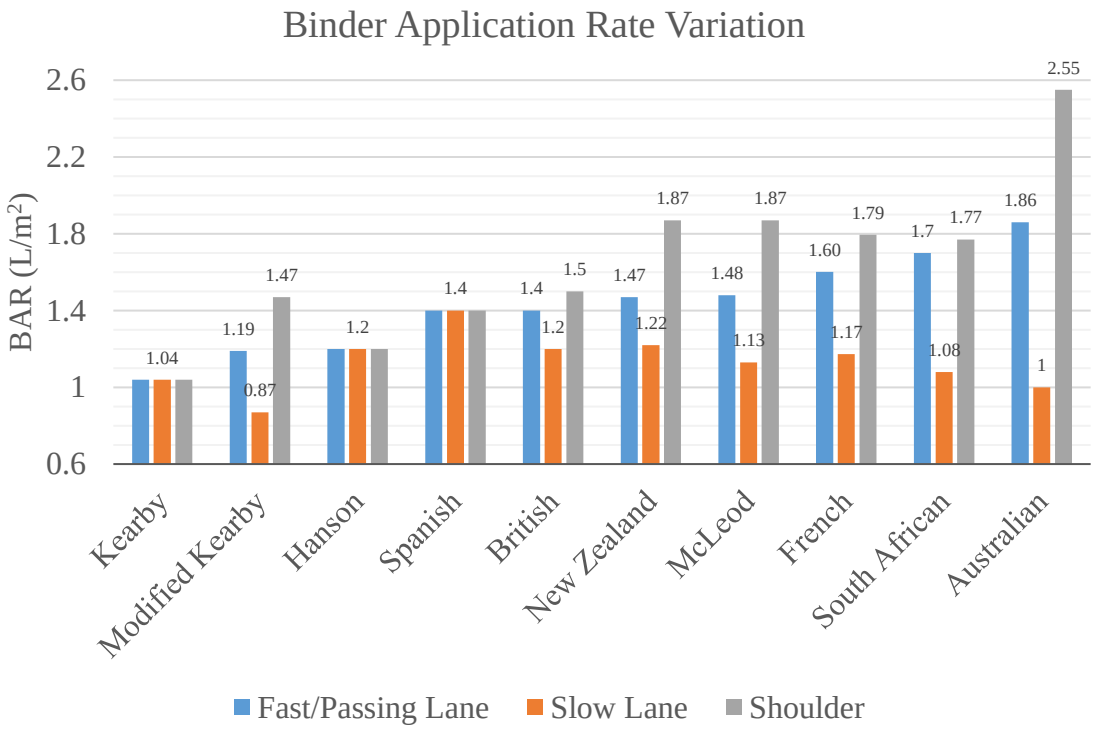

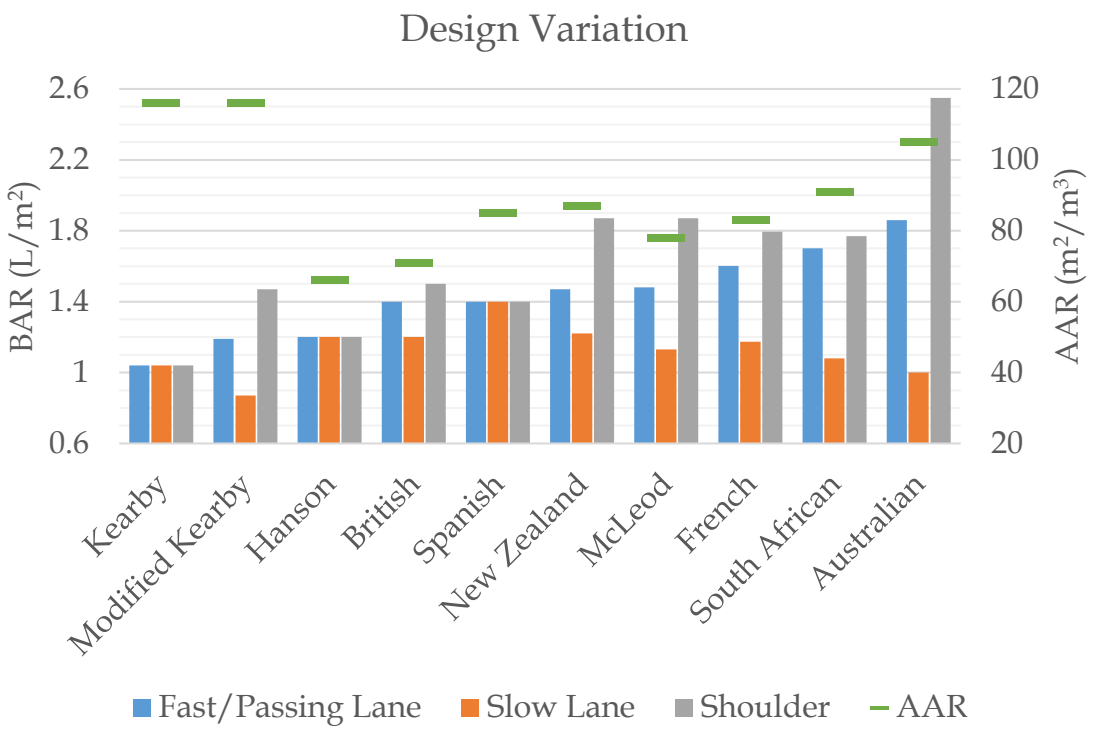

Figure 3.23 Continued

As shown in the graphs of Figure 3.23, different design methods recommend different aggregate and binder application rates. This widespread of designs is based on the inherent bias pertaining to assessing the existing site conditions and adopting different adjustment rates and factors. This makes the whole design process and assumptions questionable. Unfortunately, agencies end up having to rely on the site engineer's knowledge, common sense, and experiences in assessing the conditions on site and recommending adequate measures. In addition, the variability motivates researchers to investigate automated design methods that would quantify the site-specific conditions and eliminate the need for biased assessments. Lasers offer a high potential to quantify the surface at hand in a fast, objective, and reliable manner.

Chapter 4: UTexas AAR Improvement using 3D Laser Technology

After spraying the binder, the aggregates are spread over the width of the pavement surface in order to provide a good skid resistance by enriching the surface macro- and microtexture. This layer of aggregates also helps transmit the vehicle load to the underlying surface, and resist abrasion and deterioration of the surface. When selecting these aggregates, several properties are considered including: the aggregate availability, price, type, shape, size, gradation, hardness, acid and polish resistance, etc.

Unfortunately, there is no consensus over the aggregate application rate that is recommended for seal coat design. Different design methods would recommend different rates. These differences have been presented in Chapter 3 and are exemplified in the Appendix. There is a need to accurately estimate the right quantity of aggregates that, when applied, forms a one-aggregate-thick mat without significant wastage. Underestimating the rate results in a deficient surface (seal coat bleeding) and defeats the purpose of seal coats. Overestimating the rate is not acceptable from both an economic and safety point of view because this results in seal coat raveling. It is essential to provide an adequate application rate that meets the coverage target. This research focuses on incorporating the laser technology in the seal coat design. In particular, the laser is used to accurately measure the percent unit area coverage a specific aggregate rate achieves. Predictive models are developed in order to predict the AAR required to achieve a specific coverage percentage as a function of basic aggregate properties. The laser prototype used in this study is discussed in the following section. Afterwards, the aggregate application rate prediction model approach is described and further explained.

LASER PROTOTYPE

The incorporation of 3D laser technology into the design of seal coats could bring significant improvements and offer quantitative elements to optimize the designs. It has the potential to eliminate the bias, inaccuracy, and inconsistency pertaining to the existing design methods that are usually the result of relying on the subjective human judgement on site. In addition, the laser ensures accurate, reliable, objective, and fast measurements that improve the design and, thereby, the long-term performance of the surface treatment. For this purpose, an accurate 3D laser scanner, also referred to as Line Laser Scanner (LLS), was developed.

This prototype consists of a two-dimensional (2D) non-contact semiconductor laser scanner mounted to a motion-controlled stage. The laser is a non-destructive equipment that offers a consistent and continuous data collection process. The three-dimensional scanner setup does not need additional light and is not affected by color irregularities (Keyence, 2016). The laser's sensor head unit, model LJ-V7300, projects a visible blue to purple light with a wavelength of 405 nm. The laser head used in this study conforms to the specifications presented in Table 4.1 and Figure 4.1.

Reference distance	300 mm
Height measurement range	[-145mm, 145mm]
Height Repeatability	5 μm
Width measurement Range	[110mm, 240 mm]
Width repeatability	60 μm
Profile data interval	300 μm
Maximum sampling frequency	16μs

Table 4.1: 3D Laser Specifications

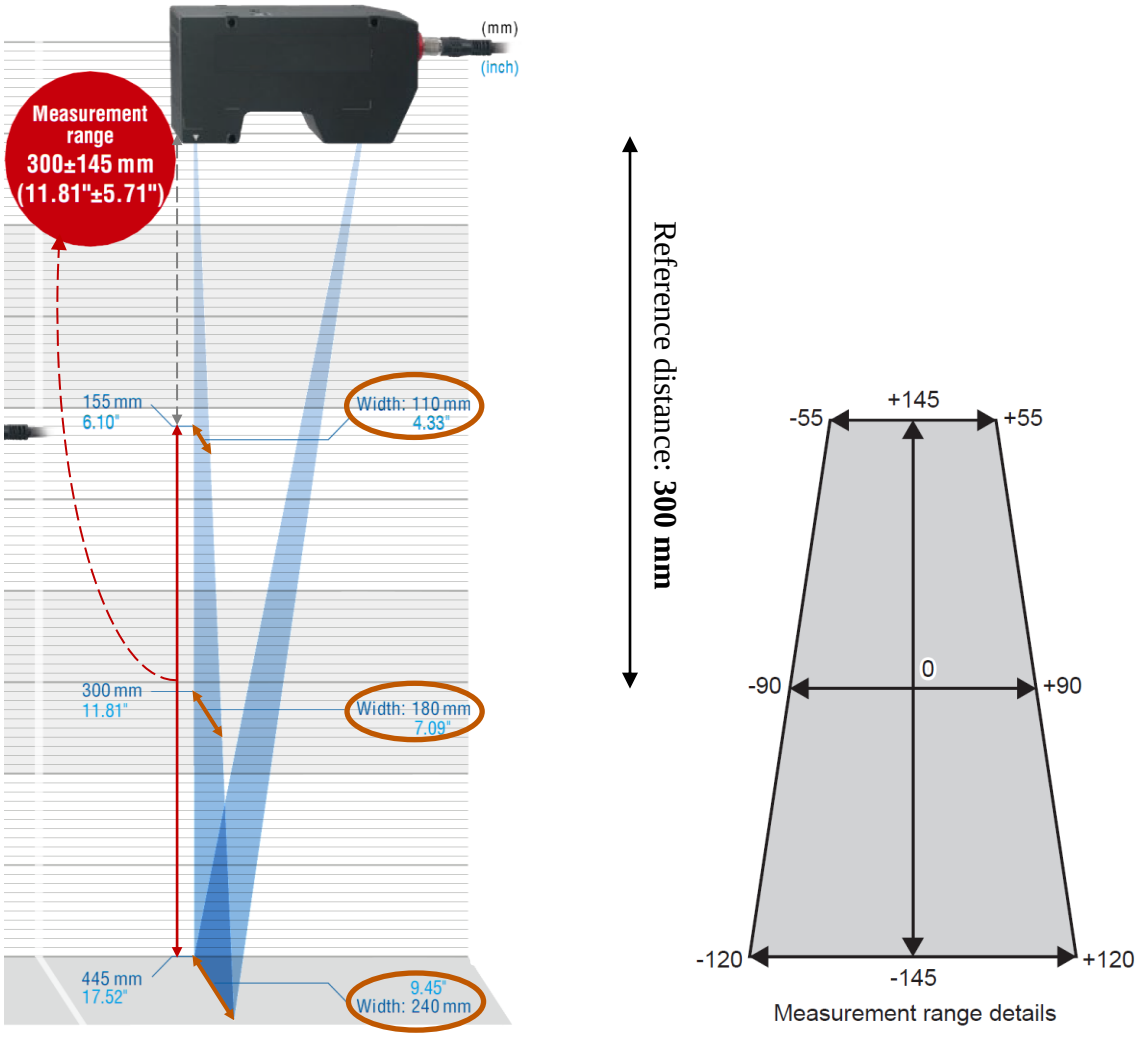

Figure 4.1: 3D Laser Specifications (Keyence, 2016)

First, the light is emitted from the laser head and projected onto the object being scanned. Then it is reflected from the object surface in all directions and captured by the camera detector within the head. As shown Figure 4.2, the angle between the emitted light and the reflected light is known and varies with height. For instance, at a reference height of 300 mm, the angle between the incidence and the reflection is 21.2°. Accordingly, triangulation is used to determine the height profile of the surface scanned relative to the reference.

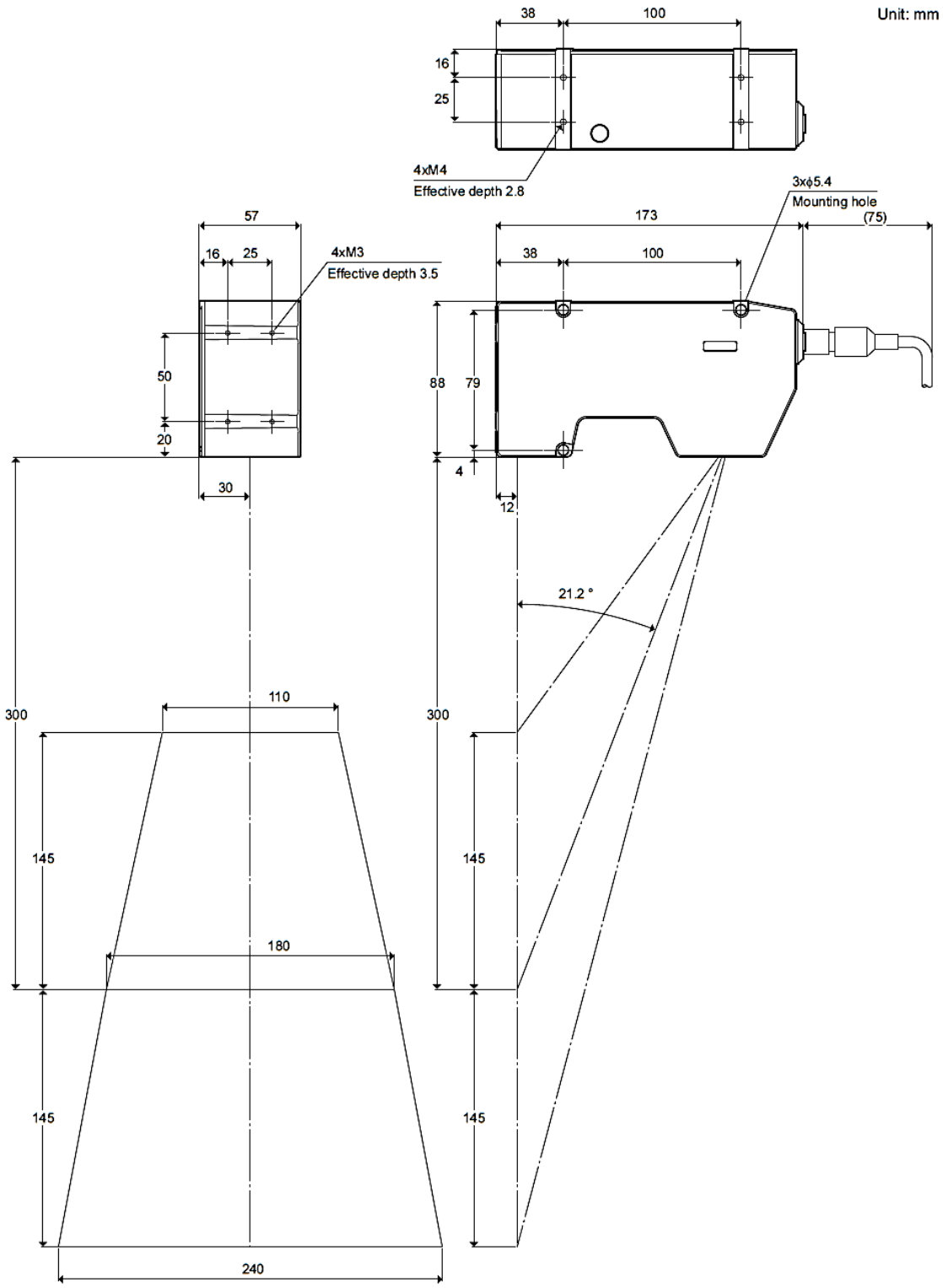

Figure 4.2: Incidence Angle Illustration and Laser Specifications (Keyence, 2016)

Small changes in height due to the texture irregularities are captured using this scanner system. The measurement principle behind the laser, as shown in Figure 4.3 and defined by the manufacturer, KEYENCE, is the following: *"The laser light is projected in a horizontal line by the cylindrical lens and diffusely reflects on the target object. This reflected light is focused on the HSE3-CMOS and by detecting changes in position and shape, displacement and shapes can be measured"* (Keyence, 2016).

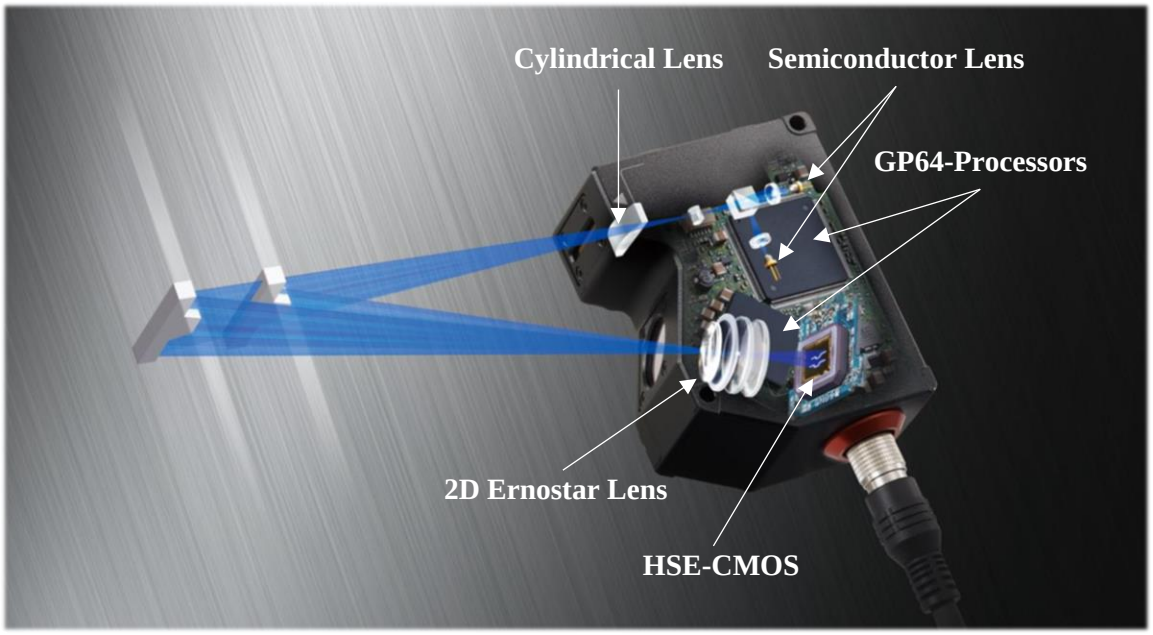

Figure 4.3: Laser Measuring Principle (Keyence, 2016)

For the purposes of this research study, the prototype consists of mounting the line laser scanner, aforementioned, to a linear-motion-controlled stage allowing the laser to travel linearly over the surface being scanned under a user-specified velocity. This allows the laser to collect height measurements along the width and across the length of the stage. The height measurements represent the Z-axis dimension, the width of the line laser represents the X-axis dimension, and the length of the stage represents the Y-axis

dimension forming the 3D scan. Figure 4.4 illustrates the frame that has the linear translation stage and the mounted laser.

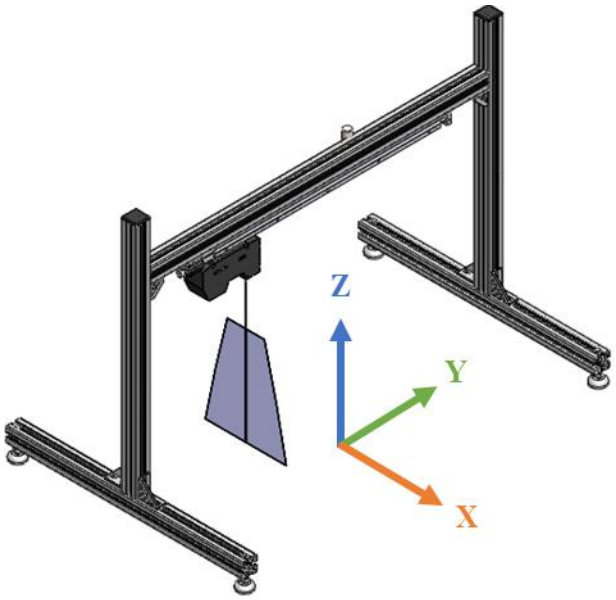

Figure 4.4: 3D Laser Scanner Prototype

This prototype is capable of collecting height measurement points, in mm, along the x-y plane whereby a maximum of 800 points 300 μm apart in the transverse X-direction and a user-defined number of points and spacing in the Y-direction are logged. The 3D surface is replicated by combining the discrete height points collected along the desired plane. The scanning interval along the Y-direction depends on the frequency of the laser light and the speed at which the laser is moving along the stage as follows:

$$\Delta Y = v \times \frac{1}{f}$$

Where v is the moving speed, in mm/s, and f is the scanning frequency, in Hz.

The linear translation stage and the laser are connected to a computer that is capable of controlling the various testing parameters and collect the scanned data in spreadsheets.

The laser scanner is a Class 2 laser, i.e. it is safe for the user to be exposed to the radiation. It operates under ambient temperature ranging between 0 and 45°C and relative humidity between 20 and 80%. Additionally, it possesses a vibration resistance of 10 to 57 Hz and 1.5 mm double amplitude in X, Y and Z directions. These operating conditions make it suitable to operate the laser in both the field and the laboratory. However, the maximum surrounding illuminance that will not cause any interference with the measurements is 10,000 Lux. This is equivalent to normal daylight without direct sunlight exposure. Henceforth, when used in the field, the laser is covered from direct sunlight to protect it from being exposed to illuminance conditions higher than the tolerable limit and eliminating possible disturbances. Parallel research studies, conducted by Kouchaki et al., showed that the developed 3D laser prototype has high accuracy and repeatability that ensures significant improvements over traditional measurement methods (Kouchaki S. , Roshani, Prozzi, & Hernandez, 2017; Kouchaki S. , Roshani, Prozzi, Cordoba, & Hernandez., 2018).

AGGREGATE APPLICATION RATE DESIGN IMPROVEMENT

The challenge in designing seal coats has always been the adjustment of the material application rates based on site-specific conditions. Most, if not all, design methods rely on empirical factor to correct for site and environmental conditions. For the aggregate application rate, most design methods recommend laboratory tests to infer the adequate quantity of aggregates needed to cover the surface. Other designs would rely on the size of the aggregate and recommend dosages based on that. The objective behind this part of the research is to employ the 3D laser scanner to accurately, automatically, and objectively measure the aggregate coverage and develop a predictive model. The predictive model would allow agencies to use easily measurable aggregate properties to predict the AAR for

specific coverage percentage. To achieve the aforementioned objective, the steps listed below were required:

- Creating a lab test that measures the aggregate coverage using the 3D laser prototype;
- Developing the algorithm that determines the aggregate coverage from the 3D scans;
- Testing different aggregate types to gather coverage data at different application rates;
- Developing a predictive model that provides the AAR for a user-defined coverage; and
- Adjusting the existing seal coat design methods.

Laboratory Experiment Setup

The 3D laser scanner prototype, previously described, was used to scan the aggregate and determine the coverage of different aggregate types. In this experiment, the laser was mounted 300 mm above the target, which is the ideal setting for this specific laser head. In this configuration, the line laser is 240 mm wide consisting of 800 points that are 300 µm apart in the transverse direction. The linear stage spans 600 mm in length allowing the laser to travel this distance above the target. This linear translation stage was set at a speed of 60 mm/s and the laser frequency at 200 Hz. Therefore, the scans in the longitudinal direction were also taken every 300 µm. Laser measurements were taken on eight different aggregate samples as discussed in a later section of this chapter. The chosen aggregates have different properties ensuring a wide variety of measurements.

To measure the aggregate coverage, a 20 mm-thick wooden tray was constructed to ensure that the aggregates are spread in a confined and specific area. The considered tray is 180 mm wide and 550 mm long. These dimensions were considered to provide a sufficient width that can still be measured by one laser scan and a suitable length that can be covered by the linear translation stage. Figure 4.5 shows the constructed tray from different views along with the relevant dimensions.

Figure 4.5: Tray Views and Dimensions

The tray surface was made of wood that had been smoothened using sandpaper with a grit size of 220 µm. This grit designation is considered very fine and recommended for sanding bare wood. Nevertheless, the tray still possessed an overall curvature and surface texture that cannot be recognized by the naked eye.

After running the initial scans, it came to the researchers' attention that the laser was not capable of scanning the first inch or so of the tray. This issue traces back to the way the laser works. The laser relies on triangulation to measure the height of a surface. During the triangulation process, the emitted ray should be captured back by the laser detector after being reflected form the surface in order for the laser to measure the height. However, if the reflected ray is obstructed by an object, the detector is not capable of

capturing it and the triangulation process is interrupted by this interference. In this particular application, the front edge of the tray was blocking the light and the laser was not capable of scanning the interference portion of the tray. Figure 4.6 illustrates the interference described.

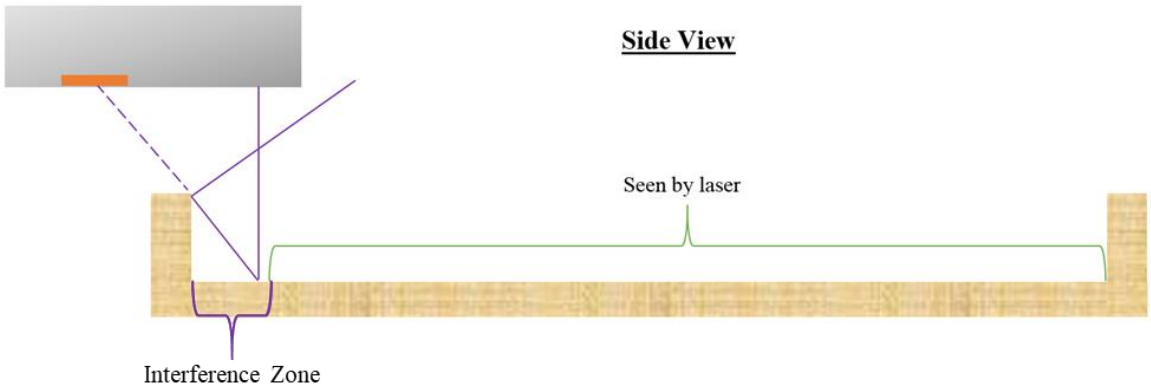

Figure 4.6: Front Edge Interference

The front edge of the tray was removed after placing the aggregates to allow the laser scanner to scan the whole surface. On the other hand, when the laser head approached the other end of the tray, the scan was affected by stray light being reflected from the surface towards the edge and from the edge towards the detector as shown in Figure 4.7.

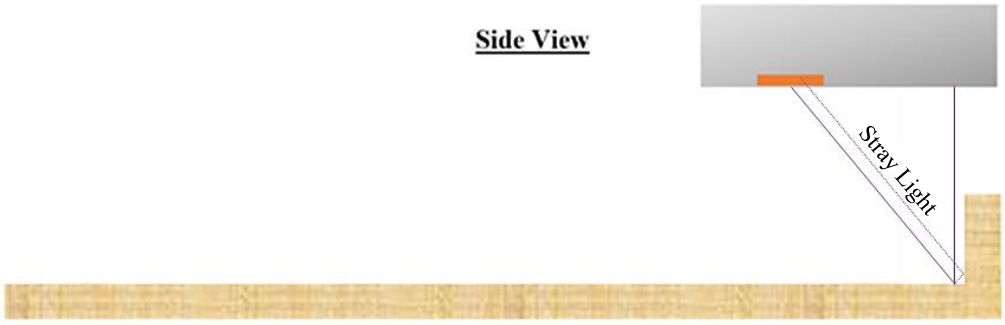

Figure 4.7: End Edge Stray Light Interference

This overestimated the height values of certain points and resulted in local spikes. Consequently, the end edge was removed when scanning, as shown in Figure 4.8, in order to minimize the interferences caused by the boundary conditions.

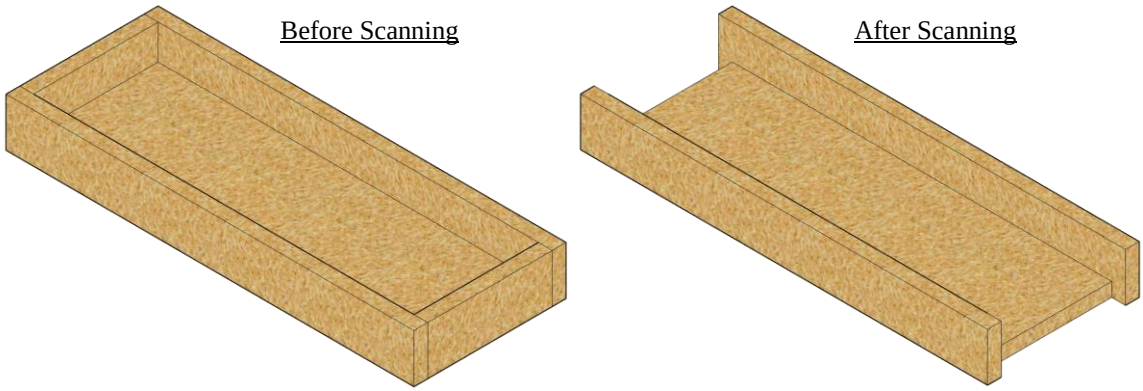

Figure 4.8: Tray Scanning Configuration

Although the laser scan width is 240 mm, the width of the tray was limited to 180 mm taking into account the potential dead points on the edges and the boundaries. While the line laser is made of 800 point that are 300 µm apart, the laser detector fails to capture all the points and ends up losing around 80 points from each side. These points are the farthest from the detector at each side and are reflected away. The system reports these points as dead points (or missing points) that are represented with an unrealistically low height value of -999.999 mm. This makes it easy for the user to identify these edge points when processing the raw data and filter them out. With the adopted tray size and configuration, the captured scan profile along the width of the tray is made of around 600 points spanning between the sides. Accordingly, the algorithm can identify the tray area as shown in Figure 4.9. This area is expected to have height values close to zero because the target plane is approximately 300 mm away from the scanning laser head.

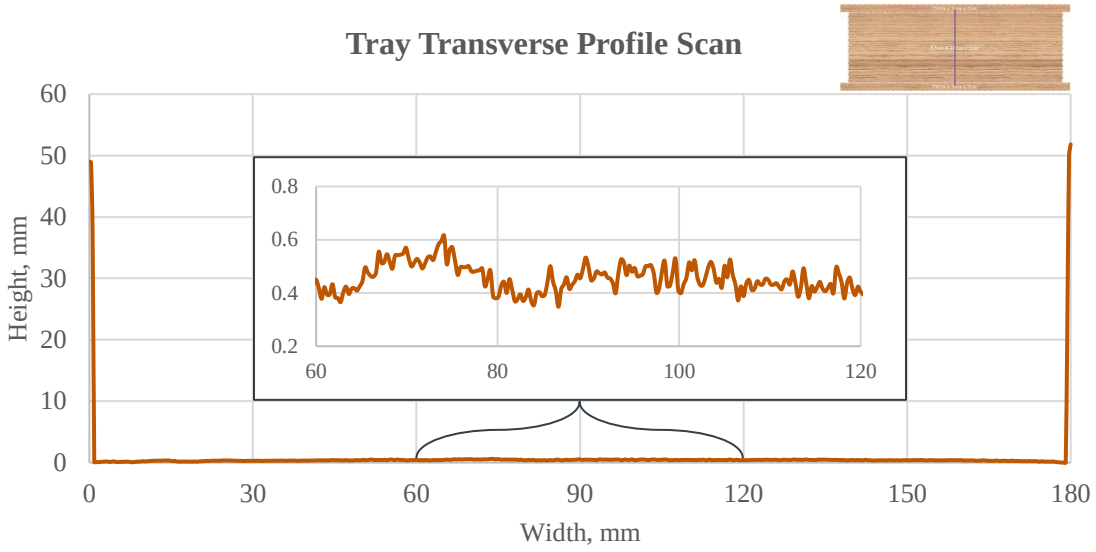

Figure 4.9: Mid-tray Transverse Profile

The tray area can be identified along the transverse direction as the edges extend 50 mm above the surface. In the longitudinal direction, the identification of the tray is different because the edges along those ends are removed to improve the scanning process. Since the translation stage is 600 mm long, it is possible to identify the front end of the tray by starting the scan few millimeters before as shown in the Figures 4.10 and 4.11.

Figure 4.10: Scanning Start Before the Tray

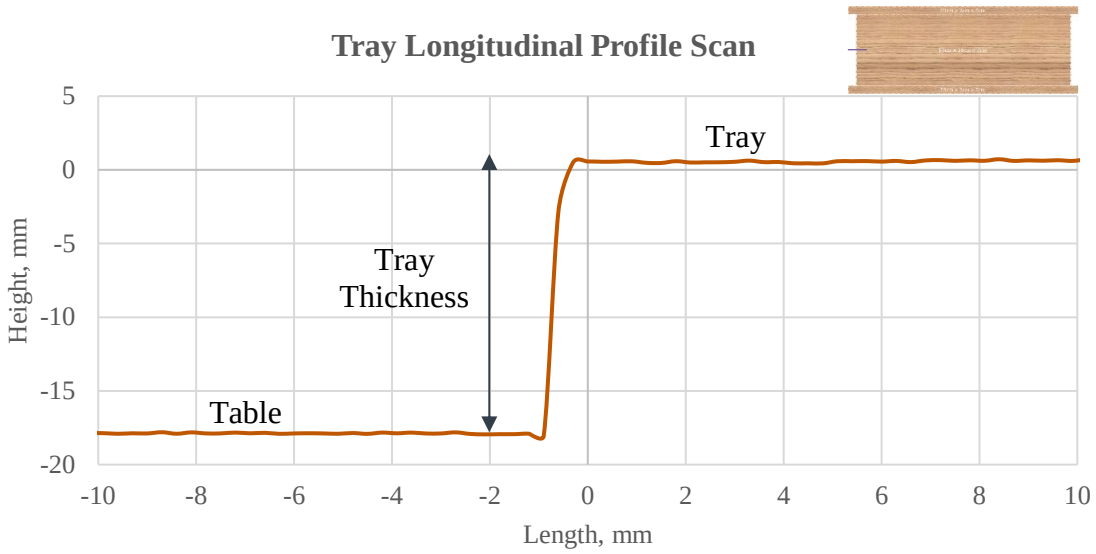

Figure 4.11: Longitudinal Profile at Beginning of Tray

Since the end edge is also removed, the laser scanner moves past the tray and onto the table. At this point, another interference zone is created whereby the reflected laser light is blocked by the thickness of the tray and is not captured by the detector. Hence, the dead points are recorded over the influence zone with values of -999.999, which are easily identifiable as shown in Figure 4.12.

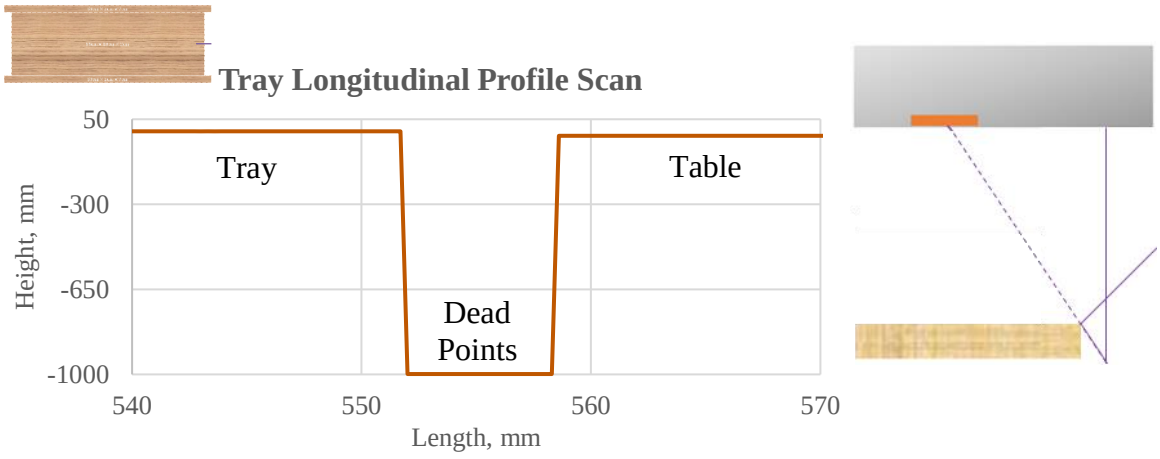

Figure 4.12: Longitudinal Profile at the End of the Tray

Accordingly, the ends of the tray are identified along the longitudinal direction. Figure 4.13 shows a full tray scan profile along the longitudinal direction, i.e. 550 mm long.

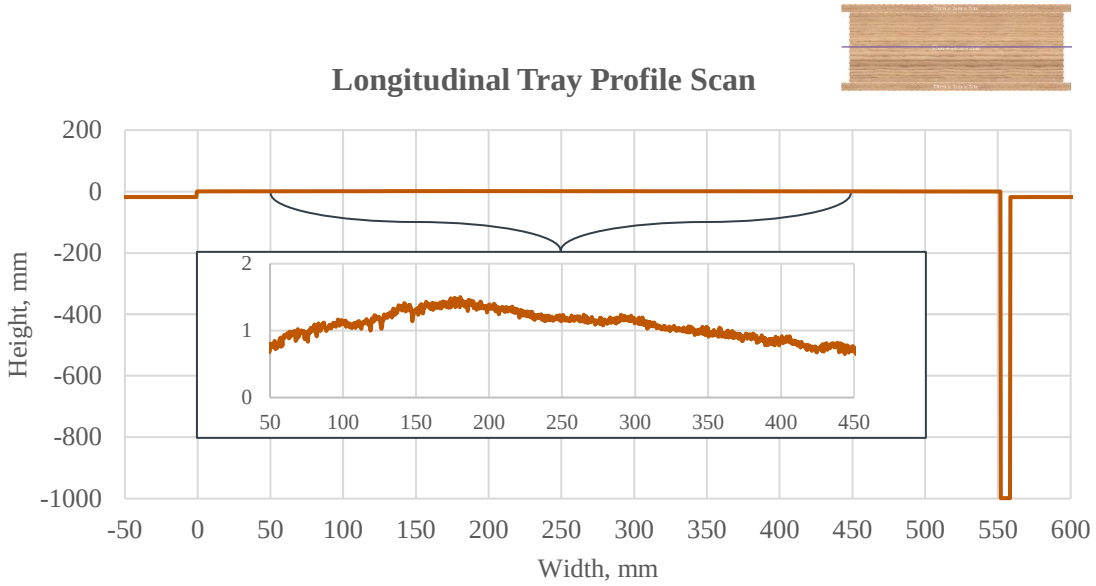

Figure 4.13: Mid-tray Longitudinal Profile

When conducting the experiments, the edges of the tray are marked down on the table in order to fix the location and ease the data collection process. In addition, the plane of the tray is almost parallel to the plane of the laser along the translation stage. Unfortunately, the wooden tray is slightly curved, and this curvature is captured in the longitudinal and transverse profiles. Henceforth, a reference scan of the tray is collected before measuring the aggregate coverage. This reference scan is later subtracted from each aggregate coverage scan to correct for the curvature, which is shown in Figure 4.18.

Aggregate Coverage Algorithm

After weighing the aggregates mass, the chips are spread on their flattest side on the tray forming when possible a one-stone thick layer. Consequently, the tray and its contents are scanned at a frequency of 200 Hz and at a speed of 60 mm/sec. In order to determine the aggregate coverage, the following algorithm is adopted:

1. The raw data is first imported from the stored csv file as shown in the Figure 4.14.
2. The dead points from the side edges are easily identified as these cells have height values of -999.999. These sides are outside the tray area and are hence removed as shown in Figure 4.15.
3. The start and the end of the tray are identified as previously explained and shown in Figure 4.15. The area outside the tray is removed as shown in Figure 4.16.

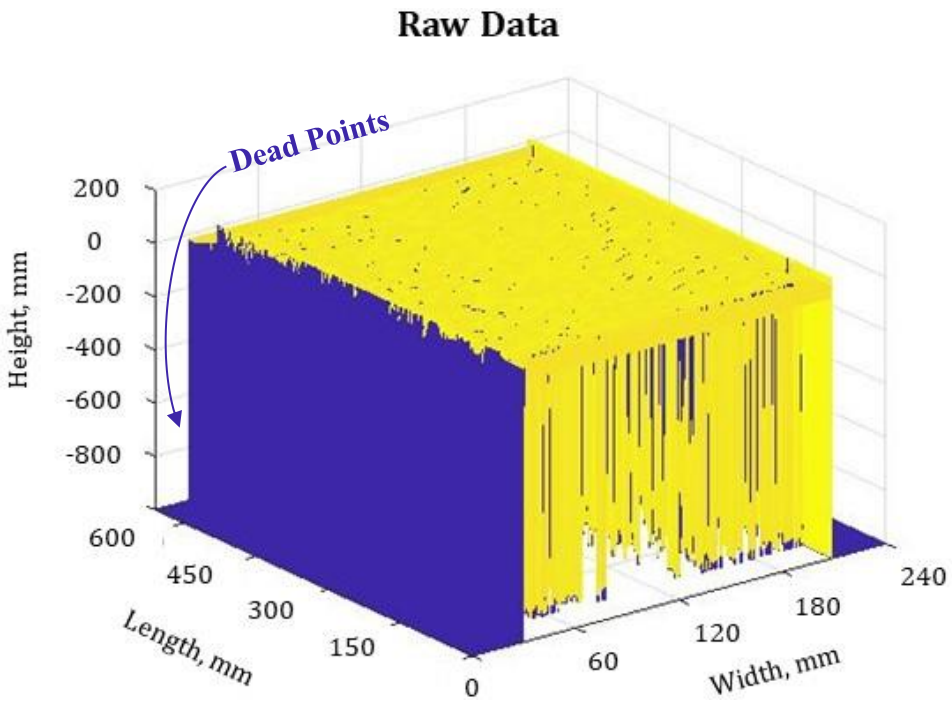

Figure 4.14: Coverage Scan Raw Data

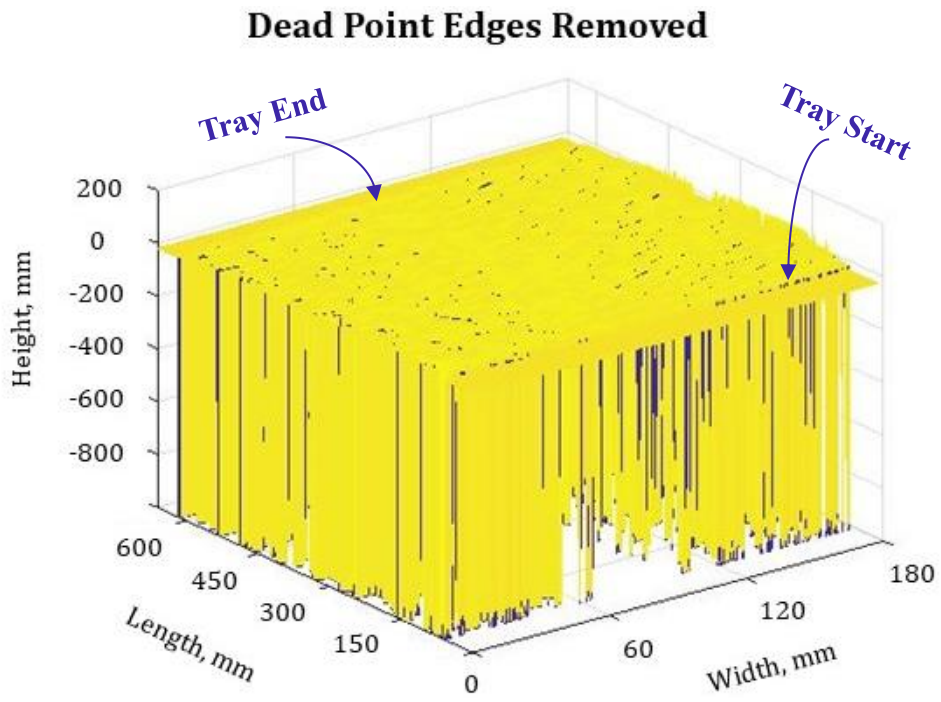

Figure 4.15: Post-Processing Edge Dead Points

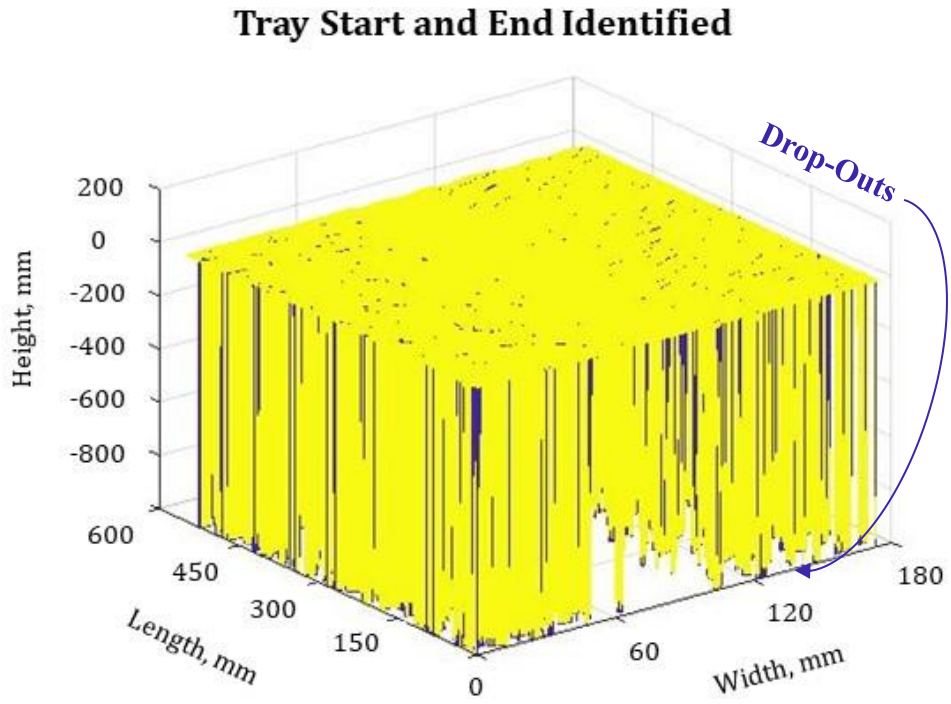

Figure 4.16: Tray Identified

4. The remaining drop-out points are corrected using a 5×5 mean filter. During the scanning process, the reflected laser light can be blocked by aggregate particles. In such cases, the detector fails to capture the light and reports the point as a drop-out with a value of -999.999 as shown in Figure 4.16. Accordingly, the mean filter will detect drop-out points and replace them by the average of the non-drop-out points that are within proximity as shown in Figure 4.17. A detailed explanation of the mean filter is provided in Chapter 6.
5. A reference scan of the tray in empty conditions, shown in Figure 4.18, is retrieved. Accordingly, the reference tray scan is subtracted from the current scan containing aggregates to obtain a virtual scan of the aggregates.

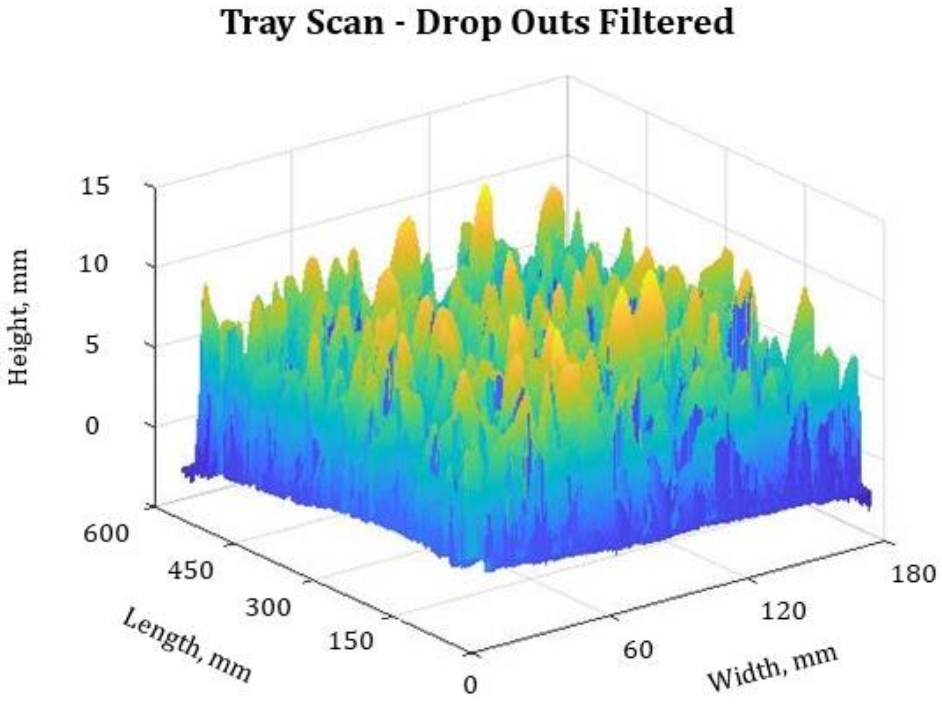

Figure 4.17: 3D Data of the Aggregates in the Tray post Drop-outs Removal

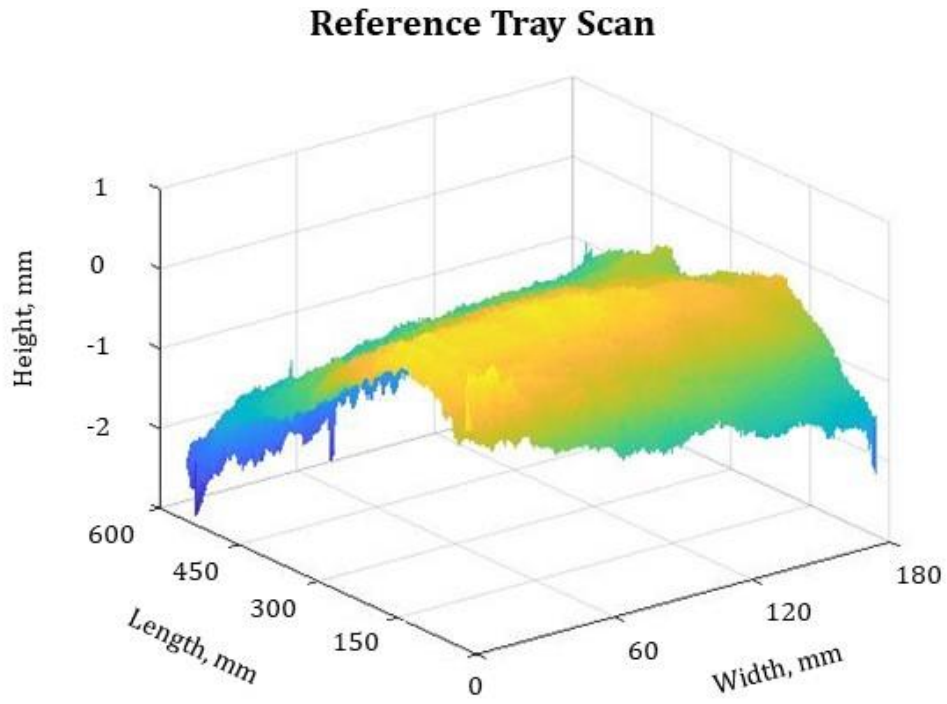

Figure 4.18: 3D Rendering of Reference Tray

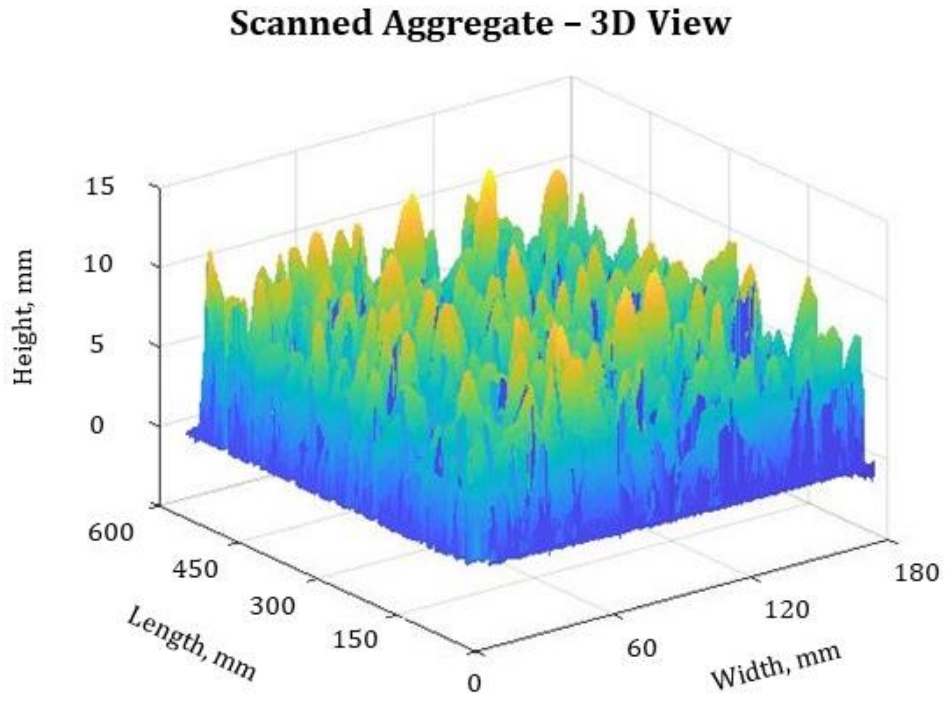

Figure 4.19: 3D Rendering of Aggregates on a Flat Surface

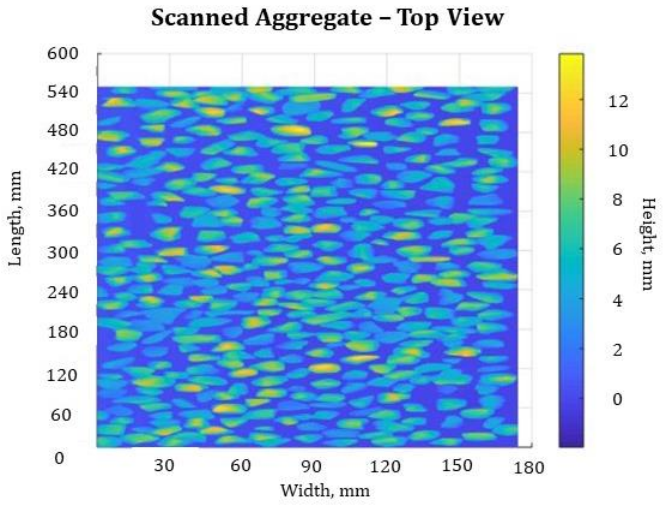

Figure 4.20: Top View of Aggregates on a Flat Surface

6. Once the aggregates are filtered from the initial scan as shown in Figures 4.19 and 4.20, the coverage ratio is determined using the following equation:

$$\text{Coverage } (\%) = \frac{\text{Area covered by aggregates}}{\text{Total Tray Area}} \times 100\%$$

The final step is to distinguish between the points on the aggregates and those on the surface of the tray. Both an image analysis and a sensitivity analysis are conducted to determine the appropriate aggregate-tray threshold. In the image analysis, several small aggregates where scanned in order to determine the height of the first scanned point above the surface. As shown Figure 4.21, the first scanned aggregate point is few millimeters above the surface.

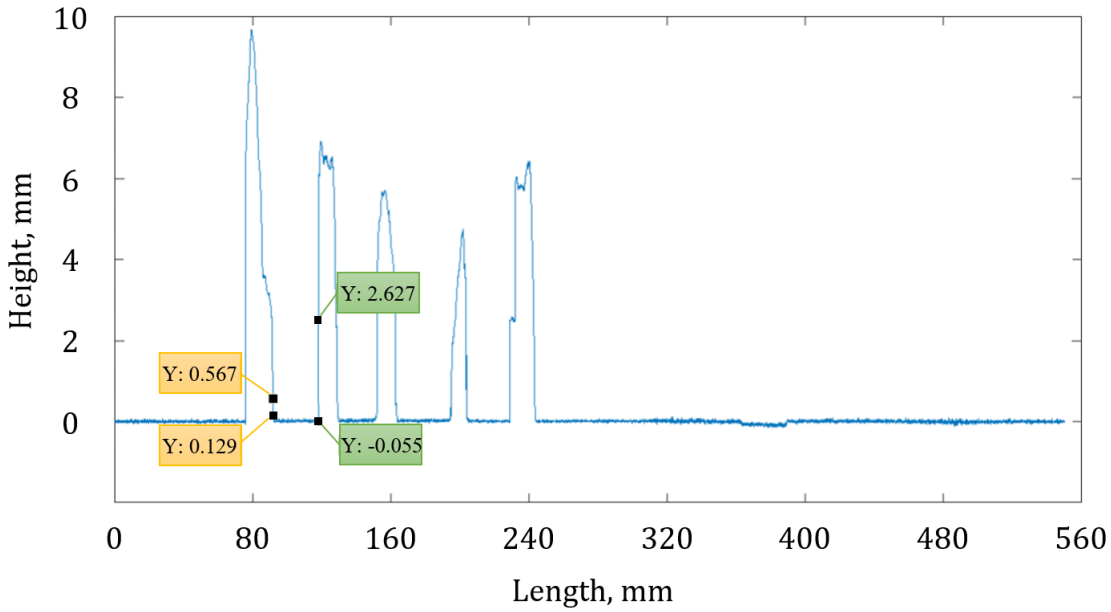

Figure 4.21: Aggregate Scan on a Flat Surface Showing Aggregate-Tray Interface

Additionally, a sensitivity analysis to determine the aggregate-tray interface threshold value is conducted with threshold values varying from 0.02 to 2.00 mm with an increment of 0.02 mm. The graph in Figure 4.22 shows the sensitivity analysis results.

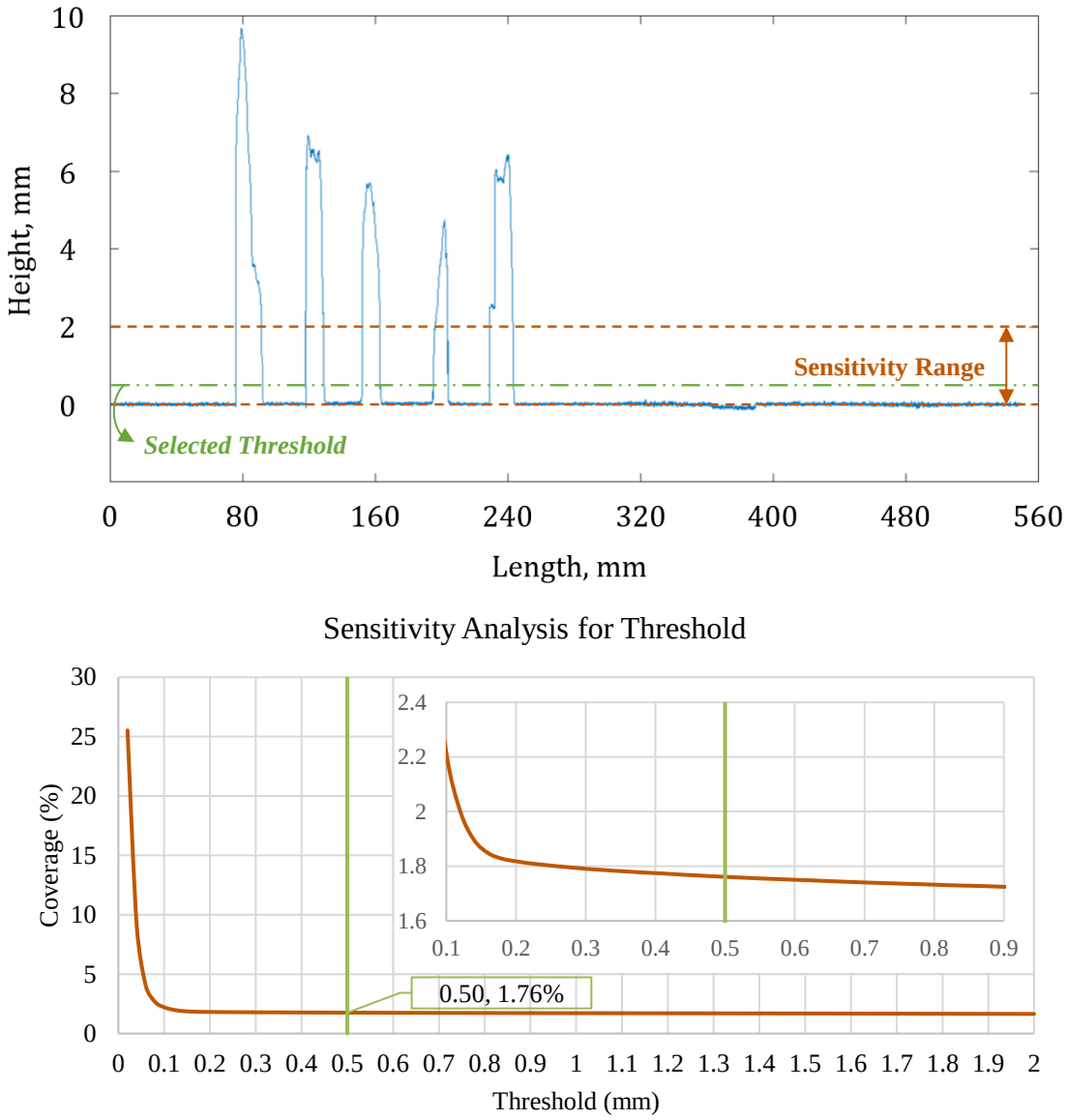

Figure 4.22: Sensitivity Analysis for Aggregate-Tray Interface

A threshold of 0.5 mm is adopted whereby the scanned points with heights greater than 0.5 mm are considered part of the aggregates and points below the threshold are considered part of the tray. Hence, the aggregate coverage of the tray is determined as

the ratio between the points belonging to the aggregates and the total number of points, i.e. the total tray surface area [549 mm by 174mm].

Laboratory Tests

After constructing the tray and developing the algorithm that determines the aggregate coverage, the following laboratory tests were conducted to capture the aggregate coverage properties for eight different aggregate samples shown in Table 4.3:

1. Sieving the aggregate samples, as shown in Figure 4.23, in accordance with TxDOT's aggregate gradation requirements for seal coats shown in Table 4.2 (TxDOT, 2017.2) and ASTM C136 for conducting sieve analysis (ASTM, 2014).

Aggregate Gradation Requirements (Cumulative % Retained[1])

Sieve	Grade								
	1	2	3S[2]	3		4S[2]	4	5S[2]	5
				Non-Lightweight	Lightweight				
1"	-	-	-	-	-	-	-	-	-
7/8"	0–2	0	-	-	-	-	-	-	-
3/4"	20–35	0–2	0	0	0	-	-	-	-
5/8"	85–100	20–40	0–5	0–5	0–2	0	0	-	-
1/2"	-	80–100	55–85	20–40	10–25	0–5	0–5	0	0
3/8"	95–100	95–100	95–100	80–100	60–80	60–85	20–40	0–5	0–5
1/4"	-	-	-	95–100	95–100	-	-	65–85	-
#4	-	-	-	-	-	95–100	95–100	95–100	50–80
#8	99–100	99–100	99–100	99–100	98–100	98–100	98–100	98–100	98–100

1. Round test results to the nearest whole number.
2. Single-size gradation.

Table 4.2: TxDOT Surface Treatment Aggregate Grades

Sample	Aggregate Type	Tag	Grade
1	Crushed Limestone	#18-0264	4S
2	Crushed Sandstone	#18-0404	5S
3	Lightweight Aggregate	#18-0394	3L
4	Crushed Trap Rock (Basalt)	#18-0471	4S
5	Crushed Trap Rock (Basalt)	#18-0471	5S
6	Crushed Sandstone	#18-0143	4S
7	Crushed Sandstone	#18-0143	5S
8	Crushed Limestone	#18-1123	3S

Table 4.3: Preliminary Properties of Scanned Aggregate Samples

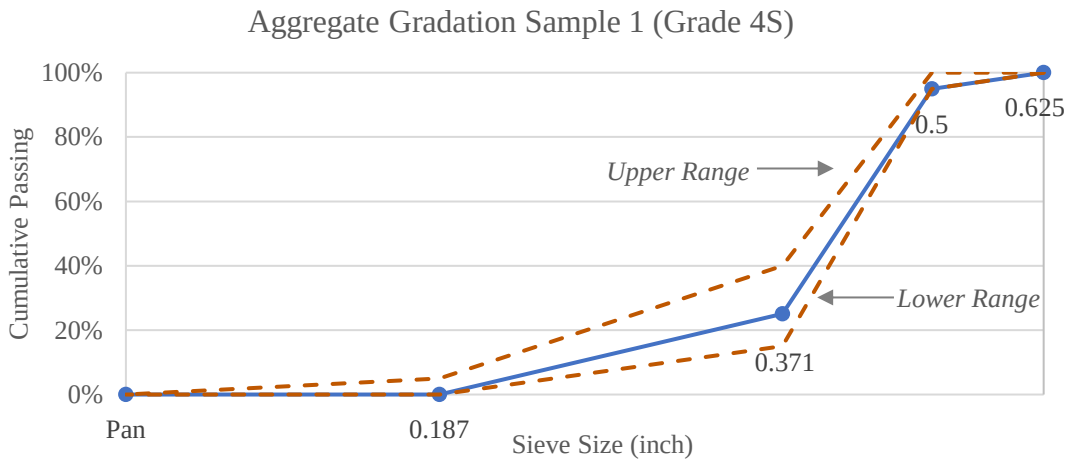

Figure 4.23: Test Samples Aggregate Gradation Complying with TxDOT Grades

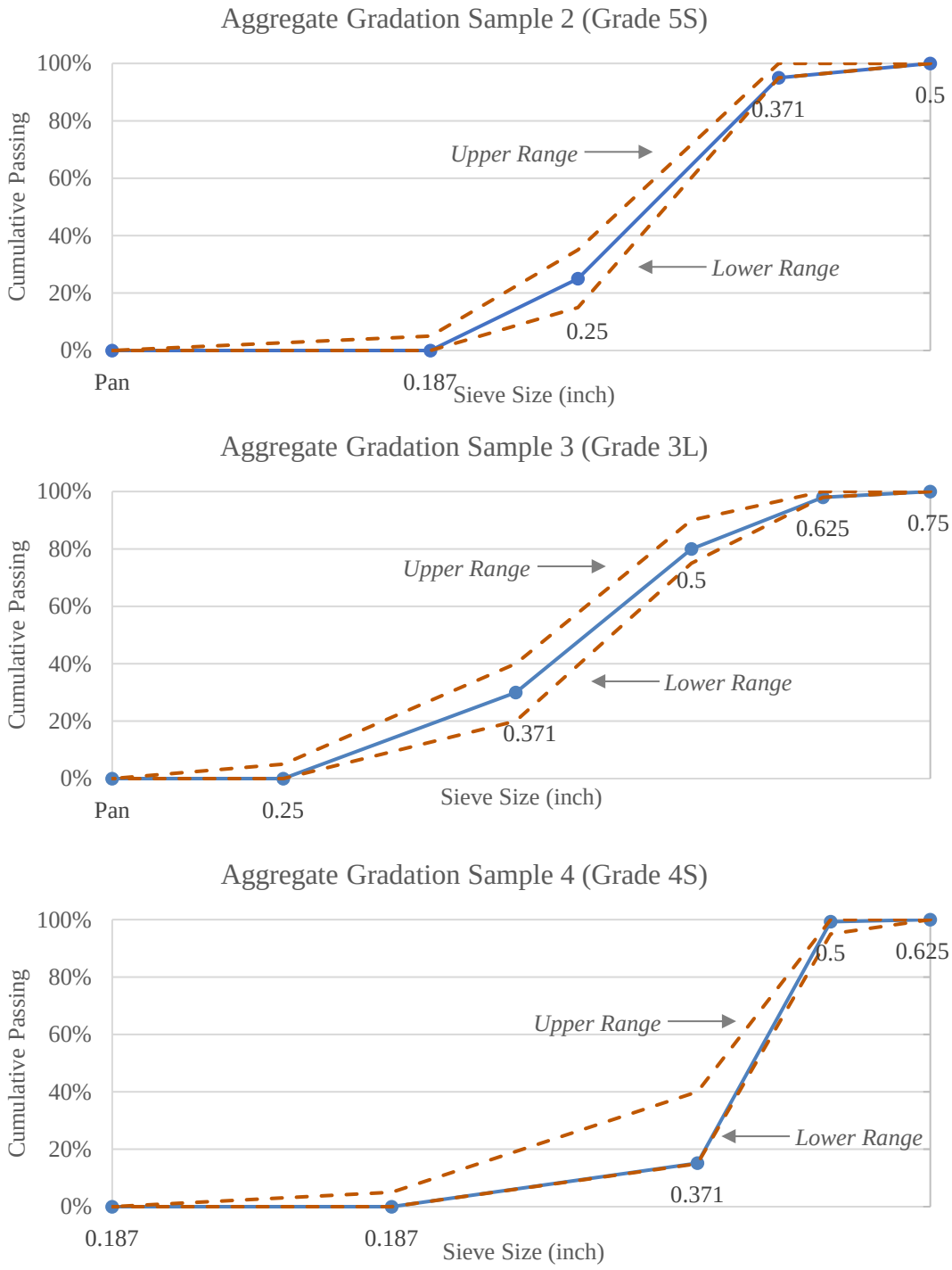

Figure 4.23 Continued

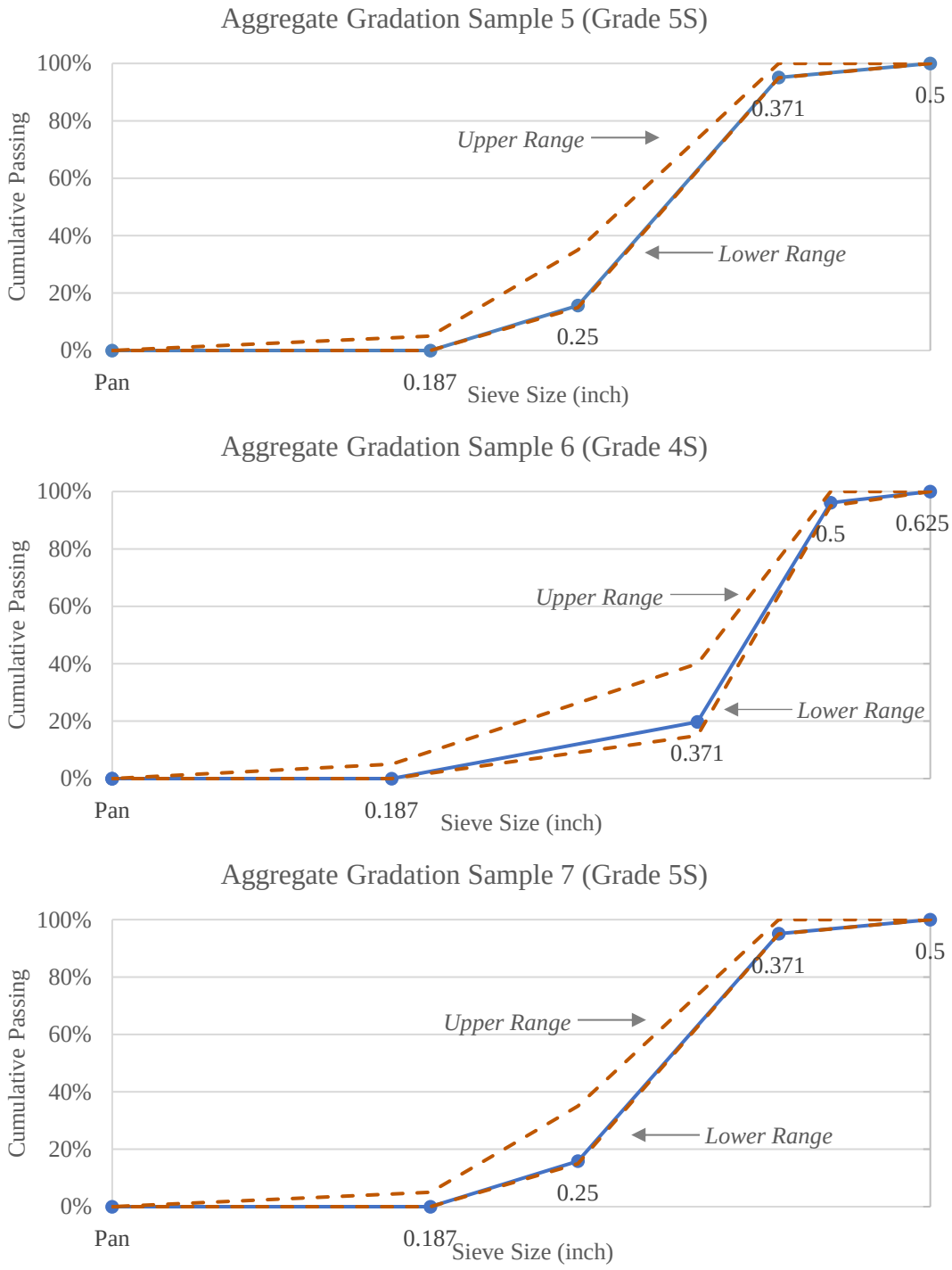
Aggregate Gradation Sample 5 (Grade 5S)
100%
80%
60%
40%
20%
0%
Cumulative Passing
Upper Range
Lower Range
0.5
0.371
0.25
Pan
0.187
Sieve Size (inch)
Aggregate Gradation Sample 6 (Grade 4S)
100%
80%
60%
40%
20%
0%
Cumulative Passing
Upper Range
Lower Range
0.625
0.5
0.371
Pan
0.187
Sieve Size (inch)
Aggregate Gradation Sample 7 (Grade 5S)
100%
80%
60%
40%
20%
0%
Cumulative Passing
Upper Range
Lower Range
0.5
0.371
0.25
Pan
0.187
Sieve Size (inch)

Figure 4.23

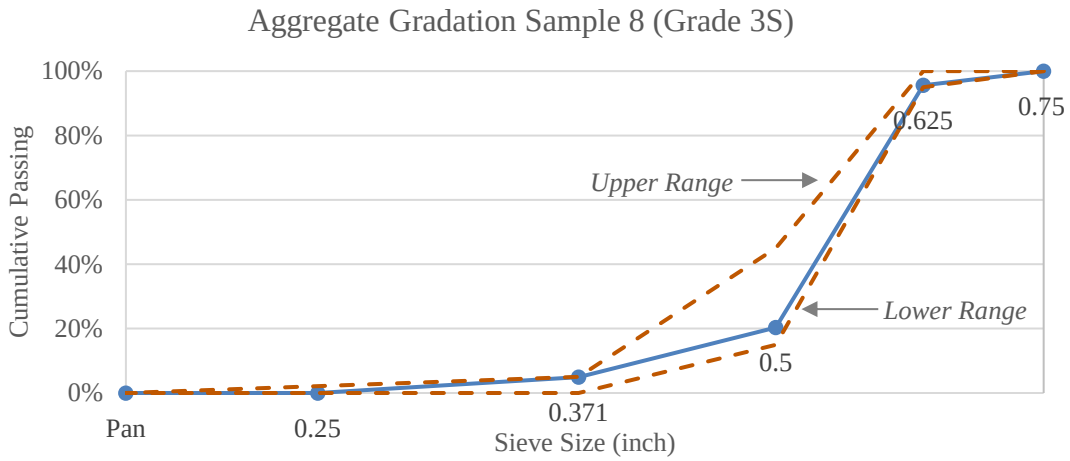

Figure 4.23 Continued

2. Determining the aggregates' unit weights in accordance with TEX-404-A (TxDOT, 2014) and verifying them with the literature as shown in Table 4.4.

Sample	Aggregate Type	Grade	Bulk Density	Literature*
1	Crushed Limestone	4S	2.69 g/cm^3	2.3 – 2.7 *[2.66]*
2	Crushed Sandstone	5S	2.32 g/cm^3	2.2 – 2.8 *[2.32]*
3	Lightweight Aggregate	3L	1.34 g/cm^3	1.0 – 2.0 *[1.40]*
4	Crushed Trap Rock (Basalt)	4S	3.00 g/cm^3	2.8 – 3.0 *[2.90]*
5	Crushed Trap Rock (Basalt)	5S	3.00 g/cm^3	2.8 – 3.0 *[2.90]*
6	Crushed Sandstone	4S	2.74 g/cm^3	2.2 – 2.8 *[2.32]*
7	Crushed Sandstone	5S	2.74 g/cm^3	2.2 – 2.8 *[2.32]*
8	Crushed Limestone	3S	2.66 g/cm^3	2.3 – 2.7 *[2.66]*

*Note: The specific gravity range is recommended by Edumine (Edumine, 2018) and the bracketed value represents the average adopted by University of Washington (Nemati, 2015).

Table 4.4: Densities of Aggregate Samples

3. Measuring the average least dimension (ALD) of the aggregates sampled using the 3D line laser scanner prototype. This method has proven to be faster, more accurate, and more reliable than just using the caliper and conducting the measurements manually (Kouchaki S. , Roshani, Prozzi, Cordoba, & Hernandez., 2018). First, the aggregates are placed on their flattest side on a horizontal surface and scanned using the 3D laser. The raw scanned data is preprocessed to result in the aggregates as shown in Figure 4.24. Afterwards, the aggregate data is pixelated and converted to an image where the boundaries of the aggregates are detected as shown in Figure 4.25. Once each aggregate is identified, the least dimension is determined as the difference in height between the highest point and the lowest point because the aggregates are placed on their flattest side. Finally, the average least dimension of the aggregate sample is determined as the arithmetic mean of the least dimensions of all the scanned aggregates. The algorithm is applied to the 8 samples determining their ALD as shown in Table 4.5

Sample	**S1G4**	**S2G5**	**S3G3L**	**S4G4**	**S5G5**	**S6G4**	**S7G5**	**S8G3**
ALD(mm)	7.96	5.05	8.42	7.42	6.35	7.78	5.68	10.24

Table 4.5: 3D Laser ALD Results

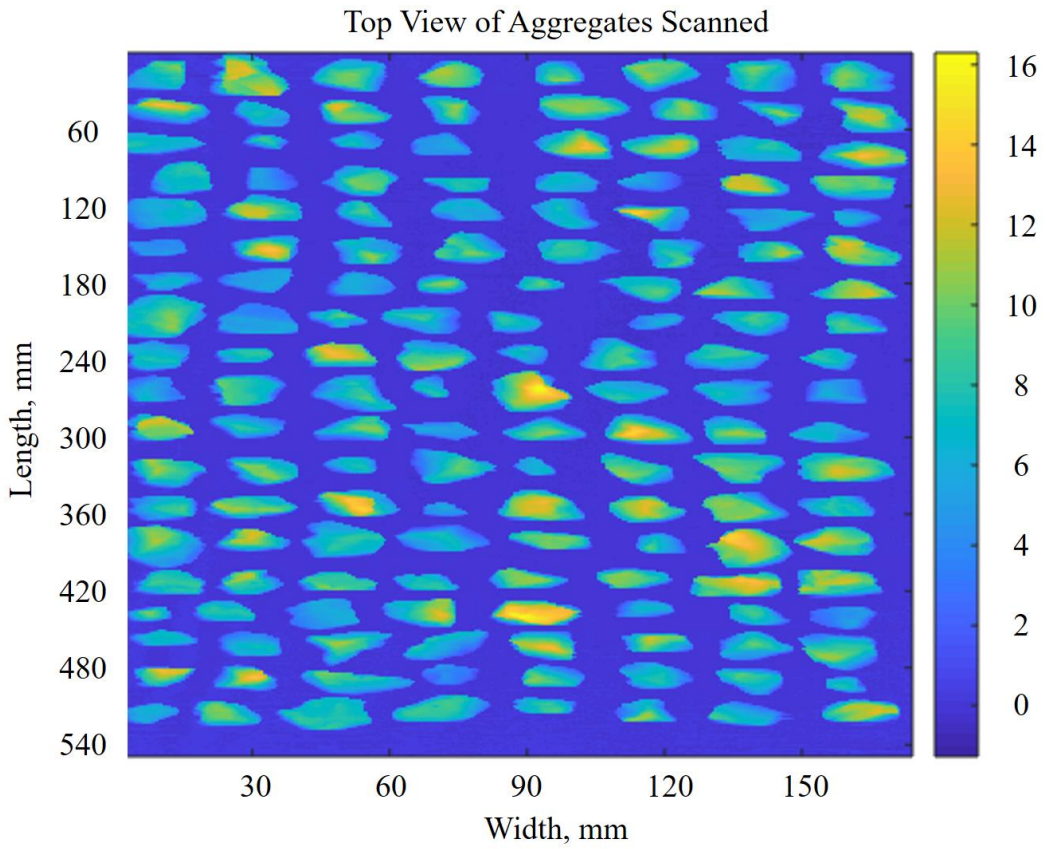

Figure 4.24: Scanned Aggregates for ALD Determination

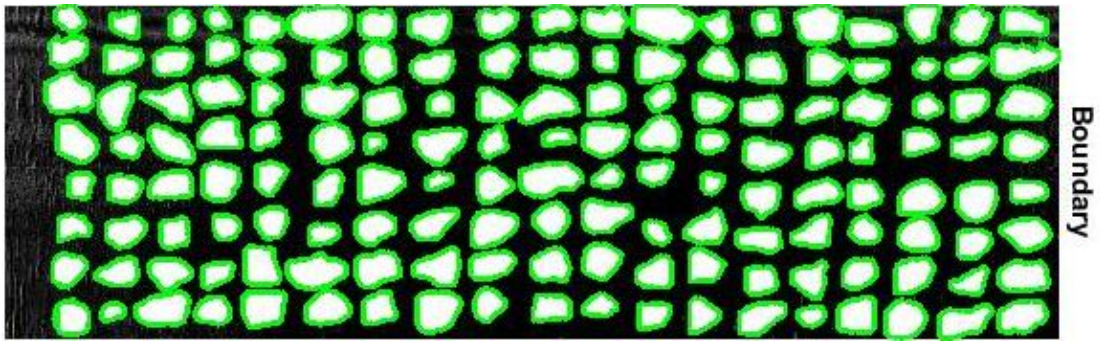

Figure 4.25: Aggregate Boundary Identification

4. Scanning the aggregates at mass increments using the 3D laser scanner and determining the aggregate coverage percentage at each scan.

5. Repeating Steps 3 and 4 until the tray is filled or the target coverage is reached.

Note: In these experiments, the target coverage was 99%. In order to achieve the target, the aggregates were required to overlap and violate the one-stone thick assumption.

The pictures in Figure 4.26 show the buildup of the aggregate scans with each aggregate mass increment until the coverage reaches 99%.

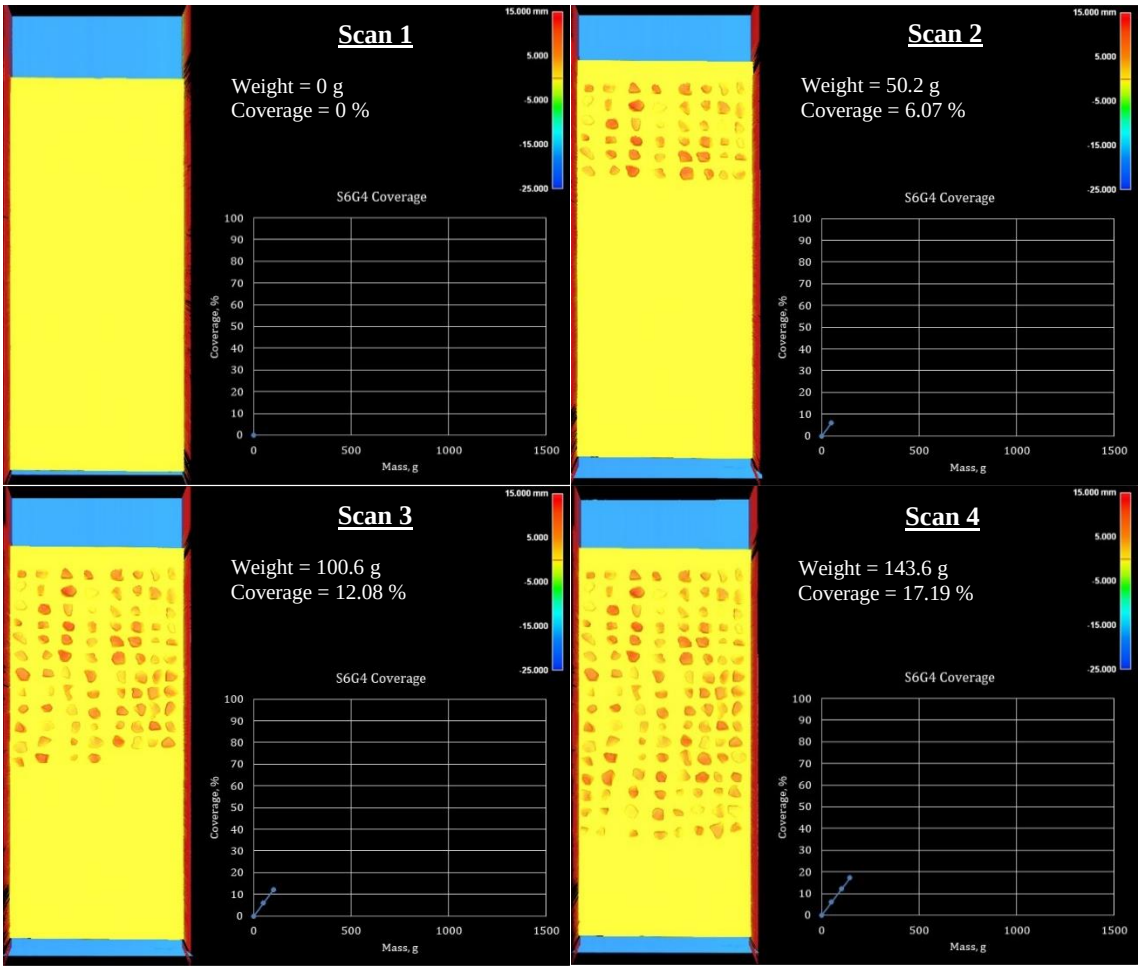

Figure 4.26: Sample 6 Grade 4 Scans From 0 Reach 99% Tray Coverage

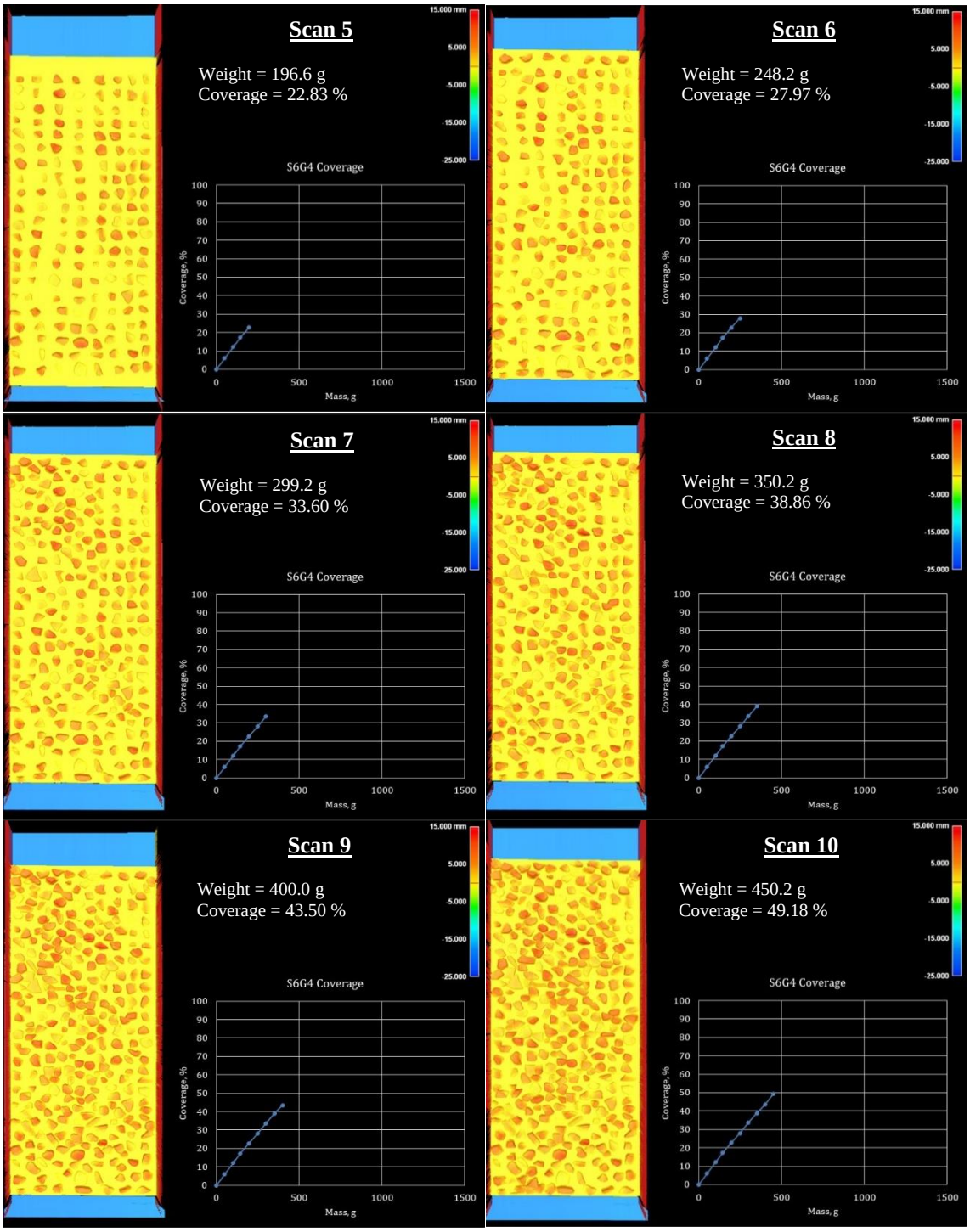

Figure 4.26 Continued

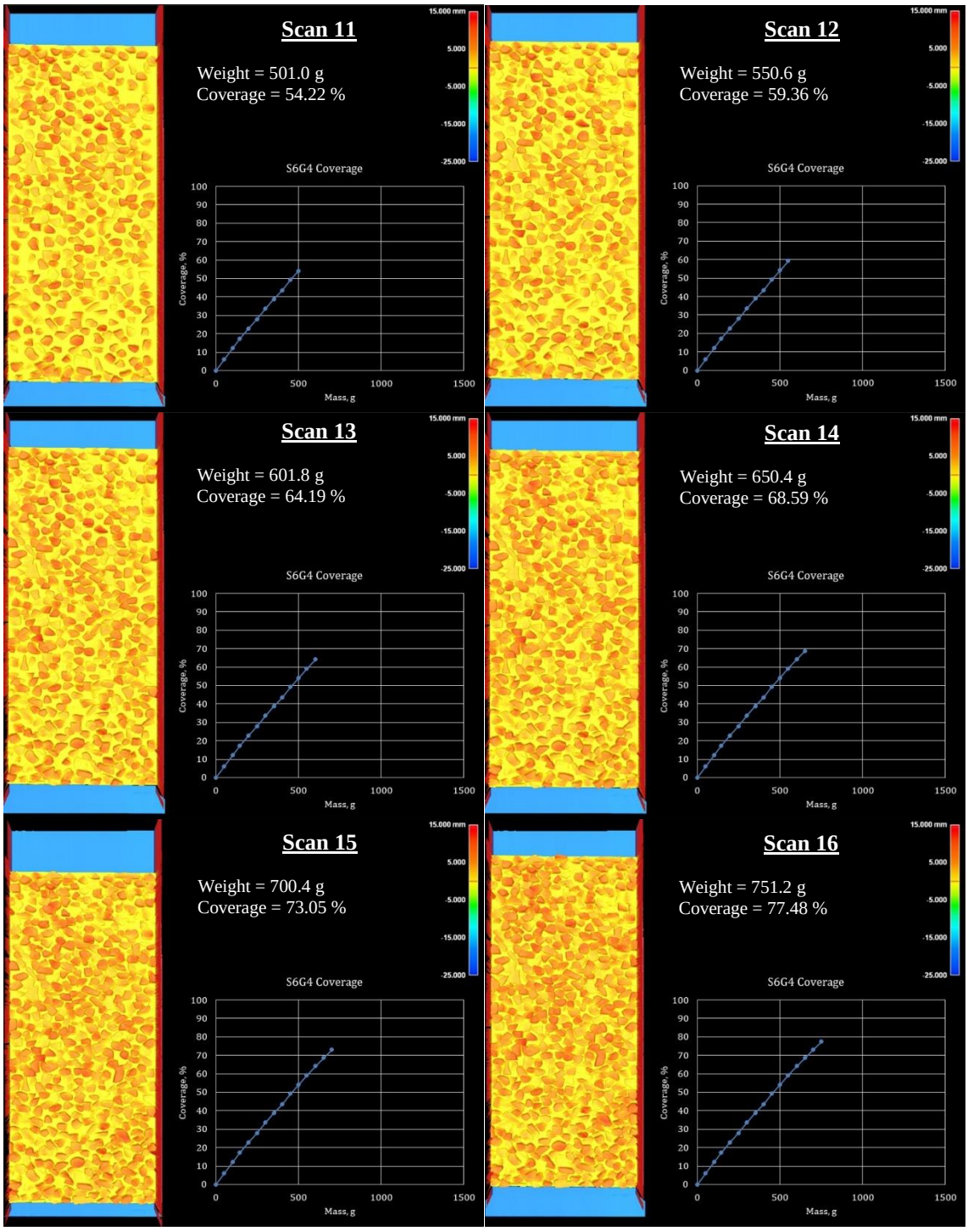

Figure 4.26 Continued

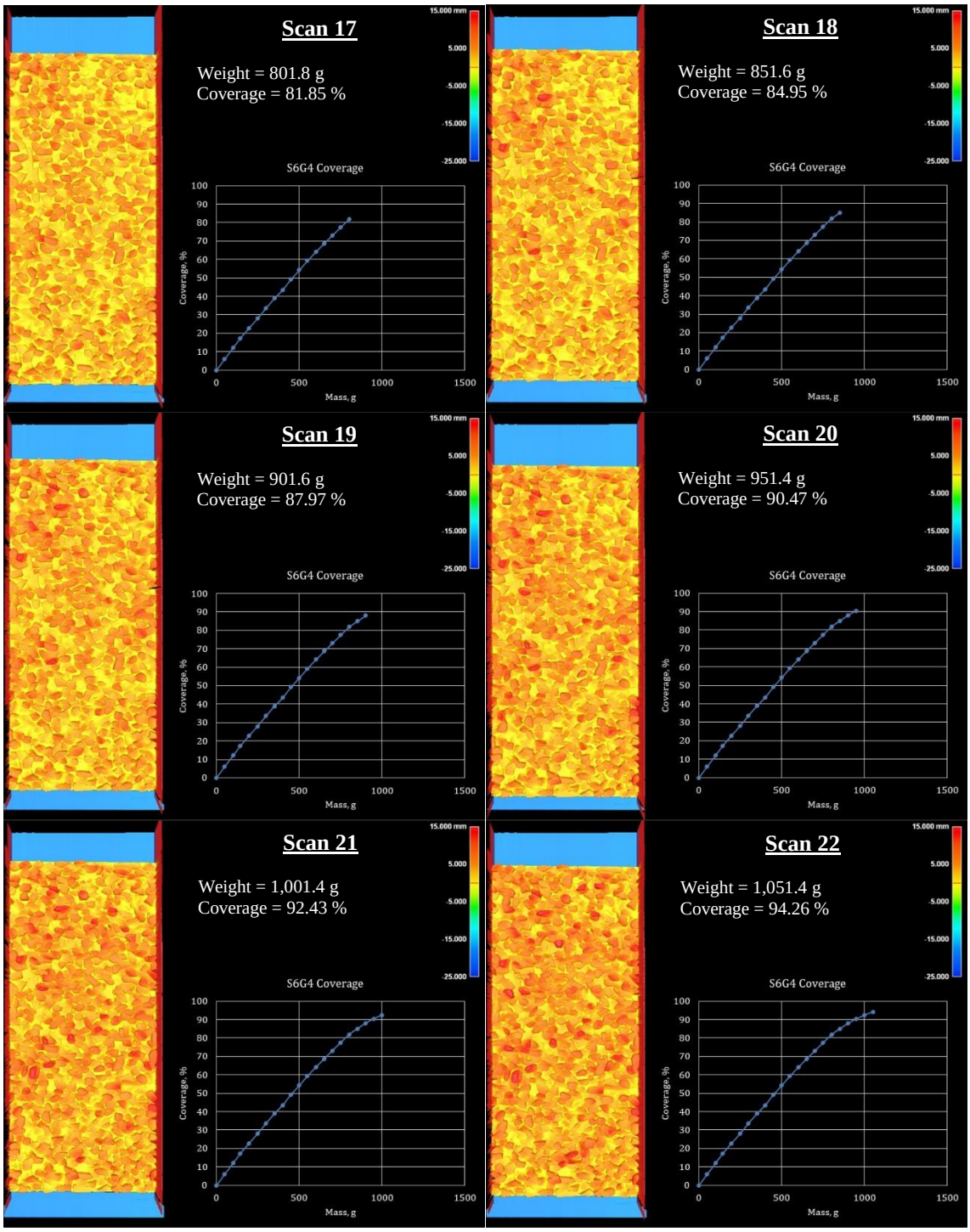

Figure 4.26 Continued

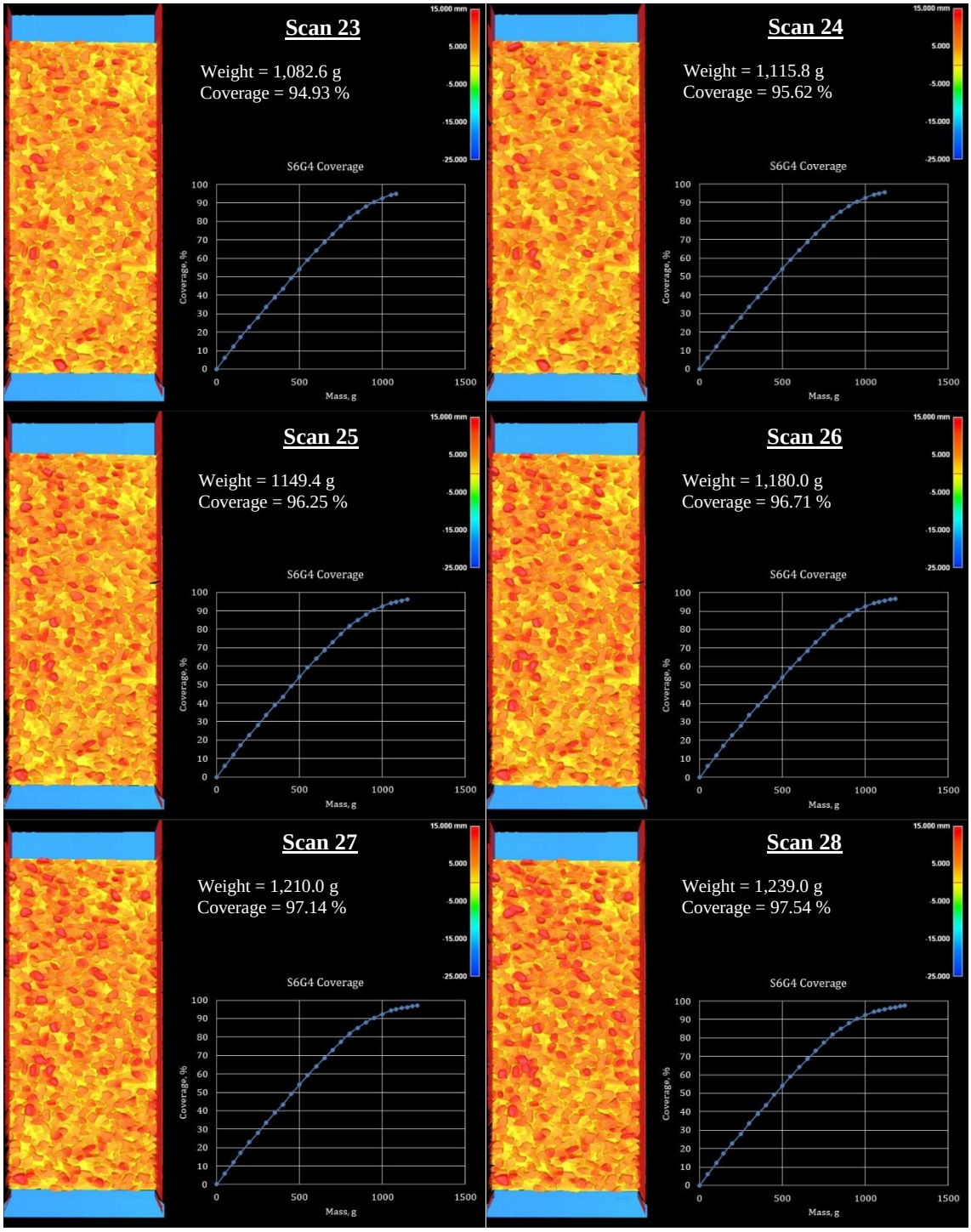

Figure 4.26 Continued

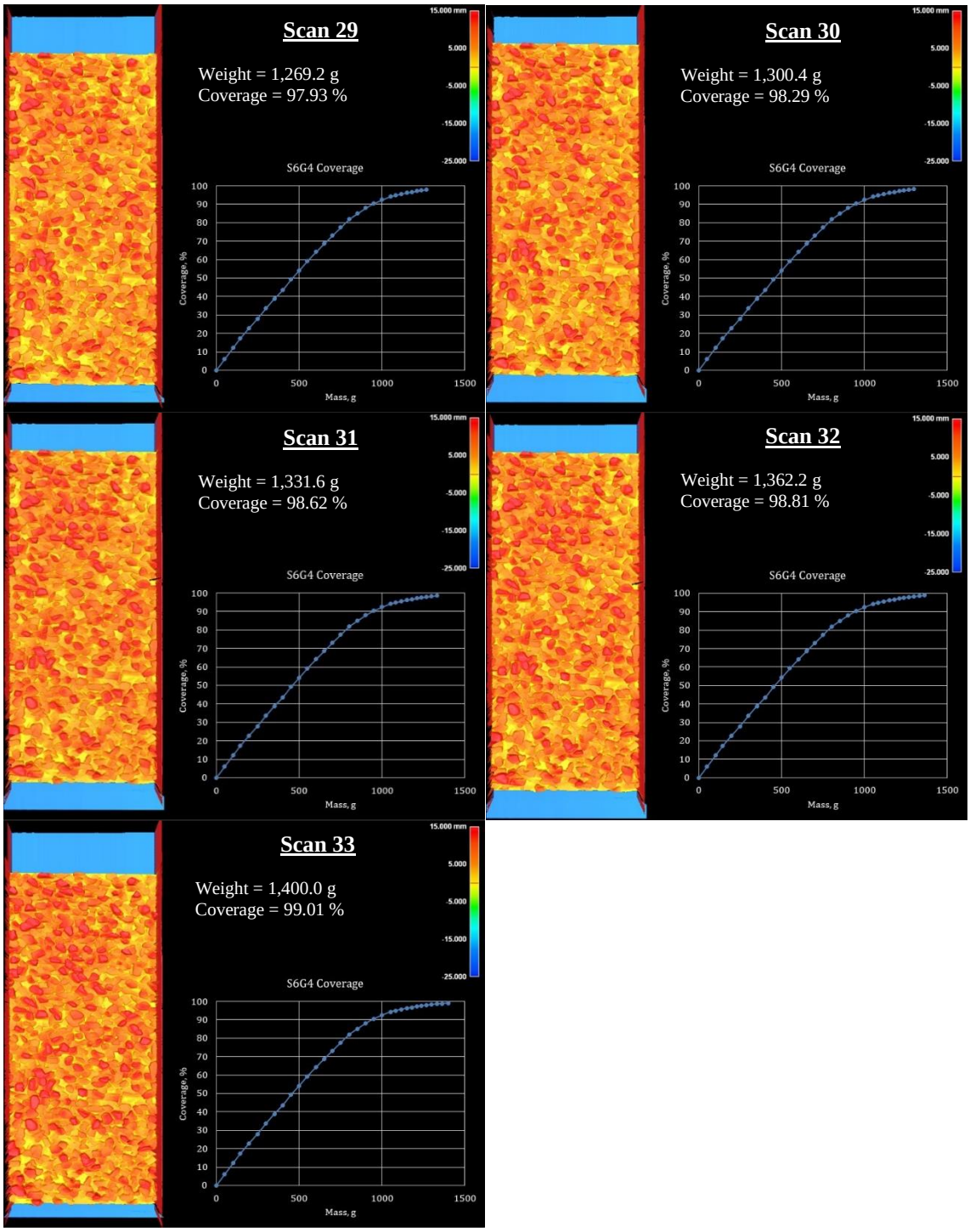

Figure 4.26 Continued

The same process is applied to the eight different aggregate samples. The nine graphs in Figure 4.27 show the raw data for aggregate coverage ratios at different mass increments of these aggregate samples.

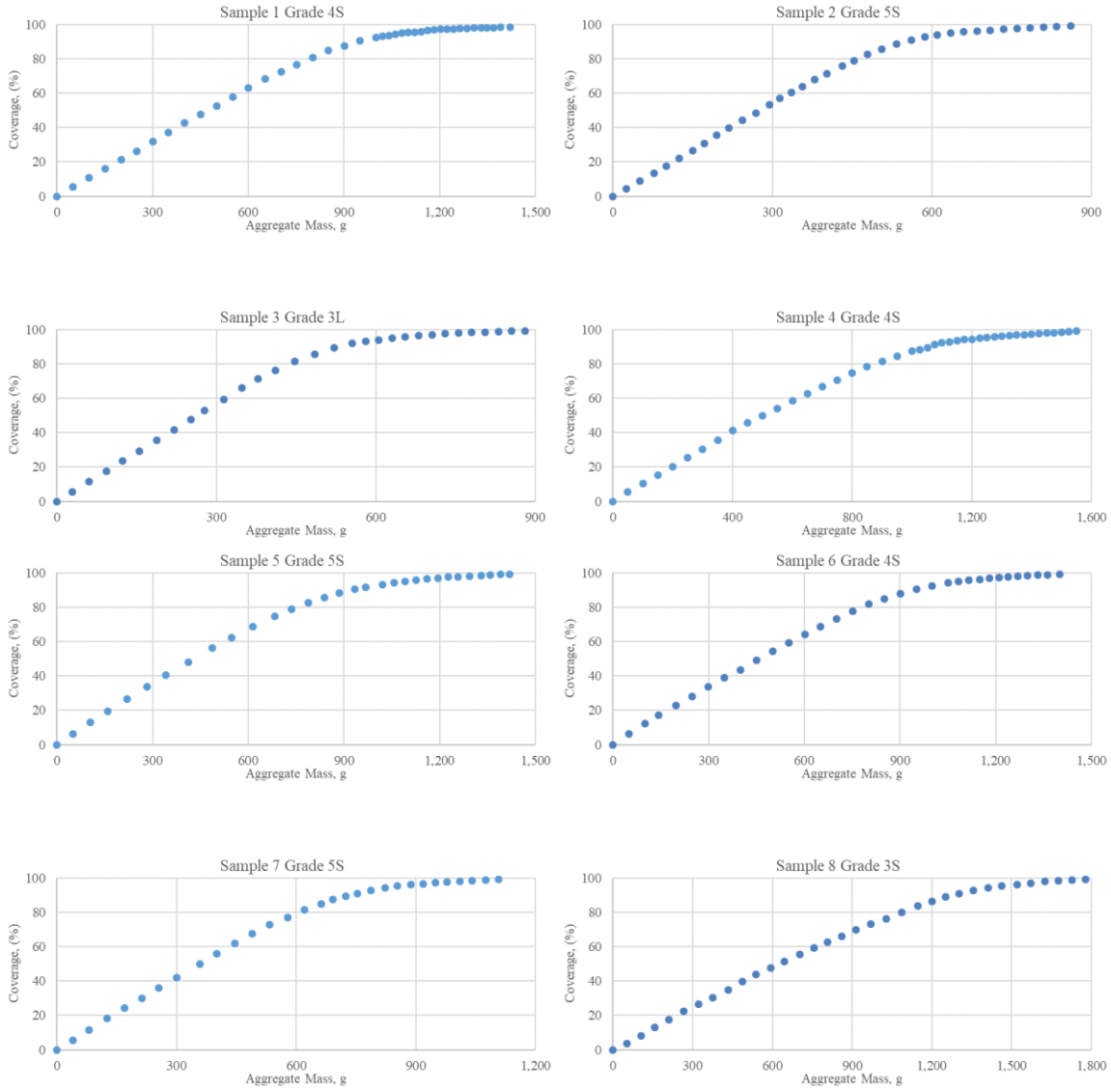

Figure 4.27: Aggregate Coverage Raw Data

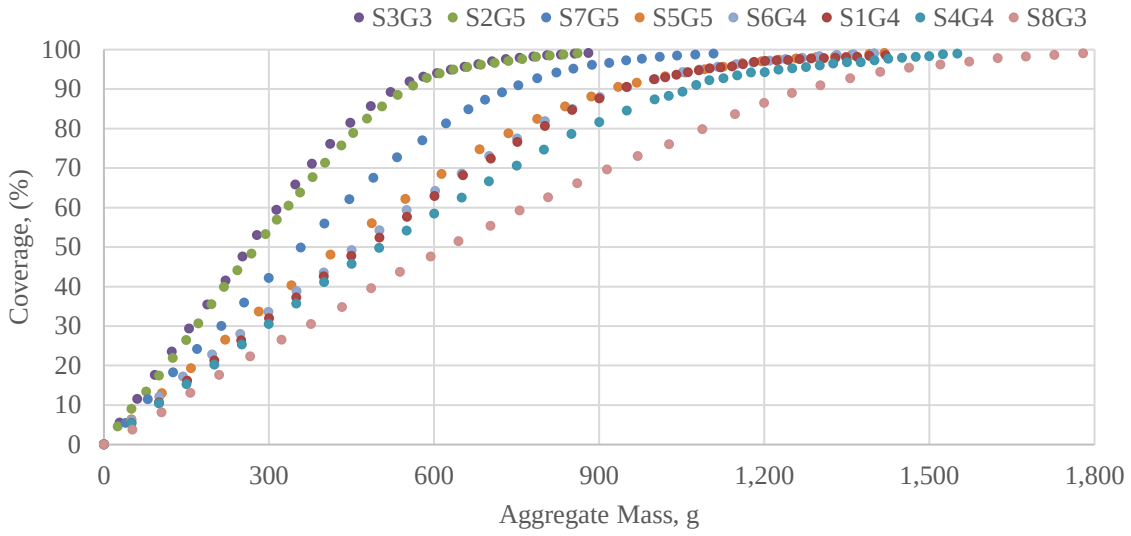

Figure 4.27 Continued

Composite Model for Aggregate Coverage

After collecting aggregate coverage data from scans of the eight different aggregate samples, a predictive model is built in order to:

- Facilitate the determination of the aggregate application rate,
- Improve the reliability of the seal coat design, specifically the AAR, and
- Enhance the consistency between designers by eliminating the need for the subjective human judgment.

Based on the results shown in Figure 4.27, a composite model was developed. This model is a combination of a linear and an exponential function. The rate of increase in aggregate coverage is constant until the tray is packed with aggregates. When the aggregates start to overlap, the rate of increase in aggregate coverage drops exponentially. In other words, when the tray area is clear, and the aggregates are being spread one-aggregate thick, the aggregate coverage fits a linear equation as a function of the aggregate weight as follows:

$$Y = b.x$$

Where Y is the aggregate coverage in percent and x is the cumulative mass in grams.

At a specific point of transition Z (X_0, Y_0) when the tray starts to get covered with aggregates, the coverage tends to follow an exponential function as follows:

$$Y = 100 - (100 - Y_0) \times e^{-d(X - X_0)}$$

For fitting this composite model, several constraints were addressed:

- Origin constraint: The coverage value is null for no aggregate application; i.e. the model passes through the origin.
- Continuity Constraint: The composite model has to be continuous at the point of transition Z. In other words, there are no jumps in coverage values or vertical asymptotes. Specifically, the following applies for coverage at the point Z:

$$Y_0 = bX_0 = 100 - (100 - Y_0) \times e^{-d(X - X_0)}$$

- Differentiability Constraint: The composite model is required to be differentiable at all mass points belonging to its domain. This implies that the function must have a non-vertical tangent line at each point in its domain and be relatively smooth without any breaks, bends, or cusps. Specifically, the derivative of Y at the point of transition Z, which is defined by two functions, should be the same.

  $\frac{dY_1}{dx} = b$; hence, $\frac{dY_1}{dx}|_{x=X_0} = b$

  $\frac{dY_2}{dx} = (100 - Y_0) \times d \times e^{d(X_0 - x)}$; hence, $\frac{dY_2}{dx}|_{x=X_0} = (100 - Y_0) \times d$

  At $Z(X_0, Y_0)$: $\frac{dY_1}{dx} = \frac{dY_2}{dx}$

  $\boldsymbol{(100 - Y_0) \times d = b}$

  The graph in Figure 4.28 is an example of the composite model with all constraints satisfied. In this example, the values of the fitting parameters b and d are taken as 0.1 and 0.004 respectively.

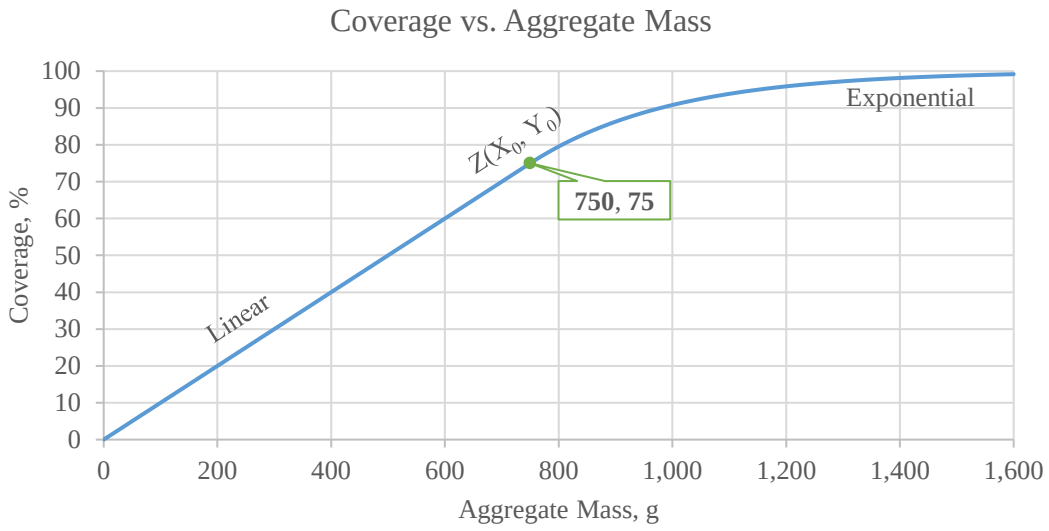

Figure 4.28: Composite Model Example

To implement this model, three different approaches were used to fit the proposed composite equations to the data collected. The three approaches are discussed in order of goodness-of-fit from the model with the highest sum of square errors (SSE) to the model with the lowest SSE, i.e. best fitting model.

Fitting Approach 1

The first fitting approach finds a good fit for the exponential tail first, then extrapolates the linear function. In order to do so, both d and Y_0 are iterated to find the best fit; then b is back-calculated for. First, Y_0 is iterated from the first data point to the last one with twenty sub-points increments. With every iteration, the raw points that are greater than Y_0 are considered for the exponential fit to determine the regression parameter d. Afterwards, the slope of the linear line, b, is determined as $\mathbf{b = (100 - Y_0) \times d}$ which is obtained from the continuity and differentiability constraints. Table 4.6 and Figure 4.29 show the composite model fitting parameters.

Sample	Bulk Density	ALD	b	d	Y_0	SSE
S1G4	2.69 g/cm^3	7.96	0.1023	0.0043	76.4	20.0
S2G5	2.32 g/cm^3	5.05	0.1756	0.0073	76.0	19.3
S3G3L	1.34 g/cm^3	8.42	0.1866	0.0070	73.4	5.0
S4G4	3.00 g/cm^3	7.42	0.0934	0.0039	75.8	85.7
S5G5	3.00 g/cm^3	6.35	0.1092	0.0042	74.1	63.4
S6G4	2.74 g/cm^3	7.78	0.1027	0.0047	77.9	81.1
S7G5	2.74 g/cm^3	5.68	0.1336	0.0058	76.8	42.7
S8G3	2.66 g/cm^3	10.24	0.0730	0.0042	82.5	192.2
						509.4

Table 4.6: Approach One Model Fit

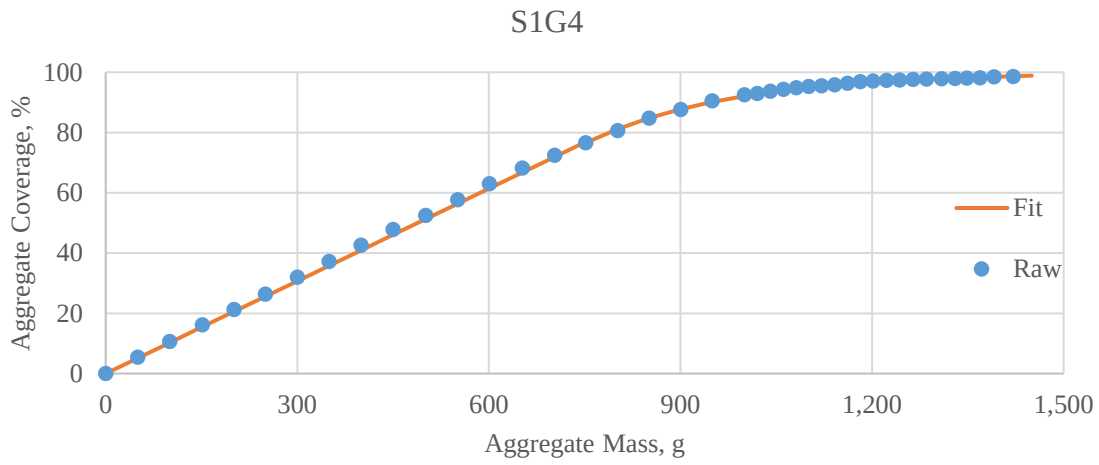

Figure 4.29: Fitting the Composite Model Using Approach One

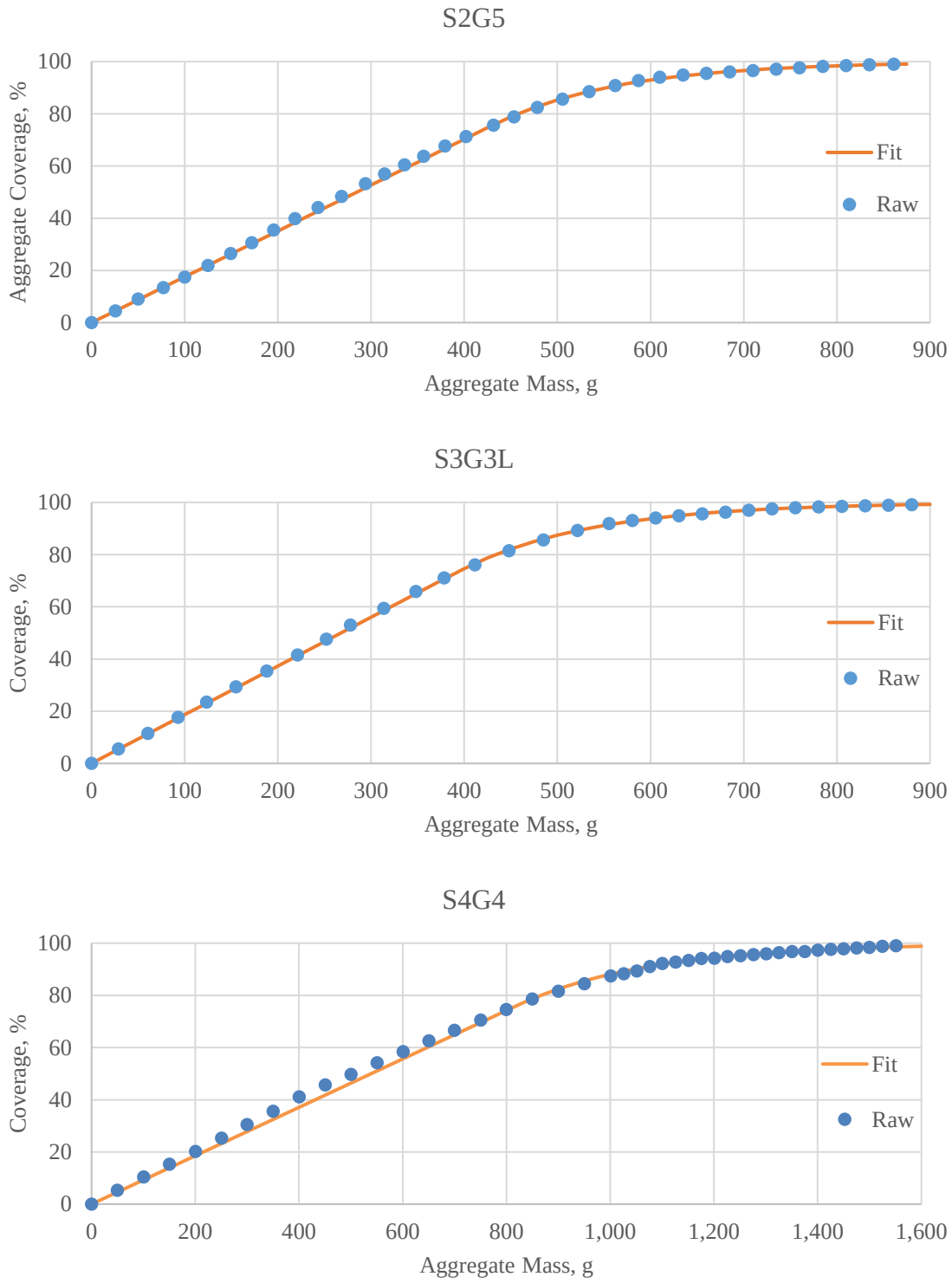

Figure 4.29 Continued

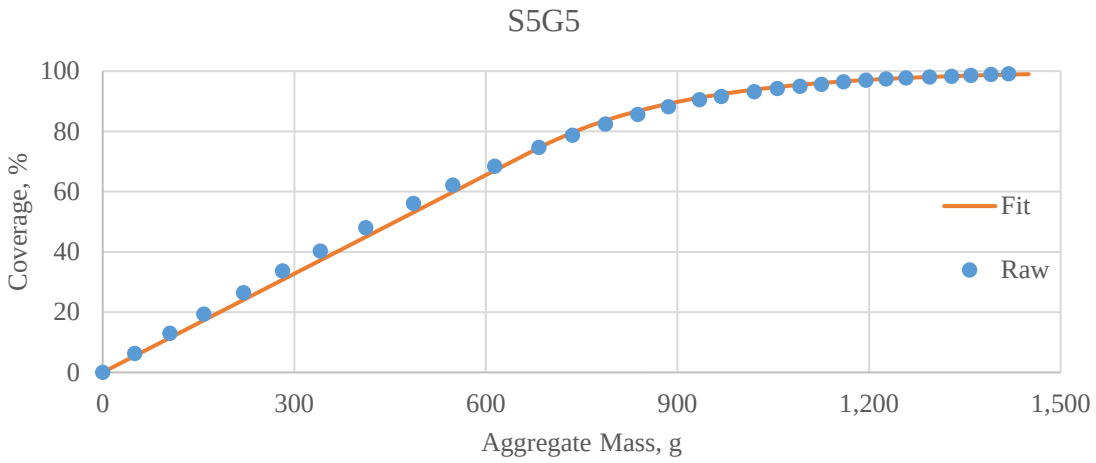

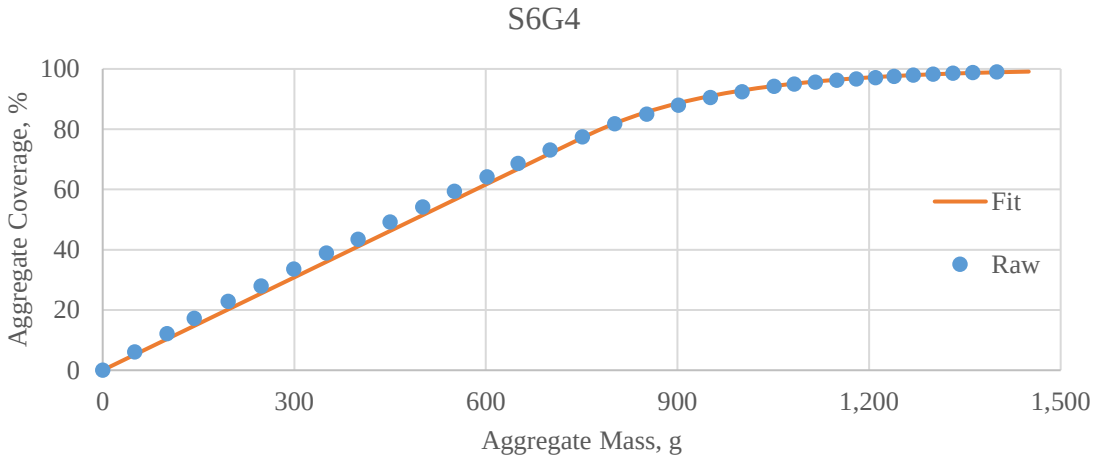

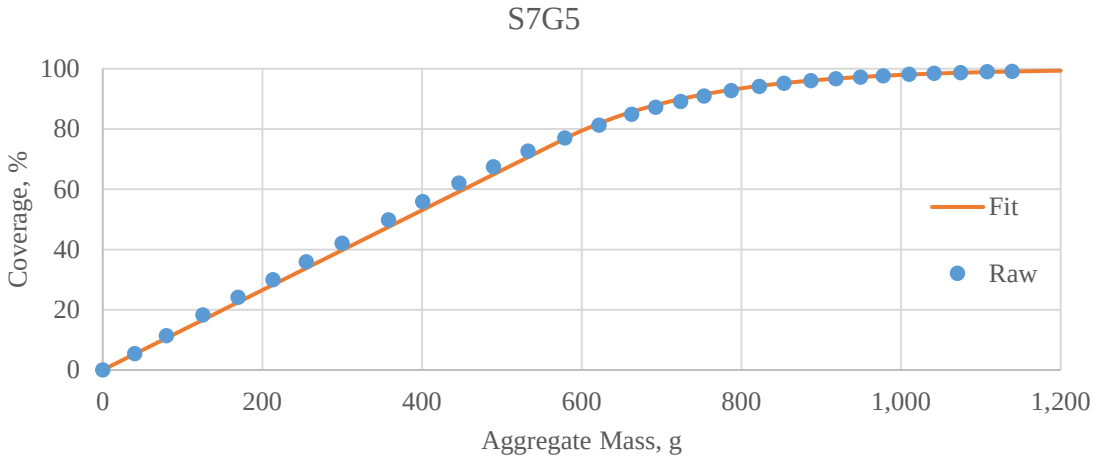

Figure 4.29 Continued

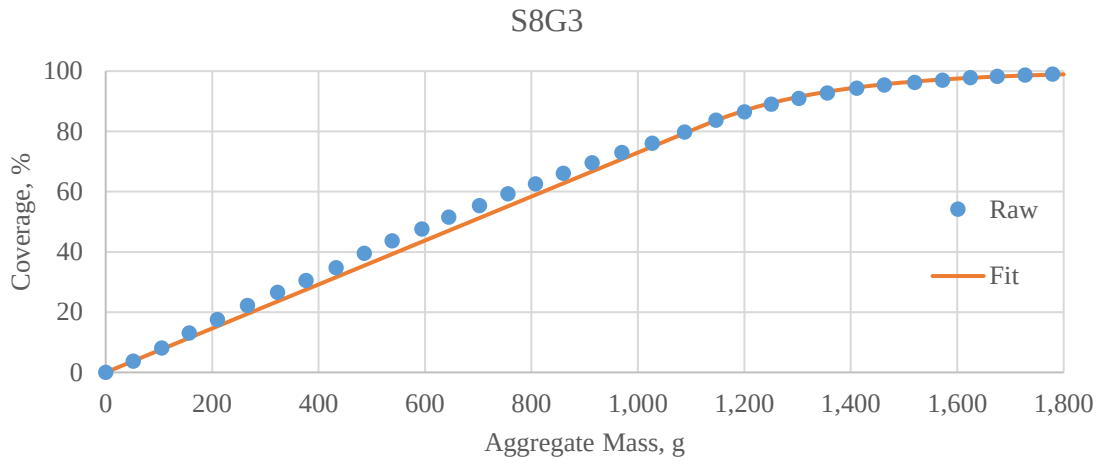

Figure 4.29 Continued

After fitting the aggregate composite model to the raw data samples, a further regression analysis was conducted to explain the fitting parameters b and d using the two measured aggregate features: ALD and density. Accordingly, agencies can simply measure the density and the average least dimension of the aggregates and predict the aggregate application rate that is recommended for a specific coverage level. The regression results of the first approach are the following:

$$b = 0.4044 - 0.06664 \times \rho - 0.0153 \times ALD$$

$$R^2 = 99.8\%;\ \text{Standard Error} = 0.0020$$

$$d = 0.0142 - 0.0022 \times \rho - 0.0005 \times ALD$$

$$R^2 = 91.0\%;\ \text{Standard Error} = 0.0005$$

As the density increases, both b and d decrease. That is, as the aggregates are denser, more aggregate weight is needed to cover the same area. As the ALD increases, both b and d decrease too. Bigger aggregate particles require more weight to cover the same area. The transition point was back-calculated based on the previously defined constraint.

$$Y_0 = 100 - \frac{b}{d} = 100 - \frac{0.4044 - 0.06664 \times \rho - 0.0153 \times ALD}{0.0142 - 0.0022 \times \rho - 0.0005 \times ALD}$$

Afterwards, the prediction model was tested against the given raw data to check its goodness-of-fit. In order to do so, the fitted values, b and d, were calculated using the regression equations presented above. Table 4.7 and Figure 4.30 show the parameters obtained from both the individual fit and the predictive model.

Sample	ρ	ALD	Individual Fit				Predictive Model			
			b	d	Y_0	SSE	b	d	Y_0	SSE
S1G4	2.69	7.96	0.1023	0.0043	76.4	20.0	0.1044	0.0046	77.3	22.8
S2G5	2.32	5.05	0.1756	0.0073	76.0	19.3	0.1734	0.0068	74.4	53.2
S3G3L	1.34	8.42	0.1866	0.0070	73.4	5.0	0.1870	0.0073	74.5	6.6
S4G4	3.00	7.42	0.0934	0.0039	75.8	85.7	0.0920	0.0042	78.0	131.7
S5G5	3.00	6.35	0.1092	0.0042	74.1	63.4	0.1085	0.0047	76.8	90.5
S6G4	2.74	7.78	0.1027	0.0047	77.9	81.1	0.1038	0.0046	77.3	59.9
S7G5	2.74	5.68	0.1336	0.0058	76.8	42.7	0.1358	0.0056	75.6	26.5
S8G3	2.66	10.24	0.0730	0.0042	82.5	192.2	0.0716	0.0036	80.1	310.6
						509.4				**701.9**

Table 4.7: Approach One Predictive Model Check

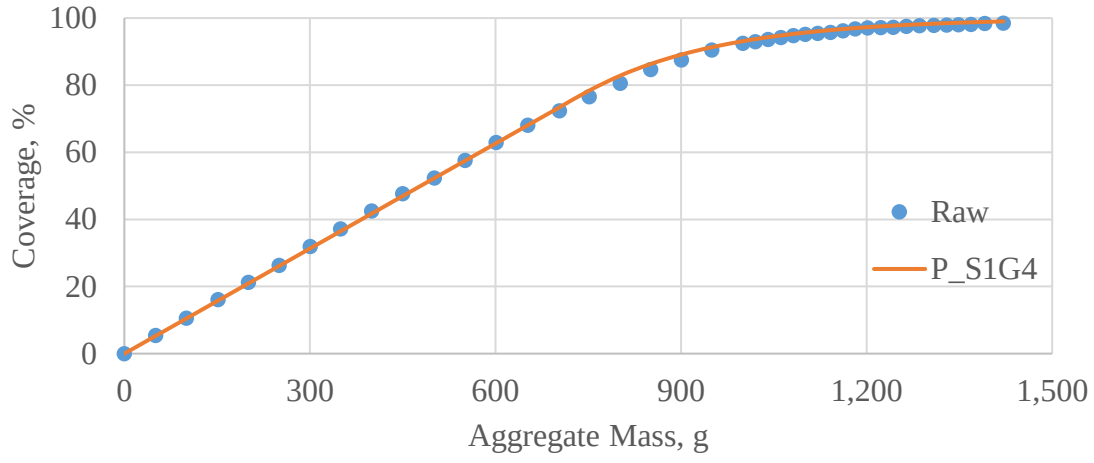

Figure 4.30: Predictive Model Graphs Using Approach One

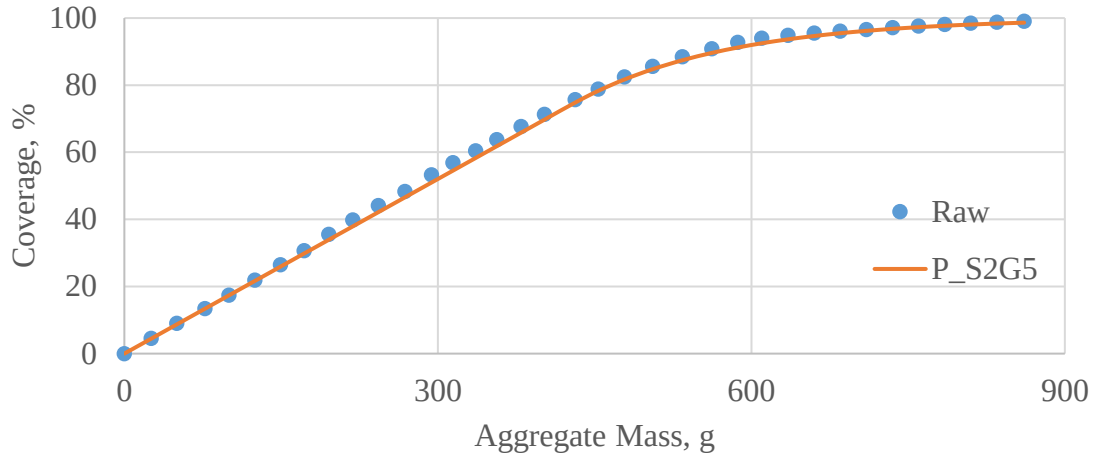

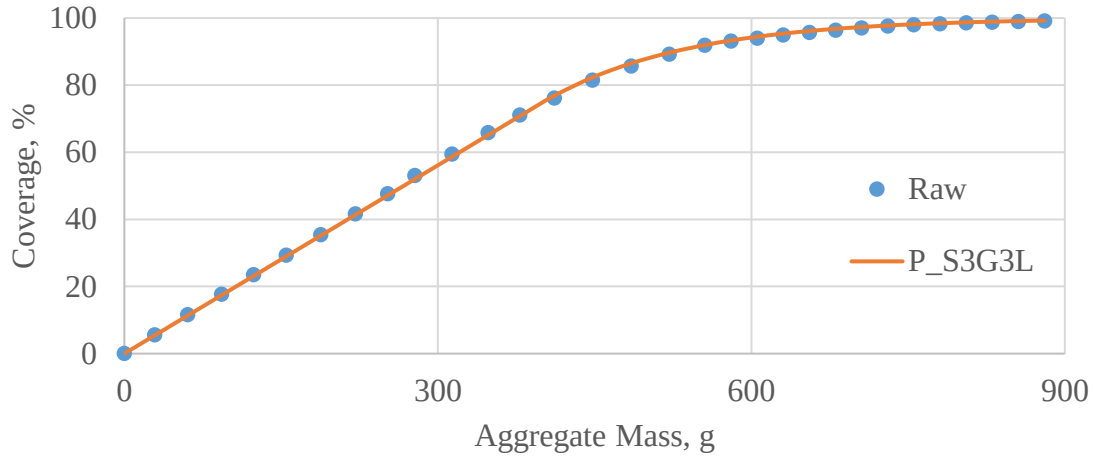

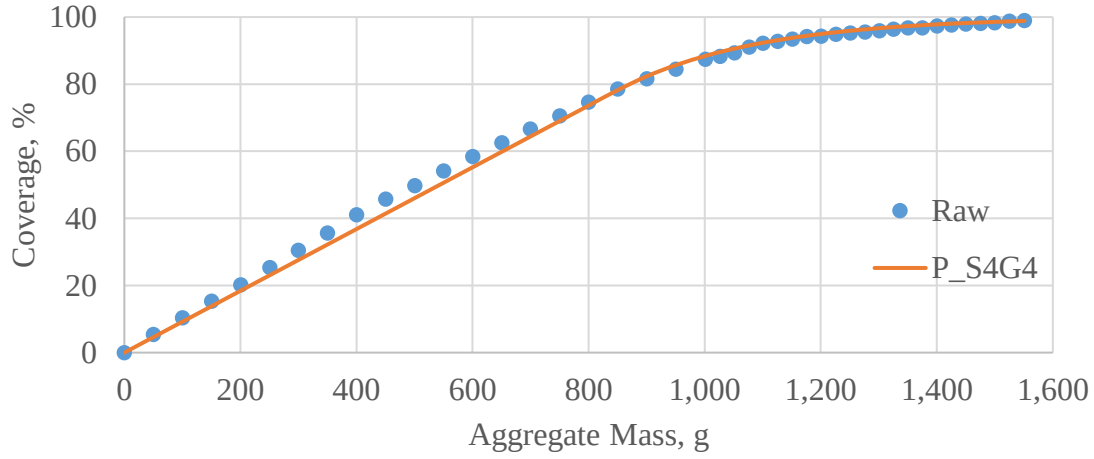

Figure 4.30 Continued

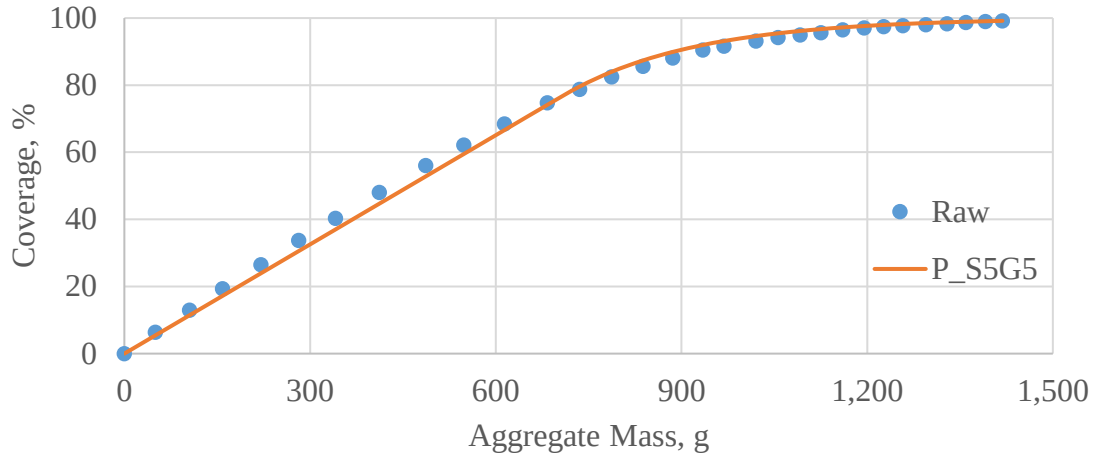

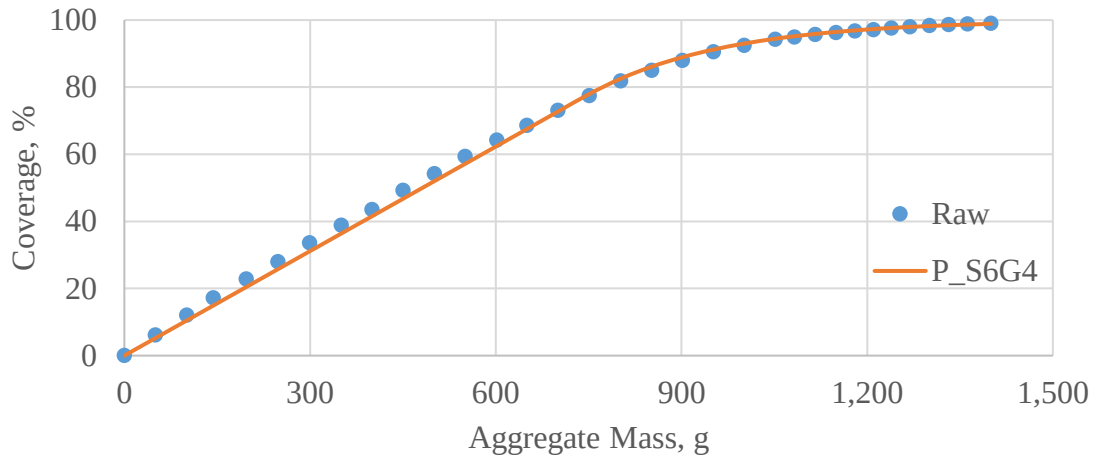

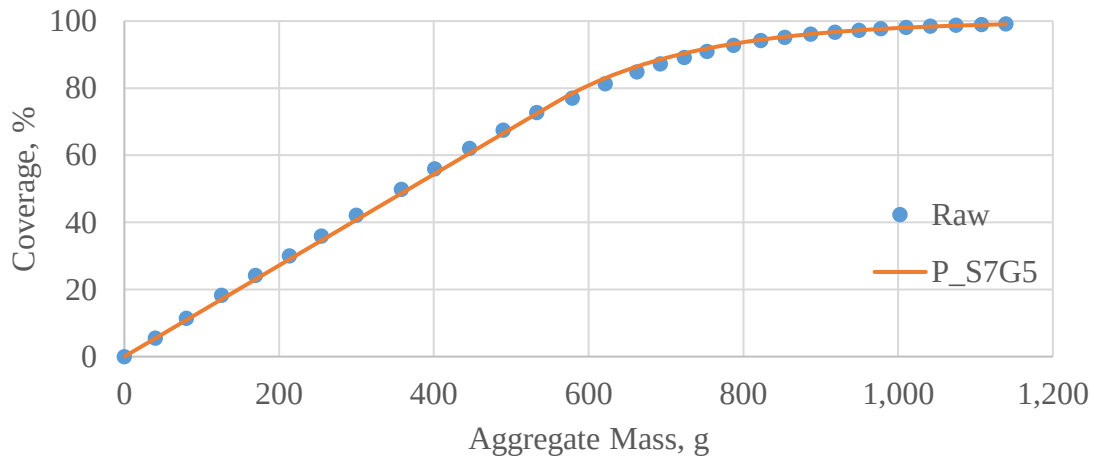

Figure 4.30 Continued

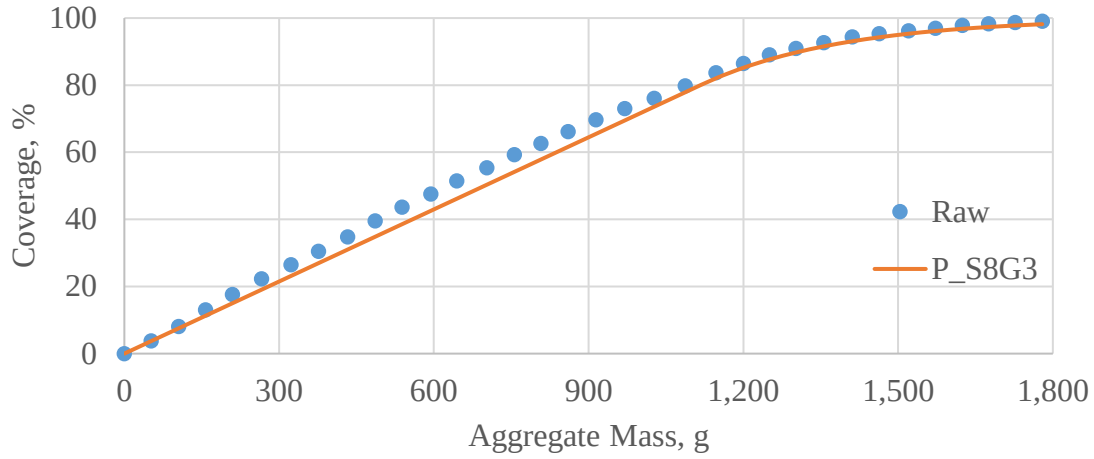

Figure 4.30 Continued

The concern with this approach is that the initial composite model fitting is based on a portion of the data that best-fits the exponential tail whereas the linear part is extrapolated. These models can be improved by fitting the whole composite model at once and back-calculating Y_0.

Fitting Approach 2

This approach aims at finding the best composite fit that results in the least sum of square error across the coverage data for each aggregate sample. In this case, both fitting parameters b and d are iterated, using Excel's Solver tool, to minimize the sum of square errors between the fit and the raw data while maintaining the constraints. Afterwards, the transition point, Y_0, is back-calculated using the previously discussed constraint $Y_0 = 100 - \frac{b}{d}$. Table 4.8 and Figure 4.31 show the composite model fitting parameters.

Sample	Bulk Density	ALD	b	d	Y_0	SSE
S1G4	2.69 g/cm^3	7.96	0.1040	0.0042	75.1	10.9
S2G5	2.32 g/cm^3	5.05	0.1784	0.0069	74.3	9.4
S3G3L	1.34 g/cm^3	8.42	0.1883	0.0068	72.4	2.8
S4G4	3.00 g/cm^3	7.42	0.0967	0.0033	71.1	46.7
S5G5	3.00 g/cm^3	6.35	0.1138	0.0036	68.3	27.9
S6G4	2.74 g/cm^3	7.78	0.1069	0.0040	73.0	32.9
S7G5	2.74 g/cm^3	5.68	0.1378	0.0049	72.1	16.5
S8G3	2.66 g/cm^3	10.24	0.0774	0.0030	74.1	58.9
						205.9

Table 4.8: Approach Two Model Fit

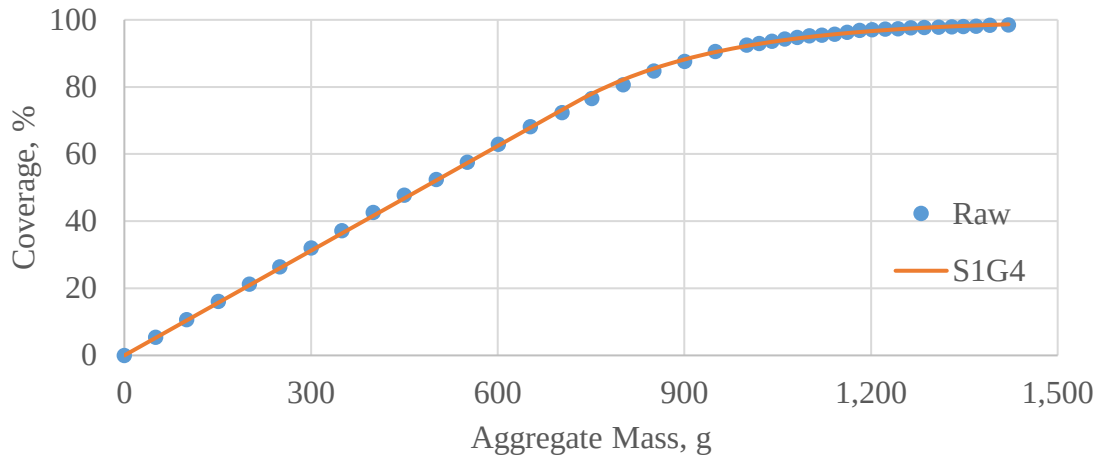

Figure 4.31: Fitting the Composite Model Using Approach Two

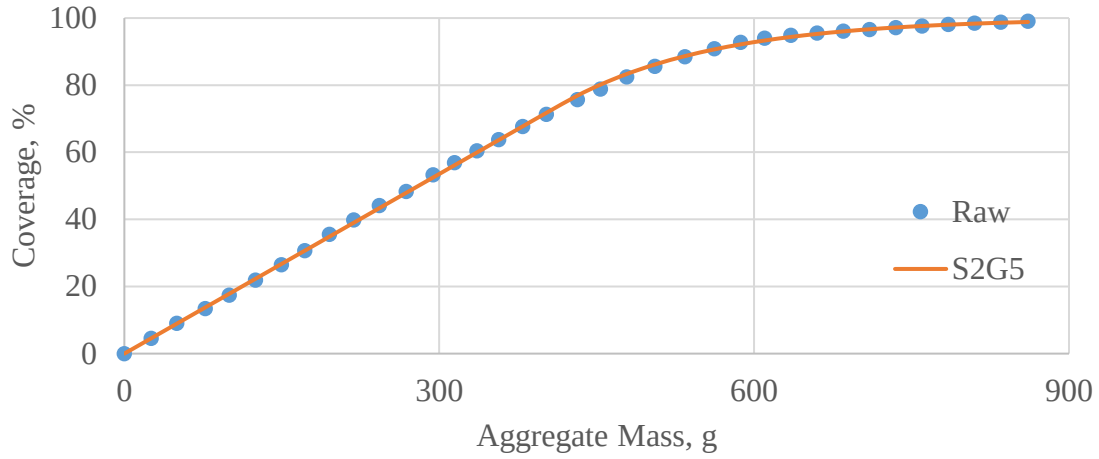

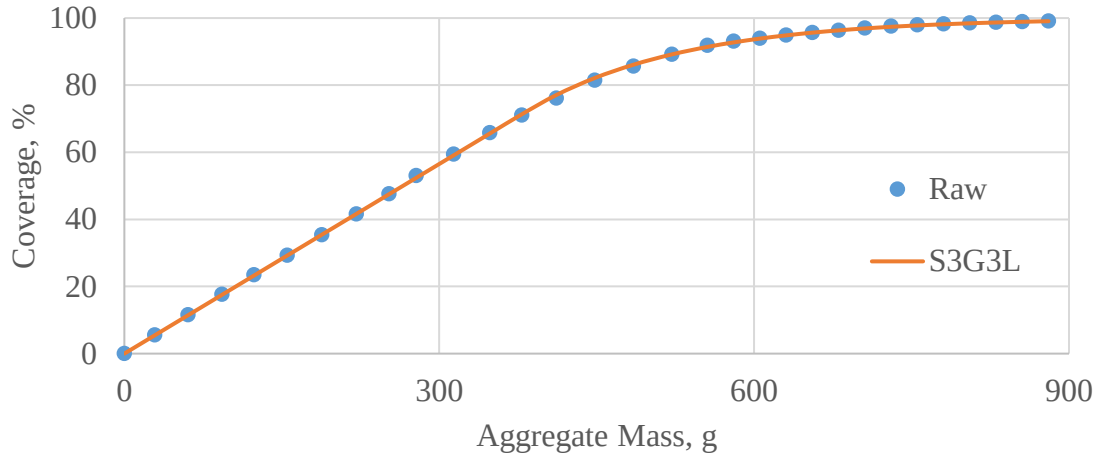

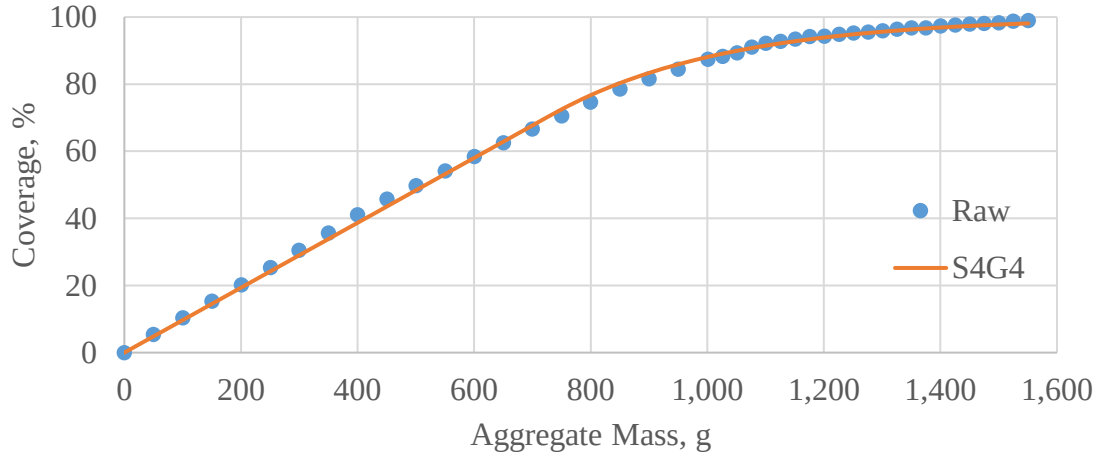

Figure 4.31 Continued

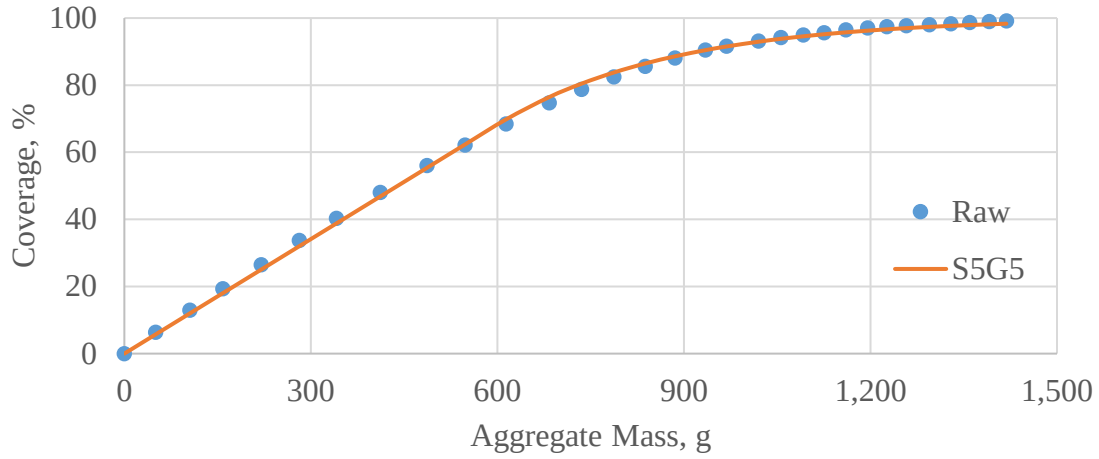

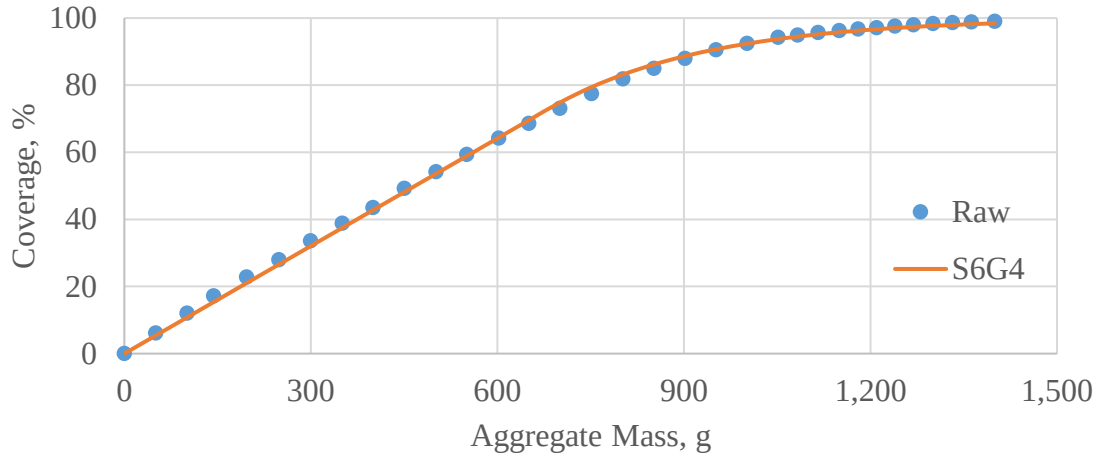

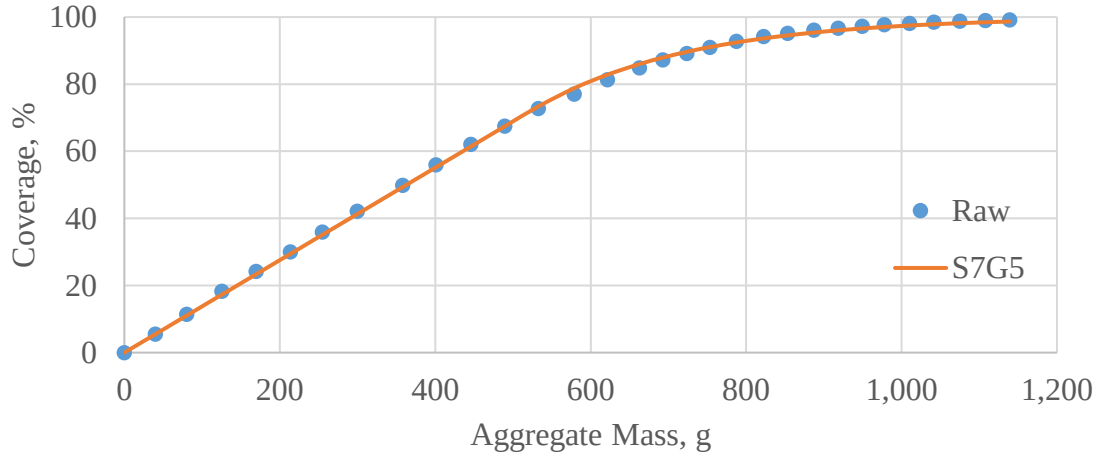

Figure 4.31 Continued

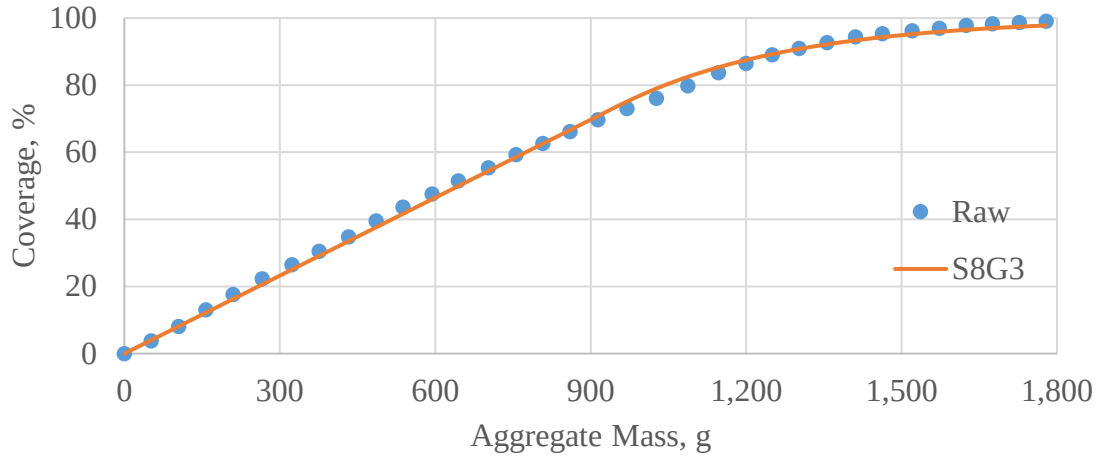

Figure 4.31 Continued

After fitting the aggregate composite model to the raw data samples, a further regression analysis, similar to approach 1, was conducted in order to explain the fitting parameters b and d using the two measured aggregate features. The regression results are the following:

$$b = 0.4036 - 0.0649 \times \rho - 0.0152 \times ALD$$

$$R^2 = 99.6\%;\ \text{Standard Error} = 0.0024$$

$$d = 0.0140 - 0.0025 \times \rho - 0.0005 \times ALD$$

$$R^2 = 96.0\%\ \text{Standard Error} = 0.0004$$

As mentioned in the first approach, when the density and the ALD increase, both b and d decrease. The transition point is back-calculated using the previously identified constraint.

$$Y_0 = 100 - \frac{b}{d} = 100 - \frac{0.4036 - 0.0649 \times \rho - 0.0152 \times ALD}{0.0140 - 0.0025 \times \rho - 0.0005 \times ALD}$$

Afterwards, the prediction model was tested against the given raw data to check the goodness-of-fit. Table 4.9 and Figure 4.32 show the fitting parameters from both the individual fit and the predictive model.

Sample	ρ	ALD	Individual Fit				Predictive Model			
			b	d	Y_0	SSE	b	d	Y_0	SSE
S1G4	2.69	7.96	0.1040	0.0042	75.1	10.9	0.1079	0.0039	72.7	53.4
S2G5	2.32	5.05	0.1784	0.0069	74.3	9.4	0.1763	0.0065	72.7	26.4
S3G3L	1.34	8.42	0.1883	0.0068	72.4	2.8	0.1886	0.0071	73.4	4.5
S4G4	3.00	7.42	0.0967	0.0033	71.1	46.7	0.0960	0.0035	72.3	48.4
S5G5	3.00	6.35	0.1138	0.0036	68.3	27.9	0.1124	0.0040	72.2	41.6
S6G4	2.74	7.78	0.1069	0.0040	73.0	32.9	0.1074	0.0039	72.6	33.6
S7G5	2.74	5.68	0.1378	0.0049	72.1	16.5	0.1394	0.0051	72.5	23.2
S8G3	2.66	10.24	0.0774	0.0030	74.1	58.9	0.0752	0.0028	73.0	116.1
						205.9				**347.3**

Table 4.9: Approach Two Predictive Model Check

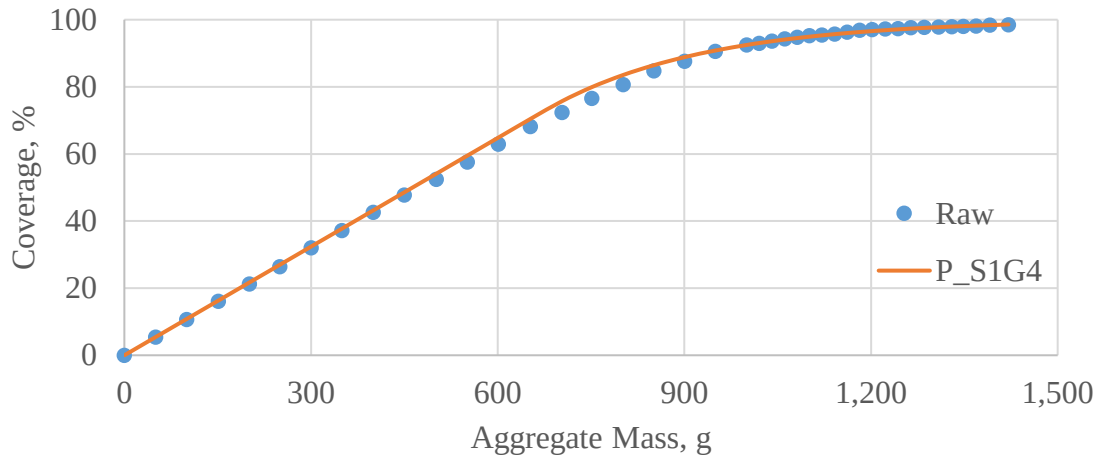

Figure 4.32: Predictive Model Graphs Using Approach Two

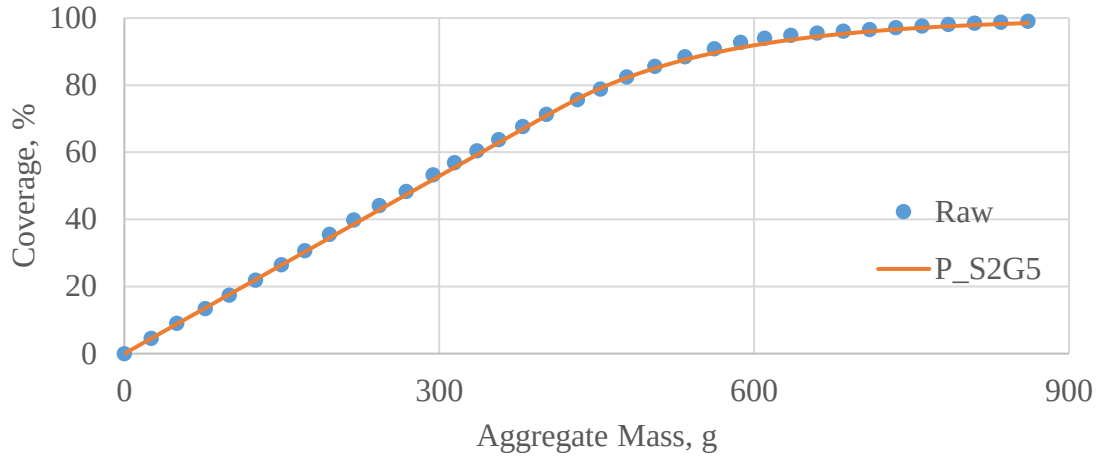

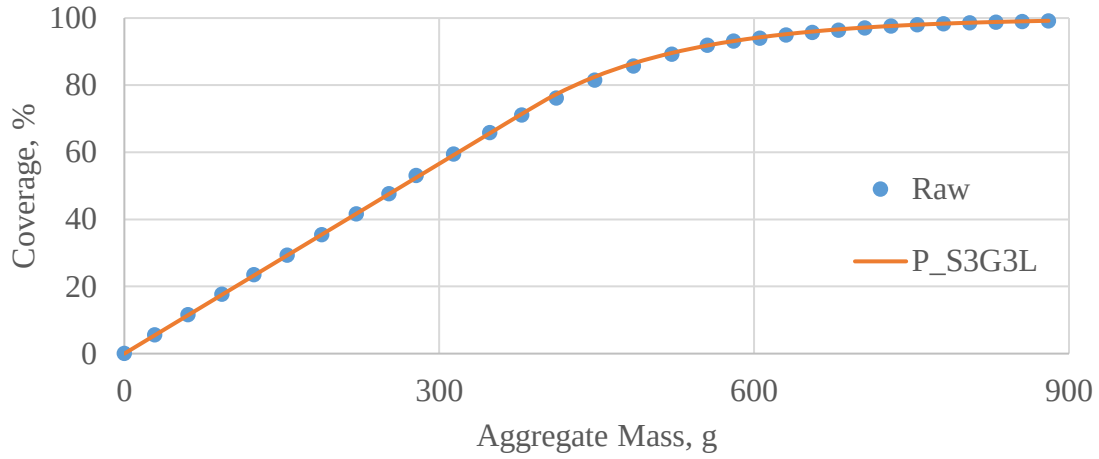

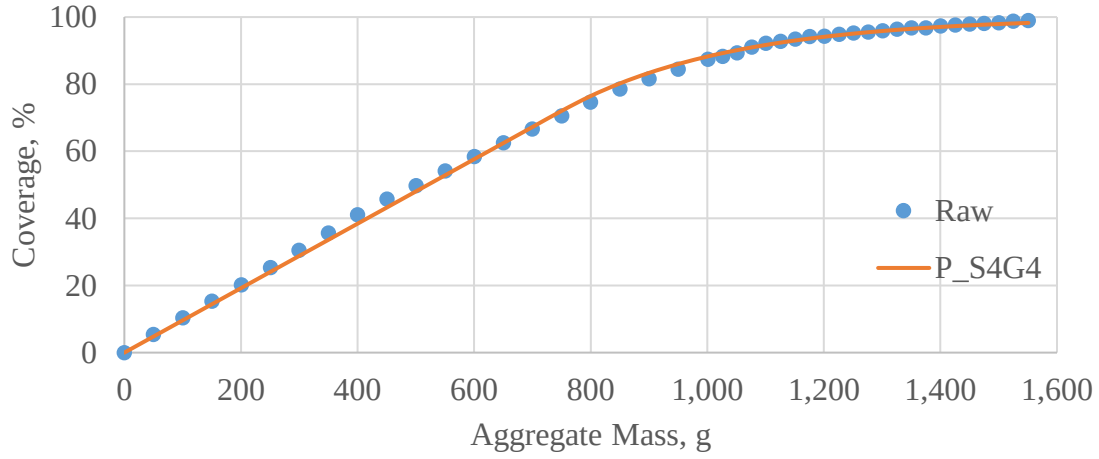

Figure 4.32 Continued

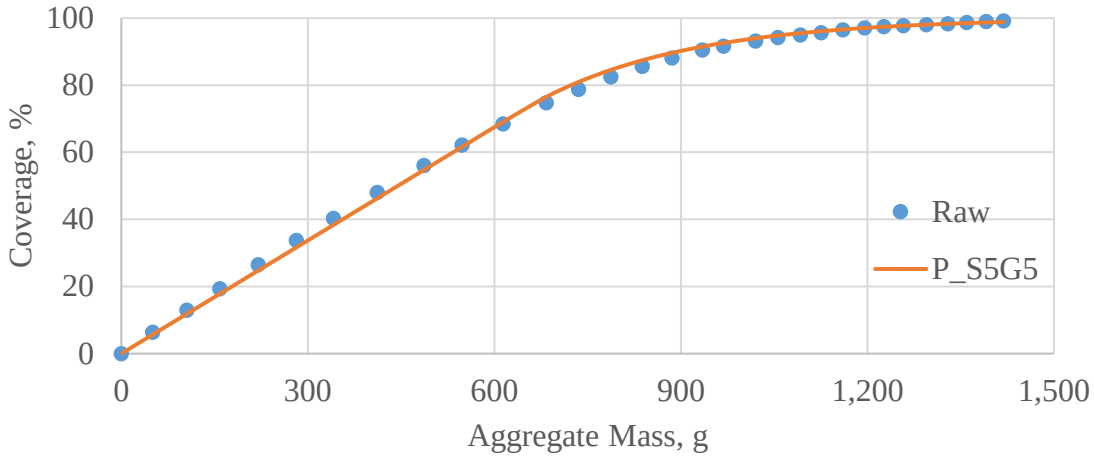

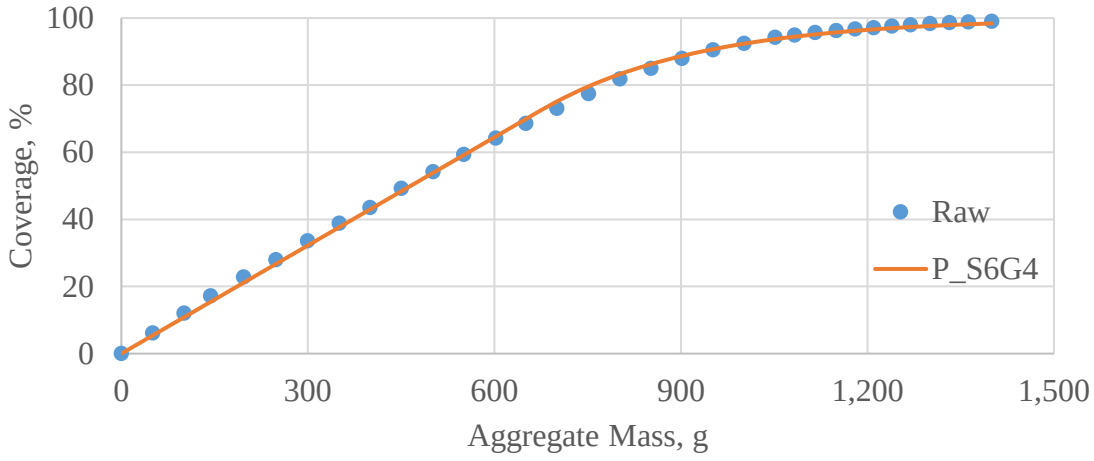

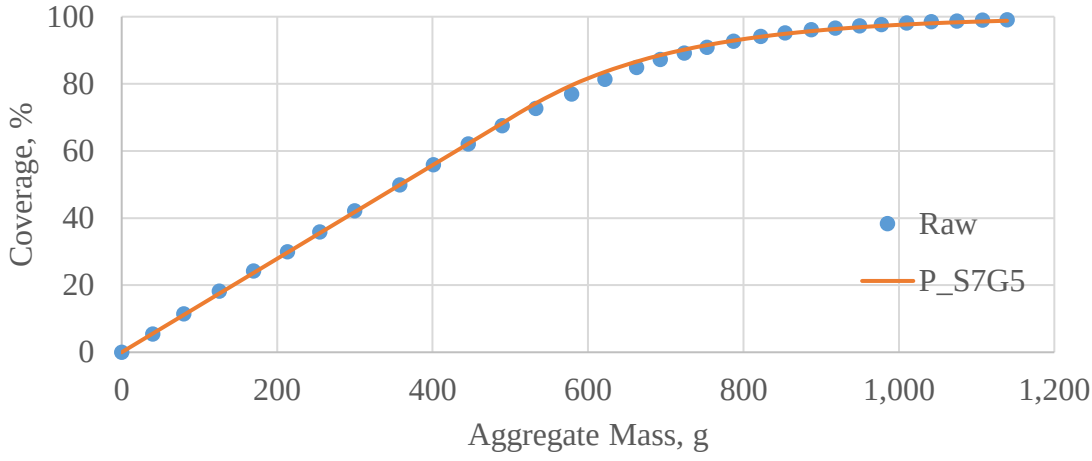

Figure 4.32 Continued

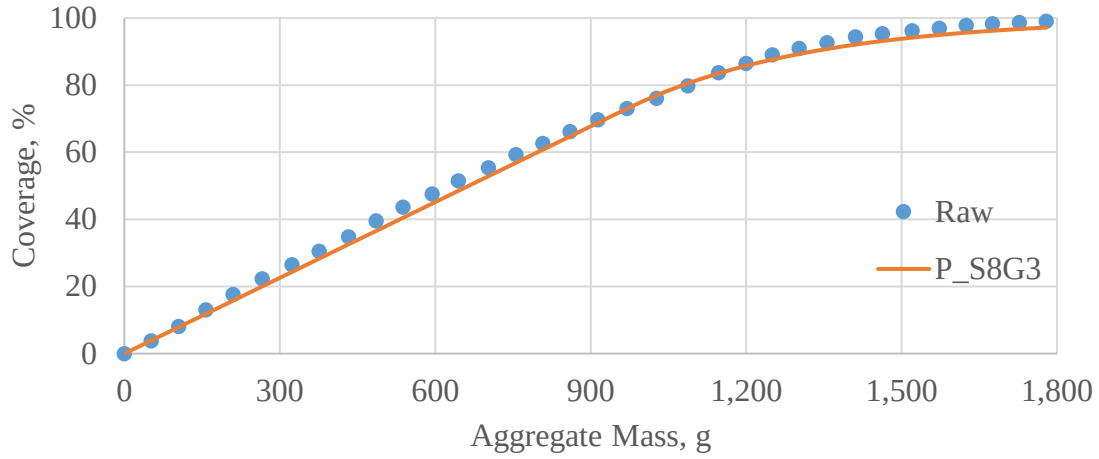

Figure 4.32 Continued

The only concern with these two models is that the fitting parameters b and d are predicted in a regression model based on eight data points. In this particular case, the reliability of the model is questionable because the data used is limited. The next and final approach address this concern and make use of more data points.

Fitting Approach 3

This approach aims at using the complete raw coverage data for all the aggregate samples to directly generate the predictive model using simultaneous linear regression. This approach provides the best fit for all the data set. In this case, the regression parameters of the composite model fitting parameters, b and d, were iterated in order to minimize the overall sum of square errors between all the fitted models and the raw data set. Similarly, the constraint was used to calculate the transition point as $Y_0 = 100 - \frac{b}{d}$. The simultaneous regression results are the following:

$$b = 0.39976 - 0.06461 \times \rho - 0.01478 \times ALD$$

$$d = 0.01508 - 0.00272 \times \rho - 0.00048 \times ALD$$

As before, as the density increases, both b and d decrease. As the ALD increases, both b and d decrease too. The transition point is calculated as before:

$$Y_0 = 100 - \frac{b}{d} = 100 - \frac{0.39976 - 0.06461 \times \rho - 0.01478 \times ALD}{0.01508 - 0.00272 \times \rho - 0.00048 \times ALD}$$

Afterwards, the prediction model was plotted against the data to check the goodness-of-fit. Table 4.10 and Figure 4.33 show the fitting parameters of the predictive model using the simultaneous regression approach.

Sample	Bulk Density	ALD	b	d	Y_0	SSE
S1G4	2.69 g/cm^3	7.96	0.1083	0.0039	72.5	61.2
S2G5	2.32 g/cm^3	5.05	0.1753	0.0063	72.4	42.0
S3G3L	1.34 g/cm^3	8.42	0.1888	0.0074	74.5	9.3
S4G4	3.00 g/cm^3	7.42	0.0962	0.0034	71.3	47.4
S5G5	3.00 g/cm^3	6.35	0.1122	0.0039	71.1	34.1
S6G4	2.74 g/cm^3	7.78	0.1077	0.0039	72.3	34.5
S7G5	2.74 g/cm^3	5.68	0.1387	0.0049	71.7	17.8
S8G3	2.66 g/cm^3	10.24	0.0766	0.0029	73.8	67.0
						313.3

Table 4.10: Predictive Model Obtained in Approach Three

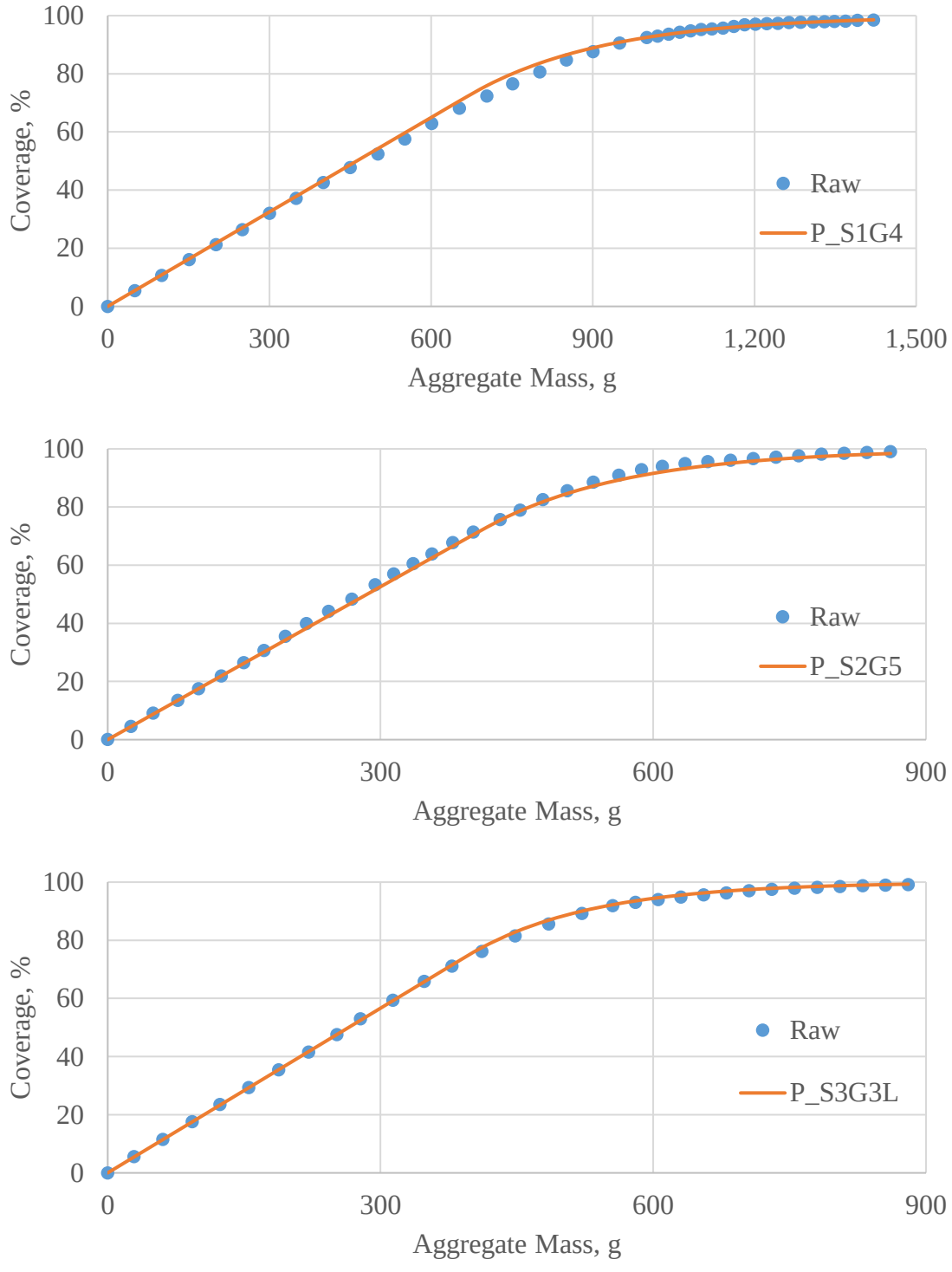

Figure 4.33: Predictive Model Graphs Using Approach Three

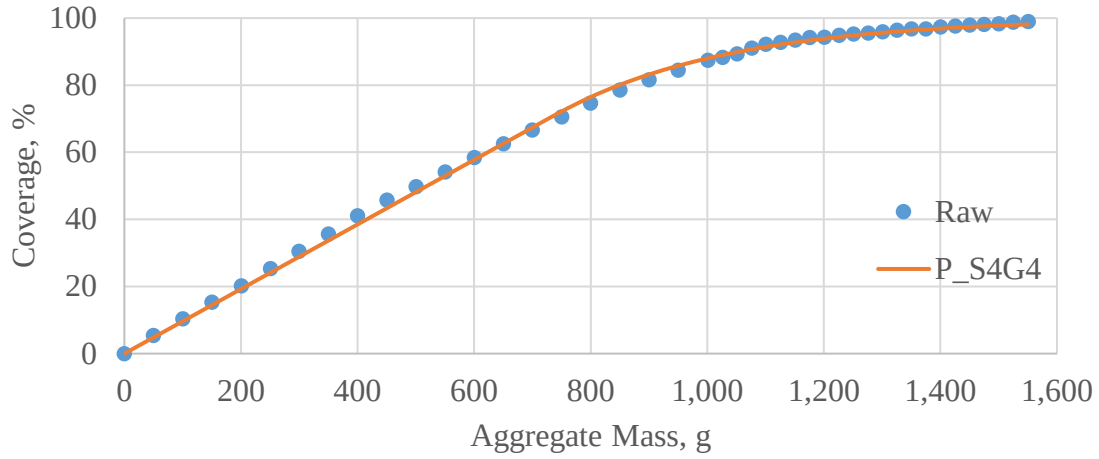

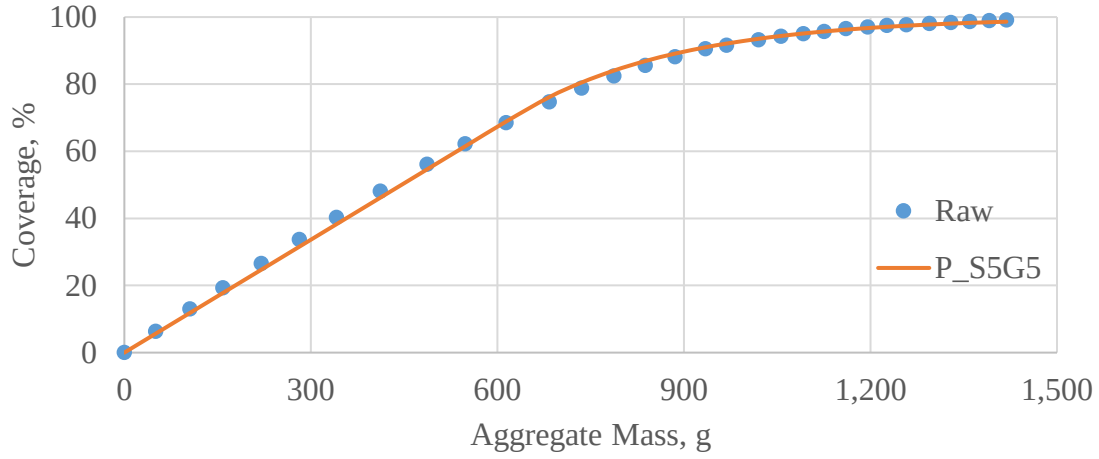

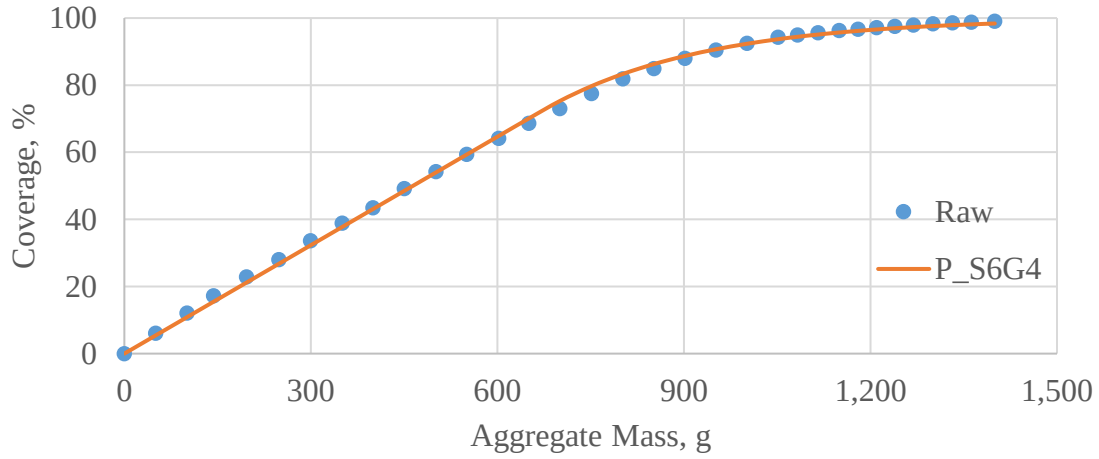

Figure 4.33 Continued

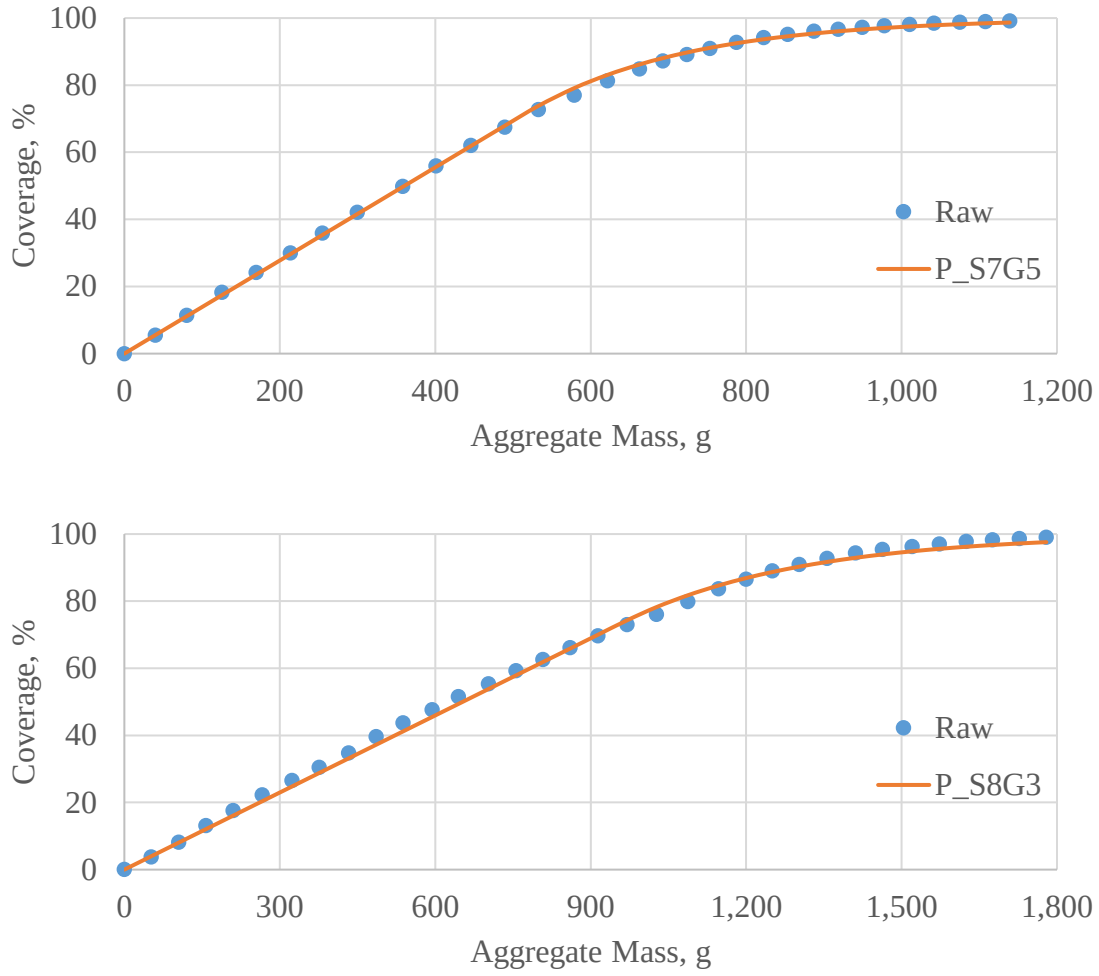

Figure 4.33 Continued

Table 4.11 shows the benefit of simultaneous regression against other trivial techniques. The second approach provides 50.5% improvement over the first one by including more data points when fitting the model. Given this improvement, the simultaneous regression provides an additional 10% improvement from the second approach enhancing the predictive model by making use of all the raw data directly in determining the regression parameters of both b and d simultaneously. Therefore, the third

model will be used as the predictive model for aggregate coverage and thereby the aggregate application rate.

Sample		S1G4	S2G5	S3G3L	S4G4	S5G5	S6G4	S7G5	S8G3	SSE	Sum of SSE's
Approach 1	b	0.1044	0.1734	0.1870	0.0920	0.1085	0.1038	0.1358	0.0716	701.9	
	d	0.0046	0.0068	0.0073	0.0042	0.0047	0.0046	0.0056	0.0036		
	Y0	77.3	74.4	74.5	78.0	76.8	77.3	75.6	80.1		
	SSE	22.8	53.2	6.6	131.7	90.5	59.9	26.5	310.6		
Approach 2	b	0.1079	0.1763	0.1886	0.0960	0.1124	0.1074	0.1394	0.0752	347.3	
	d	0.0039	0.0065	0.0071	0.0035	0.0040	0.0039	0.0051	0.0028		
	Y0	72.7	72.7	73.4	72.3	72.2	72.6	72.5	73.0		
	SSE	53.4	26.4	4.5	48.4	41.6	33.6	23.2	116.1		
Approach 3	b	0.1083	0.1753	0.1888	0.0962	0.1122	0.1077	0.1387	0.0766	313.3	
	d	0.0039	0.0063	0.0074	0.0034	0.0039	0.0039	0.0049	0.0029		
	Y0	72.5	72.4	74.5	71.3	71.1	72.3	71.7	73.8		
	SSE	61.2	42.0	9.3	47.4	34.1	34.5	17.8	67.0		

Table 4.11: Comparison of the Three Predictive Model Determination Approaches

AGGREGATE APPLICATION RECOMMENDATION

One of the objectives of this thesis is to develop a predictive model for the aggregate application rate. This model requires, as input, the density and the average least dimension of the aggregates being used. These two metrics can be easily measured or obtained from the supplier. Accordingly, the aggregate application rate is determined based on the level of coverage desired. Typically in a seal coat job, aggregates would cover between 60 and 90% of the road surface without extensive aggregate overlap (IDRRIM, 2017; TxDOT, 2017.2). Figure 4.34 shows the aggregate surface coverages of 60% and 90% respectively.

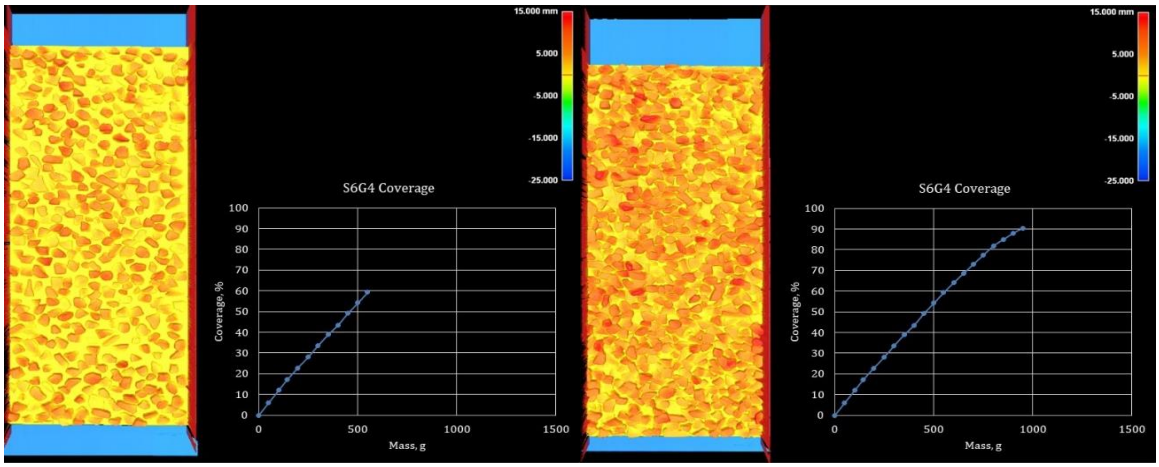

Figure 4.34: Aggregate Coverage Range of 60 and 90%

The composite predictive model for the aggregate coverage previously determined is:

$$\text{Coverage, } Y = \begin{cases} bX \dots\dots\dots\dots\dots\dots\dots\dots\dots\dots\dots & \text{for } X \le X_0 \\ 100 - (100 - Y_0) \times e^{-d(X - X_0)} & \text{otherwise} \end{cases}$$

The aggregate application rate, determined in kg/m^2, is the aggregate mass over the tray surface area. From the above equation, the aggregate mass is given by:

$$\text{Aggregate Mass in g, } X = \begin{cases} Y/b \dots\dots\dots\dots\dots\dots\dots & \text{for } Y \le Y_0 \\ X_0 - \dfrac{\ln\left(\dfrac{Y - 100}{Y_0 - 100}\right)}{d} & \text{otherwise} \end{cases}$$

$$\text{AAR in } \frac{kg}{m^2}, \frac{X}{A} = \frac{10^{-3}}{0.549 \times 0.174} \times \begin{cases} Y/b \dots\dots\dots\dots\dots\dots\dots\dots\dots\dots & \text{for } Y \le 100 - \dfrac{b}{d} \\ \dfrac{100 \times d - b\left(1 + \ln\left(\dfrac{100 - Y}{b/d}\right)\right)}{b \times d} & \text{otherwise} \end{cases}$$

Where Y is the target coverage in % point; while, b, d, and Y_0 are determined as follows:

$$b = 0.39976 - 0.06461 \times \rho - 0.01478 \times ALD;$$

$$d = 0.01508 - 0.00272 \times \rho - 0.00048 \times ALD;$$

$$Y_0 = 100 - \frac{b}{d} = 100 - \frac{0.39976 - 0.06461 \times \rho - 0.01478 \times ALD}{0.01508 - 0.00272 \times \rho - 0.00048 \times ALD}; \text{and}$$

ALD is the average least dimension in mm and ρ is the bulk density in g/cm^3

For a density of 2.5 g/cm^3 and an average least dimension of 7.5 mm, the aggregate application rate with an intended coverage of 75% is determined as follows:

$$b = 0.39976 - 0.06461 \times 2.5 - 0.01478 \times 7.5 = 0.1274$$

$$d = 0.01508 - 0.00272 \times 2.5 - 0.00048 \times 7.5 = 0.0047$$

$$Y_0 = 100 - \frac{0.1274}{0.0047} = 72.8\%$$

Since $Y > Y_0$, the aggregate application rate is given by:

$$\text{AAR}, \text{kg/m}^2 = \frac{10^{-3}}{0.549 \times 0.174}\left(\frac{100 \times 0.0047 - 0.1274\left(1 + \ln\left(\frac{100 - 75}{0.1274/0.0047}\right)\right)}{0.1274 \times 0.0047}\right)$$

$$\text{AAR} = 6.17 \text{ kg/m}^2$$

Chapter 5: UTexas BAR Improvement using 3D Laser Technology

The effectiveness of the dual aggregate-binder system, i.e. seal coat, is directly related to the adequate estimation of the application rates of both components. The amount of binder needed is directly proportional to the volume of voids in the covering aggregates and the texture of the existing pavement surface. Inadequately assessing the voids in the system, especially the existing surface texture, leads to BAR miscalculation.

REVIEW OF TEXTURE MEASUREMENT AND LASER TECHNOLOGY

According to the World Health Organization, about 1.25 million people die each year as a result of road traffic crashes in addition to 50 million injured or disabled victims (World Health Organization, 2017). Among the factors leading to fatal crashes, roadway structure, especially insufficient texture and friction, are major contributors. Hence, it is vital to understand and mitigate the effect texture could have on driver safety and be able to account for that in the design process. As defined by the AASHTO Guide for Pavement Friction, pavement surface texture is "*the deviations of the pavement surface from a true planar surface*" (Hall, Smith, Wambold, Yager, & Rado, 2009). This deviation greatly affects the tire-pavement interaction, friction, and noise. The Permanent International Association of Road Congress (PIARC) divided texture based on its wavelength size, λ, and amplitude, A, into four different categories that have a direct effect on surface friction and ride quality as shown in Table 5.1.

Unevenness is the major deviation that is felt by the bouncy behavior of the vehicle on the road. It has a significant effect on the safety and ride quality because it directly affects the dynamic components of the vehicle. Mega-texture comprises the major surface irregularities like cracks, roughness, and potholes. It has a major effect on the driver comfort. Macrotexture plays an important role in the pavement's ability to drain water. On

wet pavements, this texture component is responsible for the largest contribution for skid resistance. In fact, to mitigate the occurrence of hydroplaning, the pavement surface needs to have sufficient macrotexture in order to quickly disperse water accumulated on the surface of the pavement. Macrotexture plays an important role in the development of the hysteresis component of friction which depends on energy loss due to tire compression and decompression. Microtexture is the component that is the most vital at low speeds yet still contributes to friction at relatively higher speeds. It has a vital effect on road-tire interaction from an adhesion level. It is believed that the shape of the aggregates and the micro-asperities in the aggregate surfaces dictate low-scale friction (Hogervorst, 1974; Ong, Fwa, & Guo, 2005).

Texture	**Wavelength λ**	**Amplitude A**
Unevenness	Above 500 mm [20 in]	Above 50 mm [2 in]
Mega-texture	50 to 500 mm [2 to 20 in]	0.1 to 50 mm [0.005 to 2 in]
Macrotexture	0.5 to 50 mm [0.02 to 2 in]	0.1 to 20 mm [0.005 to 0.8 in]
Microtexture	less than 0.5 mm [0.02 in]	1 to 500 μm [0.04 to 20 mils]

Table 5.1: PARC Surface Texture Categories

One of the primary purposes for applying seal coats as pavement surface treatments is to improve the surface texture and ultimately restore or improve the skid resistance. On the other hand, the existing surface texture directly affects the design and, in particular, the binder application rate as the voids in the surface texture contribute towards the total voids in the seal coat system. Figure 5.1 shows the breakdown of different texture categories and the effects aggregates have on seal coats.

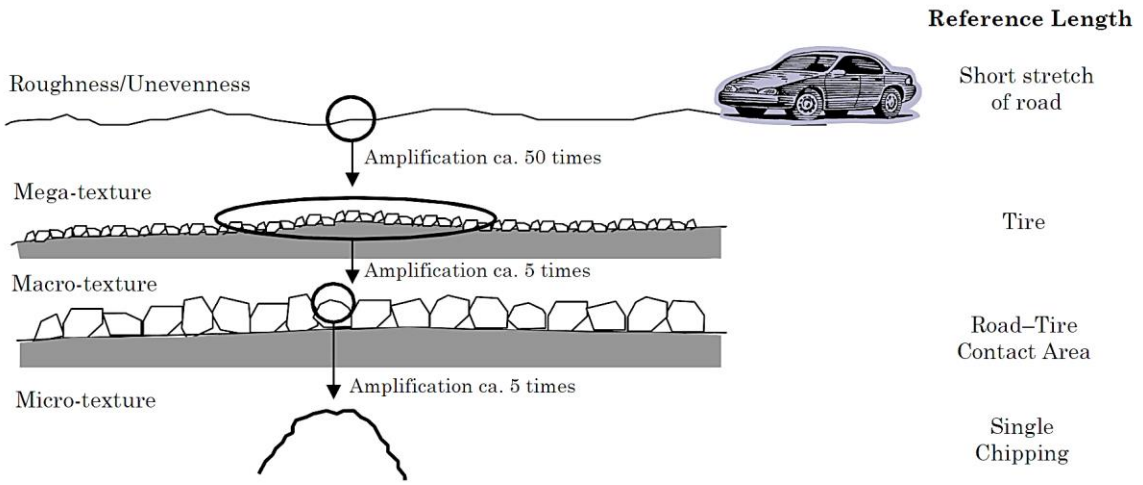

Figure 5.1: PARC Surface Texture Categories

In Chapter 3, different design methods highlighted that texture has two impacts on the seal coat design: one pertaining to the existing surface texture, and the second related to the final surface texture. With a relatively smooth surface, i.e. smaller texture values than the reference base's, the binder application rate is decreased to account for the lower volume of voids in the system. On the other hand, for relatively coarser surfaces, i.e. greater than the average texture values, the binder application rate is increased to account for the higher volume of voids in the system. These BAR adjustments are needed to obtain the final surface texture. The target surface texture after applying the seal coat also dictates the quantity of binder sprayed. The greater the binder dosage is, the higher the binder rises, and the lower the surface texture obtained. Hence, the quantity of binder directly impacts the texture of the surface obtained.

To measure surface texture, there are various techniques that differ by speed of measurement and surface contact requirement. Laser-based profilometry is one of the commonly used technique to collect pavement texture data. Most non-contact profilers in-use today measure texture using a single-point laser, which results in a two-dimensional

(2D) texture profile with distance along the pavement surface as one dimension and the texture height as the second. The Circular Track Meter (CTM) is a laser-based device that measures the mean profile depth (MPD), which is a 2D texture parameter shown in Figure 5.2 (ASTM, 2015.2). As stated in the ASTM: "*This test method uses a displacement sensor that is mounted on an arm, with a radius of 142 mm, that rotates clockwise at a fixed elevation from the surface being measured*."

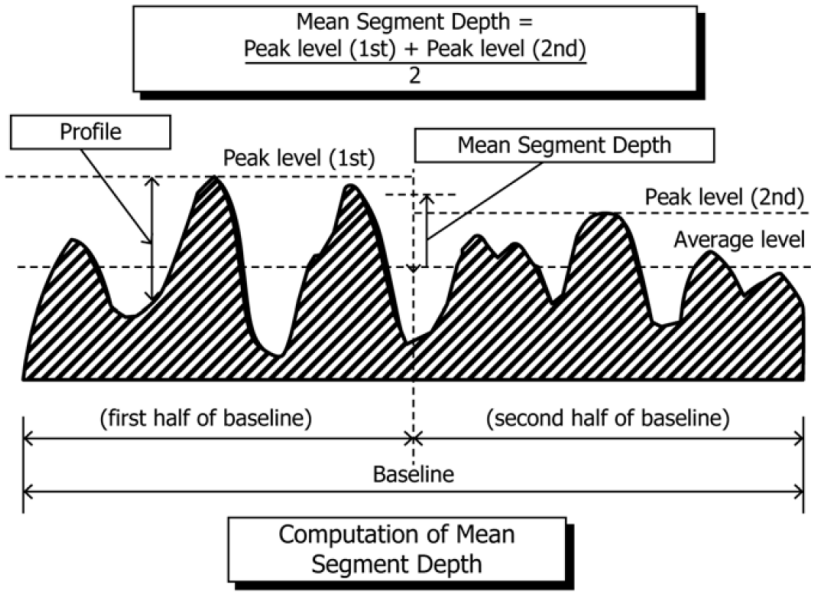

Figure 5.2: Mean Profile Depth Computation

The sand patch test (SPT) is a popular test method to assess the available texture of newly designed and existing pavements (Chamberlin & Amsler, 1982; Amsler & Quinn, 1977). This test entails the determination of an average depth of the pavement surface macrotexture and is insensitive to the characteristics of the pavement microtexture. The test method requires the use of a uniform material which historically remains the Ottawa natural silica sand or practically equivalent glass spheres of controlled properties to ensure uniform testing. According to ASTM E965, these spheres should have "*90% roundness in*

accordance with Test Method D1155 and be graded to have a minimum of 90%, by weight, passing sieve No. 60 and retained on sieve No. 80" (ASTM, 2015.1; Hayden, 1982). Additionally, a container of known volume, a wind shield, a flat spreader, a brush or vacuum cleaner, and a ruler are needed for the test as shown in Figure 5.3.

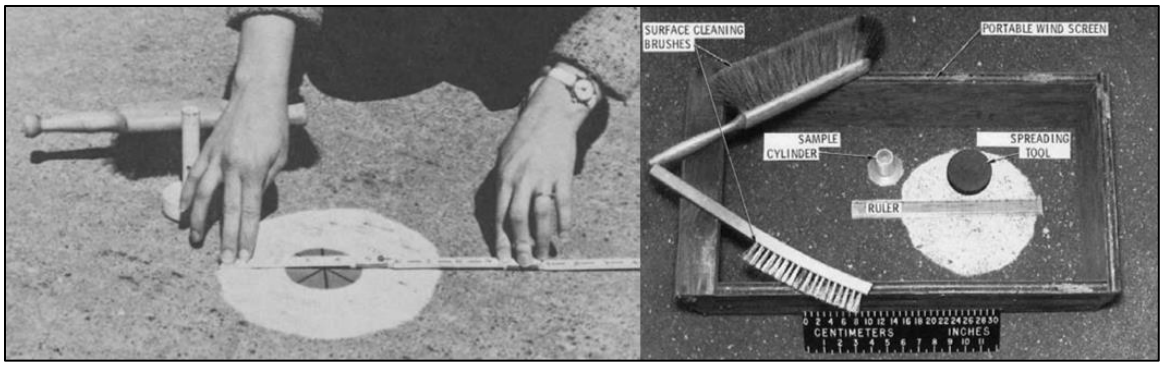

Figure 5.3: SPT Demonstration and Equipment (Chamberlin & Amsler, 1982)

First, the tested area is inspected ensuring that it is homogeneous, dry, and free from unique localized cracks or joints. Then, the surface is cleaned with the brush, a vacuum cleaner, or any other dust cleaning equipment that removes any residual debris and loose material. Afterwards, an adequate windshield is placed within the testing area in order to limit the effect of wind, vibrations, and adjacent passing vehicles on the test. Next, a specific volume of the testing sand, at least 25ml, is measured. Then, the sand is poured over the clean surface and spread uniformly in all directions using the spreader to form the widest circle possible and fill the surface voids, as illustrated in Figure 5.3. Subsequently, four distinct diameter measurements are taken 45° apart and the arithmetic mean is computed. Afterwards, the average pavement macrotexture depth, referred to as mean texture depth (MTD), is calculated using the known bulk volume of the sand and the mean of the measured diameters of the circular sand patch as follows:

$$\text{MTD} = \frac{\text{Volume of Sand}}{\text{Area Covered}} = \frac{4}{\pi \times D^2} \times V$$

Where V is the volume of the sand spread and D is the diameter of the spread.

The results of the test are used by different seal coat agencies to measure the surface texture and adjust the design accordingly. The test is simple and quick, but still requires traffic control measures to ensure the safety of the operators. It has a well-defined procedure and a controlled test method detailed within ASTM E965 (ASTM, 2015.1). However, this test is subject to human errors and has a low repeatability and reproducibility.

In recent years, the use of laser scanning techniques in engineering applications has gained increasing interest due to the advantages of being non-contact, operator-independent, rapid, and highly accurate (Wang, Yan, Huang, Chu, & Abdel, 2011; Serigos, Smit, & Prozzi, 2014; Kouchaki S. , Roshani, Prozzi, Cordoba, & Hernandez., 2018; Huang, Copenhaver, Hempel, & Mikhail, 2013). Accordingly, efforts have been made to replace the sand patch test with laser-based technologies (Chen, Zhang, Yu, & Wang, 2017; Zhang, Liu, Liu, & Chen., 2014; Wang, Liu, Wang, Ueckermann, & Oeser., 2017; Huang, Copenhaver, Hempel, & Mikhail, 2013). In 2012, Sengoz attempted to determine the surface texture using laser scans and was able to obtain comparable results (Sengoz, Topal, & Tanyel, 2012). In 2014, Yaacob et al. compared the MTD to the sensor measured texture depth (SMTD) obtained from a vehicle-mounted multi-laser profiler. The SMTD is calculated as the standard deviation of the profile amplitudes, measured by a sensor located 300 mm above the road surface (Yaacob, Hassan, & Hainin, 2014). The results showed low correlation between the two MTD measurements, but the tests were conducted months apart. However, Halil et al. in 2008 conducted a study that showed a strong correlation between the sand patch and multi-laser profiler (Halil, Nicholas, & Patrick, 2008). Currently, the vehicle-mounted laser measuring devices that are available in the market can

estimate the MTD based on some limiting assumptions and numerical interpolations. For instance, the Automatic Road Analyzer (ARAN), collects the texture profile and estimates the MTD by numerically integrating the area between the road profile and a horizontal line representing the highest value of that profile as illustrated in Figure 5.4 (Meegoda, Hettiarachchi, Rowe, Bandara, & Sharrock, 2002).

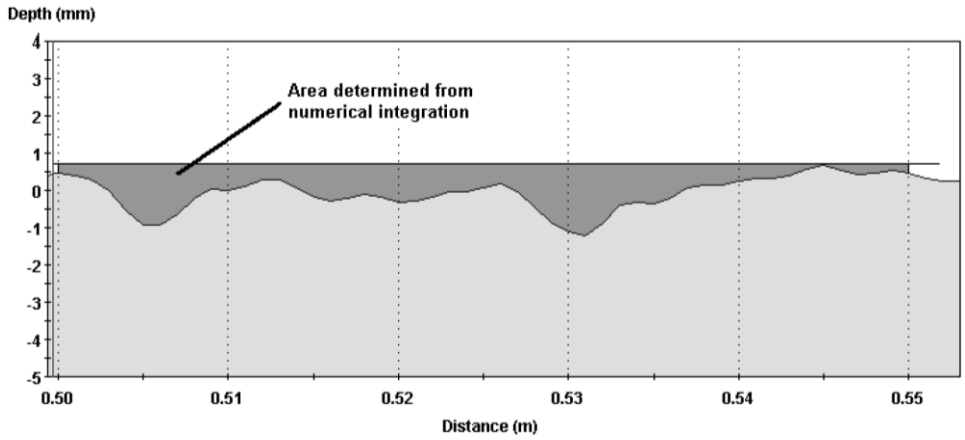

Figure 5.4: MTD Calculation Using ARAN

On the other hand, Hao et al. performed a study in 2015 using a real-time laser pavement texture meter to collect pavement surface data. To calculate the MTD using the line laser, the collected data is first divided into three segments as shown in Figure 5.5. Then a straight line is fitted to each segment using the least square method. The MTD of the scanned pavement is estimated as the average distance between the surface and the fitted lines (Hao, Sha, Sun, Li, & Zhao, 2016). However, the algorithm does not remove the slope from the collected data; henceforth, the calculated MTD is biased.

In summary, many studies have attempted to correlate the results obtained by different laser-based scanners and the sand patch test. These established models are mainly based on the analysis of two-dimensional (2D) road profiles or other limiting assumptions;

thus, the results do not reflect the MTD. Hence, the sand patch test remains the only test conducted by highway agencies to assess the volume of voids in the existing surface texture when designing seal coats.

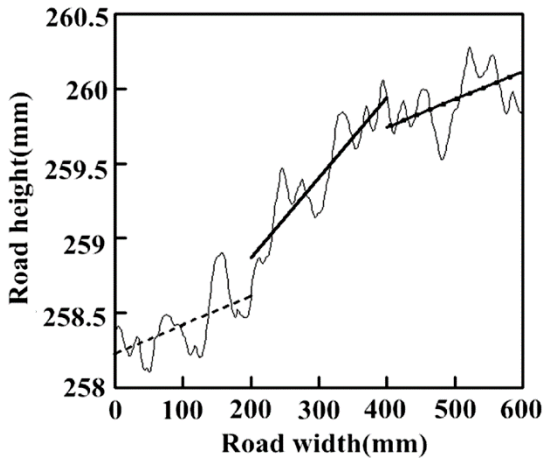

Figure 5.5: MTD Calculation Using Real-Time Laser Scanner

ASSESSING THE VARIABILITY AND LIMITATIONS OF THE SAND PATCH TEST

In this section, the variability of the SPT on asphalt pavements is evaluated in order to understand the test limitations and identify its benefits. To achieve this objective, the following steps were taken:

- Conducting SPTs on several pavement sections with different texture conditions to test the various factors affecting the variability of the SPT; and
- Conducting statistical analyses to assess the reliability, reproducibility, and repeatability of the SPT.

Three field test experiments engaging 20 operators for a total of 126 SPT's were conducted on nine distinct sections as follows:

1. The first experiment involved four operators testing seven distinct sites where each operator conducted three different SPTs per site;

2. The second experiment involved 16 operators testing two distinct surfaces, and each operator conducted one SPT in one specific fixed location on the surface; and
3. The third experiment involved one operator conducting ten SPTs in one specific fixed location on a surface.

Afterwards, an analysis of variance (ANOVA) was performed to evaluate the effect each experimental factor has on the SPT. Before analyzing the results of this experiment, a short overview of the concept behind ANOVA and its applicability in this study is provided.

ANOVA Overview

The analysis of variance, known as ANOVA, is a statistical method used to determine whether there is a significant difference between two or more sample means of the populations and assess the effects of various independent factor (Lane, 2001; Cohen & Cohen, 2008; Kass, Eden, & Brown, 2014; Schlotzhauer, 2007; Viv, Liz, & Jonathan, 2004). This method tests the null hypothesis that all population means for all conditions are equal. If the null hypothesis is rejected, then it can be concluded that at least one of the population means is different from at least one other population mean. If the null hypothesis is accepted, then it can be concluded that the population means are equal with a confidence defined by an F-statistic. The independent factors are the variables designated by the experimenter as a potential source of variance. In this study, the experimental factors tested are the different site surfaces, the distinct test trial locations within a pavement section, and the various operators conducting the SPT. Hence, the three previously mentioned experiments were conducted to assess the effect these independent factors have on the variability of the SPT results.

One-way ANOVA

One-way ANOVA is a simple technique for analysis that gives an overall conclusion whether there is a significant difference between the distinct groups by assessing one factor at a time (Viv, Liz, & Jonathan, 2004). The test is based on two estimates of the population variance, σ^2. The **first** estimate of the population variance is the mean square error (MSE). It reflects the differences among scores **within** the groups of an independent factor. In other words, the MSE can be expressed as the mean of all the different variances within each group. For example, to obtain the MSE for different surfaces, first the variances of the recorded diameters for each surface is determined; then, the MSE is calculated as the average of these variances. The MSE for a selected independent factor is given by:

$$\mathrm{MSE} = \frac{\sum_{i=1}^{n} \sigma^2{}_i}{n}$$

Where i is a distinct group of the n groups within an independent factor.

The **second** estimate of the population variance is the mean square between (MSB). It reflects the differences among scores **between** the groups of an independent factor. In other words, the MSB can be expressed as the variance of all the different means of each group of the selected independent factor. For example, to obtain the MSB for different surfaces, the averages of the recorded diameters for each surface is determined; then, the MSB is calculated as the product of the variance of the computed averages and the number of diameters per surface. The MSB for a selected independent factor is given by:

$$\mathrm{MSB} = \mathrm{k}_{(\text{elements per group})} \times \sigma^2_{\{\mu_1, \mu_2, \ \ldots \ \mu_n\}}$$

Where k is the number of elements in a group, and μ is the mean of a group.

The MSE estimates σ^2 regardless of whether the null hypothesis is true, i.e. the population means are equal. However, MSB only estimates σ^2 if the population means are equal. If

the population means are not equal, then MSB estimates a quantity larger than σ^2. Therefore, if the MSB is much larger than the MSE, then the population means are unlikely to be equal. On the other hand, if the MSB is about the same as MSE, then the data are consistent with the null hypothesis that the population means are equal with a confidence defined by the F-probability. The difference between MSB and MSE is evaluated as:

$$\mathrm{F} = \frac{\text{Variance between sample means}}{\text{Variance within the sample}} = \frac{\mathrm{MSB}}{\mathrm{MSE}}$$

Generally, the F ratio is near 1.0 when the null hypothesis is true and larger when the hypothesis is false. The statistical analysis requires identifying a significance level α that conveys the confidence interval of the testing. This is the probability of incorrectly rejecting the null hypothesis i.e. incorrectly concluding that the means are not equal (Bland, 2001). In other words, "*the chance of wrongly concluding that there is a difference between two groups when in reality there's no such difference*" (Viv, Liz, & Jonathan, 2004). Typically, a significance level of 0.05 is selected. Concurrently, the p-value, which is the probability of occurrence of a given event, can be compared to α. The null hypothesis is false when the p-value is less than α.

It is important to acknowledge the three assumptions adopted while conducting the analysis of variance for an independent factor:

1. The populations have the same variance;
2. The populations are normally distributed; and
3. Each value is sampled independently from the other values.

Applicability of ANOVA

One of the ways to analyze the sources of variation in the diameters measured in the SPT is to conduct separate studies on how each variable affects the variance of the overall results. In light of the outcome, an analysis that includes two or more independent

variables could be necessary to test the interaction between the variables. Likewise, it is interesting to test how the variance generated by one variable differs while considering other variables. In this study there are three factors of interest that potentially affect the measured diameter.

1. Site-specific: How does the diameter measurements vary depending on the selected site? This would test the ability of the SPT to differentiate between two surfaces;
2. Selected locations within a specific site: How does the SPT result differ depending on the selected location of the test within a specific site? This would assess the homogeneity of the site in regard to the actual texture; and
3. Operator: How does the diameter measurements vary depending on the operator? This would test the reproducibility and repeatability of the sand patch test.

Measurement Processes and Results

First Experiment

In the first experiment, a total of 84 sand patch tests were conducted in accordance with ASTM E965 (ASTM, 2015.1). Four operators (O1 - O4) tested seven different surfaces (S1 - S7) with three distinct trial locations per operator per surface type, i.e. site. In each SPT, four diameters (D1 - D4) were recorded 45° apart. Figure 5.6 illustrates the first experiment.

All the operators were well trained to do the SPT in accordance with ASTM E965 (ASTM, 2015.1). Each surface was well defined with set boundaries, and the operators measured three different sand patch tests within each surface (site). The tests were conducted independently to avoid affecting the operator's perception. The volume of sand was measured by the test coordinator in all the tests to avoid unnecessary biases.

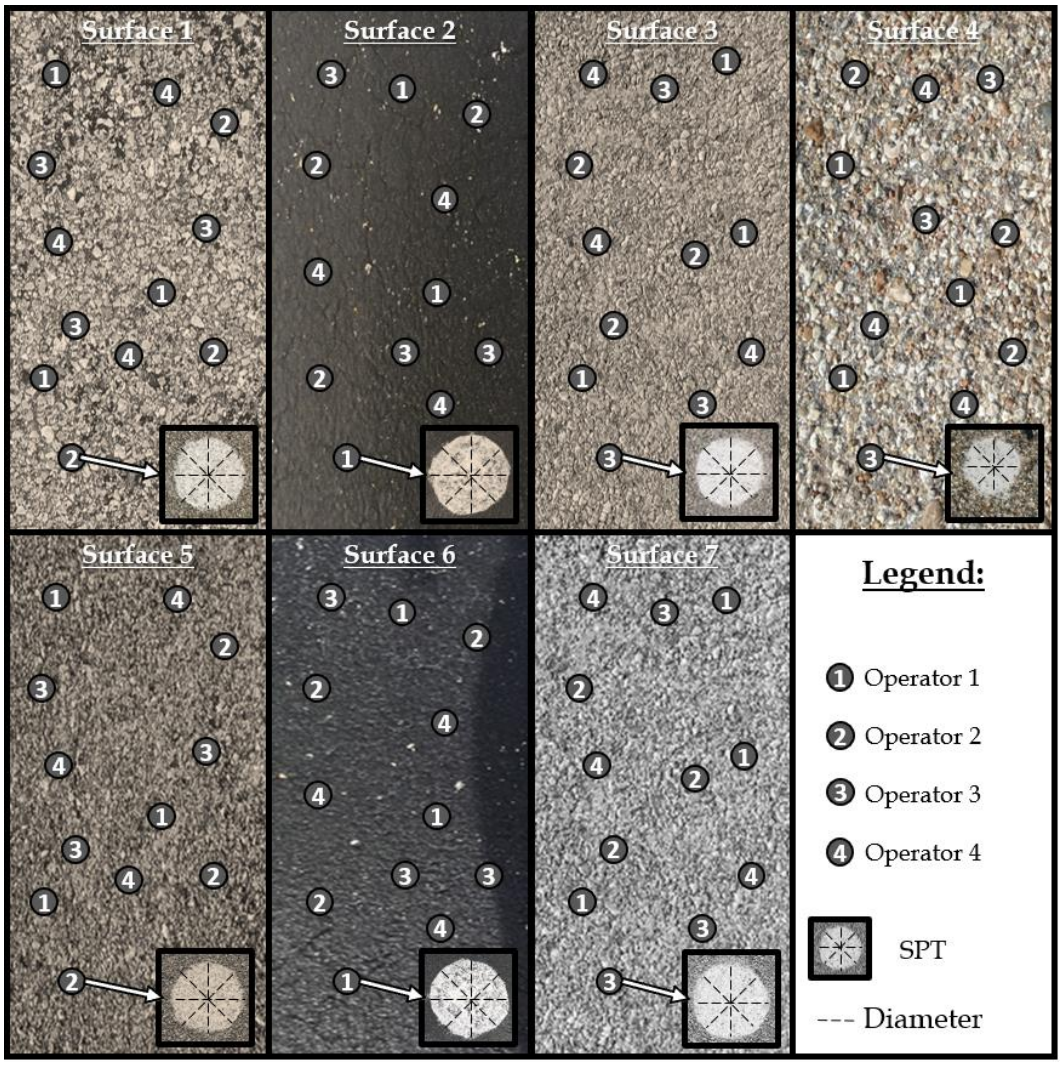

Figure 5.6: Layout of the First Experiment.

Variability between Site Sections (1st Factor)

First, the variance associated with the selected site was analyzed to verify the SPT's ability to differentiate between different site surfaces and estimate the MTD of each surface. Table 5.2 summarizes the one-way ANOVA that assesses the ability of the SPT to distinguish between different sections (bearing all other factors insignificant regarding variability). Since the p-value is lower than the selected significance ($\alpha = 0.05$), it is valid

to reject the null hypothesis that the means of all the site-surfaces' diameters are the same. This implies that there exists at least one surface diameter mean which is significantly different from the rest. In addition, the high F-value indicates that the variance between the site's means is higher than the variance within the site surfaces themselves.

One Way ANOVA: Site-Specific Surface						
Surfaces	**# of Operators**	**SPT's per Operator**	**Diameters per SPT**	**Count**	**Average (mm)**	**Variance**
Surface 1	4	3	4	48	186.6	26.2
Surface 2	4	3	4	48	251.6	92.8
Surface 3	4	3	4	48	173.9	36.4
Surface 4	4	3	4	48	115.5	49.1
Surface 5	4	3	4	48	206.7	247.9
Surface 6	4	3	4	48	238.8	204.1
Surface 7	4	3	4	48	137.6	37.8
ANOVA						
Variation Source	**SS**	**df**	**MS**	**F**	**P-value**	**F crit**
Between Surfaces	718,740	6	119,790	1,208	**1.06E-220**	2.13
Within Surfaces	32,635	329	99			
Total	751,375	335				

Table 5.2: One-way ANOVA with the Site Surface as Independent Factor

It can be concluded that the selected section (site) has a major effect on the measured diameter in the SPT. Accordingly, this test can differentiate between different sections because the tested surfaces have different textures.

Variability within a Specific Pavement Surface Section (2nd Factor)

Each operator performed three SPTs in three distinct locations within a specific site. The variance associated with the selected SPT trial location within a specific site was analyzed to assess the homogeneity or non-homogeneity of a pavement surface deeming all other factors insignificant. Table 5.3 summarizes the one-way ANOVA that evaluates the ability of the SPT to evaluate surface homogeneity.

One Way ANOVA – Independent Factor: Location within Specific Site						
One Way ANOVA: Operators within Site 1						
Operators	**# of Surfaces**	**SPT's per Operator**	**Diameters per SPT**	**Count**	**Average**	**Variance**
Operator 1	1	3	4	12	184.8	38.0
Operator 2	1	3	4	12	187.0	15.3
Operator 3	1	3	4	12	183.9	3.9
Operator 4	1	3	4	12	190.8	24.4
ANOVA						
Variation Source	**SS**	**df**	**MS**	**F**	**P-value**	**F crit**
Between Groups	336.1	3	112.0	5.49	0.003	2.82
Within Groups	897.4	44	20.4			
Total	1,233.5	47				
…						
…						
…						
One Way ANOVA: Operators within Site 7						
Operators	**# of Surfaces**	**SPT's per Operator**	**Diameters per SPT**	**Count**	**Average**	**Variance**
Operator 1	1	3	4	12	132.7	49.3
Operator 2	1	3	4	12	141.6	22.6
Operator 3	1	3	4	12	138.2	30.2
Operator 4	1	3	4	12	137.9	15.2
ANOVA						
Variation Source	**SS**	**df**	**MS**	**F**	**P-value**	**F crit**
Between Groups	487.5	3	162.5	5.54	0.003	2.82
Within Groups	1,290.2	44	29.3			
Total	1,777.7	47				
ANOVA (Average of 7 Surfaces)						
Variation Source	**SS**	**df**	**MS**	**F**	**P-value**	**F crit**
Between Groups	1,151.2	3	383.7	6.36	0.001	2.82
Within Groups	3,510.9	44	79.8			
Total	4,662.2	47				

Table 5.3: One-way ANOVA of Operators Over Seven Surfaces

Likewise, the p-value is less than 0.05. It is safe to reject the null hypothesis that the means of all the operators' diameters within a surface are the same and conclude that at least one diameter mean is significantly different from the rest and non-homogeneity exists within the surface. If the bias generated by the operator is insignificant, one can conclude that the pavement texture within the surface is not homogeneous, and the non-homogeneity is a

main contributor to the variance. Studies have shown that the texture varies significantly across a pavement especially between the wheel-path and the center of the lane (Lee M. , 2017; Viner, et al., 2006; TxDOT, 2017.2). However, it is essential to capture the MTD of the pavement texture and the surface non-homogeneity without inherent biases within the data collection process such as those generated by the operator.

The boxplot in Figure 5.7 shows the variability of the diameters measured by each operator for the seven different site surfaces. The boxplots show the lowest recorded diameters, the highest recorded diameters, the first and third quartiles, the median highlighted by a horizontal line, and the mean displayed using an "X" mark. There are noticeable differences between the seven surfaces proving that the SPT can differentiate between different surfaces with Surface 2 being the smoothest and Surface 4 the coarsest. Ideally, the curves should be horizontal and parallel if the surfaces were perfectly homogenous and the operator variability was consistent or did not exist. However, there is a local variation in the diameters measured within each surface. This could be the result of surface non-homogeneity and/or inherent operator differences. For instance, the two suspected factors augmented the variability of the SPT conducted by Operator 3 on Surface 6 and undermined the variability of the same operator on Surface 1. For that reason, it is important to accurately measure the MTD of the pavement to determine surface non-homogeneity without inherent biases within the data collection procedure such as those generated by the operator. Hence, the ability of the SPT to measure the MTD remains questionable given the inherent operator perception variability.

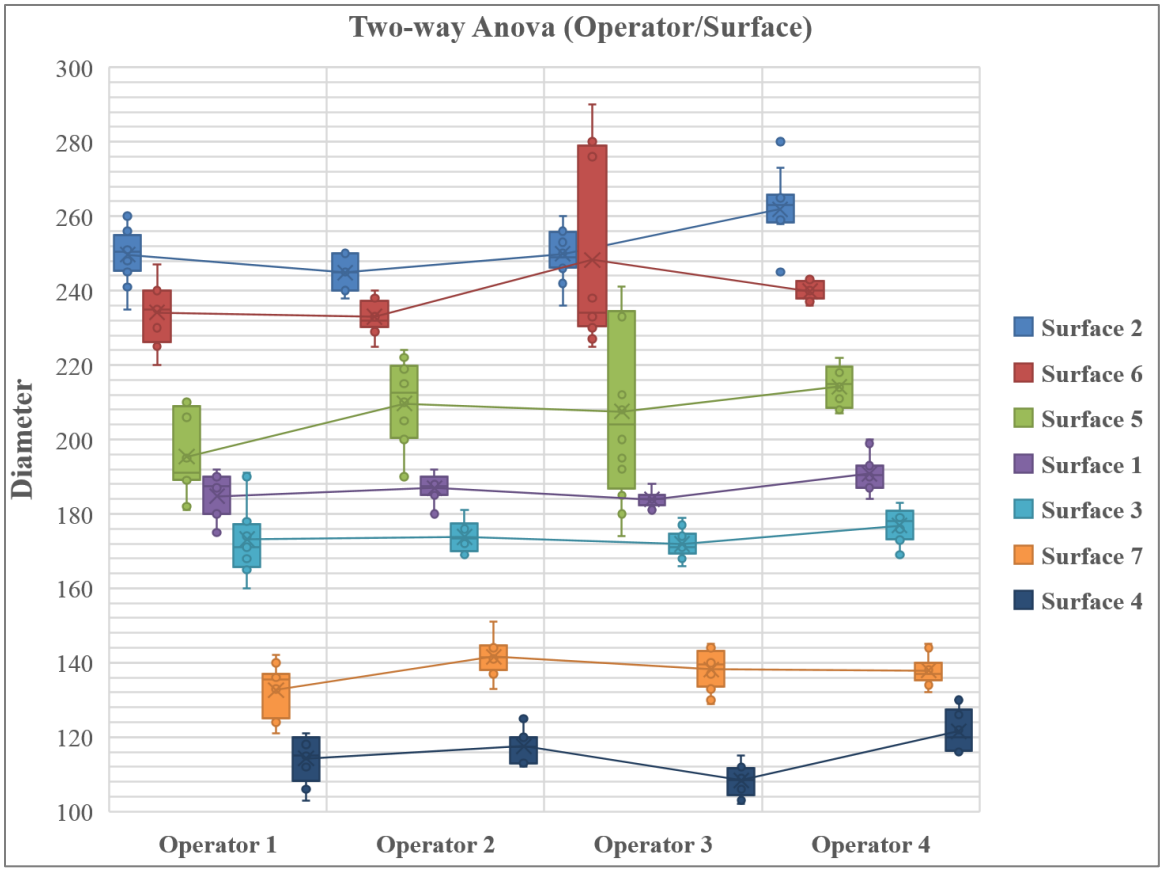

Figure 5.7: The Spread of the Measured Operator Diameters Over Seven Surfaces.

Second Experiment

This experiment involved 32 SPTs with 16 operators, each testing two distinct surfaces. The operators were given the same instructions on how and where to conduct the test. Additionally, each operator conducted the test independently to avoid skewing their perception by target diameter values. A vacuum cleaner was used to remove the remaining sand between test repeats, limiting any possible bias that could be generated. Illustrated in Figure 5.8, each operator conducted one SPT in each specific pre-defined fixed location within the surface limiting all potential biases.

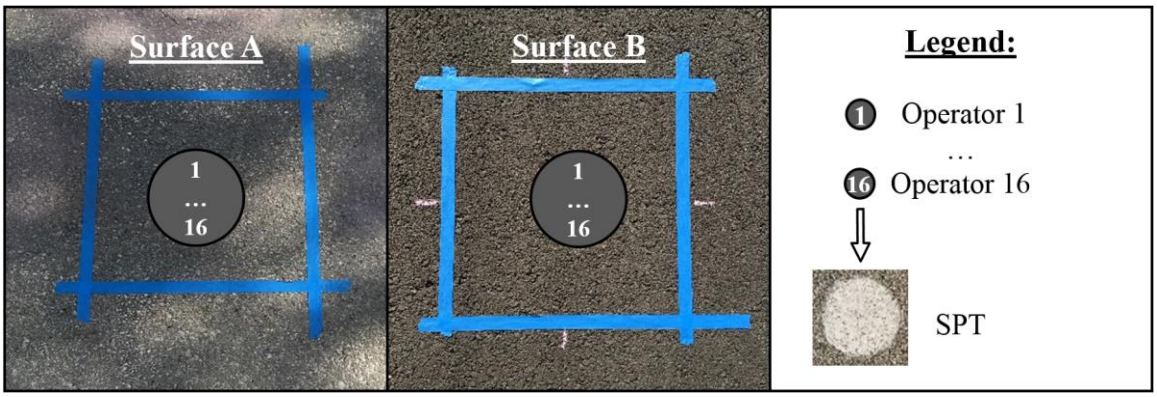

Figure 5.8: Layout of the Second Experiment.

Variability between Operators, Reproducibility

The variance associated with the operator conducting the SPT is analyzed to assess the bias pertaining to the SPT procedure and its ability to determine the MTD. A one-way ANOVA was conducted for both surfaces to assess the significance of the bias generated by the operator while limiting any other biases. The results shown Table 5.4 indicate that the p-value is lower than the selected α of 0.05. Therefore, it is safe to reject the null hypothesis that the means of all the operators' diameters are the same and conclude that there exists at least one operator diameter mean which is significantly different from the rest. The high F-value indicates that the variance between operators is much higher than the variance within the sample operators themselves. This demonstrates that the reproducibility of the SPT is much lower than its repeatability.

One Way ANOVA – Independent Factor: Operators						
Surface A: New Pavement						
Operators	**# of Surfaces**	**SPT's per Operator**	**Diameters per SPT**	**Count**	**Average**	**Variance**
Operator 1	1	1	4	4	191.0	12.0
Operator 2	1	1	4	4	195.8	87.6
Operator 3	1	1	4	4	206.5	101.7

Table 5.4: ANOVA of Operators, as Independent Factors, Over Two Surfaces

Operator 4	1	1	4	4	221.3	84.3
Operator 5	1	1	4	4	191.5	163.0
Operator 6	1	1	4	4	230.8	10.9
Operator 7	1	1	4	4	238.5	169.7
Operator 8	1	1	4	4	218.8	18.9
Operator 9	1	1	4	4	192.0	11.3
Operator 10	1	1	4	4	186.3	6.3
Operator 11	1	1	4	4	233.0	88.7
Operator 12	1	1	4	4	226.0	91.3
Operator 13	1	1	4	4	227.8	61.6
Operator 14	1	1	4	4	255.0	116.7
Operator 15	1	1	4	4	233.0	6.0
Operator 16	1	1	4	4	234.5	17.7
ANOVA						
Variation Source	**SS**	**df**	**MS**	**F**	**P-value**	**F crit**
Between Operators	26,336.9	15	1,755.8	26.82	2.9 E-18	1.88
Within Operators	3,142.5	48	65.5			
Total	29,479.4	63				
Surface B: Old Pavement						
Operators	**# of Surfaces**	**SPT's per Operator**	**Diameters per SPT**	**Count**	**Average**	**Variance**
Operator 1	1	1	4	4	215.5	43.7
Operator 2	1	1	4	4	215.0	11.3
Operator 3	1	1	4	4	213.3	24.9
Operator 4	1	1	4	4	207.8	51.6
Operator 5	1	1	4	4	220.0	16.7
Operator 6	1	1	4	4	222.0	28.0
Operator 7	1	1	4	4	231.0	20.7
Operator 8	1	1	4	4	223.0	32.7
Operator 9	1	1	4	4	225.0	50.0
Operator 10	1	1	4	4	212.5	75.0
Operator 11	1	1	4	4	248.8	289.6
Operator 12	1	1	4	4	257.0	94.0
Operator 13	1	1	4	4	271.3	590.9
Operator 14	1	1	4	4	256.3	122.9
Operator 15	1	1	4	4	276.0	11.3
Operator 16	1	1	4	4	280.0	333.3
ANOVA						
Variation Source	**SS**	**df**	**MS**	**F**	**P-value**	**F crit**
Between Operators	37,152.5	15	2,476.8	22.06	1.6E-16	1.88
Within Operators	5,389.8	48	112.3			
Total	42,542.2	63				

Table 5.4 Continued

Thus, it can be concluded that the SPT is a subjective test that depends on the perception of the operator. Although the test is capable of distinguishing between different surfaces, it is not capable of accurately estimating the MTD. The operator selected to conduct the test has a direct effect on the result leaving the ability of the SPT to objectively assess the pavement texture questionable.

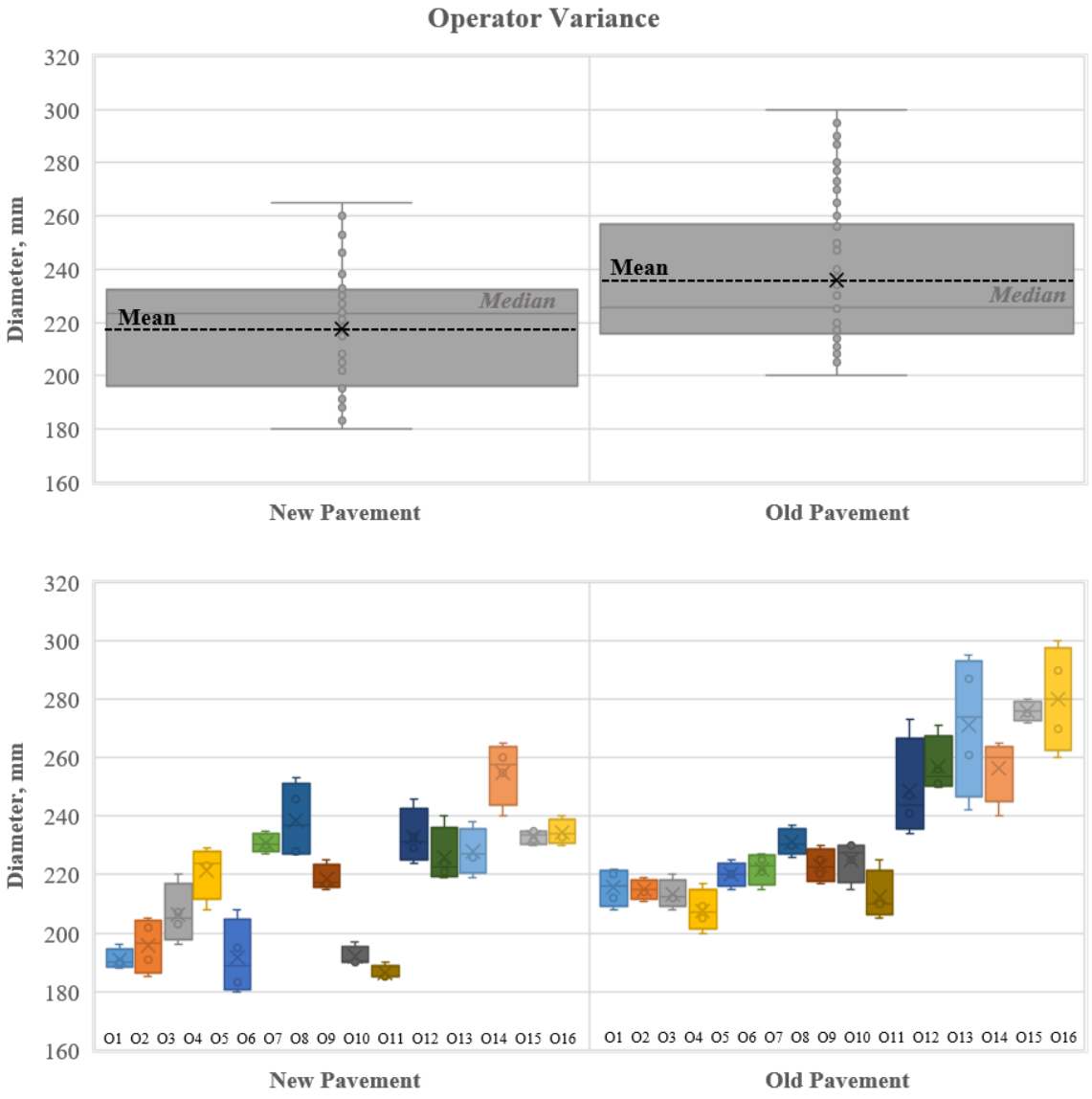

Figure 5.9: Variability of Measured Operator Diameters Over Two Surfaces

The boxplot in Figure 5.9 shows that the new pavement seems to be coarser than the old pavement since the overall mean diameter is lower, yielding a higher MTD. This conclusion is reasonable because aged pavements deteriorate with trafficking and the surface gets abraded by tires and becomes flatter. This reinforces the previous conclusion that the SPT can differentiate between two different surfaces. Theoretically, the curves shown in Figure 5.9 should be horizontal with a negligible variability relevant to the operator's bias. However, there is a wide variation in the measured diameters within each surface. This provides visual evidence supporting the conclusion obtained from the ANOVA regarding the inherent operator bias: the SPT results highly depend on the perception of the operator.

The findings from the second experiment indicate that the reproducibility of the SPT is lower than its repeatability. At the same time, it was proven that the sand patch test is not capable of reliably estimating the MTD because the operator's perception is a significant source of bias. However, the previous experiments do not provide a complete understanding of the repeatability of the sand patch test.

Third Experiment

This experiment was performed to assess the repeatability of the SPT. In this experiment, one operator conducted ten SPTs in one specific location on Surface A, shown in Figure 5.8. Similar to the second experiment, the volume of sand was measured by the test coordinator. Furthermore, a vacuum cleaner was used to remove the sand and any other debris found on the surface between two consecutive tests.

Single Operator Variability, Repeatability

A one-way ANOVA for ten SPTs done by one operator in the same location was conducted to assess the repeatability of the test while limiting other biases. The results,

shown in Table 5.5, indicate that the p-value is lower than the selected α of 0.05. Therefore, it is safe to reject the null hypothesis that the mean diameters of all the SPTs are the same and conclude that there exists at least one test trial significantly different from the rest. The high F-value indicates that the variance between the SPTs is much higher than the variance within the diameters of one SPT. It should be noted that the variance within one SPT represents the ability of the operator to form a circle (a perfect circle is formed when the four measured diameters are equal). This demonstrates that the repeatability of the SPT is low and is a significant source of variance in this ANOVA.

One Way ANOVA: Surface						
Surfaces	**# of Operators**	**# of Surfaces**	**Diameters per SPT**	**Count**	**Average D (mm)**	**Variance**
SPT1	1	1	4	4	207.75	8.92
SPT2	1	1	4	4	215.00	6.67
SPT3	1	1	4	4	199.00	6.67
SPT4	1	1	4	4	212.75	8.92
SPT5	1	1	4	4	221.00	6.67
SPT6	1	1	4	4	229.00	6.67
SPT7	1	1	4	4	217.75	9.58
SPT8	1	1	4	4	202.75	11.58
SPT9	1	1	4	4	214.00	6.67
SPT10	1	1	4	4	224.50	11.67
ANOVA						
Variation Source	**SS**	**df**	**MS**	**F**	**P-value**	**F crit**
Between Surfaces	3,161.1	9	351.2	41.81	1.5E-14	2.21
Within Surfaces	252	30	8.4			
Total	3,413.1	39				

Table 5.5: One-way ANOVA of SPTs of One Operator in One Location

Conclusion

Based on these experiments, it was concluded that the SPT is a relatively subjective test that depends on the perception of the operator. Although the test is capable of distinguishing between different surfaces, it is not capable of accurately estimating the

MTD in a repeatable and reproducible manner. These experiments reassure the previous hypothesis that the operator selected to conduct the test has a direct effect on the results. Given those circumstances, highway agencies still rely on the SPT to evaluate the available friction and level of safety of a pavement section (Henault & Jessica, 2011). The main sources of error lie within the test administration, i.e. volume determination, sand spreading, and diameter measurement. Furthermore, the sand patch test can be affected by wind, as losing sand throughout the testing process can skew the results and misestimate the available texture. Additionally, the test relies on the operator's ability to spread the material into a circular patch, which could be inconsistent between different workers. Hence, the operator's perception is the main contributor to the variability within the results, apart from the surface variability and the non-homogeneity within a pavement section. Generally, the sand patch test can differentiate between various surfaces but cannot provide accurate estimates of the mean texture depth. Nevertheless, agencies use the SPT to assess the existing surface texture and apply site-specific adjustments when it comes to pavement preservation designs such as seal coats (TxDOT, 2017.2). Thus, it is vital that the operator subjectivity be minimized or eliminated to adequately assess the MTD. Hence, there is a need to use three-dimensional (3D) pavement surface data for a more comprehensive and accurate measurement of the texture depth.

DESIGN IMPROVEMENT FOR VARYING SURFACE TEXTURE

One of the challenges of designing seal coats is the reliability of using empirical factors to correct for site-specific conditions, such as the voids in the surface texture. This part of the research aims at using the 3D laser scanner to accurately, automatically, and objectively quantify the volume of voids in the existing surface texture and incorporate it into the existing seal coat design methods to improve the BAR calculation. To achieve the goal, the steps listed below were required:

- Conducting field tests to collect 3D scans of different pavement sections using the laser system and measure the MTD using the SPT to comply with existing design methods;
- Developing the algorithm that determines the volume of voids in the scanned 3D model of the surface and comparing the results with those of the SPT; and
- Adjusting the existing seal coat design methods.

Field Tests

The 3D laser scanner prototype, described in the previous chapter, was used to scan the existing pavement surface at nine different locations in Texas and determine the volume of voids. The line laser consists of 800 points that are 300 µm apart in the transverse direction. The linear translation stage was set at a speed of 8 mm/s and the laser frequency at 1.0 kHz. Hence, the scans in the longitudinal direction were taken every 8 µm. The laser head was collecting data 300 mm above the target surface because this is the ideal height for model LJ-V7300 lasers. The chosen locations have different mix designs, ensuring a wide variety of surface textures. The test locations and their pavement mix designs are presented in Table 5.6.

Test Location No.	District/Location	Pavement Mix design
1	Speedway St, Austin	Dense-Graded Type D
2	FM 1626, Austin	Thin Overlay Mixtures
3	RM 12, Austin	Thin Overlay Mixtures
4	FM 1431, Austin	Porous Friction Course
5	IH 20, Brownwood	Dense-Graded Type D
6	SH 36, Brownwood	Dense-Graded Type C
7	SH 195, Austin	Porous Friction Course
8	US 84, Bryan	Dense-Graded Type C
9	US 181, San Antonio	Novachip

Table 5.6: Test Locations

For each pavement section, two to three locations were selected along the right wheel path where a sand patch test was conducted in accordance with ASTM E965 (ASTM, 2015.1) followed by a laser scan. To limit any bias generated by surface non-homogeneity, the SPT was conducted in the same location as that of the laser scan, as illustrated in Figure 5.10.

Figure 5.10: Field Testing Setup and Measurement Overlap

Data Collection and Processing

As shown in Figure 5.10, specific locations along the right wheel path were marked. First, the area was cleaned, and the sand patch test was conducted. Afterwards, the surface was thoroughly vacuumed to remove any sand debris, and laser scans were conducted. Figure 5.11 is an example of one of the scanned surfaces.

Figure 5.11: Scanned Surface Showing Texture Non-Homogeneity

The collected raw data, shown in Figure 5.12, was filtered to obtain a 3D model relevant to the pavement surface. Following is a detailed description of the filtering process.

1. Discarding the Dead-point Edges:

   Unfortunately, not all the emitted laser light is captured back by the detector, and hence the missing data points are reported as dead points, i.e. -999.999 mm, which are easily identifiable when processing the data. Fortunately, this issue affects the data points that

are at the edges of the scan line. Figure 5.12 illustrates the dead points, shown in blue, at both ends of the line.

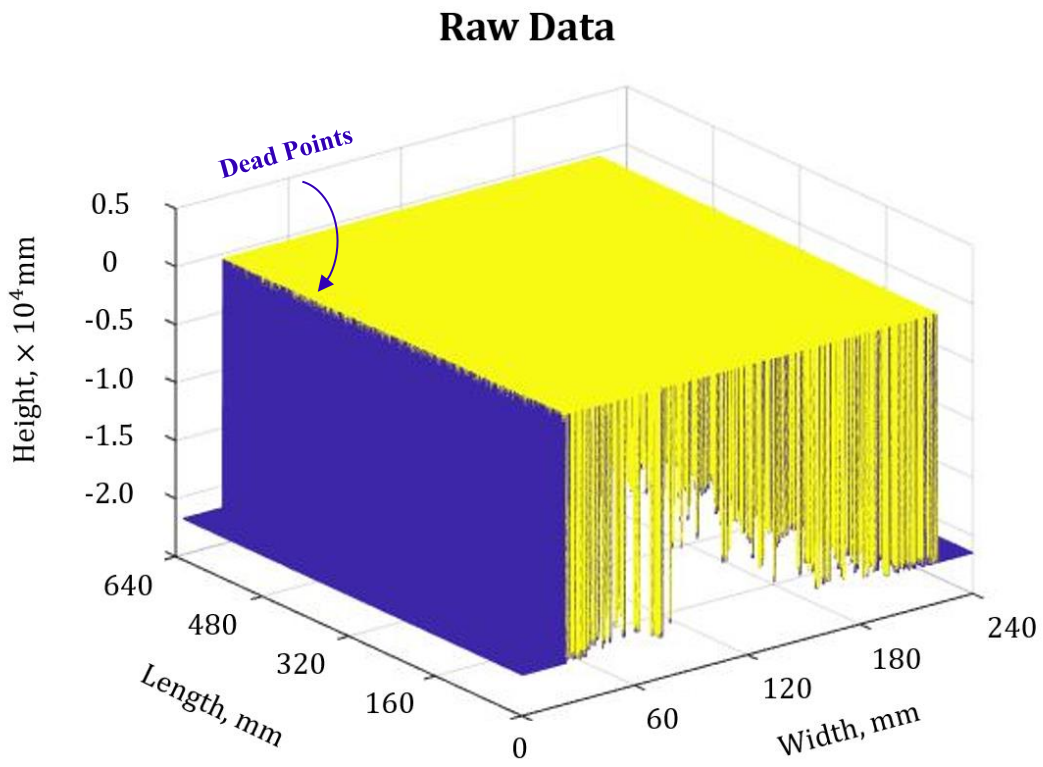

Figure 5.12: 3D Laser Scan of a Pavement Surface - Raw Data with Dead Points

These edge dead points are discarded because there isn't a reliable method to regenerate them from the existing data without overfitting. Figure 5.14 shows the surface data without the dead point on the edges.

2. Correcting the Drop-outs:

Depending on the features of the scanned surface, a drop-out, i.e. dead zone, might be created in the measurement zone. When the laser beam irradiating from the target surface is not received back by the detector due to an obstruction, the missing data are also recorded as drop-outs as shown in Figure 5.13.

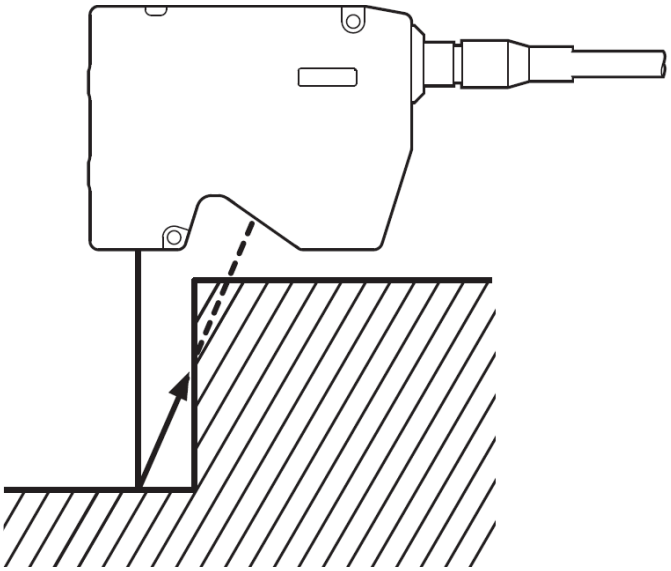

Figure 5.13: Reflected Light Obstruction Generating Drop-outs (Keyence, 2016)

When scanning the pavement surface, the aggregate features could interfere with the reflected light and cause minor local drop-outs as shown in Figure 5.14. In order to correct these drop-outs, a mean filter is applied to replace the identified drop-out points. Any point with unreasonably low height values is identified as a drop-out; usually, this value is -999.999 mm but can differ from one laser controller to the other. After identifying a drop-out, the two-dimensional mean filter first selects a 5×5 matrix centered around the drop-out point. Then the filter replaces its value by the mean (or sample average) of the remaining 24 values that are not drop-outs themselves.

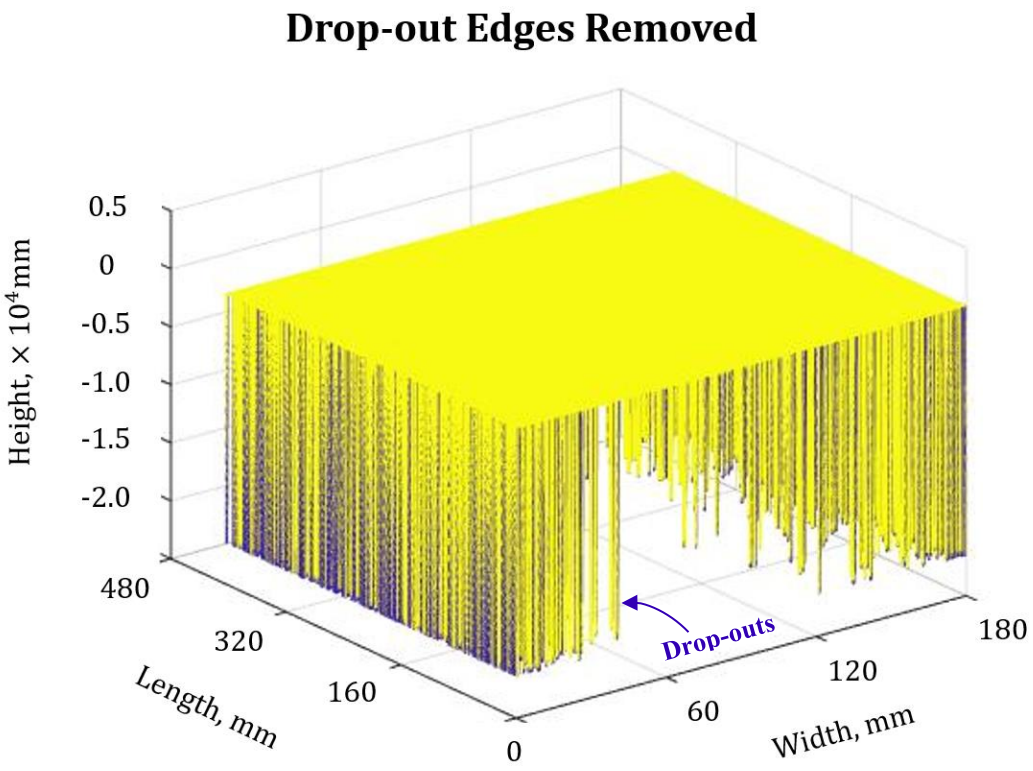

Figure 5.14: Surface Drop-outs after Removing Dead Point Edges

The example in Table 5.7 illustrates how the mean filter works. In this case, the center cell highlighted in grey and bold font is the identified drop-out. The neighboring cells forming a 5×5 matrix centered around this drop-out are identified. Their values are tested to detect which of these points are not drop-outs themselves and hence qualify as potential candidate points that replace the identified drop-out without tampering with the data. In this example, 23 out of the 24 potential points are not drop-outs themselves, and their average is used to replace the drop-out initially identified. The other corner drop-out is handled similarly by considering another 5×5 matrix centered around it. Accordingly, all the drop-outs are corrected using their neighboring data points, and the Figure 5.15 is obtained.

Before 2D Mean Filtering

-999.999	0.609	0.6074	0.6063	0.6070
0.6068	0.6068	0.6055	0.6053	0.6057
0.6069	0.6098	**-999.999**	0.6052	0.6068
0.6069	0.609	0.6085	0.6088	0.6051
0.6092	0.6098	0.6099	0.6089	0.6067

After 2D Mean Filtering

-999.999	0.6090	0.6074	0.6063	0.6070
0.6068	0.6068	0.6055	0.6053	0.6057
0.6069	0.6098	**0.6074**	0.6052	0.6068
0.6069	0.6090	0.6085	0.6088	0.6051
0.6092	0.6098	0.6099	0.6089	0.6067

Table 5.7: Example of 2D Mean Filter

3. Two-dimensional Slope Detrending

The laser used in this study has a very high precision and accuracy compared to traditional measuring techniques with a height repeatability of 5 μm. The laser is mounted onto a frame with a lower alignment precision. In addition, the surface being scanned has an inherent slope. Hence, the scanned surface shown in Figure 5.15 has a slope in both dimensions.

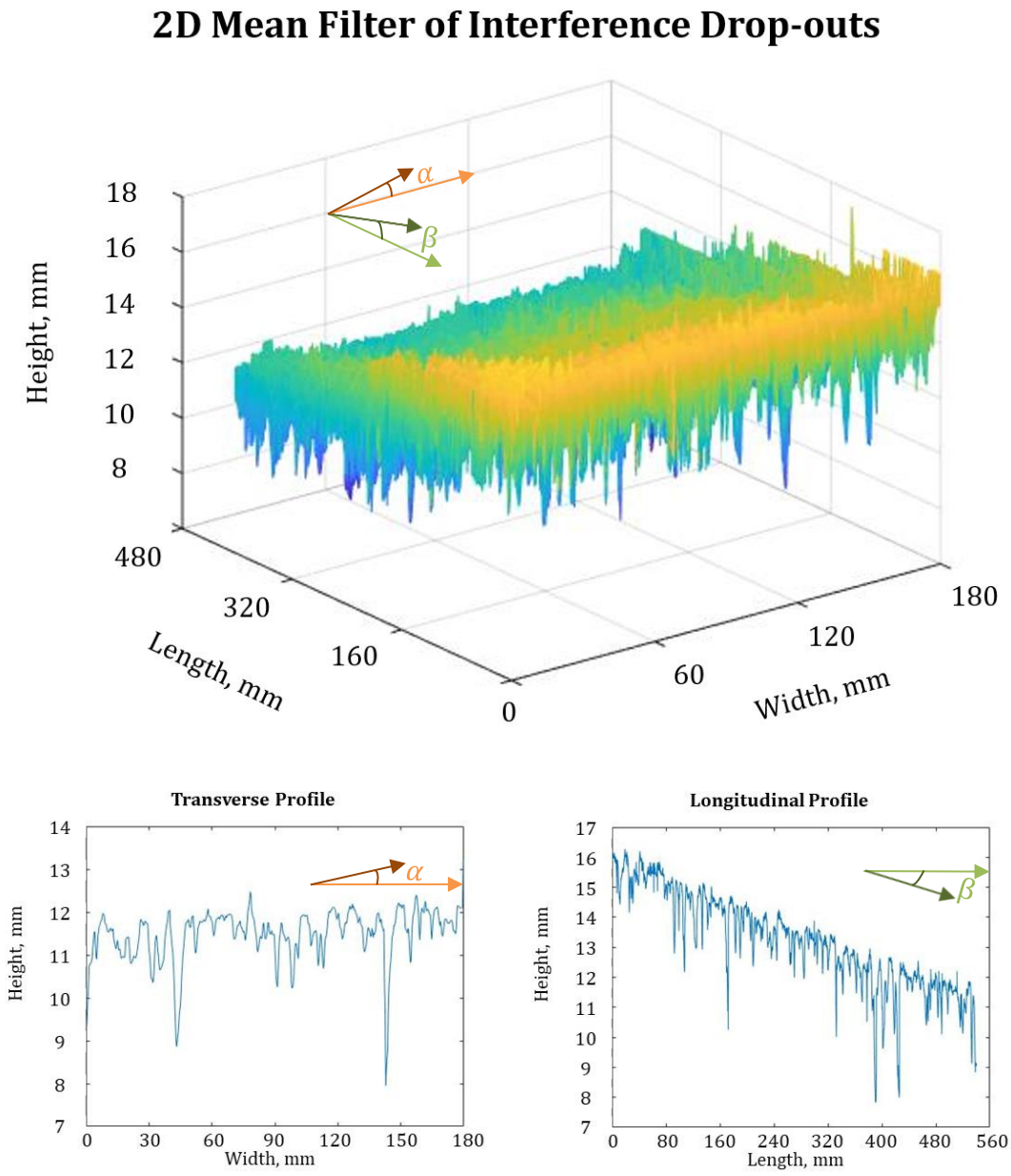

Figure 5.15: Surface & Directional Trends after Removing Drop-outs

In order to remove this slope and obtain the surface texture, first, a plane is fitted to the data by minimizing the sum of square distances between the data and the plane. Next, this surface is subtracted from the data to remove the slope. Consequently, a detrended 3D representation of the data is obtained as shown in Figure 5.16.

4. Zeroing the surface

When subtracting the best fit plane from the scanned surface, the surface obtained is centered around the x-y plane as shown in Figure 5.16. Next, the surface is shifted upwards for better visualization. Accordingly, the minimum height value recorded is subtracted from all the data shifting it upwards as shown in Figure 5.17.

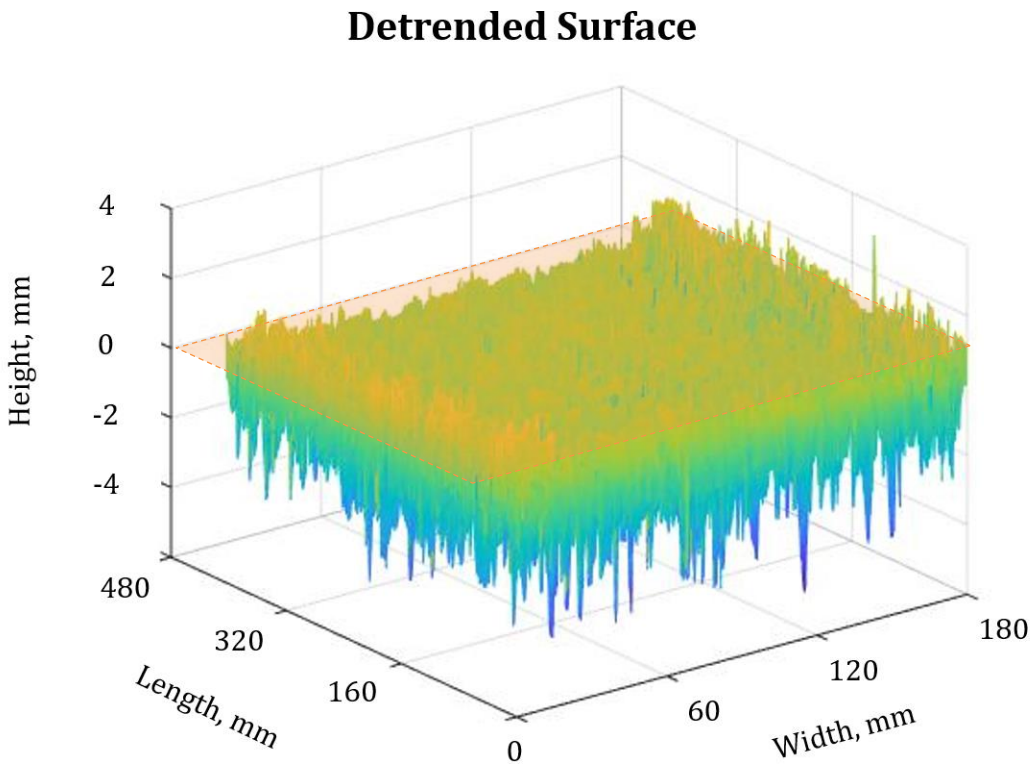

Figure 5.16: Zero-Centered Surface after Detrending

5. Local Spike Two-Dimensional Median Filtering

When subtracting the minimum from the data, the surface is shifted upwards. As shown in Figure 5.18, the surface has some local spikes that can be caused by specific features on the surface or stray light affecting the measurement. The concept of stray light is shown in Figure 5.17.

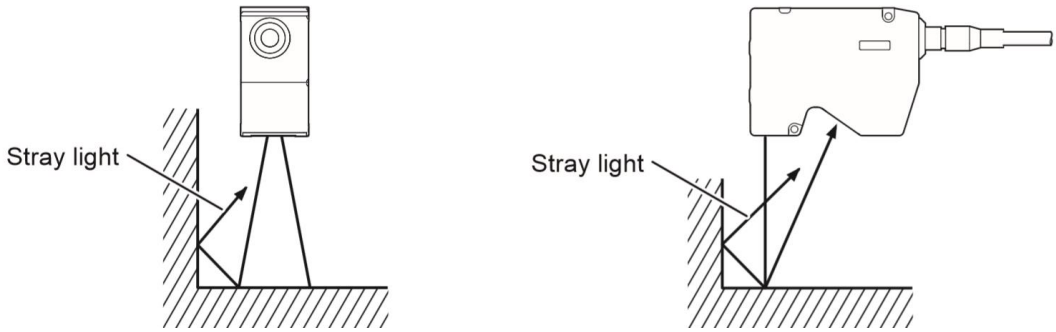

Figure 5.17: Stray Light Reflecting from edges and surface features (Keyence, 2016)

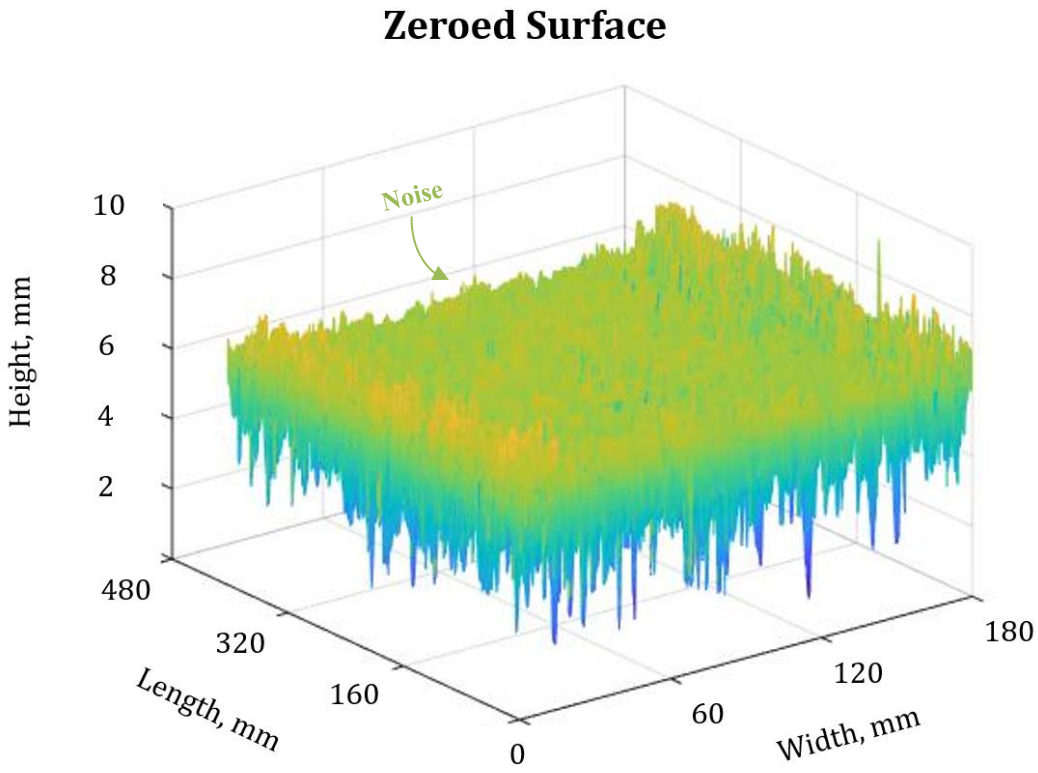

Figure 5.18: Spikes After Zeroing the Surface

When scanning the pavement surface, the laser light might stray due to aggregate features and may cause local spikes as shown Figure 5.18. In order to correct these minor spikes, a two-dimensional median filter is applied to remove these points. This

filter is applied to all the surface and does not tamper with the features but smoothens out the spikes that do not reflect local pavement features. The two-dimensional median filter first selects a 5×5 matrix centered around each point. Then the filter replaces the point value by the median of all the considered values. The example in Table 5.8 illustrates how the median filter works.

Before 2D Median Filtering

0.6167	0.6228	0.6221	0.6207	0.618
0.6182	0.6209	0.6229	0.616	0.6201
0.6263	0.6101	**0.6281**	0.6182	0.6242
0.6182	0.6192	0.6267	0.6228	0.6291
0.621	0.6168	0.6234	0.6201	0.6149

After 2D Median Filtering

0.6167	0.6228	0.6221	0.6207	0.618
0.6182	0.6209	0.6229	0.616	0.6201
0.6263	0.6101	**0.6207**	0.6182	0.6242
0.6182	0.6192	0.6267	0.6228	0.6291
0.621	0.6168	0.6234	0.6201	0.6149

Table 5.8: Example of 2D Median Filter

In this case, the center cell highlighted in grey and bold font is the target cell. The neighboring cells forming a 5×5 matrix centered around this point are identified. The median of the 25 values is used to replace the value of the cell. Accordingly, the surface is smoothened after applying the median filter (Figure 5.19).

6. Local Reference Generation Mimicking Binder Flow

   The surface is divided into different square elements of size 30 by 30 mm. For each element, a horizontal plane is created at the 98th percentile value of the surface heights; determining this percentile is discussed in a later section within this chapter.

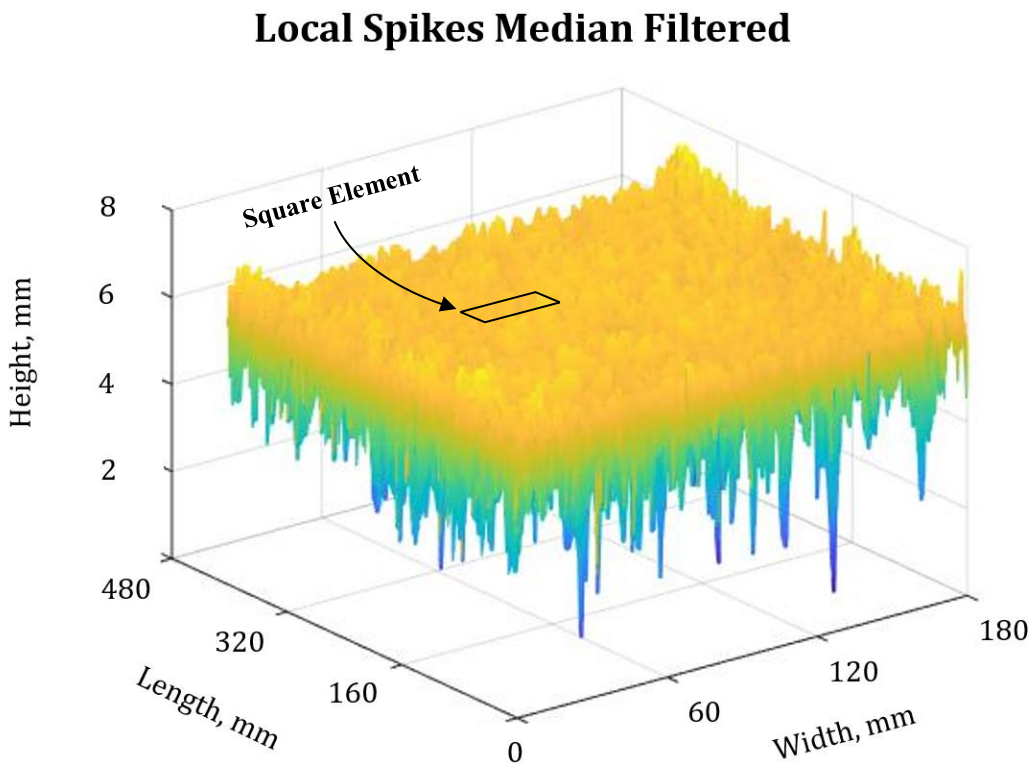

Figure 5.19: Surface Features After Median Filtering

Accordingly, the virtual horizontal plane is imposed onto the scanned surface to form a layer where the voids are virtually filled with the binder. Figure 5.20 shows the rendering for two different surfaces.

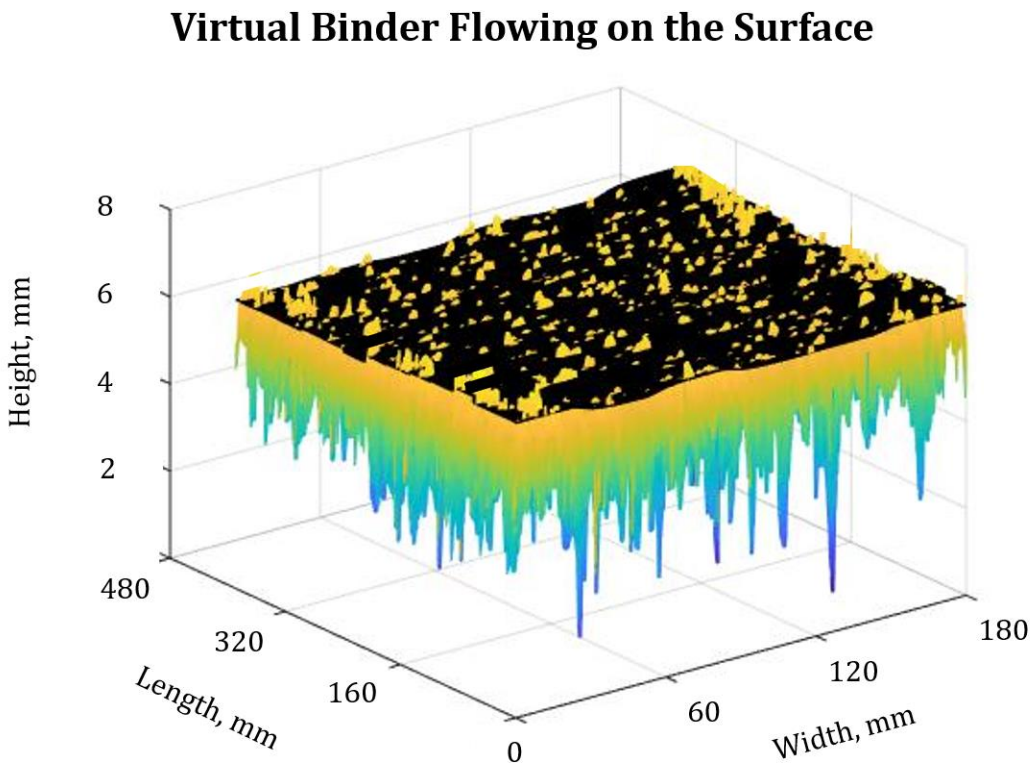

Figure 5.20: Surface Features with Virtual Binder

Reference Plane and Volume of Voids

As mentioned earlier, some design methods adjust the BAR by estimating the volume of voids in the surface texture using the MTD obtained from the SPT (Transit NZ, RCA, & Roading NZ, 2005; Alderson A. , 2006; IDRRIM, 2017; SANRAL, 2007). The MTD provides an average value of the deviations of the pavement surface from a true planar surface (ASTM, 2015.1). However, the SPT is a subjective and an operator-dependent test. Previous research attempted to replace the sand patch test with laser-based

devices that eliminate the bias associated with the operator. These studies scanned the pavement surface and demonstrated that a reference point, line, or plane is required for the calculation of the MTD (Meegoda, Hettiarachchi, Rowe, Bandara, & Sharrock, 2002; Fugro, 2017; Hao, Sha, Sun, Li, & Zhao, 2016). Nevertheless, pointing tips, debris, or few large aggregates can skew the reference point and overestimate the results. When it comes to seal coat design, the reference plane should mimic the binder flowing over the pavement surface and filling almost all the voids. Since the surface, as shown in Figure 5.20, is not homogeneous, smaller square elements (30 by 30 mm) of the surface texture were considered. Each square has its own reference plane based on the data heights contained within it. With the considered size elements, the volume in the surface texture represents the macrotexture (wavelength: 0.5 to 50 mm). Figure 5.19 displays the 3D scanned surface with one of the square regions for illustration. Note that the size of square elements can be changed to meet the needs of the user and the data at hand.

To calculate the volume of voids, the distance between the reference plane and each data point below it is calculated. The average depth is determined for each of the considered square elements. The volume of voids in the square element is the product of the square area and the average depth of the scanned surface from its reference plane. The same procedure is reiterated for each square region over the whole scanned area. The total volume of voids in the whole scanned area is the sum of the volume of voids in each individual region. The total volume of voids can then be divided by the total area of the scanned surface to obtain an estimate of the volume of voids per unit area.

Results and Analysis

Different agencies have attempted to determine the BAR of seal coats based only on the volume of voids in the aggregates as shown in part (a) of Figure 5.21. Consequently,

they rely on different subjective methods to estimate or assess the voids in the existing surface texture (illustrated in part (b) of Figure 5.21). As depicted in part (c), the existing surface texture provides a surplus of voids in excess to those accounted for when considering the aggregate matrix on a flat surface. Hence, it is recommended to accurately measure the volume of voids in the existing pavement texture, then estimate the total volume of voids, and finally calculate the binder application rate. This method eliminates the need to subjectively assess the texture and empirically correct the BAR.

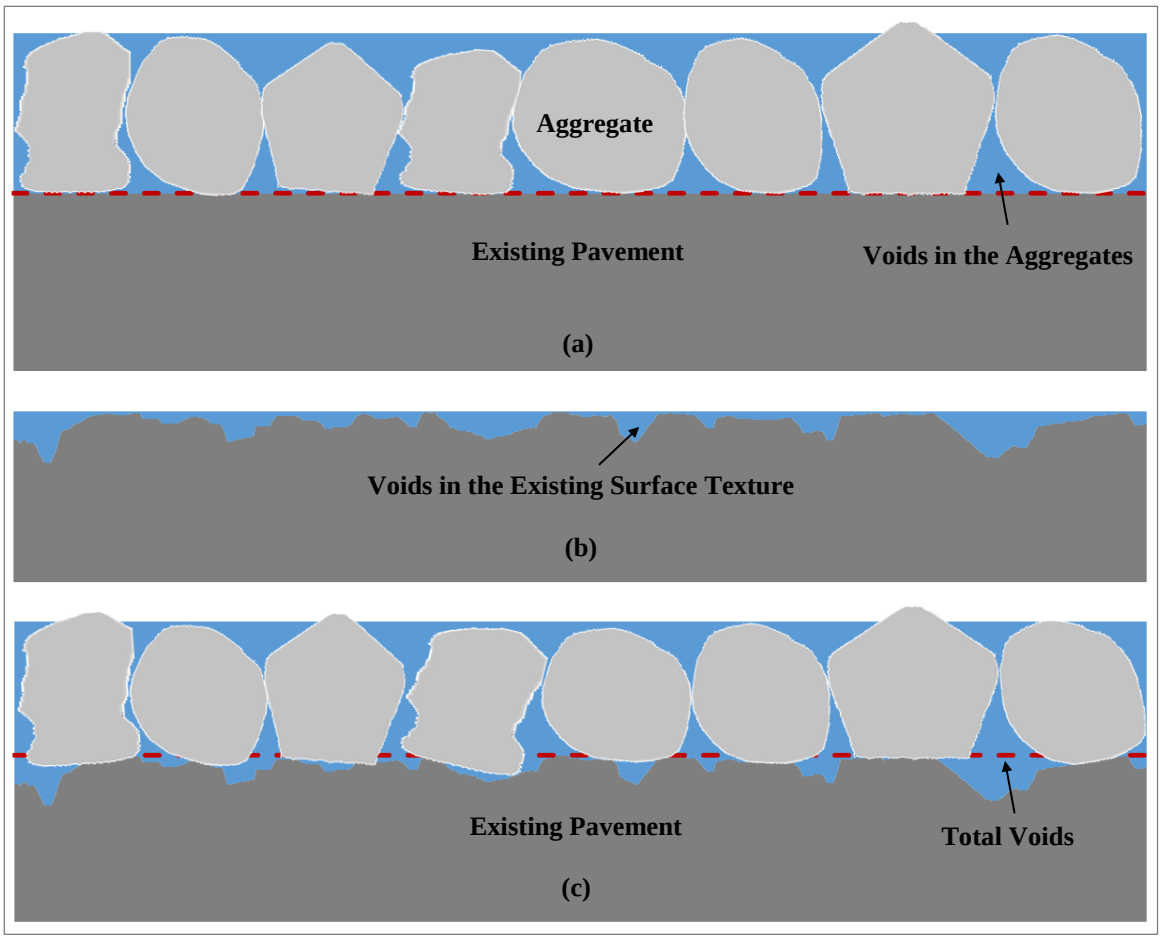

Figure 5.21: Voids in the Seal Coats Structure

Most design methods estimate the volume of voids in the existing surface texture by measuring the MTD using SPT. As shown in the previous section, the variability of the SPT is relatively high, and the test remains highly dependent on the operator's perception. Hence, an operator-independent and objective procedure capable of accurately quantifying the volume of voids in the surface texture is required.

Determining the Reference Plane

The purpose behind the reference planes is to calculate the volume of the voids in the existing surface texture and simulate the flow of the binder within these voids. Different simulations of the reference planes were performed at different percentiles ranging from 50 to 100th percentile, and the respective volume of voids were calculated as shown briefly in Table 5.9 and extensively in the Table 5.10.

Test Section	MTD (mm)	Volume of Voids in Texture $V_{V_{ES}}$(L/m^2) with the reference plate at				
		95th Perc.	96th Perc.	97th Perc.	98th Perc.	99th Perc.
Speedway (1)	0.64	0.52	0.54	0.57	**0.61**	0.66
Speedway (2)	0.63	0.52	0.54	0.56	**0.59**	0.63
FM 1431 (1)	1.24	1.46	1.50	1.55	**1.62**	1.72
FM 1431 (2)	1.34	1.46	1.50	1.55	**1.61**	1.70
FM 1431 (3)	1.24	1.60	1.65	1.70	**1.77**	1.87
FM 1626 (1)	0.75	0.64	0.66	0.69	**0.72**	0.78
FM 1626 (2)	0.73	0.67	0.69	0.71	**0.75**	0.80
FM 1626 (3)	0.68	0.69	0.71	0.74	**0.78**	0.84
IH 20 (1)	2.33	2.62	2.72	2.82	**2.93**	3.08
IH 20 (2)	2.29	2.33	2.41	2.50	**2.61**	2.76
IH 20 (3)	2.10	2.57	2.66	2.75	**2.88**	3.05
RM 12 (1)	0.45	0.39	0.41	0.43	**0.46**	0.51
RM 12 (2)	0.47	0.39	0.40	0.42	**0.45**	0.51
RM 12 (3)	0.47	0.39	0.41	0.43	**0.46**	0.51
SH 36 (1)	2.23	2.27	2.33	2.41	**2.51**	2.66
SH 36 (2)	2.04	2.21	2.27	2.35	**2.45**	2.61
SH 36 (3)	2.09	2.34	2.41	2.50	**2.61**	2.76

Table 5.9: Volume of Voids for Different Reference Planes

SH 195 (1)	1.60	1.39	1.44	1.50	**1.58**	1.70
SH 195 (2)	1.78	1.50	1.55	1.60	**1.67**	1.77
SH 195 (3)	2.16	1.59	1.64	1.70	**1.78**	1.90
US 84 (1)	1.07	0.88	0.94	1.00	**1.08**	1.18
US 84 (2)	1.18	0.93	0.99	1.06	**1.14**	1.23
US 84 (3)	1.24	1.02	1.07	1.13	**1.21**	1.31
US 181 (1)	1.36	1.22	1.26	1.32	**1.38**	1.46
US 181 (2)	1.33	1.12	1.15	1.20	**1.25**	1.33
US 181 (3)	1.24	1.29	1.33	1.38	**1.44**	1.54

Table 5.9 Continued

Test Locations	**FM 1626**		**RM 12**		**FM 1431**		**IH 20**		**SH 36**		**SH 195**		**US 84**		**US 181**	
Test Sections	**1**	**2**	**1**	**2**	**1**	**2**	**1**	**2**	**1**	**2**	**1**	**2**	**1**	**2**	**1**	**2**
MTD Obtained by Sand Patch Test	0.750	0.734	0.474	0.472	1.236	1.338	2.330	2.290	2.037	2.087	1.600	1.780	1.183	1.243	1.364	1.334
Percentiles	**MTD Obtained by Simulation Model**															
50th	0.533	0.556	0.286	0.288	1.099	1.127	1.312	1.081	1.422	1.418	1.132	1.167	0.304	0.362	0.908	0.944
60th	0.527	0.557	0.290	0.290	1.118	1.127	1.417	1.244	1.481	1.513	1.125	1.177	0.334	0.427	0.909	0.955
70th	0.530	0.566	0.299	0.299	1.141	1.148	1.584	1.425	1.532	1.638	1.146	1.210	0.386	0.511	0.924	0.972
80th	0.545	0.588	0.318	0.318	1.206	1.193	1.810	1.654	1.617	1.848	1.213	1.257	0.503	0.613	0.981	1.023
81st	0.548	0.591	0.321	0.320	1.214	1.201	1.838	1.678	1.629	1.876	1.224	1.265	0.521	0.628	0.990	1.030
82nd	0.551	0.595	0.324	0.323	1.223	1.210	1.869	1.703	1.642	1.907	1.235	1.272	0.540	0.643	0.999	1.039
83rd	0.554	0.599	0.328	0.326	1.233	1.219	1.903	1.726	1.657	1.939	1.246	1.280	0.559	0.661	1.009	1.048
84th	0.557	0.603	0.331	0.329	1.244	1.229	1.937	1.752	1.671	1.974	1.259	1.289	0.579	0.681	1.019	1.057
85th	0.561	0.608	0.335	0.333	1.256	1.238	1.968	1.781	1.687	2.015	1.273	1.298	0.603	0.702	1.031	1.067
86th	0.566	0.613	0.340	0.337	1.270	1.250	2.004	1.808	1.705	2.055	1.287	1.308	0.628	0.727	1.044	1.077
87th	0.571	0.618	0.344	0.341	1.285	1.261	2.048	1.835	1.726	2.098	1.303	1.319	0.657	0.751	1.059	1.088
88th	0.577	0.624	0.349	0.346	1.302	1.275	2.097	1.867	1.749	2.146	1.323	1.333	0.686	0.779	1.075	1.100
89th	0.583	0.631	0.354	0.351	1.322	1.290	2.151	1.901	1.774	2.198	1.344	1.349	0.715	0.814	1.090	1.115
90th	0.590	0.638	0.360	0.357	1.344	1.306	2.212	1.937	1.803	2.253	1.367	1.367	0.746	0.854	1.107	1.131
91st	0.598	0.646	0.367	0.363	1.369	1.324	2.279	1.983	1.832	2.314	1.390	1.387	0.779	0.898	1.126	1.148
92nd	0.607	0.655	0.375	0.370	1.397	1.344	2.347	2.041	1.862	2.374	1.415	1.410	0.819	0.944	1.149	1.169
93rd	0.617	0.666	0.383	0.379	1.429	1.367	2.417	2.102	1.899	2.443	1.446	1.435	0.871	1.001	1.177	1.191
94th	0.629	0.678	0.393	0.389	1.466	1.393	2.510	2.163	1.944	2.524	1.486	1.464	0.928	1.074	1.210	1.215
95th	0.644	0.693	0.404	0.400	1.511	1.424	2.613	2.259	1.998	2.620	1.535	1.497	0.990	1.148	1.246	1.244
96th	0.662	0.712	0.419	0.414	1.563	1.461	2.719	2.365	2.067	2.712	1.594	1.538	1.059	1.227	1.288	1.276
97th	0.684	0.736	0.437	0.433	1.632	1.510	2.857	2.504	2.162	2.841	1.673	1.589	1.156	1.341	1.349	1.320
98th	0.711	0.773	0.462	0.460	1.726	1.584	2.992	2.729	2.279	3.074	1.779	1.663	1.270	1.498	1.432	1.381
99th	0.756	0.834	0.505	0.503	1.859	1.723	3.155	3.083	2.472	3.360	1.927	1.791	1.412	1.913	1.564	1.490
100th	1.266	1.456	2.740	1.084	2.543	2.313	4.036	4.351	3.427	4.399	2.443	2.277	2.221	2.843	3.045	2.016
SPT	0.750	0.734	0.474	0.472	1.236	1.338	2.330	2.290	2.037	2.087	1.600	1.780	1.183	1.243	1.364	1.334

Table 5.10: Volume of Voids for Different Reference Planes - 2

By comparing the results obtained using the laser to those from the SPT, it can be observed that there are no evident outliers. Although, the values do not precisely match, they are within the normal variability of the SPT. Figure 5.22 is a graphical representation of the Table 5.10 where the sections are sorted from the lowest MTD to the highest MTD. It can be observed that at the 98th percentile the MTD values are comparable, especially for low

MTD values. However, at higher values of MTD, the variability within the sand patch test increases, and it becomes harder for the operator to run the SPT properly with limited sand volumes that fill some of the pores. Hence, there are significant differences between the MTD measured by the laser and the SPT at such levels of texture.

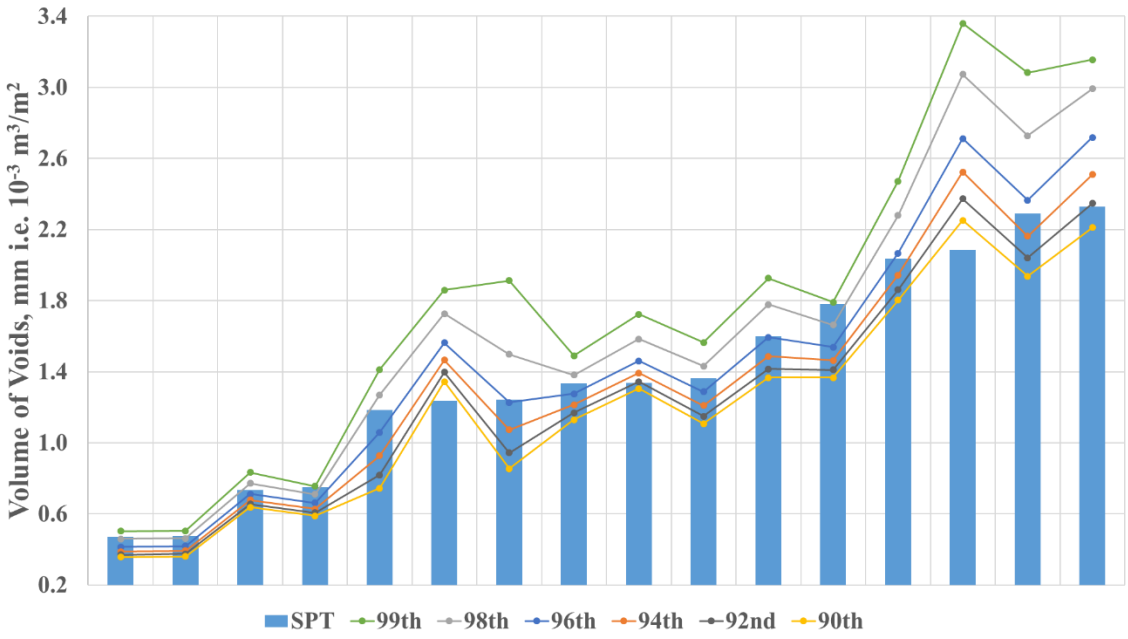

Figure 5.22: Comparison Between Various Reference Levels and MTD.

It is noteworthy to mentioning that the developed prototype mimics the flow of binder within the existing surface voids and is highly repeatable and reproducible. Several graphical representations of the flow of binder on the surface were generated in order to visualize the appropriate reference needed to determine the volume of voids in the existing pavement surface. Figure 5.23 shows a side view of the scanned pavement with the reference plane at four different percentile levels of the surface depth (94 to 100th). In this figure, several profiles are stacked next to each other, and the obtained binder flow level is easily identified.

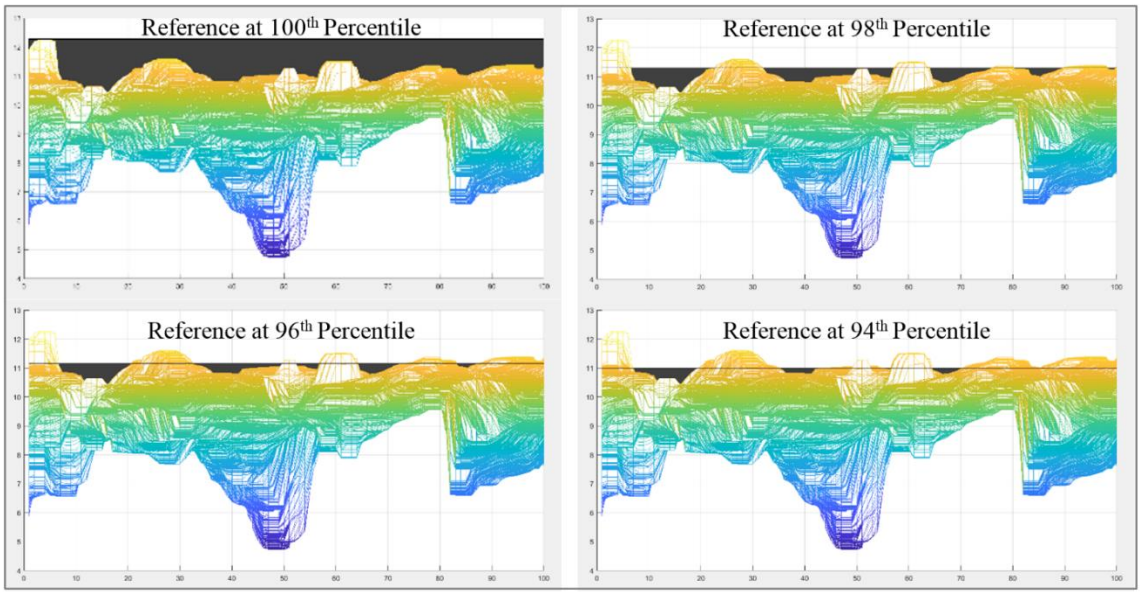

Figure 5.23: Simulated Texture Voids Filled by Binder

The volume of voids in the surface texture (highlighted in black in Figure 5.24) is calculated as the volume between the scanned surface and the reference plane. The 98th percentile is considered the best predictor plane for simulating the flow of the binder and calculating the volume of voids in the existing surface texture. Hence, the reference plane for the entire scanned surface is the mesh of the 98th percentiles of each of the smaller data blocks (30 mm squares) as represented Figure 5.24.

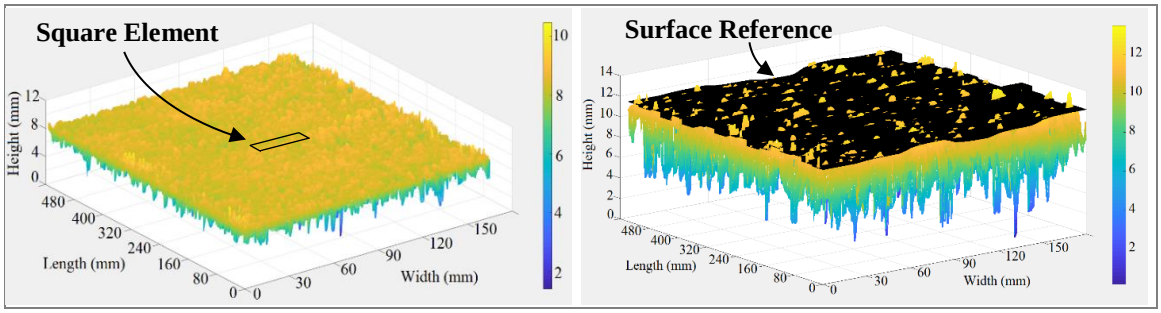

Figure 5.24: Flow of the Binder on the Existing Pavement Surface

BINDER APPLICATION RATE RECOMMENDATION

The performance of the seal coat design is directly related to the adequate estimation of the required BAR and AAR. Almost all the current design methods measure the voids in the aggregate layer, determine the BAR, and correct for voids in the texture. Since the BAR is a function of the voids in the seal coat system, the ability to measure the total volume of voids enhances the BAR estimation. At the same time, the existing surface texture is highly variable along both the width and the length of the road section. Conventional methods rely on testing few locations within the job site and applying a one-fits-all BAR. This leaves the rough-textured locations with underestimated binder and the smooth-textured areas with overestimated binder, compromising the performance of the treatment. However, the laser mitigates these deficiencies by measuring the texture of the roadway at several, if not all the locations, and modifying the BAR accordingly.

To improve the calculation of the BAR, the measured volume of voids in the existing surface texture should be added to the estimated volume of voids in the aggregate matrix before calculating the BAR. As an example, the following discussion presents the modifications that would be required for two of the existing design methods, to better calculate the BAR.

Hanson Design Method

Hanson suggested that the volume of voids in the compacted aggregate matrix occupies 20% of the total compacted volume and is given by:

$$V_{V_{Agg}} = 20\% \text{ of Compacted Aggregate Volume } = 0.2 \times \frac{ALD}{1000}$$

Where $V_{V_{Agg}}$ is the volume of voids in the aggregate matrix in m^3/m^2, and ALD is the average least dimension of the aggregates in mm.

Note: The compacted aggregate volume has a compacted depth estimated in mm to be the average least dimension (ALD) of the aggregates over an area of $1m^2$.

However, the total volume of voids, $V_{V_{Total}}$, in the seal coat matrix is the sum of the volume of voids in the aggregate matrix, $V_{V_{Agg}}$, and the volume of voids in the existing surface texture, $V_{V_{ES}}$. Hence, the total volume of voids in the seal coat is given by:

$$V_{V_{Total}} = V_{V_{Agg}} + \mathbf{V_{V_{ES}}}$$

Hanson's experience with seal coats shows that chips will be held in position if the bitumen occupies 70% of the void volume; however, Hanson did not account for the volume of voids in the existing surface texture. Instead, the BAR is calculated based on the volume of voids in aggregates. Consequently, the volume of voids in the existing surface texture could be easily incorporated in the calculations as follows:

$$\text{BAR} = 0.7 \times V_{V_{Total}} = 0.14 \times \text{ALD} + \mathbf{0.7} \times \mathbf{V_{V_{ES}}}$$

Modified Kearby Method

In the modified Kearby method, the BAR is determined in gal/yd^2 based on the average mat depth, the desired embedment depth, and the experimentally estimated proportion of voids in the aggregates. Consequently, a correction factor for predicted traffic and another factor for volume of voids in the existing surface texture are applied as follows:

$$\text{BAR} = 5.61\text{E}\left(1 - \frac{\text{W}}{62.4 \times \text{G}}\right)(\text{T}) + \text{V}$$

Where E is the embedment depth in inches, which is a percentage of the average mat depth d, $\left(1 - \frac{\text{W}}{62.4 \times \text{G}}\right)$ is the proportion of voids in the aggregate matrix, W is the dry loose unit weight of aggregates, G is the dry bulk specific gravity of aggregates, T is the traffic correction factor, and V is the empirical correction for existing surface texture in gal/yd^2.

The total volume of voids can be used to estimate the BAR without the need to empirically correct for the existing surface texture. In the original equation, the proportion of voids is relevant to the volume of voids in the aggregate matrix (shown in part (a) of Figure 5.21). This is replaced by a proportion of voids relevant to the whole seal coat system (shown in part (c) of Figure 5.21) as follows:

$$\text{Proportion of Voids} = 1 - \frac{\text{Volume of Solids}}{\text{Total Volume}} = 1 - \frac{\frac{W}{62.4 \times G} \times d}{d + \mathbf{V_{V_{ES}}}} = 1 - \left\{\frac{W}{62.4 \times G} \times \frac{d}{d + V_{V_{ES}}}\right\}$$

Consequently, the BAR is calculated as follows:

$$BAR = 5.61E \left(1 - \left\{\frac{W}{62.4 \times G} \times \frac{\mathbf{d}}{\mathbf{d} + \mathbf{V_{V_{ES}}}}\right\}\right)(T)$$

Where $\left(1 - \left\{\frac{W}{62.4 \times G} \times \frac{\mathbf{d}}{\mathbf{d} + \mathbf{V_{V_{ES}}}}\right\}\right)$ is the proportion of voids in the entire system.

This proposed modification to the existing design methods could help highway agencies and state DOTs better assess the required BAR and improve the performance of the seal coat system. The ability to incorporate an automated and accurate method for calculating the volume of voids in the existing surface texture would constitute a significant enhancement in the field of pavement preservation in general and seal coat treatments in particular. This enhancement would lead to a better design and, consequently, significant savings in tax payer dollars.

Chapter 6: Conclusion and Recommendations

This chapter presents a summary of the research work conducted during the fulfillment of the master's work at The University of Texas at Austin. Discussed below are the most important findings and recommendations for possible future work in developing the UTexas Seal Coat Design Method Using Laser Technologies.

SUMMARY

Pavement preservation has recently become common practice for highway agencies due to their cost-effectiveness. Seal coats rank among the most popular surface treatments. First, the asphalt binder is sprayed on top of the surface. Subsequently, the aggregate is spread over the asphalt, and the system is rolled and compacted. The performance of this dual system depends on the adequate estimation of the material application rates. The over-estimation or underestimation of these application rates leads to premature failures that compromise the safety of the road users.

Many highway agencies worldwide have developed their own design methods stemming from Hanson's initial design guide in 1935. Currently there is at least ten different seal coat design methods that are in-use around the world. Unfortunately, the different design methods recommend different application rates. The root for such differences is the empirical nature of most designs along with the engineering judgement required in assessing site-specific conditions such as: surface texture, aggregate coverage, estimated traffic, surface hardness, embedment depths, and many more. This disparity questions the reliability of these methods and raises the need for an analytical, objective, and consistent design method.

With recent advancements in the laser technology, highway agencies, Departments of Transportations, and research institutes are gearing towards improving and employing

such developments to contribute towards better seal coat designs, among other practices. The advantage of using laser technology is the ability to capture 3D data of pavement surfaces using a non-destructive, quick, and simple operation. These versatile laser systems can be used in both the laboratory and the field for design, quality assurance, quality control, and performance assessment. With this objective, a laser scanning prototype was developed at The University of Texas at Austin. It consists of a line laser scanner that can measure height values along a line. This scanner is mounted onto a linear translation stage allowing it to move in the longitudinal direction. The whole system is computer-controlled allowing the users to set their preferred settings. Ultimately, the 3D laser scanner should be mounted to seal coat sprayers making them capable of measuring the pavement surface in real-time while paving. Accordingly, the volume of voids in the existing texture could be constantly quantified to determine the adequate binder application rate. This rate should be varied along both the width and the length of the roadway due to the non-homogeneous nature of the surface texture. In order to measure the volume of voids in the existing surface texture, the raw data of the surface scan is filtered and processed to extract the texture features. The 3D model of the surface is then divided into square elements with specific reference planes that mimic the flow of the binder on the surface. Accordingly, the volume of voids, calculated between the surface and the reference plane, is used to improve the binder application rate estimation and provide the right dosage for the right location instead of having a one dosage that fits all.

Another part of the research work focused on developing a predictive model for the aggregate application rate. This model requires the input of two aggregate parameters: the aggregate density and the average least dimension (ALD). Subsequently, the aggregate dosage is determined based on an aggregate coverage ratio; the higher the surface coverage the higher the AAR. This model was developed from a series of tests conducted on different

aggregate types, densities, and sizes. These tests involved spreading the aggregate samples at different mass increments. The 3D laser was then used to measure the aggregate coverage levels. Afterwards, a simultaneous linear regression was used to determine the predictive model that best fits the data collected. This model showed that higher application rates are needed with denser and larger aggregates to obtain the same coverage level. This technique could become the foundation for an analytical design method that tailors for site-specific conditions and mitigates the deficiencies of conventional methods and practices. It simply requires retrofitting the binder sprayer trucks with lasers, CPU processors, and nozzle dosage gauges to better design the seal coat and enhance the overall performance.

IMPORTANT FINDINGS

The major findings and conclusions attributed to his study are presented in the bullet points below:

- Seal coats are popular cost-effective surface treatments used to maintain pavement surfaced. Their performance is directly affected by the adequate estimation of the binder and aggregate application rates.
    - Overestimating the binder application rate or underestimating the aggregate application rate would lead to bleeding surfaces.
    - Underestimating the binder application rate or overestimating the aggregate application rate would lead to raveling.
- Different design methods are used worldwide where each design method has its own philosophy for determining the material dosages based on experimental studies, laboratory tests, or engineering judgements.
- Unfortunately, there is no consensus on the dosages recommended for the construction of the seal coat. A case study was conducted through a design exercise that showed

quite a high variability and inconsistency between the dosages obtained by different design methods for seal coating a specific road.

- Incorporating the 3D laser technology in the seal coat design and construction practices provides a significant improvement in the consistency of seal coat products worldwide. The laser technology provides an accurate, reliable, and objective tool for assessing site-specific conditions.
- A predictive model was developed to enhance the calculation of the aggregate application rate. The model requires as inputs the aggregate density, average least dimension, and the surface coverage proportion to determine the aggregate dosage, according to the following equation:

$$\text{AAR, kg/m}^2 = \frac{10}{54.9 \times 17.4} \times \begin{cases} \text{Y/b} \ldots\ldots\ldots\ldots\ldots\ldots\ldots\ldots\ldots\ldots & \text{for Y} \leq 100 - \frac{\text{b}}{\text{d}} \\ \dfrac{100 \times \text{d} - \text{b}\left(1 - \ln\left(\dfrac{100 - \text{Y}}{\text{b/d}}\right)\right)}{\text{b} \times \text{d}} & \text{otherwise} \end{cases}$$

Where Y is the target coverage in % point; while, b, d, and Y_0 are determined as:

$$\text{b} = 0.3998 - 0.0646 \times \rho - 0.0148 \times \text{ALD};$$

$$\text{d} = 0.0151 - 0.0027 \times \rho - 0.0005 \times \text{ALD};$$

$$Y_0 = 100 - \frac{\text{b}}{\text{d}} = 100 - \frac{0.3998 - 0.0646 \times \rho - 0.0148 \times \text{ALD}}{0.0151 - 0.0027 \times \rho - 0.0005 \times \text{ALD}}; \text{and}$$

ALD is the average least dimension in mm and ρ is the bulk density in g/cm^3

- Sand patch test is one of the most common macrotexture characterization and assessment techniques because it is relatively cheap and easy to perform. Unfortunately, the analysis of variance of the sand patch test showed that this test is subjective and highly dependent on the perception of the operator. The test is capable of distinguishing between different surfaces, but it is not capable of accurately estimating the volume of voids in the surface texture. This negatively affects the correction of the binder application rate for surface texture.

- The 3D laser scanner was used to measure the volume of voids in the existing surface mitigating the shortcomings of the existing methods. In addition, an algorithm was developed to objectively estimate the MTD, and adjustments to commonly used seal coat design methods were proposed.
- The UTexas seal coat design method is the first analytical design method that minimizes the subjective judgement of the operator and allows for simple modification of existing designs and practices around the world.

RECOMMENDATIONS

The objective of this research work was to develop an analytical seal coat design method that limits the subjective assessments pertaining to site-specific features. The methodology consists of incorporating the 3D laser scanner prototype in a laboratory-setting to develop an AAR predictive model and in a field-setting to quantify the volume of voids in the existing surface texture. This approach is one of its kind in both applications, but, as part of this study, it could not be compared to reliable references or practices for calibration. It is recommended to move this method forward onto a pilot program that makes use of the prototype in order to design and build the seal coat and monitor the long-term performance. As for the AAR predictive model, a higher reliability could be obtained by testing a larger sample of aggregates with various densities, grades, or ALDs.

Glossary of Abbreviations

This section compiles a comprehensive list of abbreviations used throughout the thesis making it easier for the reader to refer to.

AAR	=	Aggregate Application Rate
ADT	=	Average Daily Traffic
AFNOR	=	Association Francaise de Normalisation
AGD	=	Average Greatest Dimension
ALD	=	Average Least Dimension
ANOVA	=	Analysis of Variance
ASCE	=	American Society of Civil Engineers
ASTM	=	American Society for Testing and Materials
BAR	=	Binder Application Rate
BSI	=	British Standard Institute
CISA	=	Cybersecurity and Infrastructure Security Agency
COLTO	=	Committee of Land Transport Officials
DHS	=	Department of Homeland Security
DOT	=	Department of Transportation
EHV	=	Equivalent Heavy Vehilces
ELT	=	Effective Layer Thickness
ELV	=	Equivalent Light Vehicle
FHWA	=	Federal Highway Administration
GGBFS	=	Ground Granulated Blast-Furnace Slag
GNP	=	Gross National Product
HCV	=	Heavy Commercial Vehicle

HV	=	Heavy Vehicle
LASER	=	Light Amplification by Stimulated Emission of Radiation
LHV	=	Long Heavy Vehicle
LLS	=	Line Laser Scanner
MPD	=	Mean Profile Depth
MTD	=	Mean Texture Depth
PCI	=	Pavement Condition Index
PM	=	Preventive Maintenance
PPD	=	Presidential Policy Directive
PSV	=	Polished Stone Value
SABS	=	South African Bureau of Standards
SANRAL	=	South African National Roads Agency Ltd.
SMTD	=	Sensor Measured Texture Depth
SPT	=	Sand Patch Test
SSE	=	Sum of Square Errors
ST	=	Standard Test
TMH	=	Technical Methods for Highways
TVAR	=	Transversely Varying Asphalt Rates
TxDOT	=	Texas Department of Transportation
USDOT	=	United States Department of Transportation
VAD	=	Visual Assessment Level of Defects

Appendix : Comparing the Popular Seal Coat Design Methods Used Worldwide

This appendix presents a comparative study of the most popular seal coat design methods that are being employed around the world. In order to objectively compare the outcomes of those methods, the following case study was conducted whereby a specific highway section was considered for surface treatment using seal coats. Sufficient input data is provided to make all the design methods possible.

CASE STUDY

The single carriageway road (undivided Highway), shown in Figure A.1, is scheduled for preventative maintenance with the objective of providing a waterproof surface and enhance the skid resistance for the next five years. Afterwards, the pavement is scheduled for a major rehabilitation as well as potential lane upgrades. The area to be resurfaced has the following characteristics:

- Geometry
    - Long uphill section with a gradient of 4%;
    - Two lanes in each direction with shoulders 2.7 m wide; and
    - Lane width of 3.7 m [12 ft]
- Surface Condition
    - 10 mm-seal as existing surface;
    - Variable texture across the width of the pavement;
        - The slow moving lane is somewhat uniform and very smooth. Sand patch test results showed MTD values between 0.4 and 0.6 mm.
        - The fast/passing lane is uniform and coarse with an MTD of 1.5 mm.
        - The shoulder is uniform and coarser with an MTD of 2.4 mm, and

        - The lanes are coarser along the edges and between the wheel paths.
    - Surface hardness ball penetration: 1.0 to 2.0 mm (not punch-able).
    - Impermeable surface.
- Distresses
    - The heavily trafficked slow lane previously experienced minor rutting and some distresses (low severity cracks and potholes) that had been fixed and adequately treated.
- Aggregates
    - 14 mm crushed basalt;
    - Average Least Dimension 8.6 mm;
    - 22% Flakiness; and
    - Gradation D/d ~ 14/10 mm shown in Table A.1.

Sieve Size	**1 in. 25.4 mm**	**¾ in. 19.6 mm**	**0.530 in. 13.2 mm**	**3/8 in. 9.5 mm**	**0.265 in. 6.7 mm**	**No. 4 4.76 mm**	**No. 35 0.5 mm**
% Pass	100	98-100	85-99	0-15	0-5	<1	<1

Table A.1: Aggregate Gradation

- Traffic
    - AADT = 5,000 vehicle/day
    - 18% Heavy Vehicles (greater than 3.5 metric tons)
        - 10 % Heavy vehicles; and
        - 8 % Large heavy vehicles.
    - 50% directional split
        - 60 % of vehicles travel on the slow lane;
        - 40 % of vehicles travel on the fast/passing lane;

- Shoulder traffic: less than 50 veh/lane/day; and
- Heavy vehicles are required to use the slow lane for travel.

Shoulder				
←		←	**Fast/Passing Lane**	←
←		←	**Slow Lane**	←
→	**Fast/Passing Lane**	→		→
→	**Slow Lane**	→		→
Shoulder				

Figure A.1: Schematic Representation of the Considered Roadway Section

- Design Traffic Characterization
  - Slow Lane: $5{,}000 \times 0.5 \times 0.6 = 1{,}500$ vehicles/lane/day
    - $5{,}000 \times 0.5 \times 0.18 = 450$ truck
      - $5{,}000 \times 0.5 \times 0.10 = 250$ heavy vehicles/lane/day
      - $5{,}000 \times 0.5 \times 0.08 = 200$ large heavy vehicles/lane/day
      - Equivalent Heavy Vehicles (%) = HV(%) + LHV(%) × 3

        $$\text{EHV}\ (\%) \ = \ 250/1500 + 3 \times 200/1500 = 0.566 = 56.6\%$$
    - 1,050 light vehicles
  - Fast/Passing Lane: $5{,}000 \times 0.5 \times 0.4 = 1{,}000$ vehicles/lane/day
  - Shoulder: 50 vehicles/lane/day

The following sections represents the determination of the BAR and AAR across the roadway using different design methods.

HANSON DESIGN METHOD (HANSON, 1935)

Aggregate Application Rate:

$\text{AAR} = 0.0016 \times \text{ALD} \quad (\text{m}^3/\text{m}^2)$

$\text{AAR} = 0.0016 \times 8.6 = 0.01376\ \text{m}^3/\text{m}^2$

After considering a 10% whip-off factor $\text{AAR} = 0.01376 \times 1.1 = 0.015136\ \text{m}^3/\text{m}^2$

$\mathbf{AAR = 66\ m^2/m^3}$

Binder application rate:

$\text{BAR} = 0.14 \times \text{ALD} \quad \text{L/m}^2$

$\mathbf{BAR = 1.204\ L/m^2}$

Recommendations:

Adjustment to the design needs to take into account the existing surface, the use of emulsions, and the amount of remaining aggregate.

KEARBY DESIGN METHOD (KEARBY, 1953)

Aggregate Application Rate:

$$\text{AAR} = \text{Spread Ratio} = \frac{\text{lb/yd}^3}{\text{lb/yd}^2} = \text{yd}^2/\text{yd}^3$$

The average least dimension of the aggregates is given as 8.6mm or 0.34 in. The Kearby design method for seal coats requires the determination of the spread ratio, which is the number of square yards covered by one cubic yard of aggregate. Hence, the unit weight (lb/yd^3) and the board test (lb/yd^2) should be conducted for the proposed aggregates. Since the average mat thickness is based on the spread ratio using this formula:

$$\text{Average Mat Thickness (in)} = \frac{36}{\text{SR } (\text{yd}^2/\text{yd}^3)}$$

The average least dimension is equated to the average mat thickness in order to back-calculate the spread ratio without the need of conducting the lab test.

$$\text{Average mat thichness} = \frac{36}{\text{Spread ratio}}$$

$$\text{Spread Ratio} = \frac{36}{\text{Average mat thickness}} = 106.3\text{yd}^2/\text{yd}^3 = 116.25\text{m}^2/\text{m}^3$$

$$\mathbf{AAR = 116.25 m^2/m^3}$$

Binder application rate:

Determining the asphalt application rate for an average aggregate mat thickness of 0.34 inch, percent of voids in aggregate of 40%, and desired embedded depth of 30%

Average Mat Thickness (in)	Binder Application Rate (gal/yd^2)
0.375	0.25
0.250	0.17
0.340	0.23

Table A.2: Interpolating the Binder Application Rate for a thickness of 0.34 inch

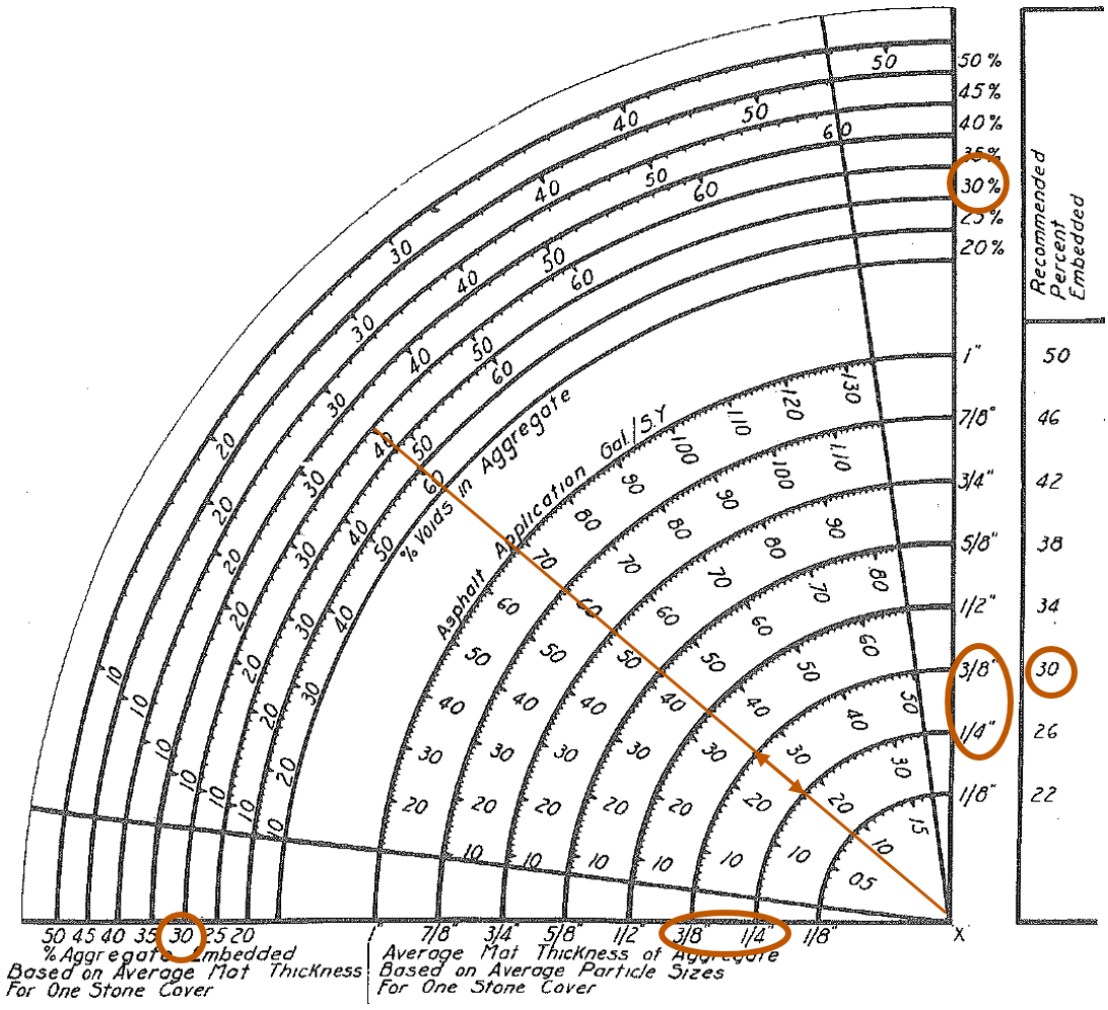

Figure A.2: Binder Application Rate Determination using Kearby's Nomograph

$$\text{BAR} = 0.23(\text{gal/yd}^2) \times 4.52731\left(\frac{\text{L/m}^2}{\text{gal/yd}^2}\right) = 1.04\ \text{L/m}^2$$

$$\mathbf{BAR = 1.04\ L/m^2}$$

<u>Design Considerations</u>

- Bleeding or soft existing surface ➔ ↓ BAR
- High traffic volumes ➔ ↓ BAR + use large aggregates
- High % of heavy vehicles ➔ ↓ BAR + use large aggregates
- Light traffic ➔ ↑ BAR

McLeod Design Method (McLeod, 1969)

Slow Lane

Aggregate Application Rate:

$$\text{AAR}(\text{lb/yd}^2) = \left(\frac{36 \times 36 \times 0.8\ \text{ALD(in)}}{1728}\right) \times 62.4(\text{lb/ft}^3) \times \text{G} \times \text{E}$$

$\text{ALD} = 8.6\ \text{mm} = 0.34\text{in}$

Since no data is available for the dry bulk specific gravity, the average of the bulk specific gravities of the one-sized aggregates test data present in McLeod's design method is used.

G … Dry bulk specific gravity of aggregate = 2.7

E … Wastage factor $\left(1 + \frac{\%}{100}\right)$ = 1.1

$$\text{AAR}\left(\frac{\text{lb}}{\text{yd}^2}\right) = \left(\frac{36 \times 36 \times 0.8\ \times 0.34}{1728}\right) \times 62.4\left(\frac{\text{lb}}{\text{ft}^3}\right) \times 2.7 \times 1.1 = 37.81\text{lb/yd}^2$$

$\text{AAR} = 20.51\ \text{kg/m}^2 = 0.0128\text{m}^3/\text{m}^2$ (Using bulk unit weight of 1,600 kg/m^2)

$\mathbf{AAR = 78\ m^2/m^3}$

Binder application rate:

$$\text{BAR}(\text{gal/yd}^2) = \left(\frac{36 \times 36 \times 0.2\ \text{ALD(in)}}{231}\right)\left(\frac{\text{T}}{\text{R}}\right) + \frac{\text{S} + \text{A}}{\text{R}}$$

The net retained residual binder is used to compare the BAR obtained by various methods. When an emulsion is used, a modification for the BAR is required to determine the emulsion application rate based on the required residual binder. Hence, R = 1.0;

Based on Table A.3, the traffic correction factor $\text{T} = 0.65$

Asphalt Application Rate – Correction Due to Traffic, T					
Vehicles per day per lane	< 100	100 – 500	500 – 1000	1000-2000	> 2000
Traffic Correction Factor	0.85	0.75	0.70	0.65	0.60

Table A.3: Slow Lane McLeod Traffic Correction Factor

Based on Table A.4, the surface correction factor $S = 0$ gal/yd^2

Existing Surface Texture Rating	US gal/yd^2	SI L/m^2
Black	- 0.06	- 0.272
Smooth	-	-
Hungry 1h	+ 0.03	+ 0.136
Hungry 2h	+ 0.06	+ 0.272
Hungry 3h	+ 0.09	+ 0.408

Table A.4: Slow Lane McLeod Surface Correction Factor

$\text{ALD} = 0.34\text{in}$

The aggregate used in this example does not constitute one of the absorptive aggregates.

Thus, the aggregate absorption factor is $A = 0$ gal/yd^2.

$$\text{BAR(gal/yd}^2) = \left(\frac{36 \times 36 \times 0.2 \times 0.34}{231}\right)\left(\frac{0.65}{1.0}\right) + \frac{0+0}{1.0} = 0.25 \text{ gal/yd}^2$$

$$\mathbf{BAR = 1.13\ L/m^2}$$

Fast/Passing Lane

Aggregate Application Rate:

$$\text{AAR}(\text{lb/yd}^2) = \left(\frac{36 \times 36 \times 0.8\ \text{ALD(in)}}{1728}\right) \times 62.4(\text{lb/ft}^3) \times \text{G} \times \text{E}$$

$\text{ALD} = 8.6\ \text{mm} = 0.34\text{in}$

G … Dry bulk specific gravity of aggregate = 2.7

E … Wastage factor $\left(1 + \frac{\%}{100}\right)$ = 1.1

$$\text{AAR}\left(\frac{\text{lb}}{\text{yd}^2}\right) = \left(\frac{36 \times 36 \times 0.8\ \times 0.34}{1728}\right) \times 62.4\left(\frac{\text{lb}}{\text{ft}^3}\right) \times 2.7 \times 1.1 = 37.81\text{lb/yd}^2$$

$\text{AAR} = 20.51\ \text{kg/m}^2 = 0.0128\text{m}^3/\text{m}^2$ (Using bulk specific gravity of 1,600 kg/m^2)

$\mathbf{AAR = 78\ m^2/m^3}$

Binder application rate:

$$\text{BAR}(\text{gal/yd}^2) = \left(\frac{36 \times 36 \times 0.2\ \text{ALD(in)}}{231}\right)\left(\frac{\text{T}}{\text{R}}\right) + \frac{\text{S} + \text{A}}{\text{R}}$$

The net retained residual binder is used to compare the BAR obtained by various methods. When an emulsion is used, a modification for the BAR is required to determine the emulsion application rate based on the required residual binder. Hence, R = 1.0;

Based on Table A.5, the traffic correction factor $\text{T} = 0.70$

Asphalt Application Rate – Correction Due to Traffic, T					
Vehicles per day per lane	< 100	100 – 500	500 – 1000	1000-2000	> 2000
Traffic Correction Factor	0.85	0.75	0.70	0.65	0.60

Table A.5: Fast/Passing Lane McLeod Traffic Correction Factor

Based on Table A.6, the surface correction factor $\text{S} = 0.06\ \text{gal/yd}^2$

Existing Surface Texture Rating	US gal/yd^2	SI L/m^2
Black	- 0.06	- 0.272
Smooth	-	-
Hungry 1h	+ 0.03	+ 0.136
Hungry 2h	+ 0.06	+ 0.272
Hungry 3h	+ 0.09	+ 0.408

Table A.6: Fast/Passing Lane McLeod Surface Correction Factor

The aggregate used in this example does not constitute one of the absorptive aggregates. Thus, the aggregate absorption factor is $A = 0$ gal/yd^2.

$ALD = 0.34$in

$$BAR(\text{gal/yd}^2) = \left(\frac{36 \times 36 \times 0.2 \times 0.34}{231}\right)\left(\frac{0.70}{1.0}\right) + \frac{0.06 + 0}{1.0} = 0.33 \text{ gal/yd}^2$$

$$\mathbf{BAR = 1.48\ L/m^2}$$

Shoulder

Aggregate Application Rate:

$$\text{AAR}(\text{lb/yd}^2) = \left(\frac{36 \times 36 \times 0.8\ \text{ALD(in)}}{1728}\right) \times 62.4(\text{lb/ft}^3) \times \text{G} \times \text{E}$$

$\text{ALD} = 8.6\ \text{mm} = 0.34\text{in}$

G … Dry bulk specific gravity of aggregate = 2.7

E … Wastage factor $\left(1 + \frac{\%}{100}\right)$ = 1.1

$$\text{AAR}\left(\frac{\text{lb}}{\text{yd}^2}\right) = \left(\frac{36 \times 36 \times 0.8\ \times 0.34}{1728}\right) \times 62.4\left(\frac{\text{lb}}{\text{ft}^3}\right) \times 2.7 \times 1.1 = 37.81\text{lb/yd}^2$$

$\text{AAR} = 20.51\ \text{kg/m}^2 = 0.0128\text{m}^3/\text{m}^2$ (Using bulk specific gravity of 1,600 kg/m^2)

$\mathbf{AAR = 78\ m^2/m^3}$

Binder application rate:

$$\text{BAR}(\text{gal/yd}^2) = \left(\frac{36 \times 36 \times 0.2\ \text{ALD(in)}}{231}\right)\left(\frac{\text{T}}{\text{R}}\right) + \frac{\text{S} + \text{A}}{\text{R}}$$

The net retained residual binder is used to compare the BAR obtained by various methods. When an emulsion is used, a modification for the BAR is required to determine the emulsion application rate based on the required residual binder. Hence, R = 1.0;

Based on Table A.7, the traffic correction factor $\text{T} = 0.85$

Asphalt Application Rate – Correction Due to Traffic, T					
Vehicles per day per lane	< 100	100 – 500	500 – 1000	1000-2000	> 2000
Traffic Correction Factor	0.85	0.75	0.70	0.65	0.60

Table A.7: Shoulder McLeod Traffic Correction Factor

Based on Table A.8, the surface correction factor $\text{S} = 0.09\ \text{gal/yd}^2$

Existing Surface Texture Rating	US gal/yd^2	SI L/m^2
Black	- 0.06	- 0.272
Smooth	-	-
Hungry 1h	+ 0.03	+ 0.136
Hungry 2h	+ 0.06	+ 0.272
Hungry 3h	+ 0.09	+ 0.408

Table A.8: Shoulder McLeod Surface Correction Factor

The aggregate used in this example does not constitute one of the absorptive aggregates. Thus, the aggregate absorption factor is $A = 0$ gal/yd^2.

ALD $= 0.34$in

$$\text{BAR}(\text{gal/yd}^2) = \left(\frac{36 \times 36 \times 0.2 \times 0.34}{231}\right)\left(\frac{0.85}{1.0}\right) + \frac{0.09 + 0}{1.0} = 0.41 \text{ gal/yd}^2$$

$$\mathbf{BAR = 1.87\ L/m^2}$$

MODIFIED KEARBY DESIGN METHOD (EPPS, GALLAWAY, & HUGHES, 1981)

Slow Lane

Aggregate Application Rate:

$$\text{AAR}(\text{yd}^2/\text{yd}^3) = \frac{27\ \text{W}\ (\text{lb/ft}^3)}{\text{Q}\ (\text{lb/yd}^2)}$$

W = Dry Loose Unit Weight (lb/ft^3) in accordance with TEX 404 A

Q = Quantity of Aggregates determined from Board Test (lb/yd^2)

The average mat thickness, $\text{d (in)} = \frac{4}{3} \times \frac{\text{Q}\ (\text{lb/yd}^2)}{\text{W}\ (\text{lb/ft}^3)}$

In the problem statement, the average least dimension of the aggregates is given as 8.6mm or 0.34 in. The modified Kearby design method for seal coats requires the determination of both the dry loose unit weight of the aggregate, W, and the quantity of aggregates from the board test, Q. The average mat thickness is based on W and Q using this formula:

$$\text{d (in)} = \frac{4}{3} \times \frac{\text{Q}\ (\text{lb/yd}^2)}{\text{W}\ (\text{lb/ft}^3)}$$

The average least dimension is equated to the average mat thickness in order to back calculate the ratio of Q/W without the need of conducting the lab test.

$$\frac{\text{Q}}{\text{W}}\left(\frac{\text{lb/yd}^2}{\text{lb/ft}^3}\right) = \frac{3}{4} \times \text{d(in)}$$

$$\frac{\text{Q}}{\text{W}} = 0.254$$

$$\text{AAR} = 27 \times \frac{\text{W}}{\text{Q}} = \frac{27}{0.254} = \frac{106.3\text{yd}^2}{\text{yd}^3} = 116.25\text{m}^2/\text{m}^3$$

$$\mathbf{AAR = 116.25 m^2/m^3}$$

Binder application rate:

$$\text{BAR}(\text{gal/yd}^2) = 5.61\text{E (in)}\left(1 - \frac{\text{W}}{62.4\text{G}}\right)(\text{T}) + \text{V}(\text{gal/yd}^2)$$

The embedment depth $\text{E} = \text{ed}$

The average mat thickness $\text{d} = 0.34$ in

As shown in Figure A.3, the percent embedment e = 29%

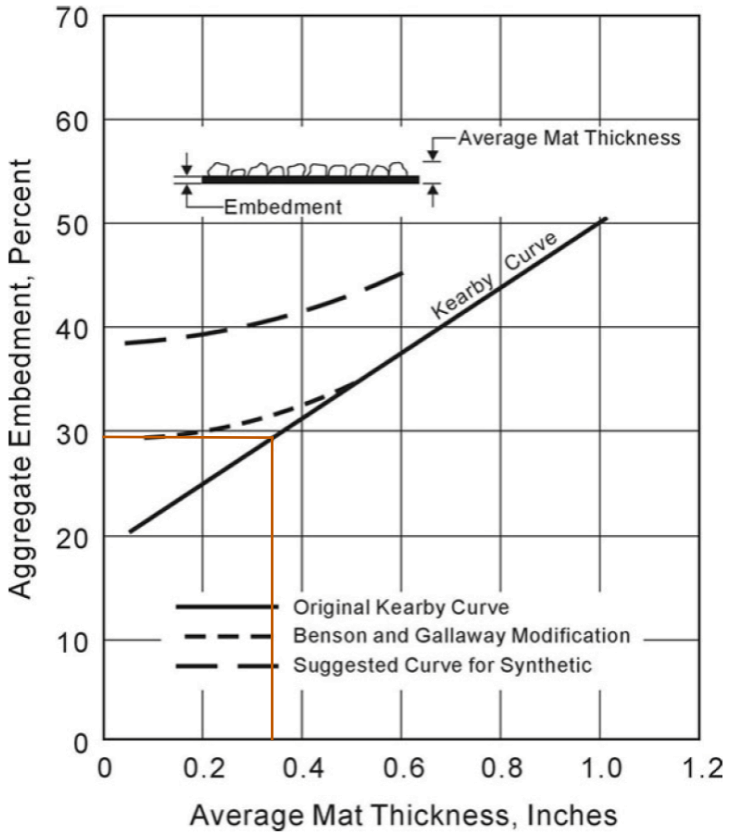

Figure A.3: Slow Lane Percent Embedment, e

The percent of voids in aggregates is given by:

$$1 - \frac{W}{62.4G}$$

Conforming to the assumptions made for the Kearby design method, the voids in aggregates for the purpose of this exercise is assumed to be 40%. Hence,

$$1 - \frac{W}{62.4G} = 0.4$$

Traffic Correction Factor T = 1.00 (Table A.9)

Asphalt Application Rate – Correction Due to Traffic, T					
Vehicles per day per lane	>1000	500-1000	250-500	100-250	<100
Traffic Correction Factor	1	1.05	1.1	1.15	1.2

Table A.9: Slow Lane Modified Kearby Traffic Correction Factor

Correction for surface condition $V = -0.03$ gal/yd^2(Table A.10)

Asphalt Application Rate Correction due to Existing Pavement Surface Condition	
Description of Existing Surface	**Correction (V), gal/SY**
Flushing, slightly bleeding surface	-0.06
Smooth, nonporous surface	-0.03
Slightly porous, slightly oxidized surface	0
Slightly pocked, porous, oxidized surface	0.03
Badly pocked, porous, oxidized surface	0.06

Table A.10: Slow Lane Modified Kearby Surface Correction Factor

$\text{BAR(gal/yd}^2) = 5.61 \times (0.29 \times 0.34) \times (0.4)(1.0) - 0.03 = 0.19 \text{ gal/yd}^2$

$\mathbf{BAR = 0.87\ L/m^2}$

Fast/Passing Lane

Aggregate Application Rate:

$$\text{AAR}(\text{yd}^2/\text{yd}^3) = \frac{27\ \text{W}\ (\text{lb}/\text{ft}^3)}{\text{Q}\ (\text{lb}/\text{yd}^2)}$$

W = Dry Loose Unit Weight (lb/ft^3) in accordance with TEX 404 A

Q = Quantity of Aggregates determined from Board Test (lb/yd^2)

The average mat thickness, $\text{d}\ (\text{in}) = \frac{4}{3} \times \frac{\text{Q}\ (\text{lb}/\text{yd}^2)}{\text{W}\ (\text{lb}/\text{ft}^3)}$

In the problem statement, the average least dimension of the aggregates is given as 8.6mm or 0.34 in. The modified Kearby design method for seal coats requires the determination of both the dry loose unit weight of the aggregate, W, and the quantity of aggregates from the board test, Q. The average mat thickness is based on W and Q using this formula:

$$\text{d}\ (\text{in}) = \frac{4}{3} \times \frac{\text{Q}\ (\text{lb}/\text{yd}^2)}{\text{W}\ (\text{lb}/\text{ft}^3)}$$

The average least dimension is equated to the average mat thickness in order to back calculate the ratio of Q/W without the need of conducting the lab test.

$$\frac{\text{Q}}{\text{W}}\left(\frac{\text{lb}/\text{yd}^2}{\text{lb}/\text{ft}^3}\right) = \frac{3}{4} \times \text{d(in)}$$

$$\frac{\text{Q}}{\text{W}} = 0.254$$

$$\text{AAR} = 27 \times \frac{\text{W}}{\text{Q}} = \frac{27}{0.254} = \frac{106.3\text{yd}^2}{\text{yd}^3} = 116.25\text{m}^2/\text{m}^3$$

$$\mathbf{AAR = 116.25 m^2/m^3}$$

Binder application rate:

$$\text{BAR}(\text{gal}/\text{yd}^2) = 5.61\text{E}\ (\text{in})\left(1 - \frac{\text{W}}{62.4\text{G}}\right)(\text{T}) + \text{V}(\text{gal}/\text{yd}^2)$$

The embedment depth $\text{E} = \text{ed}$

The average mat thickness $\text{d} = 0.34$ in

As shown in Figure A.4, the percent embedment $\text{e} = 29\%$

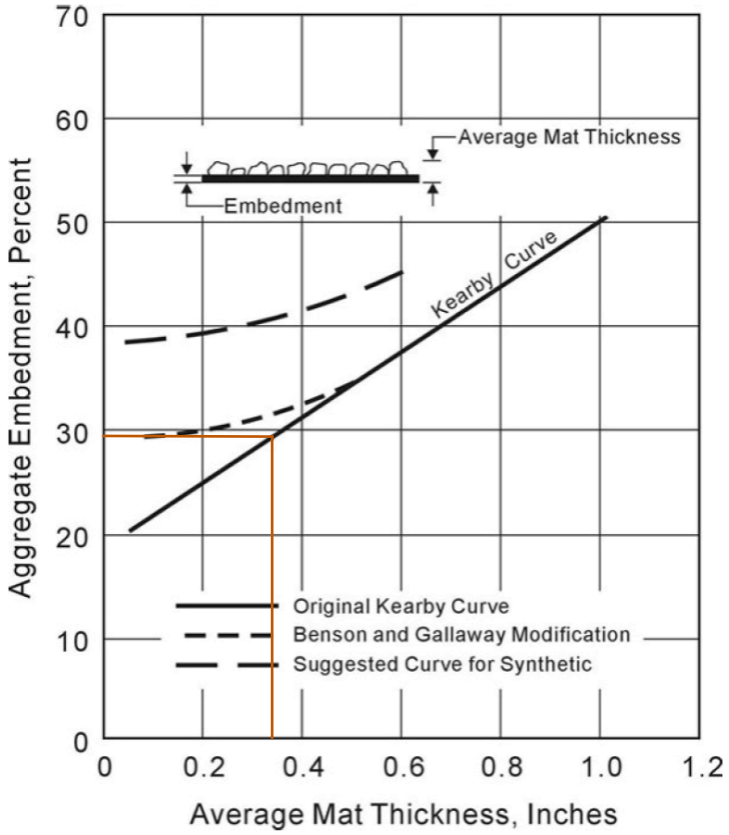

Figure A.4: Fast/Passing Lane Percent Embedment, e

The percent of voids in aggregates is given by:

$$1 - \frac{W}{62.4G}$$

Conforming to the assumptions made for the Kearby design method, the voids in aggregates for the purpose of this exercise is assumed to be 40%. Hence,

$$1 - \frac{W}{62.4G} = 0.4$$

Traffic Correction Factor $T = 1.05$ (Table A.11)

Asphalt Application Rate – Correction Due to Traffic, T					
Vehicles per day per lane	>1000	500-1000	250-500	100-250	<100
Traffic Correction Factor	1	1.05	1.1	1.15	1.2

Table A.11: Fast/Passing Lane Modified Kearby Traffic Correction Factor

Correction for surface condition $V = +0.03\ \text{gal/yd}^2$ (Table A.12)

Asphalt Application Rate Correction due to Existing Pavement Surface Condition	
Description of Existing Surface	**Correction (V), gal/SY**
Flushing, slightly bleeding surface	-0.06
Smooth, nonporous surface	-0.03
Slightly porous, slightly oxidized surface	0
Slightly pocked, porous, oxidized surface	0.03
Badly pocked, porous, oxidized surface	0.06

Table A.12: Fast/Passing Lane Modified Kearby Surface Correction Factor

$\text{BAR}(\text{gal/yd}^2) = 5.61 \times (0.29 \times 0.34) \times (0.4)(1.05) + 0.03 = 0.26\ \text{gal/yd}^2$

$\mathbf{BAR = 1.19\ L/m^2}$

Shoulder

Aggregate Application Rate:

$$\text{AAR}(\text{yd}^2/\text{yd}^3) = \frac{27\ \text{W}\ (\text{lb}/\text{ft}^3)}{\text{Q}\ (\text{lb}/\text{yd}^2)}$$

W = Dry Loose Unit Weight (lb/ft^3) in accordance with TEX 404 A

Q = Quantity of Aggregates determined from Board Test (lb/yd^2)

The average mat thickness, $\text{d}\ (\text{in}) = \frac{4}{3} \times \frac{\text{Q}\ (\text{lb}/\text{yd}^2)}{\text{W}\ (\text{lb}/\text{ft}^3)}$

In the problem statement, the average least dimension of the aggregates is given as 8.6mm or 0.34 in. The modified Kearby design method for seal coats requires the determination of both the dry loose unit weight of the aggregate, W, and the quantity of aggregates from the board test, Q. The average mat thickness is based on W and Q using this formula:

$$\text{d}\ (\text{in}) = \frac{4}{3} \times \frac{\text{Q}\ (\text{lb}/\text{yd}^2)}{\text{W}\ (\text{lb}/\text{ft}^3)}$$

The average least dimension is equated to the average mat thickness in order to back calculate the ratio of Q/W without the need of conducting the lab test.

$$\frac{\text{Q}}{\text{W}}\left(\frac{\text{lb}/\text{yd}^2}{\text{lb}/\text{ft}^3}\right) = \frac{3}{4} \times \text{d(in)}$$

$$\frac{\text{Q}}{\text{W}} = 0.254$$

$$\text{AAR} = 27 \times \frac{\text{W}}{\text{Q}} = \frac{27}{0.254} = \frac{106.3\text{yd}^2}{\text{yd}^3} = 116.25\text{m}^2/\text{m}^3$$

$$\mathbf{AAR = 116.25 m^2/m^3}$$

Binder application rate:

$$\text{BAR}(\text{gal}/\text{yd}^2) = 5.61\text{E}\ (\text{in})\left(1 - \frac{\text{W}}{62.4\text{G}}\right)(\text{T}) + \text{V}(\text{gal}/\text{yd}^2)$$

The embedment depth $\text{E} = \text{ed}$

The average mat thickness $\text{d} = 0.34$ in

Shown in Figure A.5, the percent embedment $\text{e} = 29\%$

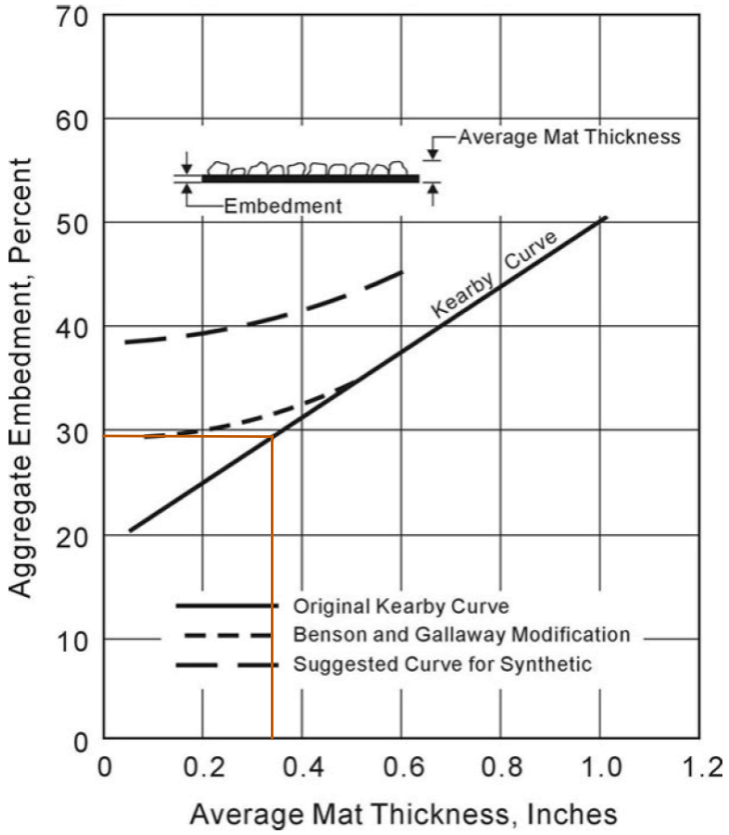

Figure A.5: Shoulder Lane Percent Embedment, e

The percent of voids in aggregates is given by:

$$1 - \frac{W}{62.4G}$$

Conforming to the assumptions made for the Kearby design method, the voids in aggregates for the purpose of this exercise is assumed to be 40%. Hence,

$$1 - \frac{W}{62.4G} = 0.4$$

Traffic Correction Factor $T = 1.20$ (Table A.13)

Asphalt Application Rate – Correction Due to Traffic, T					
Vehicles per day per lane	>1000	500-1000	250-500	100-250	<100
Traffic Correction Factor	1	1.05	1.1	1.15	1.2

Table A.13: Shoulder Modified Kearby Traffic Correction Factor

Correction for surface condition $V = +0.06$ gal/yd^2 (Table A.14)

Asphalt Application Rate Correction due to Existing Pavement Surface Condition	
Description of Existing Surface	**Correction (V), gal/SY**
Flushing, slightly bleeding surface	-0.06
Smooth, nonporous surface	-0.03
Slightly porous, slightly oxidized surface	0
Slightly pocked, porous, oxidized surface	0.03
Badly pocked, porous, oxidized surface	0.06

Table A.14: Shoulder Modified Kearby Surface Correction Factor

$\text{BAR}(\text{gal/yd}^2) = 5.61 \times (0.29 \times 0.34) \times (0.4)(1.20) + 0.06 = 0.33 \text{ gal/yd}^2$

$\mathbf{BAR = 1.47\ L/m^2}$

SPANISH DESIGN METHOD (BARDESI & TOMAS, 2004)

C.R.R. (Centre de Recherches Routiers) Method

Aggregate Application Rate (L/m^2):

D = 14mm → Smallest sieve opening (in mm) with percent passing ≥ 90%

d = 10mm → Largest sieve opening (in mm) with percent passing ≤ 10%

Δ = average aggregate size (mm)

$$\Delta = \frac{(D + d)}{2} = 12\text{mm}$$

R = Correction factor for aggregate losses (Table A.15)

R=1.0 L/m²	**Δ = 5mm**	**R=1.5 L/m²**	**Δ = 20mm**
R=1.23 L/m²		Δ = 12mm	

Table A.15: CRR Correction Factor for Aggregate Losses

$$\text{AAR} = \Delta - 0.01\Delta^2 + \text{R}$$

$$\text{AAR} = 12 - 0.01(12)^2 + 1.23$$

$$\mathbf{AAR = 11.79\ L/m^2}$$

Binder Application Rate (kg/m^2):

BAR is the amount of RESIDUAL binder applied

$$\text{BAR} = \text{a} + \text{b}.\,\text{AAR}$$

Factor	Description	Correction Factor
Road Surface Texture (a)	Bleeding	a = 0.00
	Normal	a = 0.34
	Porous, dry, or cracked	a = 0.59
Aggregate Type (b)	Pre-Coated	b = 0.06
	Artificial	b = 0.07
	Natural	b = 0.09

Table A.16: CRR Aggregate Type and Road Surface Texture

$\text{BAR} = 0.34 + 0.09 \times 11.79$

$\mathbf{BAR = 1.4\ kg/m^2}$

Linckenheyl Method or the Decimal Rule

Aggregate Application Rate (L/m^2):

$\text{AAR} = 0.9 \times \Delta = 0.9 \times 12$

$\mathbf{AAR = 10.8\ L/m^2}$

Binder Application Rate (kg/m^2):

$\text{BAR} = 0.1 \times \text{AAR} = 0.1 \times 10.8$

$\mathbf{BAR = 1.08\ kg/m^2}$

NEW ZEALAND DESIGN METHOD (TRANSIT NZ, RCA, & ROADING NZ, 2005)

Slow Lane

Traffic Characterization

T is the equivalent light vehicle elv, $T = ADT \times (1 + 0.09 \times p)$

$ADT = veh/ln/day$ and $p = \%$ of HCV

$ADT = 5{,}000 \times 0.5 \times 0.6 = 1{,}500$ vehicles/lane/day

$$p = \frac{18\% \times (2{,}500)}{1{,}500} = 30\%$$

$T = 1{,}500 \times (1 + 0.09 \times 60) = 5{,}550$ elv

Basic Binder Application Rate

$$V_B = ALD \times \left(0.291 - 0.025 \times \log(T \times 100)\right)$$

$$V_B = 8.6 \times \left(0.291 - 0.025 \times \log(5{,}550 \times 100)\right) = 1.27\ L/m^2$$

Adjustment for Texture and aggregate Embedment

$$V_B = (ALD + MTD - 0.3 \times MTD)(0.291 - 0.025 \times \log(T \times 100))$$

MTD~0.5mm

$$V_B = (8.6 + 0.5 - 0.3 \times 0.5)(0.291 - 0.025 \times \log(5{,}550 \times 100)) = 1.32 L/m^2$$

Site Specific Adjustments

Soft Substrate adjustment $Ss = 0\ L/m^2$ (Table A.17)

Soft Substrate Adjustment (Ball Penetration Test)			
Ball Penetration Value	≤ 1mm	1 – 3 mm	3 – 4 mm
ALD adjustment	+ 1 mm	-	- 1 mm

Table A.17: Slow Lane New Zealand Soft Substrate Adjustment

Absorptive Surfaces adjustment $As = 0\ L/m^2$ as the surface at hand is not absorptive

"If sealing the surface first with a small chip is not possible, the basic application rate could be increased in the order of 0.1 to 0.2 L/m^2"

Steep grade adjustment $\mathrm{Gs} = -0.1\ \mathrm{L/m^2}$

"On steep uphill grades, slow moving heavy vehicles can cause premature flushing. A reduction of 0.1 to 0.15 L /m^2 in binder application rate for these areas is commonly used to minimize the chance of binder pick-up from the truck tires, which causes tracking and potential for flushing of the surface."

Chip Shape adjustment $\mathrm{Cs} = 0\ \mathrm{L/m^2}$

"Chip shape is controlled by a maximum ratio of ALD:AGD of 1:2.25, although typical ratios of 1:2 have been found in practice. These shapes are preferred as they pack in with maximum shoulder-to-shoulder contact."

Binder Application Rate

$$V_B = (\mathrm{ALD} + 0.7\mathrm{MTD})\left(0.291 - 0.025 \times \log(\mathrm{T} \times 100)\right) + \mathrm{As} + \mathrm{Ss} + \mathrm{Gs} + \mathrm{Cs} + \mathrm{U_S}$$

$$\mathrm{V_B} = 1.32 - 0.1$$

$$\mathbf{BAR = 1.22 L/m^2}$$

Aggregate Application Rate

$$\mathrm{AAR} = \frac{750}{\mathrm{ALD}} = \frac{750}{8.6}$$

$$\mathbf{AAR = 87\ m^2/m^3}$$

This allows for approximately 10% for whip off but assumes a good standard of uniformity of chip spread of grade 2 to grade 5 sealing chips.

Fast/Passing Lane

Traffic Characterization

T is the equivalent light vehicle elv, $T = ADT \times (1 + 0.09 \times p)$

ADT = veh/ln/day and p = % of HCV

$ADT = 5{,}000 \times 0.5 \times 0.4 = 1{,}000$ vehicles/lane/day

Assume $< 10\%$ of the trucks use the passing lane.

$$p = \frac{10\% \times 18\% \times (2{,}500)}{1{,}000} = 4.5\%$$

$T = 1{,}000 \times (1 + 0.09 \times 4.5) = 1{,}405$ elv

Basic Binder Application Rate

$V_B = ALD \times \left(0.291 - 0.025 \times \log(T \times 100)\right)$

$V_B = 8.6 \times \left(0.291 - 0.025 \times \log(1{,}405 \times 100)\right) = 1.40 L/m^2$

Adjustment for Texture and aggregate Embedment

$V_B = (ALD + MTD - 0.3 \times MTD)(0.291 - 0.025 \times \log(T \times 100))$

$MTD \sim 1.5mm$

$V_B = (8.6 + 1.5 - 0.3 \times 1.5)(0.291 - 0.025 \times \log(1{,}405 \times 100)) = 1.57 L/m^2$

Site Specific Adjustments

Soft Substrate adjustment Ss = 0 L/m^2 (Table A.18)

Soft Substrate Adjustment (Ball Penetration Test)			
Ball Penetration Value	≤ 1mm	1 – 3 mm	3 – 4 mm
ALD adjustment	+ 1 mm	-	- 1 mm

Table A.18: Fast/Passing Lane New Zealand Soft Substrate Adjustment

Absorptive Surfaces adjustment As = 0 L/m^2 as the surface at hand is not absorptive

"If sealing the surface first with a small chip is not possible, the basic application rate could be increased in the order of 0.1 to 0.2 L/m^2"

Steep grade adjustment $\mathrm{Gs} = -0.1\ \mathrm{L/m^2}$

"On steep uphill grades, slow moving heavy vehicles can cause premature flushing. A reduction of 0.1 to 0.15 L /m^2 in binder application rate for these areas is commonly used to minimize the chance of binder pick-up from the truck tires, which causes tracking and potential for flushing of the surface."

Chip Shape adjustment $\mathrm{Cs} = 0\ \mathrm{L/m^2}$

"Chip shape is controlled by a maximum ratio of ALD:AGD of 1:2.25, although typical ratios of 1:2 have been found in practice. These shapes are preferred as they pack in with maximum shoulder-to-shoulder contact."

Binder Application Rate

$$V_B = (\mathrm{ALD} + 0.7\mathrm{MTD})\left(0.291 - 0.025 \times \log(\mathrm{T} \times 100)\right) + \mathrm{As} + \mathrm{Ss} + \mathrm{Gs} + \mathrm{Cs} + \mathrm{U_S}$$

$$\mathrm{V_B} = 1.57 - 0.1$$

$$\mathbf{BAR = 1.47 L/m^2}$$

Aggregate Application Rate

$$\mathrm{AAR} = \frac{750}{\mathrm{ALD}} = \frac{750}{8.6}$$

$$\mathbf{AAR = 87\ m^2/m^3}$$

This allows for approximately 10% for whip off but assumes a good standard of uniformity of chip spread of grade 2 to grade 5 sealing chips.

Shoulder

Traffic Characterization

T is the equivalent light vehicle elv, $T = ADT \times (1 + 0.09 \times p)$

$ADT = veh/ln/day$ and $p = \%$ of HCV

$ADT < 50$ vehicles/lane/day

Assume $< 1\%$ of the trucks use the shoulder.

$$p = \frac{1\% \times 18\% \times (2{,}500)}{50} = 9\%$$

$T = 50 \times (1 + 0.09 \times 9) = 91$ elv

Basic Binder Application Rate

$V_B = ALD \times (0.291 - 0.025 \times \log(T \times 100))$

$V_B = 8.6 \times (0.291 - 0.025 \times \log(91 \times 100)) = 1.65 L/m^2$

Adjustment for Texture and aggregate Embedment

$V_B = (ALD + MTD - 0.3 \times MTD)(0.291 - 0.025 \times \log(T \times 100))$

$MTD \sim 2.4mm$

$V_B = (8.6 + 2.4 - 0.3 \times 2.4)(0.291 - 0.025 \times \log(91 \times 100)) = 1.97 L/m^2$

Site Specific Adjustments

Soft Substrate adjustment $Ss = 0\ L/m^2$ (Table A.19)

Soft Substrate Adjustment (Ball Penetration Test)			
Ball Penetration Value	$\leq$ 1mm	1 – 3 mm	3 – 4 mm
ALD adjustment	+ 1 mm	-	- 1 mm

Table A.19: Shoulder Lane New Zealand Soft Substrate Adjustment

Absorptive Surfaces adjustment $As = 0\ L/m^2$ as the surface at hand is not absorptive

"If sealing the surface first with a small chip is not possible, the basic application rate could be increased in the order of 0.1 to 0.2 L/m^2"

Steep grade adjustment $\mathrm{Gs} = -0.1\ \mathrm{L/m^2}$

"On steep uphill grades, slow moving heavy vehicles can cause premature flushing. A reduction of 0.1 to 0.15 L /m^2 in binder application rate for these areas is commonly used to minimize the chance of binder pick-up from the truck tires, which causes tracking and potential for flushing of the surface."

Chip Shape adjustment $\mathrm{Cs} = 0\ \mathrm{L/m^2}$

"Chip shape is controlled by a maximum ratio of ALD:AGD of 1:2.25, although typical ratios of 1:2 have been found in practice. These shapes are preferred as they pack in with maximum shoulder-to-shoulder contact."

Binder Application Rate

$$V_B = (\mathrm{ALD} + 0.7\mathrm{MTD})\left(0.291 - 0.025 \times \log(\mathrm{T} \times 100)\right) + \mathrm{As} + \mathrm{Ss} + \mathrm{Gs} + \mathrm{Cs} + \mathrm{U_S}$$

$$\mathrm{V_B} = 1.97 - 0.1$$

$$\mathbf{BAR = 1.87 L/m^2}$$

1.87 L/m^2 for the shoulder is an expensive option for a reseal and has a high risk of binder bleeding in hot weather. The preferred alternative is to consider selecting 7 mm aggregate (or 10 mm) as this will be cheaper whilst providing the necessary waterproofing, and texture is not an issue.

Aggregate Application Rate

$$\mathrm{AAR} = \frac{750}{\mathrm{ALD}} = \frac{750}{8.6}$$

$$\mathbf{AAR = 87\ m^2/m^3}$$

This allows for approximately 10% for whip off but assumes a good standard of uniformity of chip spread of grade 2 to grade 5 sealing chips.

AUSTRALIAN DESIGN METHOD (ALDERSON A. , 2006)

Slow Lane

The design traffic characterization

- $5{,}000 \times 0.5 \times 0.6 = 1{,}500$ vehicles/lane/day
- $5{,}000 \times 0.5 \times 0.18 = 450$ truck
    - 250 heavy vehicles/lane/day 200 large heavy vehicles/lane/day
        - Equivalent Heavy Vehicles (%) = HV(%) + LHV(%) × 3

          $\text{EHV}\ (\%) = 250/1500 + 3 \times 200/1500 = 0.566 = 56.6\%$
        - Equivalent heavy vehicles: $\text{HV} + 3 \times \text{LHV} = 250 + 600 = 850$ EHV
- 1,050 light vehicles
- Equivalent light vehicles: $\text{LV} + 10 \times \text{EHV} = 9{,}550$ ELV

Basic Voids Factor $V_f = 0.15\ \text{L/m}^2/\text{mm}$ (Figure A.6)

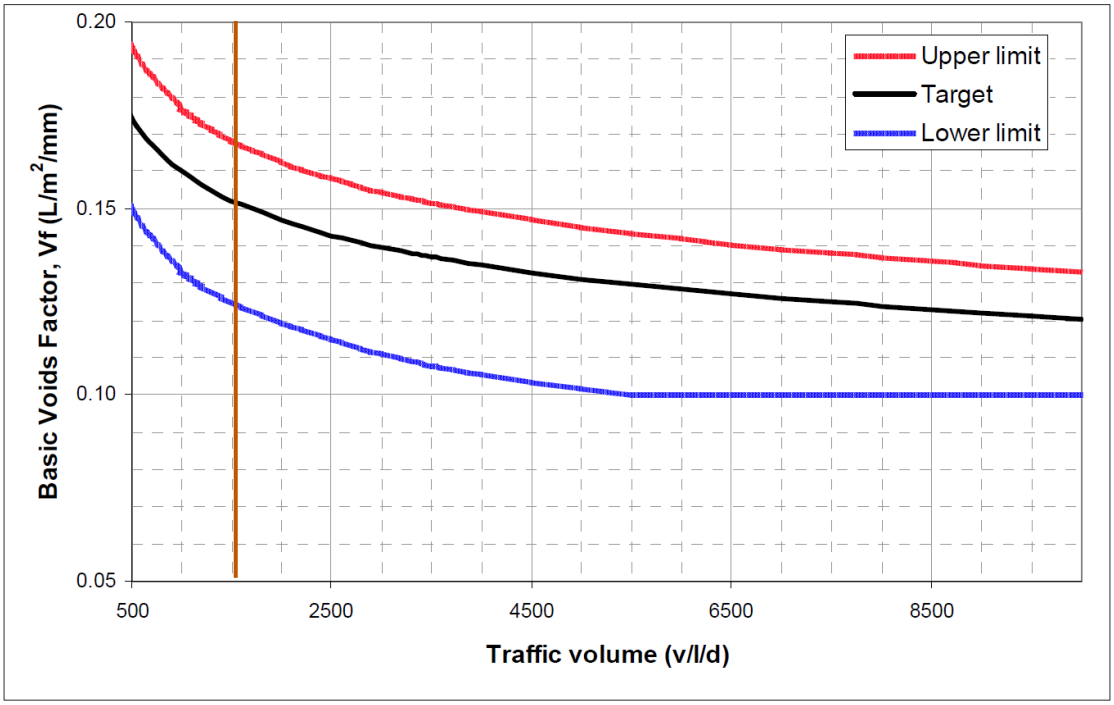

Figure A.6: Slow Lane Australian Basic Void Factor

Adjustment to the aggregate shape V_a is nil (Table A.20)

Aggregate type	Aggregate shape	Flakiness index (%)	Shape adjustment Va (L/m²/mm)
Crushed or partly crushed	Very flaky	> 35	Considered too flaky and not recommended for sealing
	Flaky	26 to 35	0 to - 0.01
	Angular	15 to 25	Nil
	Cubic	< 15	+ 0.01
	Rounded	n.a	0 to + 0.10
Not crushed	Rounded	n.a	+ 0.01

Table A.20: Slow Lane Australian Aggregate Shape Factor

Adjustment to the traffic effect V_t is -0.04 L/m^2/mm (Table A.21)

Traffic	Adjustment to Basic Voids Factor (L/m²/mm)			
	Flat or downhill		Slow moving – climbing lanes	
	Normal	Channelised*	Normal	Channelised*
On overtaking lanes of multi-lane rural roads where traffic is mainly cars with ≤10% of HV	+0.01	0.00	n.a.	n.a.
Non-trafficked areas such as shoulders, medians, parking areas	+0.02	n.a.	n.a.	n.a.
0 to 15% Equivalent Heavy Vehicles (EHV)	Nil	-0.01	-0.01	-0.02
16 to 25% Equivalent Heavy Vehicles (EHV)	-0.01	-0.02	-0.02	-0.03
26 to 45% Equivalent Heavy Vehicles (EHV)	- 0.02	- 0.03	- 0.03	- 0.04**
> 45% Equivalent Heavy Vehicles (EHV)	- 0.03	- 0.04**	- 0.04**	- 0.05**

Table A.21: Slow Lane Australian Traffic Correction Factor

** If adjustments for aggregate shape and traffic effects result in a reduction in Basic Voids Factor of 0.4 L/m^2/mm or more, special consideration should be given to the suitability of the treatment and possible selection of alternative treatments. Note that the recommended minimum Design Voids Factor is 0.10 L/m^2/mm in all cases.

Design Voids Factor V_F

$VF = V_f + V_a + V_t = 0.15 - 0.04 = 0.11$ L/m^2/mm

Basic Binder Application Rate

$BAR_{Basic} = V_F \times ALD = 0.11 \times 8.6 = 0.95 L/m^2$

Allowance applied to the basic binder application rate

Existing surface is a 10 mm seal with a small MTD of approx. 0.5mm

Surface texture allowance A_{st} = +0.1 L/m^2 (Table A.22)

Aggregate size of proposed seal	Measured texture depth (mm)	Surface texture allowance (L/m^2)
Existing: 10 mm seal		
14 mm	0 to 0.2	Note 1
	0.3 to 0.6	+0.1
	0.7 to 0.9	+0.2
	1.0 to 1.2	+0.3
	1.3 to 1.7	+0.4
	>1.7	Note 3

Table A.22: Slow Lane Australian Surface Texture Allowance

Embedment allowance A_e is -0.1 as shown Figure A.7.

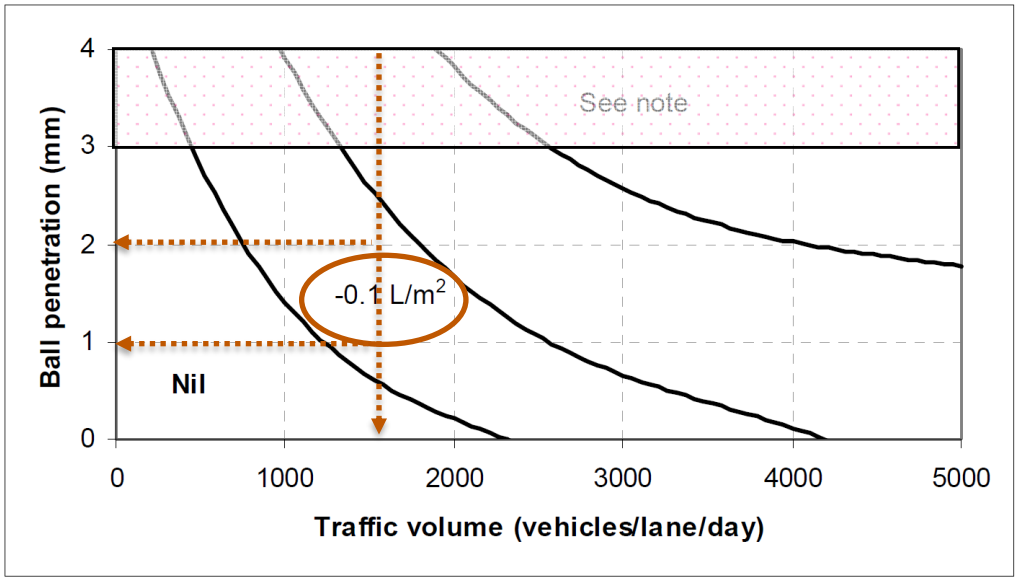

Figure A.7: Slow Lane Australian Surface Hardness Adjustment Factor

Binder absorption allowance (Aba) is nil because the existing surface does not fall under the category of an absorptive pavement nor a granular pavement.

Binder absorption by aggregate (Aaa) is nil because the aggregates considered are not absorptive.

Binder Application Rate

$\text{BAR} = \text{BAR}_{\text{Basic}} + \text{Allowances} = 0.95 + 0.1 - 0.1 + 0 + 0 = 0.95\text{L/m}^2$

$\mathbf{BAR = 1.0\ L/m^2}$ (rounded to nearest 0.1)

Aggregate Application Rate

$\text{AAR} = \frac{900}{ALD} = \frac{900}{8.6} = 104.6\ m^2/m^3$

$\text{AAR} = 105\ \text{m}^2/\text{m}^3$

To achieve a satisfactory aggregate mosaic, the actual spread rates may have to be varied in practice by as much as ±10 m^2/m^3

$\mathbf{AAR = [95\ to\ 115]\ m^2/m^3}$

Fast/Passing Lane

Design Traffic Characterization

- $5{,}000 \times 0.5 \times 0.4 = 1{,}000$ vehicle
    - Heavy vehicles will be less than 5%

Basic Voids Factor V_f

$V_f = 0.16\ L/m^2/mm$ (Figure A.8)

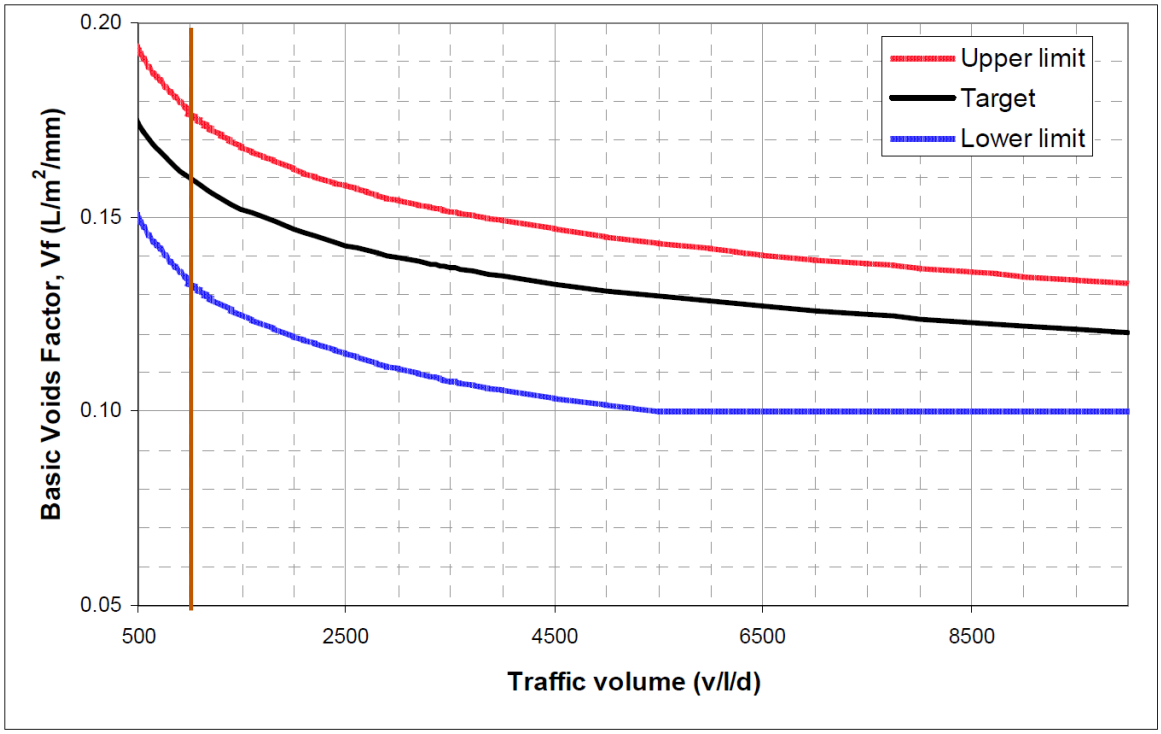

Figure A.8: Fast/Passing Lane Australian Basic Void Factor

Adjustment to the aggregate shape V_a is nil (Table A.23)

Aggregate type	Aggregate shape	Flakiness index (%)	Shape adjustment Va (L/m²/mm)
Crushed or partly crushed	Very flaky	> 35	Considered too flaky and not recommended for sealing
	Flaky	26 to 35	0 to - 0.01
	Angular	15 to 25	Nil
	Cubic	< 15	+ 0.01
	Rounded	n.a	0 to + 0.10
Not crushed	Rounded	n.a	+ 0.01

Table A.23: Fast/Passing Lane Australian Aggregate Shape Factor

Adjustment to the traffic effect V_t is $+ 0.01 L/m^2/mm$ (Table A.24)

Traffic	Adjustment to Basic Voids Factor (L/m²/mm)			
	Flat or downhill		Slow moving – climbing lanes	
	Normal	Channelised*	Normal	Channelised*
On overtaking lanes of multi-lane rural roads where traffic is mainly cars with ≤10% of HV	+0.01	0.00	n.a.	n.a.
Non-trafficked areas such as shoulders, medians, parking areas	+0.02	n.a.	n.a.	n.a.
0 to 15% Equivalent Heavy Vehicles (EHV)	Nil	-0.01	-0.01	-0.02
16 to 25% Equivalent Heavy Vehicles (EHV)	-0.01	-0.02	-0.02	-0.03
26 to 45% Equivalent Heavy Vehicles (EHV)	- 0.02	- 0.03	- 0.03	- 0.04**
> 45% Equivalent Heavy Vehicles (EHV)	- 0.03	- 0.04**	- 0.04**	- 0.05**

Table A.24: Fast/Passing Lane Australian Traffic Correction Factor

Note: As shown in the table, when considering sloped roads, the climbing lane is designed separately and has its own adjustments. The slope does not affect light vehicle's running speed as much as it affects heavy climbing vehicles.

Design Voids Factor VF

$$VF = V_f + V_a + V_t = 0.17 L/m^2/mm$$

Basic Binder Application Rate

$$BAR_{Basic} = V_F \times ALD = 0.17 \times 8.6 = 1.46 L/m^2$$

Allowance applied to the basic binder application rate

Existing surface is a 10 mm seal with MTD of 1.5mm

Surface texture allowance A_{st} = +0.4 L/m^2 (Table A.25)

Aggregate size of proposed seal	Measured texture depth (mm)	Surface texture allowance (L/m^2)
Existing: 10 mm seal		
14 mm	0 to 0.2	Note 1
	0.3 to 0.6	+0.1
	0.7 to 0.9	+0.2
	1.0 to 1.2	+0.3
	1.3 to 1.7	+0.4
	>1.7	Note 3

Table A.25: Fast/Pass Lane Australian Surface Texture Allowance

Binder absorption allowance (Aba) is nil because the existing surface does not fall under the category of an absorptive pavement nor a granular pavement.

Binder absorption by aggregate (Aaa) is nil because the aggregates are not absorptive.

Embedment allowance A_e is nil as shown Figure A.9.

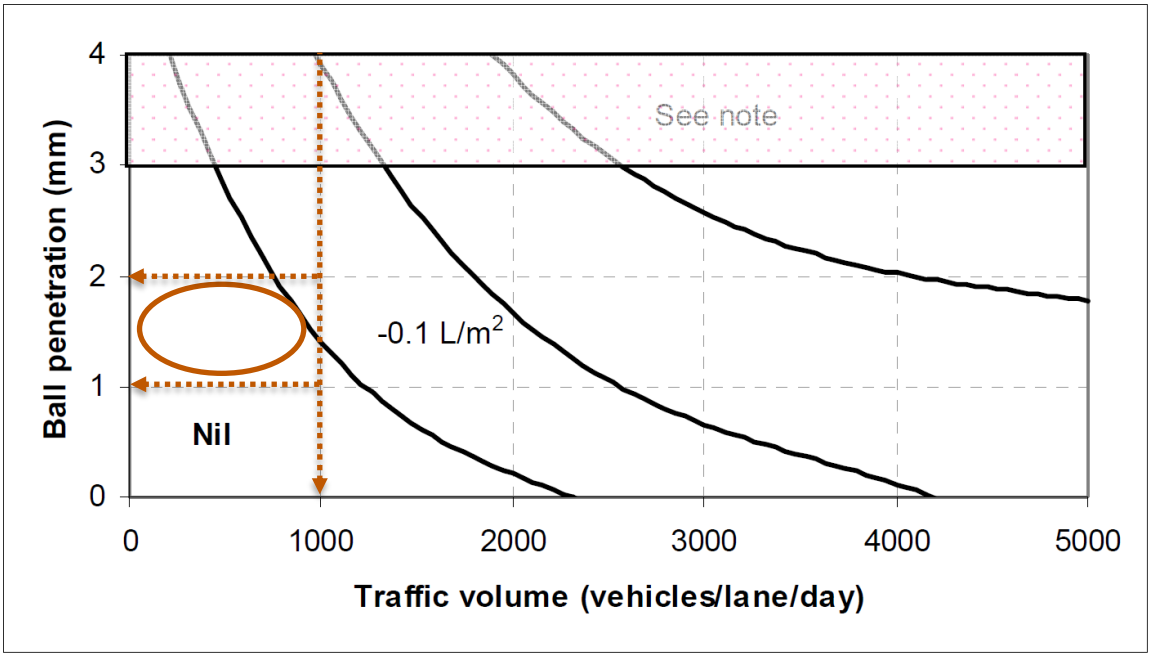

Figure A.9: Fast/Passing Lane Australian Surface Hardness Adjustment Factor

Binder Application Rate

$\text{BAR} = \text{BAR}_{\text{Basic}} + \text{Allowances} = 1.46 + 0.4$

$\mathbf{BAR = 1.86 L/m^2}$

Aggregate Application Rate

$\text{AAR} = \frac{900}{\text{ALD}} = \frac{900}{8.6} = 104.6\ \text{m}^2/\text{m}^3$

$\text{AAR} = 105\ \text{m}^2/\text{m}^3$

To achieve a satisfactory aggregate mosaic, the actual spread rates may have to be varied in practice by as much as ±10 m^2/m^3

$\mathbf{AAR = [95\ to\ 115]\ m^2/m^3}$

Shoulder

Design Traffic Characterization

- Traffic = 50v/l/d
- No or very few heavy vehicles

Basic Voids Factor V_f

$V_f = 0.23$ (Figure A.10)

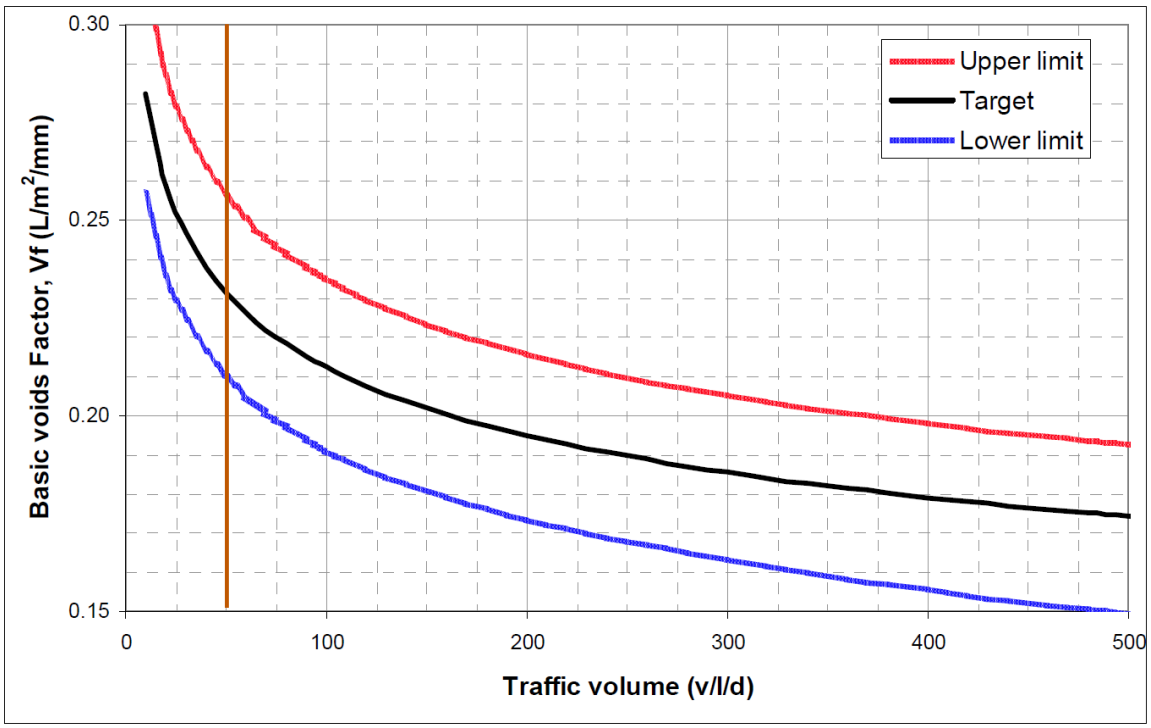

Figure A.10: Shoulder Australian Basic Void Factor

Adjustment to the aggregate shape V_a is nil (Table A.26)

.

Aggregate type	Aggregate shape	Flakiness index (%)	Shape adjustment Va (L/m²/mm)
Crushed or partly crushed	Very flaky	> 35	Considered too flaky and not recommended for sealing
	Flaky	26 to 35	0 to - 0.01
	Angular	15 to 25	Nil
	Cubic	< 15	+ 0.01
	Rounded	n.a	0 to + 0.10
Not crushed	Rounded	n.a	+ 0.01

Table A.26: Shoulder Australian Aggregate Shape Factor

Adjustment to the traffic effect V_t is $+ 0.02 L/m^2/mm$ (Table A.27)

Traffic	Adjustment to Basic Voids Factor (L/m²/mm)			
	Flat or downhill		Slow moving – climbing lanes	
	Normal	Channelised*	Normal	Channelised*
On overtaking lanes of multi-lane rural roads where traffic is mainly cars with ≤10% of HV	+0.01	0.00	n.a.	n.a.
Non-trafficked areas such as shoulders, medians, parking areas	+0.02	n.a.	n.a.	n.a.
0 to 15% Equivalent Heavy Vehicles (EHV)	Nil	-0.01	-0.01	-0.02
16 to 25% Equivalent Heavy Vehicles (EHV)	-0.01	-0.02	-0.02	-0.03
26 to 45% Equivalent Heavy Vehicles (EHV)	- 0.02	- 0.03	- 0.03	- 0.04**
> 45% Equivalent Heavy Vehicles (EHV)	- 0.03	- 0.04**	- 0.04**	- 0.05**

Table A.27: Shoulder Australian Traffic Correction Factor

Design Voids Factor VF

$VF = V_f + V_a + V_t = 0.25 L/m^2/mm$

Basic Binder Application Rate

$BAR_{Basic} = V_F \times ALD = 0.25 \times 8.6 = 2.15 L/m^2$

Allowance applied to the basic binder application rate

Existing shoulder surface is a 10 mm seal with MTD of 2.4mm

Surface texture allowance A_{st} = +0.4 L/m^2 (Table A.28)

Aggregate size of proposed seal	Measured texture depth (mm)	Surface texture allowance (L/m²)
Existing: 10 mm seal		
14 mm	0 to 0.2	Note 1
	0.3 to 0.6	+0.1
	0.7 to 0.9	+0.2
	1.0 to 1.2	+0.3
	1.3 to 1.7	+0.4
	>1.7	Note 3

Table A.28: Shoulder Australian Surface Texture Allowance

Note: The treatment might not be advisable depending on the shape and interlock of aggregates so alternative treatments might need to be considered.

Embedment allowance A_e is nil because the surface has a low ball-penetration value as shown Figure A.11.

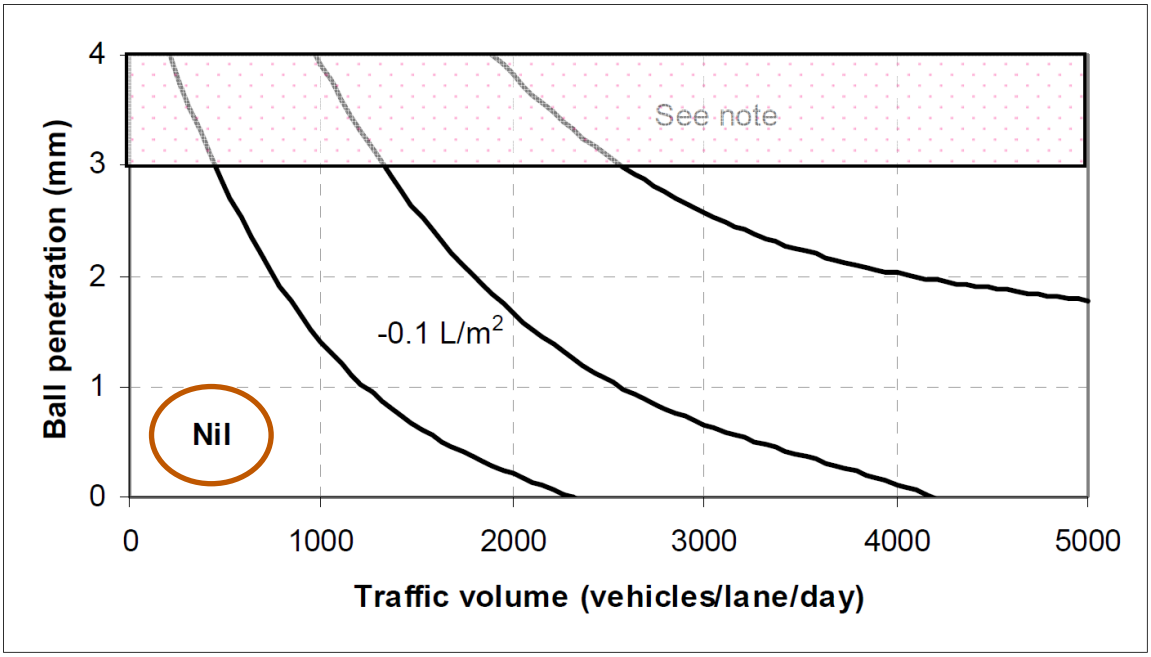

Figure A.11: Shoulder Australian Surface Hardness Adjustment Factor

Binder absorption allowance (Aba) is nil because the existing surface does not fall under the category of an absorptive pavement nor a granular pavement.

Binder absorption by aggregate (Aaa) is nil because the aggregates at hand are not absorptive.

Binder Application Rate

$$\mathbf{BAR = BAR_{Basic} + Allowances = 2.55 L/m^2}$$

"2.55 L/m^2 for the shoulder is considered to be an expensive option for a reseal and has a high risk of binder bleeding in hot weather. The preferred alternative is to consider selecting 7 mm aggregate (or 10 mm) as this will be cheaper while providing the necessary waterproofing, and texture is not an issue."

Aggregate Application Rate

$$\text{AAR} = \frac{900}{\text{ALD}} = \frac{900}{8.6} = 104.6\,\text{m}^2/\text{m}^3$$

$$\mathbf{AAR = 105 m^2/m^3}$$

SOUTH AFRICAN DESIGN METHOD (SANRAL, 2007)

Slow Lane

Aggregate Application Rate:

The average least dimension is 8.6 mm.

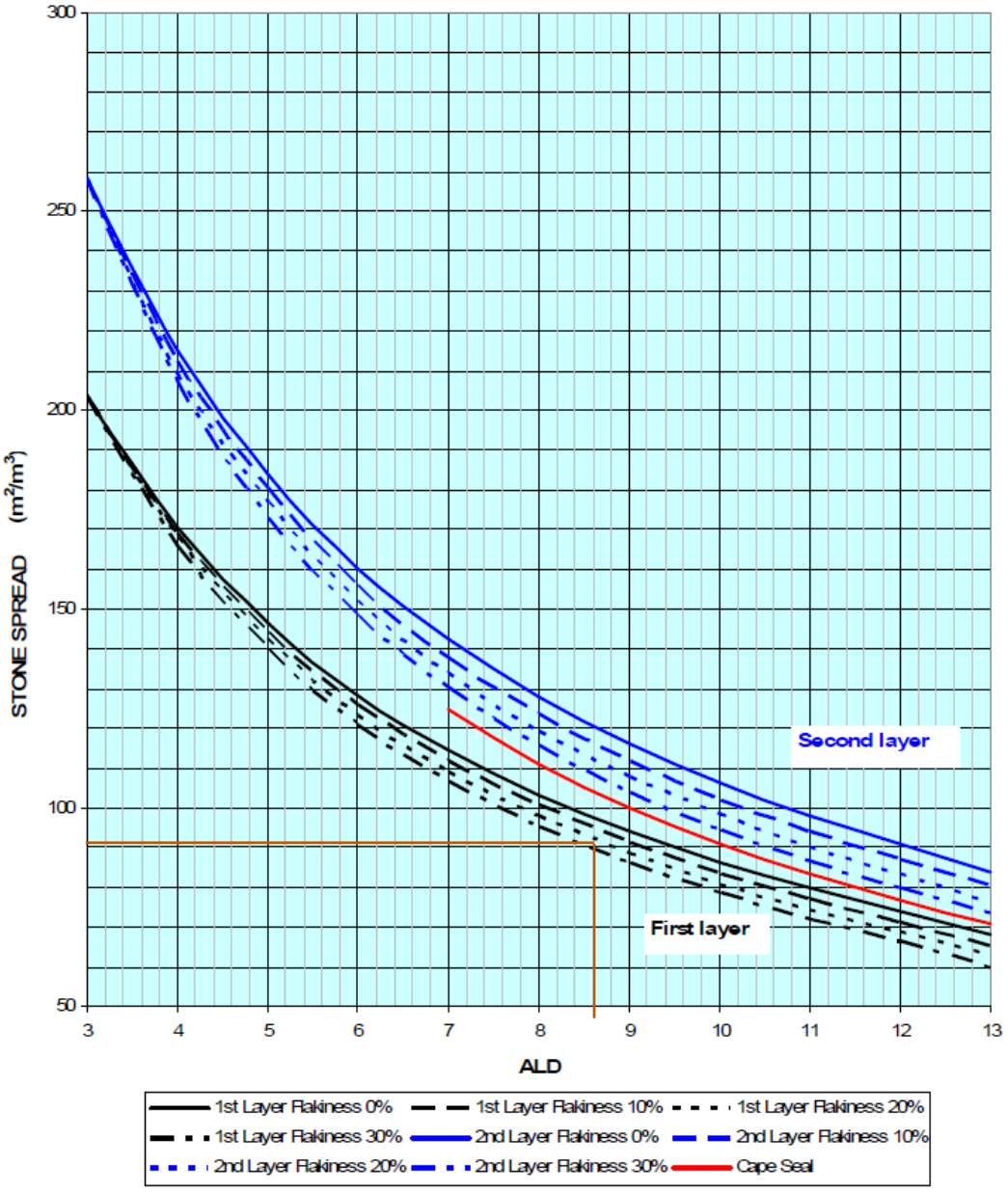

Figure A.12: Slow Lane South African AAR

AAR = 91 m^2/m^3 (Figure A.12)

Binder Application Rate:

$ADT = 5{,}000 \times 0.5 \times 0.6 = 1{,}500$ vehicles/lane/day

Heavy Vehicles $= 5{,}000 \times 0.5 \times 0.18 = 450$ HV/lane/day

$ELV = L + 40H = 1{,}050 + 40 \times 450 = 19{,}050$ ELV/lane/day

TRAFFIC VOLUME (elv/lane/day)	RECOMMENDED SURFACING TYPES FOR INITIAL SURFACING									
	S3	S7	S1	S2(9)	S2(13)	S4(13)	S2(13/6)	S4(19)	S2(19/9) S2(19/6)	AC
< 750	√	√	√	√	√	√	√	√	√	√
750 - 2000	x	√	√	√	√	√	√	√	√	√
2000 - 5000	x	x	√a	√a	√a	√	√	√	√	√
5000 - 10000	x	x	x	x	√a	√	√	√	√	√
10000 - 20000	x	x	x	x	x	√a	√	√	√	√
20000 - 40000	x	x	x	x	x	x	√a	√a	√	√
> 40000	x	x	x	x	x	x	x	√a	√a	√

Notes:

a - Good performance has been noted in several cases. The use of modified binders and trials on site can reduce risks in these situations. Typical problems expected are bleeding and loss of skid resistance

x - Not recommended

Table A.29: Slow Lane South African Surface Treatment Recommended Type

As shown in Table A.29, a single seal coat is not recommended for an ELV count of 19,000. In addition, a nominal aggregate size of 19mm is guided to provide a better skid resistance. However, for the purpose of comparing the different design methods, a single seal coat will be used with a nominal aggregate size of 14mm.

The effective layer thickness ELT is a function of the average least dimension:

$$\text{ELT} = 0.85679 \times \text{ALD} + 0.46715 \text{ mm} = 7.84\text{mm}$$

The percentage of void content in the aggregate layer is a function of the ELT:

$$\text{Void } \% = 45.333 - 0.333 \times \text{ELT} = 42.72\%$$

A corrected ball penetration of 1mm is adopted for the design.

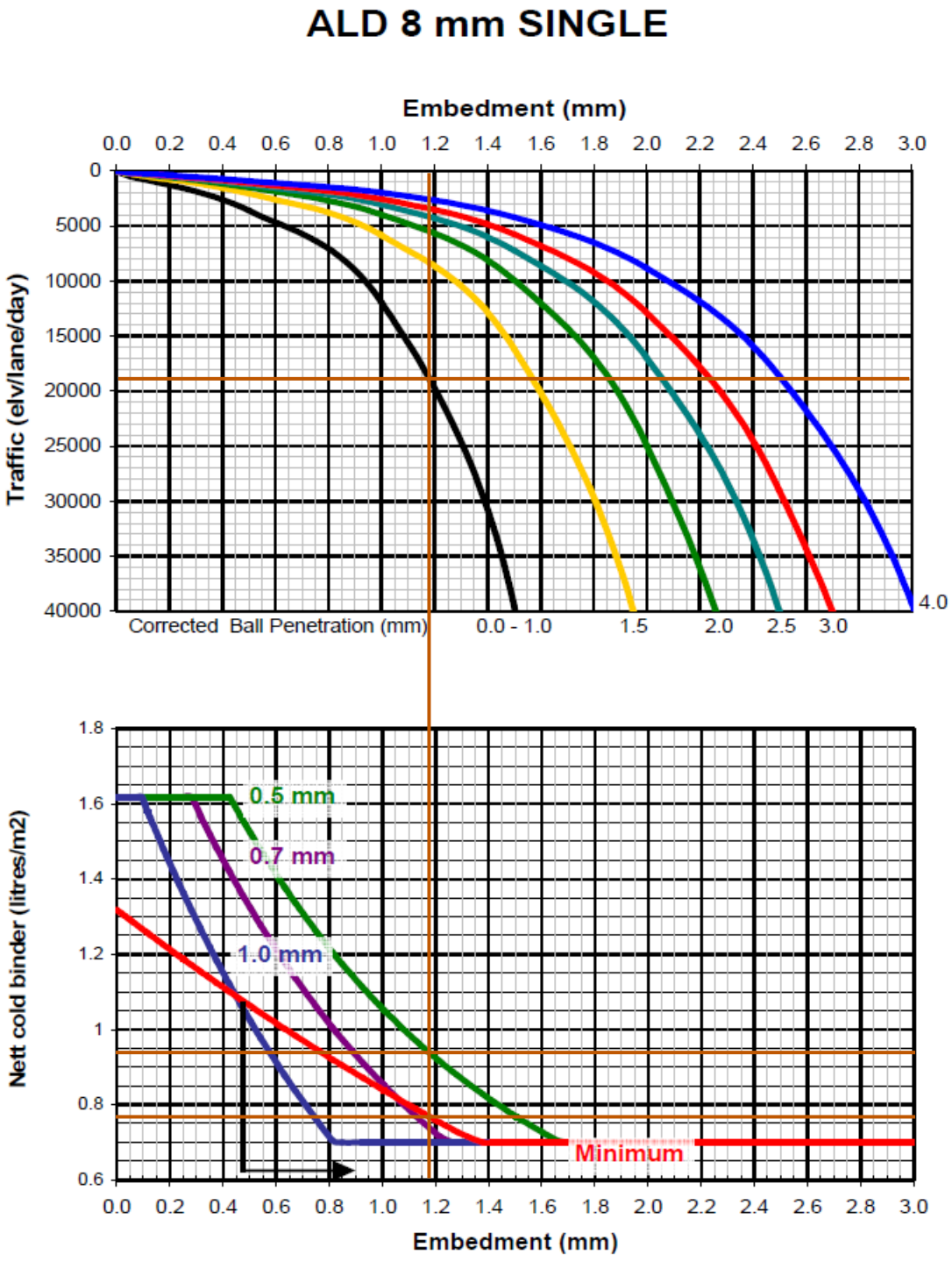

Figure A.13: Slow Lane South African BAR for Different ALDs

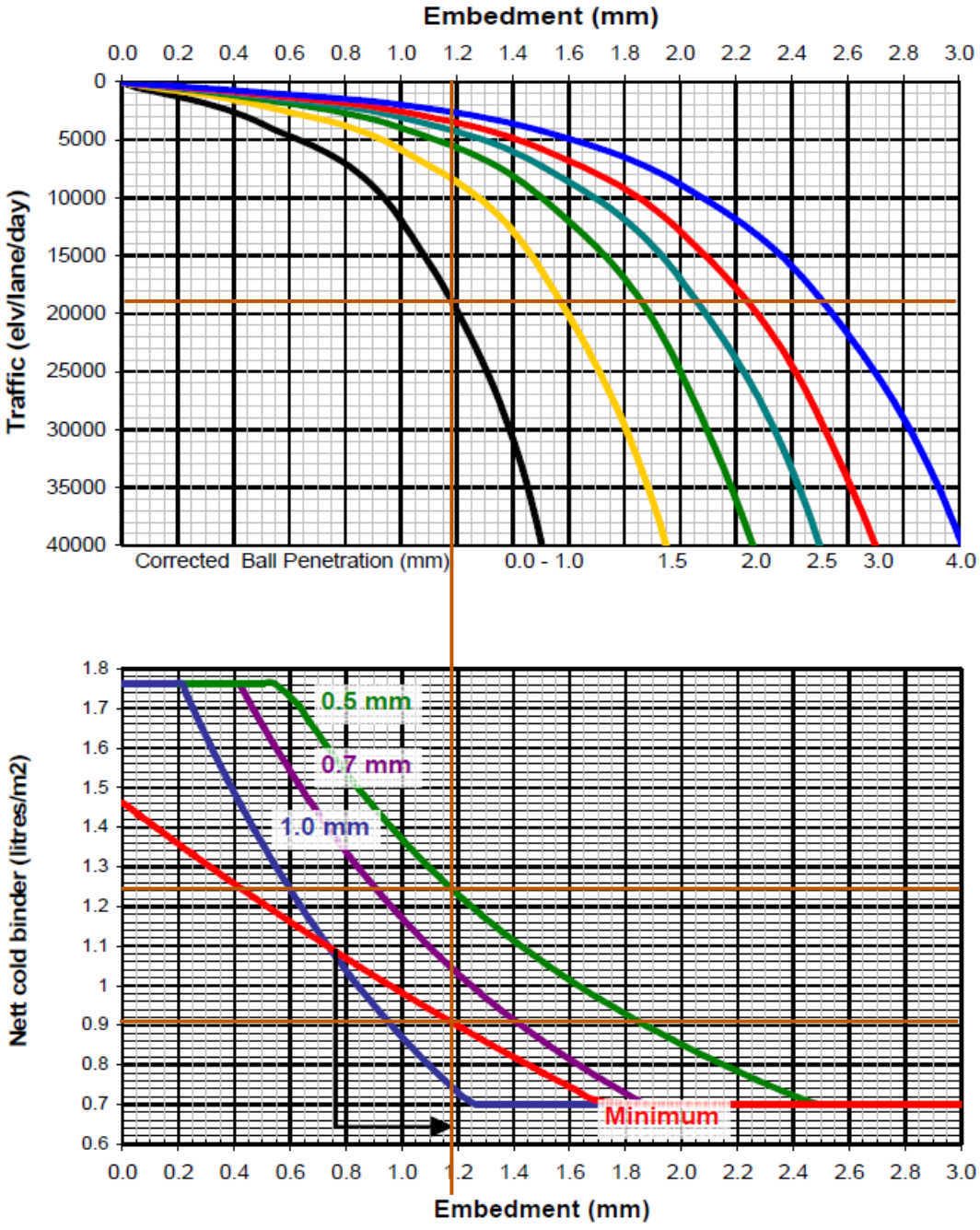

Figure A.13 Continued

ALD	Min BAR (L/m^2)	Max BAR (L/m^2)
8 mm	0.77	0.94
9 mm	0.91	1.24
8.6 mm	0.85	1.12

Table A.30: Slow Lane South African BAR

$\text{BAR}_{\text{Base}} = \frac{0.85+1.12}{2} = 0.99\ \text{L/m}^2$ (Table A.30 and Figure A.13)

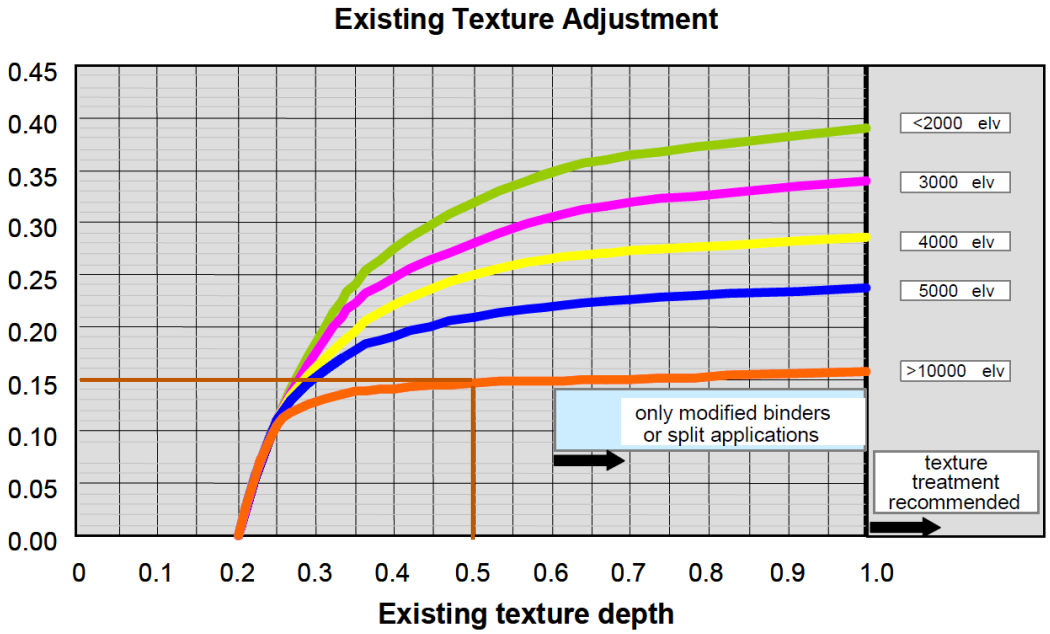

Figure A.14: Slow Lane South African BAR Texture Adjustment

A texture correction recommends increasing the binder application rate by 0.15 L/m^2

A moderate climate is assumed with a correction factor of zero.

It is recommended to reduce the binder content up to 10% for slow climbing lanes. A reduction of 5% will be adopted.

As for the aggregate spread, a dense matrix is adopted without the need for adjustments.

$\mathbf{BAR = (0.99 + 0.15) \times 0.95 = 1.08\ L/m^2}$

Fast/Passing Lane

Aggregate Application Rate:

The average least dimension is 8.6 mm.

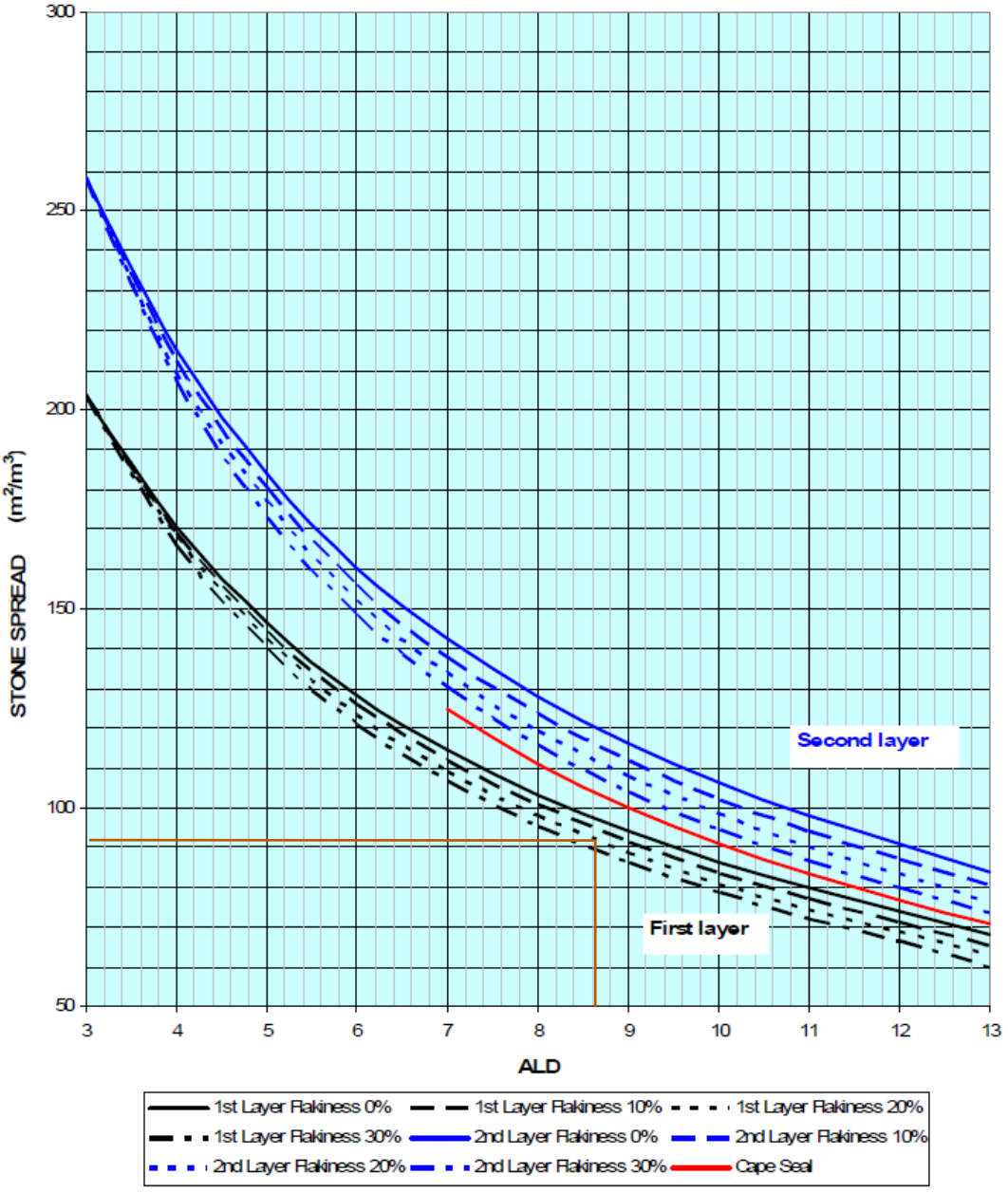

Figure A.15: Fast/Passing Lane South African AAR

AAR = 91 m^2/m^3 (Figure A.15)

Binder Application Rate:

ADT = 5,000 × 0.5 × 0.6 = 1,500 vehicles/lane/day

Heavy Vehicles = (5,000 × 0.5 × 0.18) × 10% = 45 HV/lane/day

ELV = L + 40H = 1,000 + 40 × 45 = 2,800 ELV/lane/day

TRAFFIC VOLUME (elv/lane/day)	RECOMMENDED SURFACING TYPES FOR INITIAL SURFACING									
	S3	S7	S1	S2(9)	S2(13)	S4(13)	S2(13/6)	S4(19)	S2(19/9) S2(19/6)	AC
< 750	√	√	√	√	√	√	√	√	√	√
750 - 2000	x	√	√	√	√	√	√	√	√	√
2000 - 5000	x	x	√a	√a	√a	√	√	√	√	√
5000 - 10000	x	x	x	x	√a	√	√	√	√	√
10000 - 20000	x	x	x	x	x	√a	√	√	√	√
20000 - 40000	x	x	x	x	x	x	√a	√a	√	√
> 40000	x	x	x	x	x	x	x	√a	√a	√

Table A.31: Fast/Passing Lane South African Surface Treatment Recommended Type

As shown in Table A.31, a single seal coat is recommended for this traffic level.

The effective layer thickness ELT is a function of the average least dimension:

$$\text{ELT} = 0.85679 \times \text{ALD} + 0.46715 \text{ mm} = 7.84\text{mm}$$

The percentage of void content in the aggregate layer is a function of the ELT:

$$\text{Void \%} = 45.333 - 0.333 \times \text{ELT} = 42.72\%$$

A corrected ball penetration of 1mm is adopted for the design.

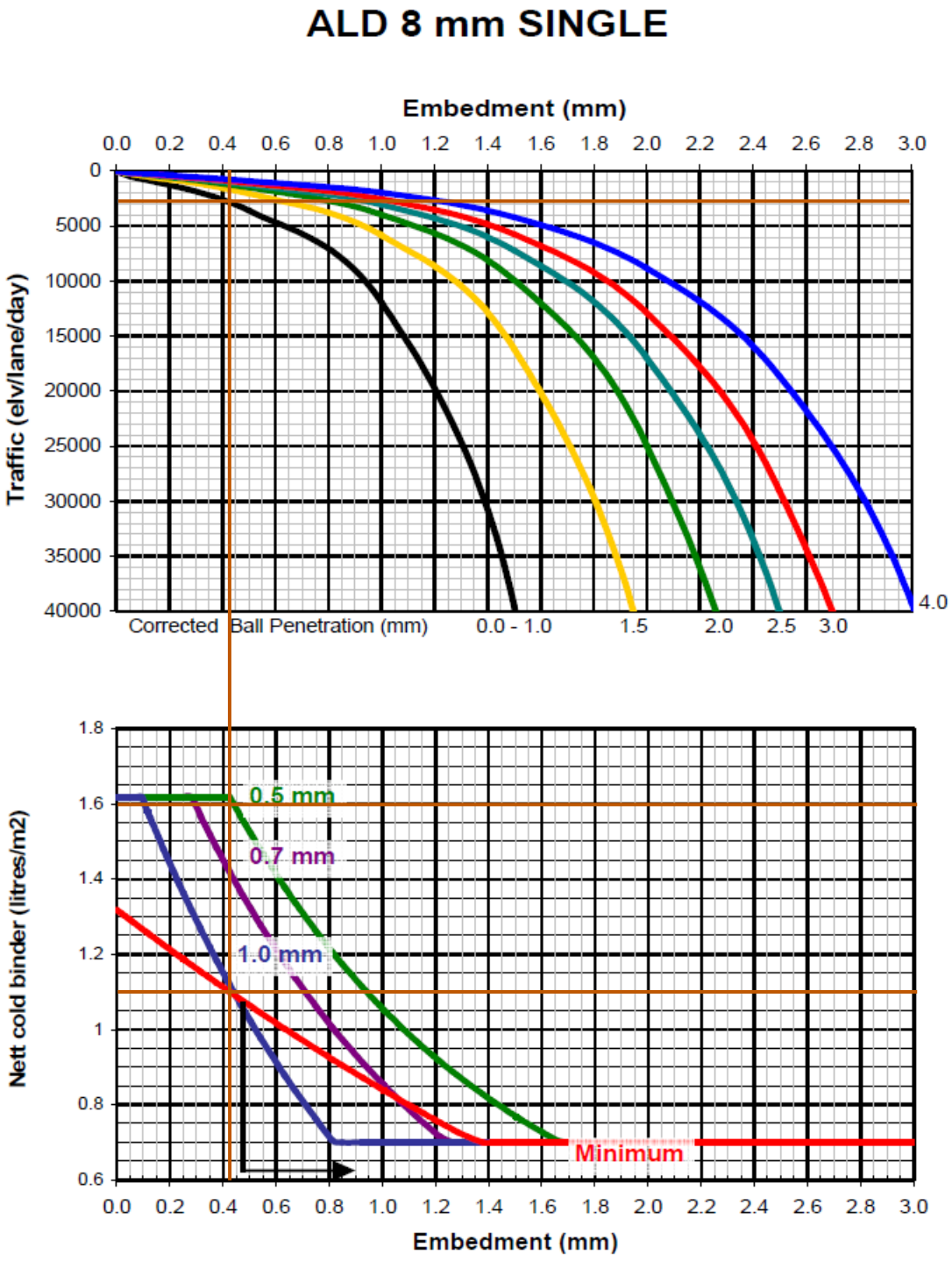

Figure A.16: Fast/Passing South African BAR for Different ALDs

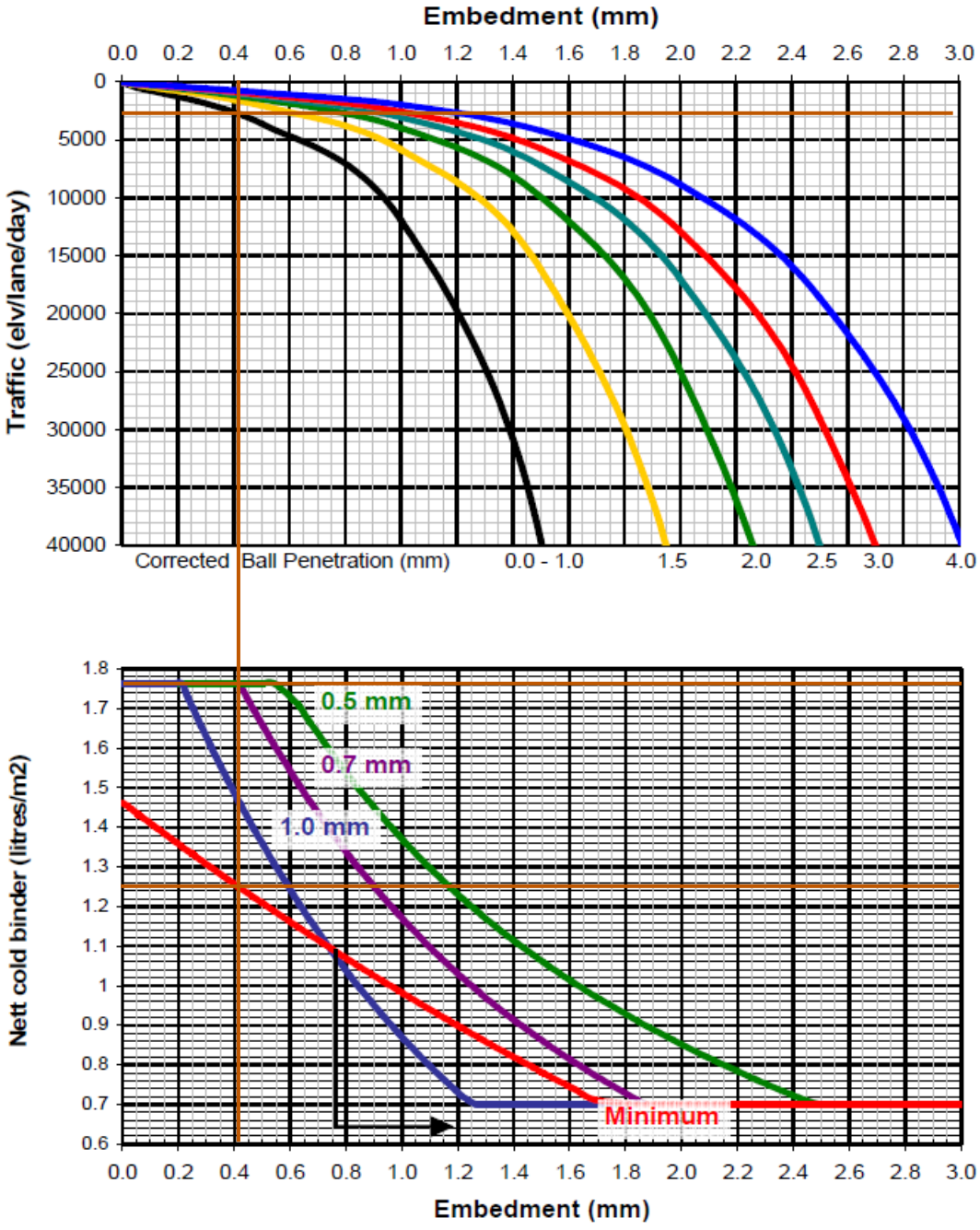

Figure A.16 Continued

ALD	Min BAR **(L/m²)**	Max BAR **(L/m²)**
8 mm	1.10	1.60
9 mm	1.26	1.76
8.6 mm	1.18	1.68

Table A.32: Fast/Passing Lane South African BAR

$\text{BAR}_{\text{Base}} = \frac{1.18+1.68}{2} = 1.43\ \text{L/m}^2$ (Table A.32 and Figure A.16)

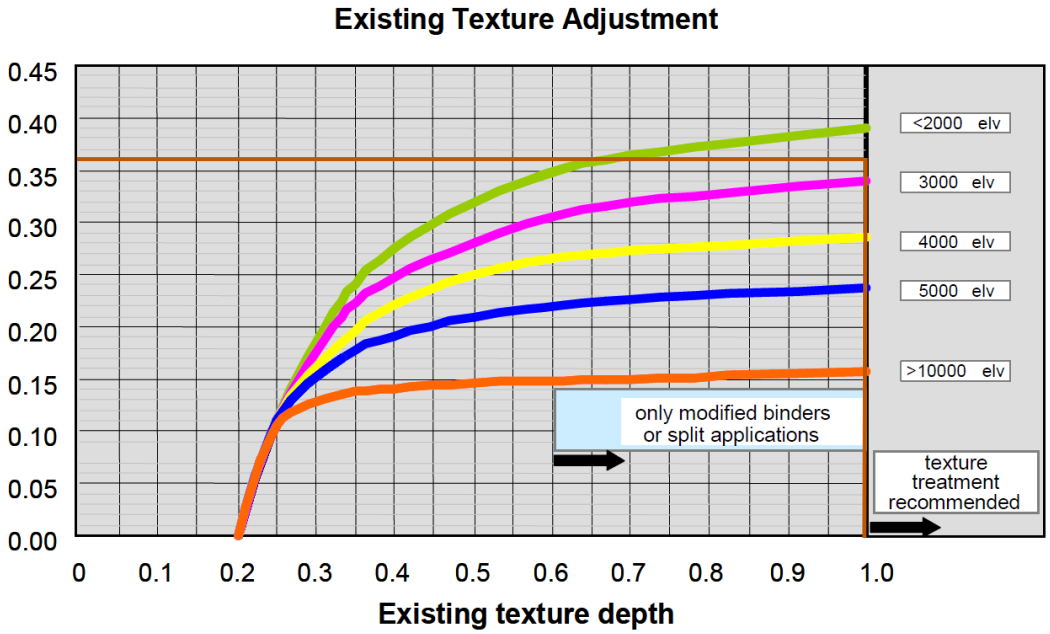

Figure A.17: Fast/Passing Lane South African BAR Texture Adjustment

A texture treatment is recommended with an additional binder rate of 0.36 L/m^2

A moderate climate is assumed with a correction factor of zero. It is recommended to reduce the binder content up to 10% for uphill climbs. A reduction of 5% will be adopted. As for the aggregate spread, a dense matrix is adopted without the need for adjustments.

$\mathbf{BAR = (1.43 + 0.36) \times 0.95 = 1.70\ L/m^2}$

Shoulder

Aggregate Application Rate:

The average least dimension is 8.6 mm.

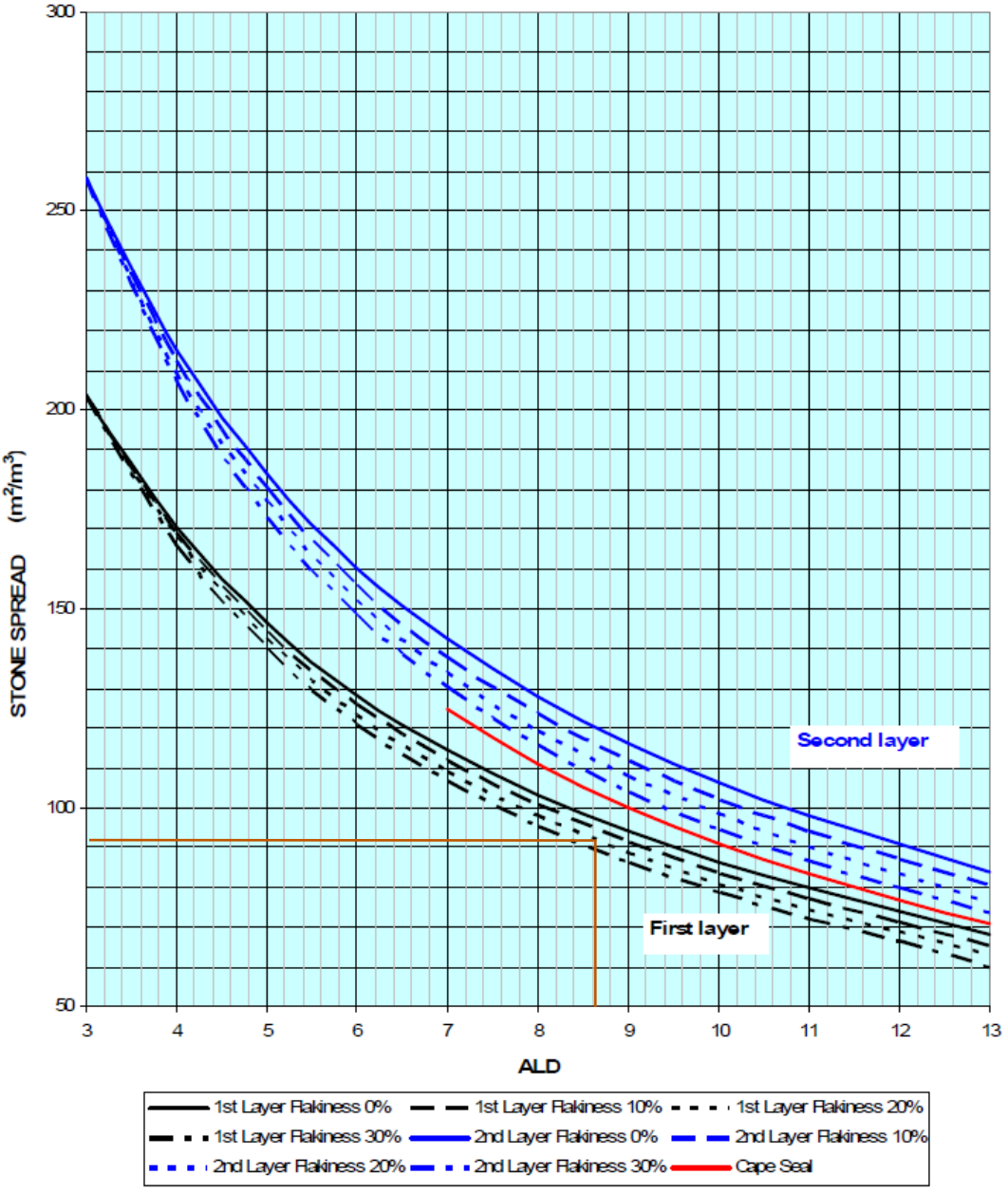

Figure A.18: Shoulder South African AAR

$\mathbf{AAR = 91\ m^2/m^3}$ (Figure A.18)

Binder Application Rate:

$\text{ADT} = 50\ \text{vehicles/lane/day}$

$\text{Heavy Vehicles} = (5{,}000 \times 0.5 \times 0.18) \times 1\% = 5\ \text{HV/lane/day}$

$\text{ELV} = \text{L} + 40\text{H} = 1{,}000 + 40 \times 45 = 1{,}850\ \text{ELV/lane/day}$

TRAFFIC VOLUME (elv/lane/day)	RECOMMENDED SURFACING TYPES FOR INITIAL SURFACING									
	S3	S7	S1	S2(9)	S2(13)	S4(13)	S2(13/6)	S4(19)	S2(19/9) S2(19/6)	AC
< 750	√	√	√	√	√	√	√	√	√	√
750 - 2000	x	√	√	√	√	√	√	√	√	√
2000 - 5000	x	x	√a	√a	√a	√	√	√	√	√
5000 - 10000	x	x	x	x	√a	√	√	√	√	√
10000 - 20000	x	x	x	x	x	√a	√	√	√	√
20000 - 40000	x	x	x	x	x	x	√a	√a	√	√
> 40000	x	x	x	x	x	x	x	√a	√a	√

Table A.33: Shoulder South African Surface Treatment Recommended Type

As shown in Table A.33, a single seal coat is recommended for this traffic level.

The effective layer thickness ELT is a function of the average least dimension:

$$\text{ELT} = 0.85679 \times \text{ALD} + 0.46715\ \text{mm} = 7.84\text{mm}$$

The percentage of void content in the aggregate layer is a function of the ELT:

$$\text{Void \%} = 45.333 - 0.333 \times \text{ELT} = 42.72\%$$

A corrected ball penetration of 1mm is adopted for the design.

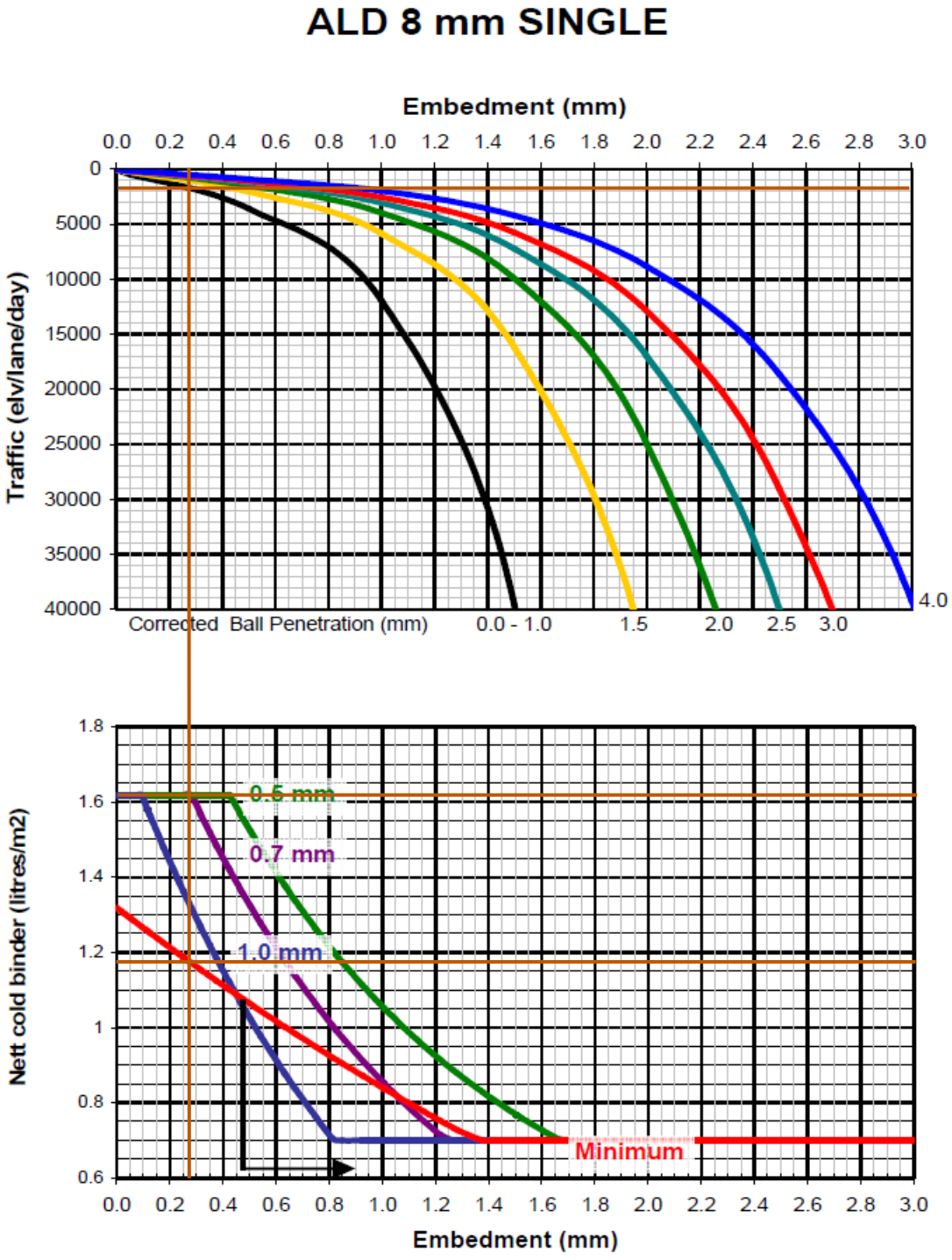

Figure A.19: Shoulder South African BAR for Different ALDs

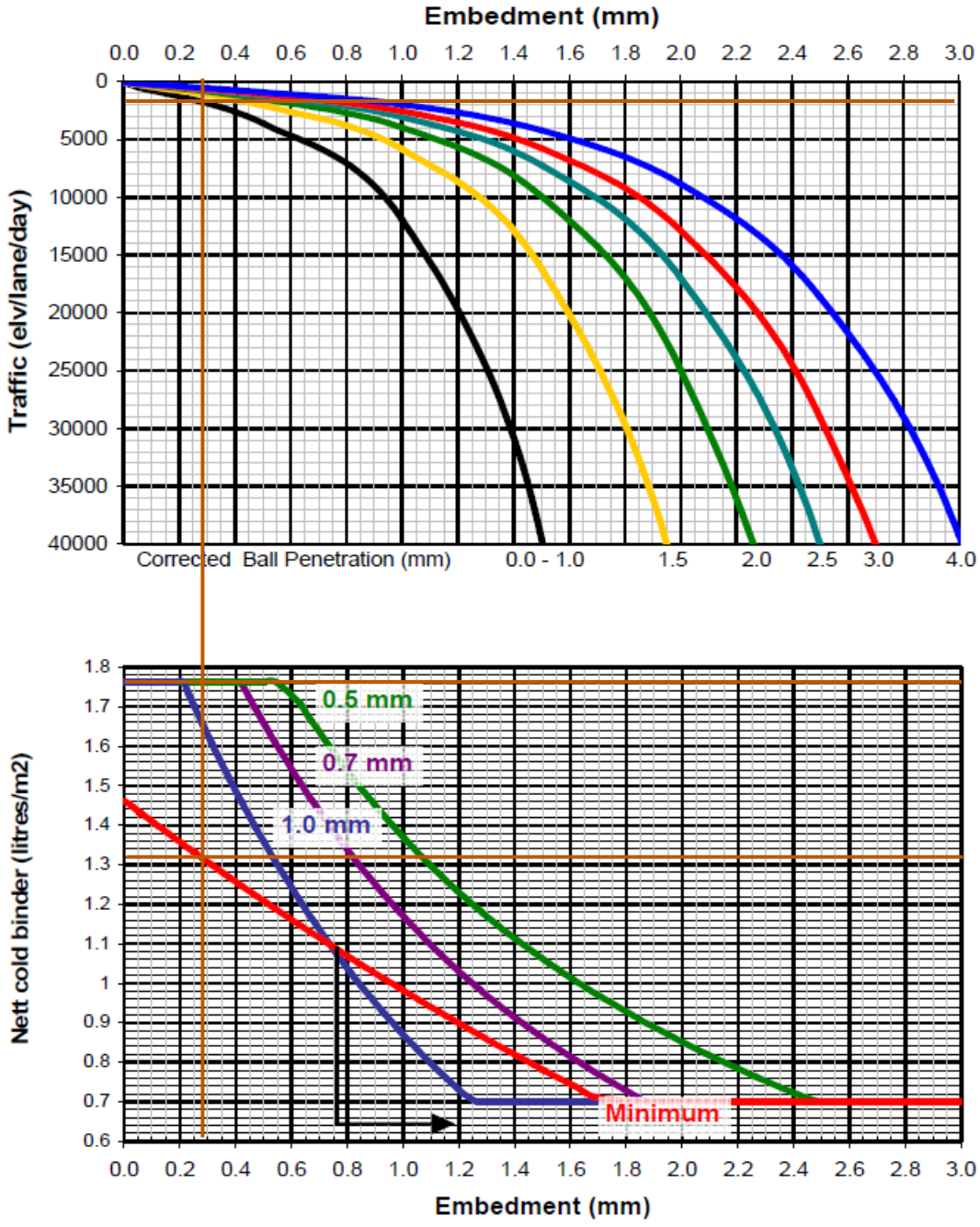

Figure A.19 Continued

ALD	Min BAR **(L/m²)**	Max BAR **(L/m²)**
8 mm	1.18	1.63
9 mm	1.32	1.75
8.6 mm	1.25	1.69

Table A.34: Shoulder South African BAR

$\text{BAR}_{\text{Base}} = \frac{1.25+1.69}{2} = 1.47\ \text{L/m}^2$ (Table A.34 and Figure A.19)

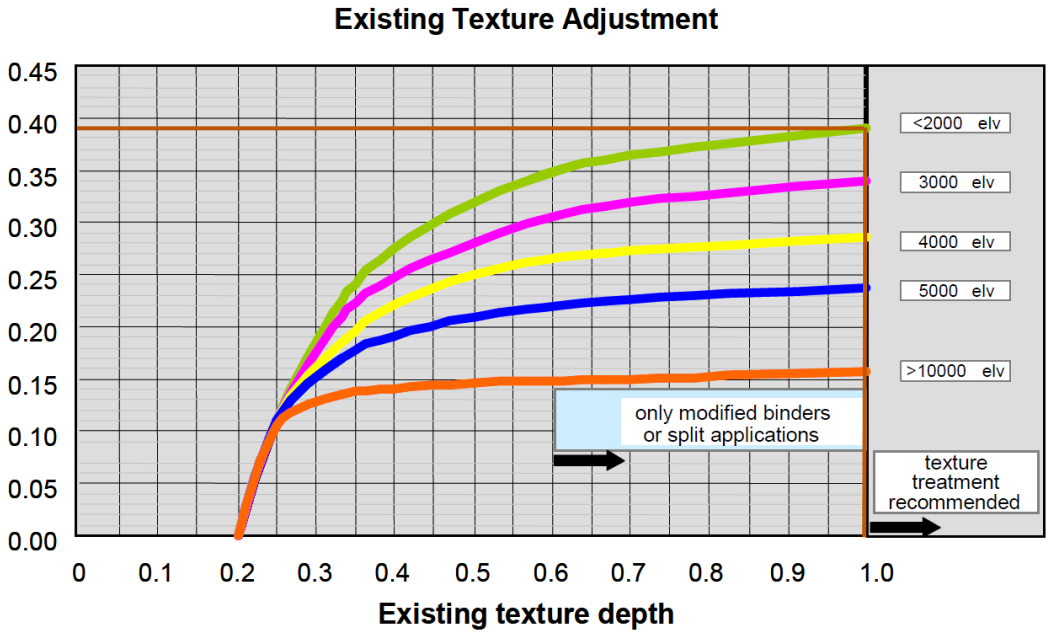

Figure A.20: Shoulder African BAR Texture Adjustment

A texture treatment is recommended with an additional binder rate of 0.39 L/m²

A moderate climate is assumed with a correction factor of zero.

It is recommended to reduce the binder content up to 10% for climbing lanes. A reduction of 5% will be adopted.

As for the aggregate spread, a dense matrix is adopted without the need for adjustments.

$\mathbf{BAR = (1.47 + 0.39) \times 0.95 = 1.77\ L/m^2}$

BRITISH DESIGN METHOD (BATEMAN, 2016)

Slow Lane

Aggregate Application Rate:

Assume: surface category A, probe penetration of 2 mm, and 15°C surface temperature.

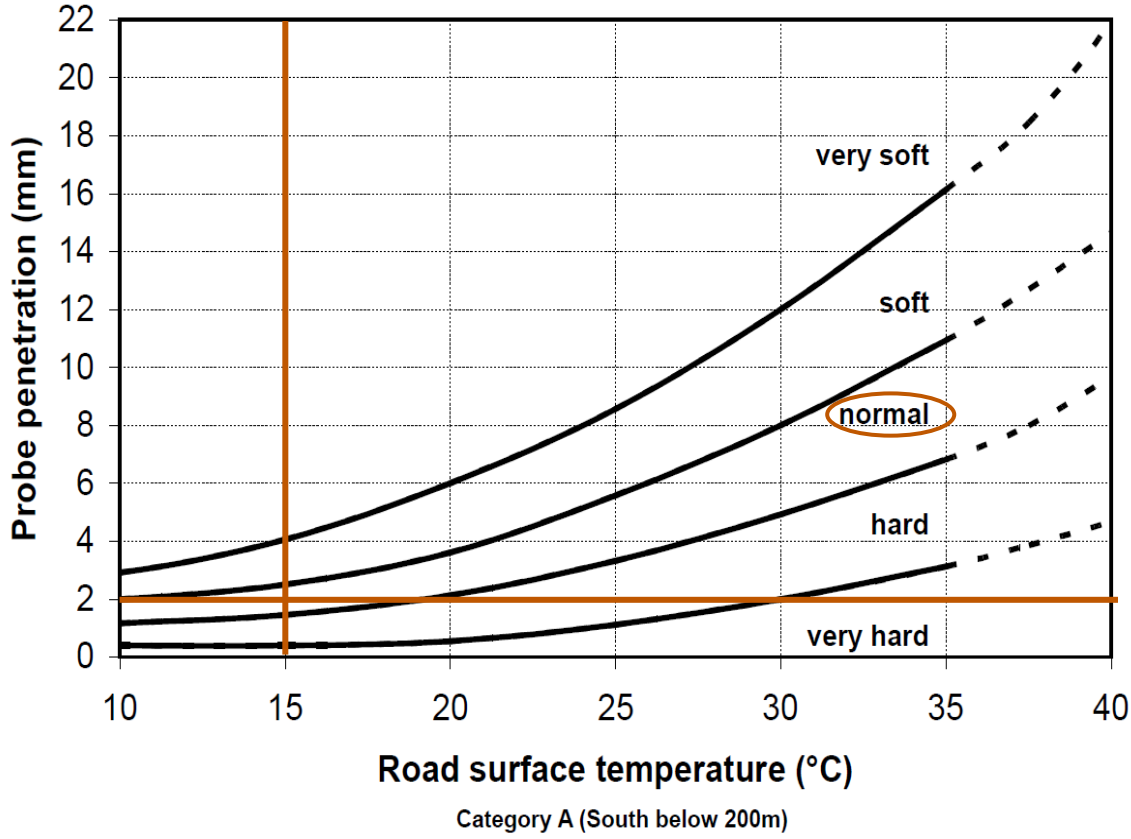

Figure A.21: Slow Lane British Surface Hardness

Medium & heavy vehicles / lane / day	0 to 50	51 to 125	126 to 250	251 to 500	501 to 1250	1251 to 2000	2001 to 2500	2501 to 3250	Over 3250
Traffic Category	H	G	F	E	D	C	B	B	A
NRSWA Road Type	4	4	3	3	2	1	1	0	0

Table A.35: Slow Lane British Traffic Characterization

Based on the following diagram, it is recommended to use a racked-in or a double seal coat. However, a single seal coat with premium grade binder can be adopted. For the sake of comparing the different design methods, a single seal coat will be used.

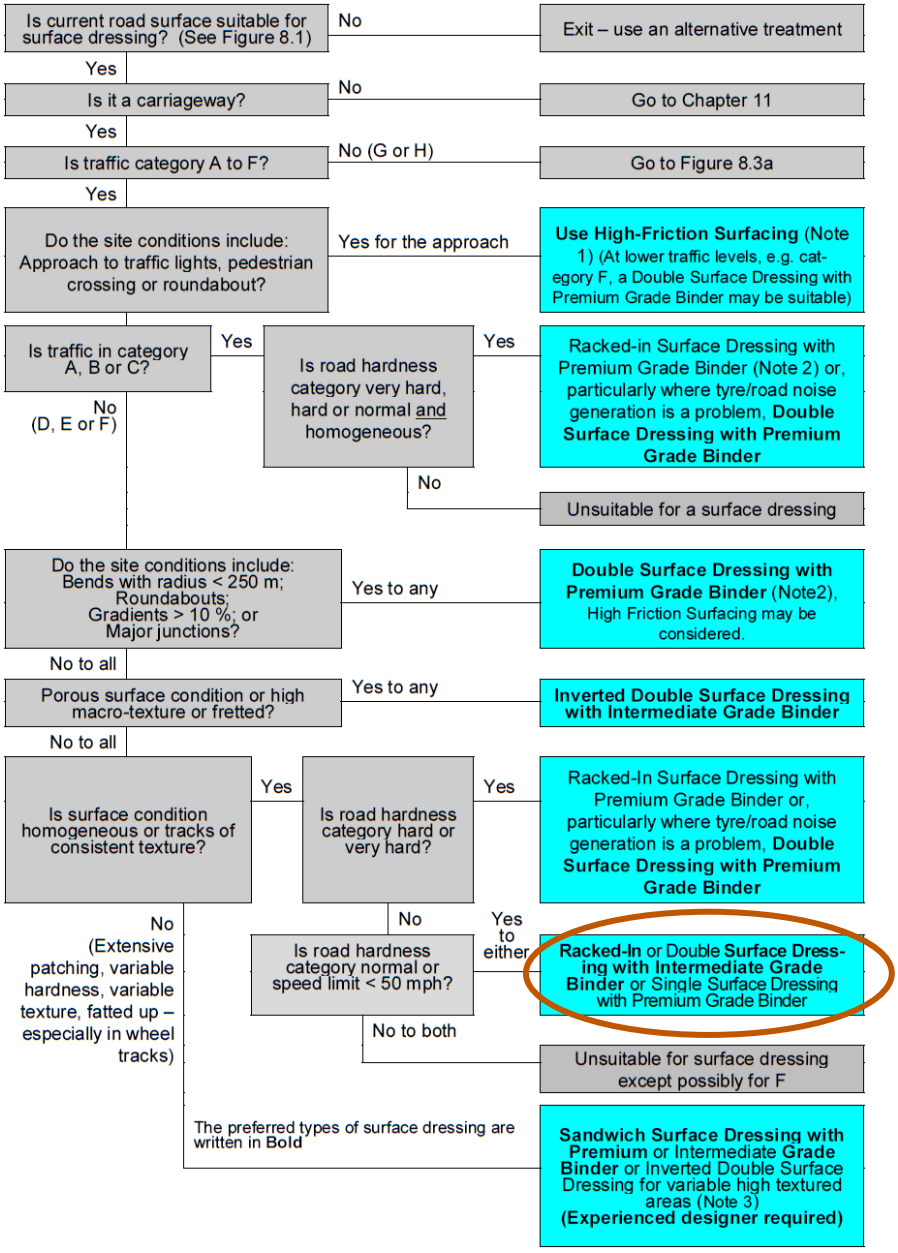

Figure A.22: Slow Lane Seal Coat Type British Recommendation

Traffic Category	Hardness Category of Road Surface									
	Very Hard		Hard		Normal		Soft		Very Soft	
	Size of Chipping	Binder Rate (L/m²)	Size of Chipping (mm)	Binder Rate (L/m²)	Size of Chipping (mm)	Binder Rate (L/m²)	Size of Chipping (mm)	Binder Rate (L/m²)	Size of Chipping (mm)	Binder Rate (L/m²)
A	(a)		(a)		(a)		(b)		(b)	
B	S10	1.8 (c)	(a)		(a)		(a)		(b)	
C	S10	1.8 (c)	S10	1.6 (c)	(a)		(a)		(b)	
D	S6	1.5 (c)	S10	1.6 (c)	(a)		(a)		(a)	
E	S6	1.5 (c)	S10	1.6 (c)	S10	1.6 (c)	S10	1.6 (c)	(a)	
F	S6	1.5 (c)	S6	1.5 (c)	S10	1.6 (c)	S10	1.6 (c)	(a)	
G	S6	1.5	S6	1.5	S6	1.5	S10	1.6	(a)	
H	S6	1.5	S6	1.5	S6	1.5	S6	1.4	S6	1.4

Notes: (a) Multiple layer surface dressing preferred – see Figures 8.3a and 8.3b.
(b) Conditions not suitable for single surface dressings – see Figure 8.3b.
(c) Polymer-modified versions of this type of binder are preferred in those conditions – see Section 5.3.4 and Figure 8.3b.
(d) The surface dressing types are coded for convenience: S is for single and the chipping sizes are the maximums so S6 is a 2.8/6.3 chipping single surface dressing and S10 is a 6.3/10 chipping.

Aggregate Size	Range of Spread Rates	
	kg/m^2	$m^2/tonne$
2.8/6.3 mm	8 – 11	125 – 91
6.3/10 mm	10 – 14	100 – 71
8 / 14 mm	12 – 16	83 – 62

Table A.36: Slow Lane British Aggregate Size and Application Rate

$AAR = 14\ kg/m^2$

A single seal coat with a minimal nominal aggregate size of 10mm is recommended; thus, an aggregate size of 14 mm is deemed appropriate.

Binder Application Rate:

$BAR_{BASE} = 1.6 L/m^2$

Influence	Property	Effect (L/m²)	Comments
Season	Early and mid-season	0	Late season work is very risky especially with S10, double surface dressing is recommended if the work has to be completed, see Fig 7.3.2.
	Late season	+0.2	
Aggregate type	Crushed rock or slag	0	Gravel is only appropriate for Traffic Categories G and H.
	Gravel	+0.1	
Shape	Flakiness category		Flakiness index should conform to PD 6882-2. Adjustment is only required for non-conforming aggregates. Very cubical chippings, FI_{10}, require more binder to hold them initially. Flaky chippings (>FI_{20}) may result in early loss of texture depending on traffic.
	FI_{10}	+0.1	
	FI_{15}	0	
	FI_{20}	-0.1	
	FI_{25} and above	Consider design	
Shade	Un-shaded, open to sun	0	Shaded areas are cooler and, therefore, the road is effectively harder so more binder is required. Double surface dressing is recommended for fully shaded areas (see Table 9.2.3).
	Partially shaded	+0.1	
	Fully shaded	+0.2	
Surface condition (Consider suitability, see Figure 8.1 and type of surface dressing Figures 8.3a and 8.3b)	Very binder rich	-0.2	For variable soft binder rich areas a sandwich surface dressing should be considered. Above F traffic category if there is tracking due to being binder rich, larger chippings should be considered for the wheel tracks as part of a double surface dressing. A pad coat is recommended to normalise and seal porous road surfaces (see Section 9.2.4). Double surface dressing with intermediate binder is recommended for variable hard and binder lean substrates (see Table 9.2.3).
	Binder rich	-0.1	
	Normal	0	
	Texture in wheel tracks	+0.1	
	Binder lean / porous	+0.2	
	Very binder lean and porous, high macro-texture, or variable and hard.	Consider Design	
Gradient	> 5 % uphill	-0.2	The gradient affects the traffic stress on the surface dressing and, therefore, the rate of embedment. Racked-in or double surface dressings are recommended for hills and downhill high-speed sections (see Tables 9.2.2 and 9.2.3).
	< 5 %	0	
	> 5 % downhill	+0.1	
	> 10 % downhill	+0.2	
Traffic Speed	High speed (≥50 mph limit)	+0.1	Roads subject to high-speed traffic induce greater surface stress. Racked-in or double surface dressings with premium binders are recommended.
	Low speed (<50 mph limit)	0	
Local traffic	Design range	0	Un-trafficked areas, such as hatched sections, and also between the wheel tracks and edges of carriageways, require more binder. Hard shoulders, unless a contra flow is planned, and sizeable areas with hatched lines to exclude traffic are effectively untrafficked.
	Effectively un-trafficked	+0.2	

$$\mathrm{BAR} = \mathrm{BAR}_{\mathrm{BASE}} - \mathrm{Adhjustments} = 1.6 - 0.1 - 0.1 - 0.2$$

$$\mathbf{BAR = 1.2 L/m^2}$$

Design of road surface dressings to Road Note 39 (Seventh Edition)

Road number: Example # | Region/Area: ...

Section location: ...

Length: # m | Width: 15.5 m | No. of lanes: 4 | Area: m^2

Lane(s): 2 | Medium/Heavy Traffic: 450 cv/l/d | NRSWA road type: 3

Traffic Speed: * 40 mph

Traffic category: * ~~A~~ ~~B~~ ~~C~~ ~~D~~ **E** ~~F~~ ~~G~~ ~~H~~

Location: * South ~~Central~~ ~~North~~ | Temperature Category: * **A** ~~B~~ ~~C~~ ~~D~~

Road Hardness (RH) probe depth: 2 mm at 15 °C | Min. PSV: 60 | Max. AAV: 8

RH Category:* ~~Very Hard~~ ~~Hard~~ Normal ~~Soft~~ ~~Very Soft~~ ~~Variable~~

Surface condition: * ~~Very binder rich~~ | Binder rich | ~~Normal~~ | ~~Texture in wheel tracks~~ | ~~Binder lean/porous~~

Radius of curvature: * Under 100 m | ~~100 – 250 m~~ | ~~over 250 m~~ | Expected Month on Site:

Junction or crossing: * ~~Approach~~ | Non-approach

Overall gradient: * ~~up to 5 %~~ | 5 – 10 % | ~~Over 10 %~~ | Uphill | ~~Downhill~~

Type of surface dressing: * Single | ~~Racked In~~ | ~~Double~~ | ~~Inverted Double~~ | ~~Sandwich~~

Chipping size: * 8/14 mm | ~~6.3/10 mm~~ | ~~2.8/6.3 mm~~ | Other:
~~8/14 & 2.8/6.3 mm~~ | ~~6.3/10 & 2.8/6.3 mm~~ | ~~6.3/10 & 4/2 mm~~

Aggregate type: * Crushed rock | ~~Blast-furnace~~ | ~~Steel slag~~ | ~~Gravel~~

Flakiness index: * ~~Less than 10 %~~ | ~~10 % to 15 %~~ | ~~15 % to 20 %~~ | More than 20 %

Bituminous emulsion binder: ~~Unmodified~~ | ~~Intermediate~~ | ~~Premium Grade~~ | Super-Premium

Seasonal risk category: ~~High~~ | ~~Significant~~ | Low

Binder spread rate: First layer 1.6 L/m² | Second layer * L/m²

Location	Season	Aggregate type	Flakiness	Increase of chipping size	Shade	Surface condition	Gradient	Traffic Speed	Untrafficked area	Sum of factors	Rate of spread of binder
First Layer	0	0	-0.1	0	0	-0.1	-0.2	0	0	-0.4	1.2 L/m²
											L/m²
											L/m²
											L/m²

Designer: | Initials: | Date: / /

Fast/Passing Lane

Aggregate Application Rate:

Similar to the slow lane, the fast/passing lane surface hardness is normal assuming surface category A, probe penetration of 2 mm, and 15°C surface temperature.

Medium & heavy vehicles / lane / day	0 to 50	51 to 125	126 to 250	251 to 500	501 to 1250	1251 to 2000	2001 to 2500	2501 to 3250	Over 3250
Traffic Category	H	G	F	E	D	C	B	B	A
NRSWA Road Type	4	4	3	3	2	1	1	0	0

Table A.37: Fast Lane British Traffic Characterization

Based on the following diagram, it is recommended to use a single unmodified seal coat.

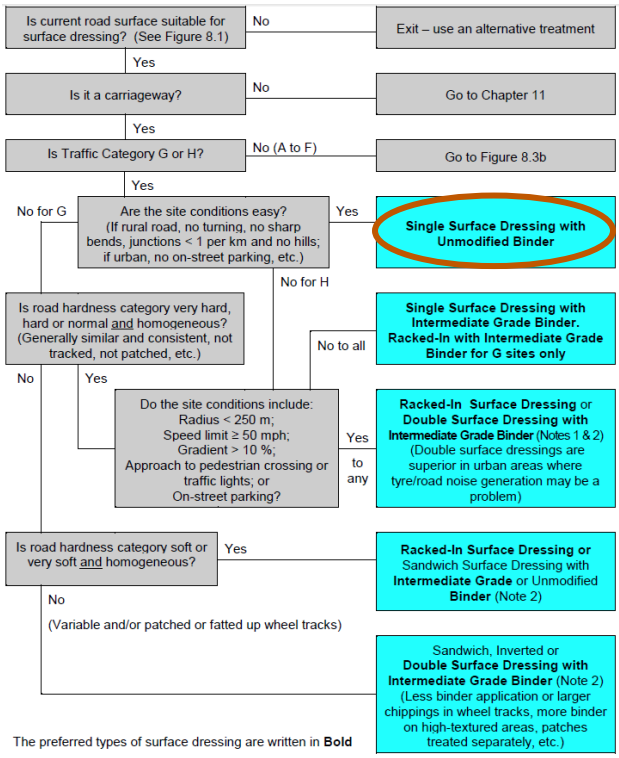

Figure A.23: Fast Lane Seal Coat Type British Recommendation

Traffic Category	Hardness Category of Road Surface									
	Very Hard		Hard		Normal		Soft		Very Soft	
	Size of Chipping	Binder Rate (L/m²)	Size of Chipping (mm)	Binder Rate (L/m²)	Size of Chipping (mm)	Binder Rate (L/m²)	Size of Chipping (mm)	Binder Rate (L/m²)	Size of Chipping (mm)	Binder Rate (L/m²)
A	(a)		(a)		(a)		(b)		(b)	
B	S10	1.8 (c)	(a)		(a)		(a)		(b)	
C	S10	1.8 (c)	S10	1.6 (c)	(a)		(a)		(b)	
D	S6	1.5 (c)	S10	1.6 (c)	(a)		(a)		(a)	
E	S6	1.5 (c)	S10	1.6 (c)	S10	1.6 (c)	S10	1.6 (c)	(a)	
F	S6	1.5 (c)	S6	1.5 (c)	S10	1.6 (c)	S10	1.6 (c)	(a)	
G	S6	1.5	S6	1.5	S6	1.5	S10	1.6	(a)	
H	S6	1.5	S6	1.5	S6	1.5	S6	1.4	S6	1.4

Notes: (a) Multiple layer surface dressing preferred – see Figures 8.3a and 8.3b.
(b) Conditions not suitable for single surface dressings – see Figure 8.3b.
(c) Polymer-modified versions of this type of binder are preferred in those conditions – see Section 5.3.4 and Figure 8.3b.
(d) The surface dressing types are coded for convenience: S is for single and the chipping sizes are the maximums so S6 is a 2.8/6.3 chipping single surface dressing and S10 is a 6.3/10 chipping.

Aggregate Size	Range of Spread Rates	
	kg/m^2	$m^2/tonne$
2.8/6.3 mm	8 – 11	125 – 91
6.3/10 mm	10 – 14	100 – 71
8 / 14 mm	12 – 16	83 – 62

$$\mathbf{AAR = 14\ kg/m^2}$$

Table A.38: Fast Lane British Aggregate Size and Application Rate

A single seal coat with a minimal nominal aggregate size of 10mm is recommended; thus, an aggregate size of 14 mm is deemed appropriate.

Binder Application Rate:

$BAR_{BASE} = 1.6 L/m^2$

Influence	Property	Effect (L/m²)	Comments
Season	Early and mid-season	0	Late season work is very risky especially with S10, double surface dressing is recommended if the work has to be completed, see Fig 7.3.2.
	Late season	+0.2	
Aggregate type	Crushed rock or slag	0	Gravel is only appropriate for Traffic Categories G and H.
	Gravel	+0.1	
Shape	Flakiness category		Flakiness index should conform to PD 6882-2. Adjustment is only required for non-conforming aggregates. Very cubical chippings, FI_{10}, require more binder to hold them initially. Flaky chippings (>FI_{20}) may result in early loss of texture depending on traffic.
	FI_{10}	+0.1	
	FI_{15}	0	
	FI_{20}	-0.1	
	FI_{25} and above	Consider design	
Shade	Un-shaded, open to sun	0	Shaded areas are cooler and, therefore, the road is effectively harder so more binder is required. Double surface dressing is recommended for fully shaded areas (see Table 9.2.3).
	Partially shaded	+0.1	
	Fully shaded	+0.2	
Surface condition (Consider suitability, see Figure 8.1 and type of surface dressing Figures 8.3a and 8.3b)	Very binder rich	-0.2	For variable soft binder rich areas a sandwich surface dressing should be considered. Above F traffic category if there is tracking due to being binder rich, larger chippings should be considered for the wheel tracks as part of a double surface dressing. A pad coat is recommended to normalise and seal porous road surfaces (see Section 9.2.4). Double surface dressing with intermediate binder is recommended for variable hard and binder lean substrates (see Table 9.2.3).
	Binder rich	-0.1	
	Normal	0	
	Texture in wheel tracks	+0.1	
	Binder lean / porous	+0.2	
	Very binder lean and porous, high macro-texture, or variable and hard.	Consider Design	
Gradient	> 5 % uphill	-0.2	The gradient affects the traffic stress on the surface dressing and, therefore, the rate of embedment. Racked-in or double surface dressings are recommended for hills and downhill high-speed sections (see Tables 9.2.2 and 9.2.3).
	< 5 %	0	
	> 5 % downhill	+0.1	
	> 10 % downhill	+0.2	
Traffic Speed	High speed (≥50 mph limit)	+0.1	Roads subject to high-speed traffic induce greater surface stress. Racked-in or double surface dressings with premium binders are recommended.
	Low speed (<50 mph limit)	0	
Local traffic	Design range	0	Un-trafficked areas, such as hatched sections, and also between the wheel tracks and edges of carriageways, require more binder. Hard shoulders, unless a contra flow is planned, and sizeable areas with hatched lines to exclude traffic are effectively untrafficked.
	Effectively un-trafficked	+0.2	

$$\mathrm{BAR} = \mathrm{BAR}_{\mathrm{BASE}} - \mathrm{Adhjustments} = 1.6 - 0.1 + 0.1 - 0.2$$

$$\mathbf{BAR = 1.4 L/m^2}$$

Design of road surface dressings to Road Note 39 (Seventh Edition)

Road number: Example # | Region/Area: ...

Section location: ...

Length: # m | Width: 15.5 m | No. of lanes: 4 | Area: m²

Lane(s): 2 | Medium/Heavy Traffic: 45 cv/l/d | NRSWA road type: 4

Traffic Speed: * 40 mph

Traffic category: * ~~A~~ ~~B~~ ~~C~~ ~~D~~ ~~E~~ ~~F~~ ~~G~~ (H)

Location: * South | ~~Central~~ | ~~North~~ | Temperature Category: * (A) | ~~B~~ | ~~C~~ | ~~D~~

Road Hardness (RH) probe depth: 2 mm at 15 °C | Min. PSV: 60 | Max. AAV: 8

RH Category:* ~~Very Hard~~ | ~~Hard~~ | Normal | ~~Soft~~ | ~~Very Soft~~ | ~~Variable~~

Surface condition: * ~~Very binder rich~~ | ~~Binder rich~~ | ~~Normal~~ | Texture in wheel tracks | ~~Binder lean/porous~~

Radius of curvature: * Under 100 m | ~~100 – 250 m~~ | ~~over 250 m~~ | Expected Month on Site:

Junction or crossing: * ~~Approach~~ | Non-approach

Overall gradient: * ~~up to 5 %~~ | 5 – 10 % | ~~Over 10 %~~ | Uphill | ~~Downhill~~

Type of surface dressing: * Single | ~~Racked In~~ | ~~Double~~ | ~~Inverted Double~~ | ~~Sandwich~~

Chipping size: *

8/14 mm	~~6.3/10 mm~~	~~2.8/6.3 mm~~	Other:
~~8/14 & 2.8/6.3 mm~~	~~6.3/10 & 2.8/6.3 mm~~	~~6.3/10 & 4/2 mm~~	

Aggregate type: * Crushed rock | ~~Blast-furnace~~ | ~~Steel slag~~ | ~~Gravel~~

Flakiness index: * ~~Less than 10 %~~ | ~~10 % to 15 %~~ | ~~15 % to 20 %~~ | More than 20 %

Bituminous emulsion binder: ~~Unmodified~~ | ~~Intermediate~~ | ~~Premium Grade~~ | Super-Premium

Seasonal risk category: ~~High~~ | ~~Significant~~ | Low

Binder spread rate: First layer 1.6 L/m² | Second layer * L/m²

Location	Season	Aggregate type	Flakiness	Increase of chipping size	Shade	Surface condition	Gradient	Traffic Speed	Untrafficked area	Sum of factors	Rate of spread of binder
First Layer	0	0	-0.1	0	0	+0.1	-0.2	0	0	-0.2	1.4 L/m²
											L/m²
											L/m²
											L/m²

Designer: | Initials: | Date: / /

Shoulder

Aggregate Application Rate:

Similarly, the shoulder surface hardness is normal assuming surface category A, probe penetration of 2 mm, and 15°C surface temperature.

Medium & heavy vehicles / lane / day	0 to 50	51 to 125	126 to 250	251 to 500	501 to 1250	1251 to 2000	2001 to 2500	2501 to 3250	Over 3250
Traffic Category	H	G	F	E	D	C	B	B	A
NRSWA Road Type	4	4	3	3	2	1	1	0	0

Table A.39: Shoulder British Traffic Characterization

Based on the following diagram, it is recommended to use a single unmodified seal coat.

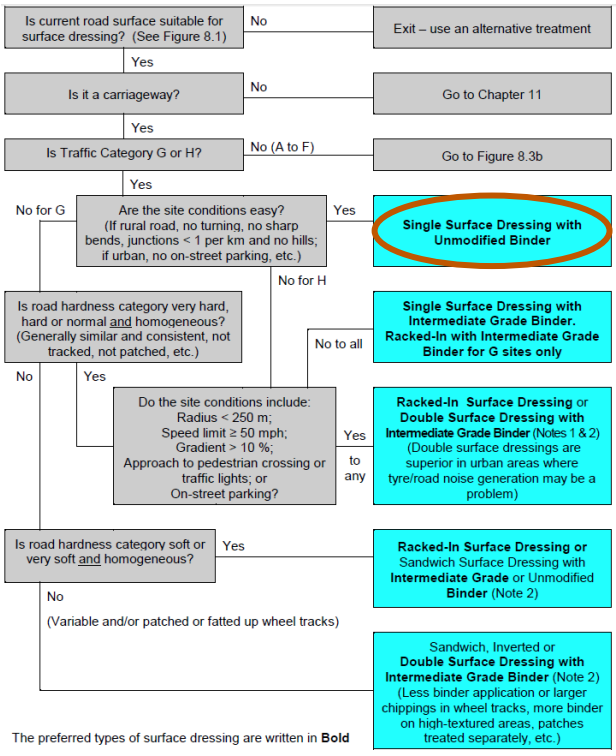

Figure A.24: Shoulder Seal Coat Type British Recommendation

Traffic Category	Hardness Category of Road Surface									
	Very Hard		Hard		Normal		Soft		Very Soft	
	Size of Chipping	Binder Rate (L/m²)	Size of Chipping (mm)	Binder Rate (L/m²)	Size of Chipping (mm)	Binder Rate (L/m²)	Size of Chipping (mm)	Binder Rate (L/m²)	Size of Chipping (mm)	Binder Rate (L/m²)
A	(a)		(a)		(a)		(b)		(b)	
B	S10	1.8 (c)	(a)		(a)		(a)		(b)	
C	S10	1.8 (c)	S10	1.6 (c)	(a)		(a)		(b)	
D	S6	1.5 (c)	S10	1.6 (c)	(a)		(a)		(a)	
E	S6	1.5 (c)	S10	1.6 (c)	S10	1.6 (c)	S10	1.6 (c)	(a)	
F	S6	1.5 (c)	S6	1.5 (c)	S10	1.6 (c)	S10	1.6 (c)	(a)	
G	S6	1.5	S6	1.5	S6	1.5	S10	1.6	(a)	
H	S6	1.5	S6	1.5	S6	1.5	S6	1.4	S6	1.4

Notes: (a) Multiple layer surface dressing preferred – see Figures 8.3a and 8.3b.
(b) Conditions not suitable for single surface dressings – see Figure 8.3b.
(c) Polymer-modified versions of this type of binder are preferred in those conditions – see Section 5.3.4 and Figure 8.3b.
(d) The surface dressing types are coded for convenience: S is for single and the chipping sizes are the maximums so S6 is a 2.8/6.3 chipping single surface dressing and S10 is a 6.3/10 chipping.

Aggregate Size	Range of Spread Rates	
	kg/m^2	$m^2/tonne$
2.8/6.3 mm	8 – 11	125 – 91
6.3/10 mm	10 – 14	100 – 71
8 / 14 mm	12 – 16	83 – 62

Table A.40: Shoulder British Aggregate Size and Application Rate

$$\mathbf{AAR = 14\ kg/m^2}$$

A single seal coat with a minimal nominal aggregate size of 10mm is recommended; thus, an aggregate size of 14 mm is deemed appropriate.

Binder Application Rate:

$BAR_{BASE} = 1.6 L/m^2$

Influence	Property	Effect (L/m²)	Comments
Season	Early and mid-season	0	Late season work is very risky especially with S10, double surface dressing is recommended if the work has to be completed, see Fig 7.3.2.
	Late season	+0.2	
Aggregate type	Crushed rock or slag	0	Gravel is only appropriate for Traffic Categories G and H.
	Gravel	+0.1	
Shape	Flakiness category		Flakiness index should conform to PD 6882-2. Adjustment is only required for non-conforming aggregates. Very cubical chippings, FI_{10}, require more binder to hold them initially. Flaky chippings (>FI_{20}) may result in early loss of texture depending on traffic.
	FI_{10}	+0.1	
	FI_{15}	0	
	FI_{20}	-0.1	
	FI_{25} and above	Consider design	
Shade	Un-shaded, open to sun	0	Shaded areas are cooler and, therefore, the road is effectively harder so more binder is required. Double surface dressing is recommended for fully shaded areas (see Table 9.2.3).
	Partially shaded	+0.1	
	Fully shaded	+0.2	
Surface condition (Consider suitability, see Figure 8.1 and type of surface dressing Figures 8.3a and 8.3b)	Very binder rich	-0.2	For variable soft binder rich areas a sandwich surface dressing should be considered. Above F traffic category if there is tracking due to being binder rich, larger chippings should be considered for the wheel tracks as part of a double surface dressing.
	Binder rich	-0.1	
	Normal	0	
	Texture in wheel tracks	+0.1	
	Binder lean / porous	+0.2	A pad coat is recommended to normalise and seal porous road surfaces (see Section 9.2.4).
	Very binder lean and porous, high macro-texture, or variable and hard.	Consider Design	Double surface dressing with intermediate binder is recommended for variable hard and binder lean substrates (see Table 9.2.3).
Gradient	> 5 % uphill	-0.2	The gradient affects the traffic stress on the surface dressing and, therefore, the rate of embedment. Racked-in or double surface dressings are recommended for hills and downhill high-speed sections (see Tables 9.2.2 and 9.2.3).
	< 5 %	0	
	> 5 % downhill	+0.1	
	> 10 % downhill	+0.2	
Traffic Speed	High speed (≥50 mph limit)	+0.1	Roads subject to high-speed traffic induce greater surface stress. Racked-in or double surface dressings with premium binders are recommended.
	Low speed (<50 mph limit)	0	
Local traffic	Design range	0	Un-trafficked areas, such as hatched sections, and also between the wheel tracks and edges of carriageways, require more binder. Hard shoulders, unless a contra flow is planned, and sizeable areas with hatched lines to exclude traffic are effectively untrafficked.
	Effectively un-trafficked	+0.2	

$$\mathrm{BAR} = \mathrm{BAR}_{\mathrm{BASE}} - \mathrm{Adhjustments} = 1.6 - 0.1 + 0.2 - 0.2$$

$$\mathbf{BAR = 1.5 L/m^2}$$

Design of road surface dressings to Road Note 39 (Seventh Edition)

Road number: Example # | Region/Area: ...

Section location: ...

Length: # m | Width: 15.5 m | No. of lanes: 4 | Area: m^2

Lane(s): 2 | Medium/Heavy Traffic: 45 cv/l/d | NRSWA road type: 4

Traffic Speed: * 40 mph

Traffic category: * ~~A~~ ~~B~~ ~~C~~ ~~D~~ ~~E~~ ~~F~~ ~~G~~ (H)

Location: * South | ~~Central~~ | ~~North~~ | Temperature Category: * (A) ~~B~~ ~~C~~ ~~D~~

Road Hardness (RH) probe depth: 2 mm at 15 °C | Min. PSV: 60 | Max. AAV: 8

RH Category:* ~~Very Hard~~ | ~~Hard~~ | Normal | ~~Soft~~ | ~~Very Soft~~ | ~~Variable~~

Surface condition: * ~~Very binder rich~~ | ~~Binder rich~~ | ~~Normal~~ | ~~Texture in wheel tracks~~ | Binder lean/porous

Radius of curvature: * Under 100 m | ~~100 – 250 m~~ | ~~over 250 m~~ | Expected Month on Site:

Junction or crossing: * ~~Approach~~ | Non-approach

Overall gradient: * ~~up to 5 %~~ | 5 – 10 % | ~~Over 10 %~~ | Uphill | ~~Downhill~~

Type of surface dressing: * Single | ~~Racked In~~ | ~~Double~~ | ~~Inverted Double~~ | ~~Sandwich~~

Chipping size: *

8/14 mm	~~6.3/10 mm~~	~~2.8/6.3 mm~~	Other:
~~8/14 & 2.8/6.3 mm~~	~~6.3/10 & 2.8/6.3 mm~~	~~6.3/10 & 4/2 mm~~	

Aggregate type: * Crushed rock | ~~Blast-furnace~~ | ~~Steel slag~~ | ~~Gravel~~

Flakiness index: * ~~Less than 10 %~~ | ~~10 % to 15 %~~ | ~~15 % to 20 %~~ | More than 20 %

Bituminous emulsion binder: ~~Unmodified~~ | ~~Intermediate~~ | ~~Premium Grade~~ | Super-Premium

Seasonal risk category: ~~High~~ | ~~Significant~~ | Low

Binder spread rate: First layer 1.6 L/m² | Second layer * L/m²

Location	Season	Aggregate type	Flakiness	Increase of chipping size	Shade	Surface condition	Gradient	Traffic Speed	Untrafficked area	Sum of factors	Rate of spread of binder
First Layer	0	0	-0.1	0	0	+0.2	-0.2	0	0	-0.1	1.5 L/m²
											L/m²
											L/m²
											L/m²

Designer: | Initials: | Date: / /

FRENCH DESIGN METHOD (IDRRIM, 2017; AFNOR, 2007)

Slow Lane

Traffic Class	Average Annual Daily Truck Traffic AADTT
T5	between 0 and 25
T4	between 25 and 50
T3-	between 50 and 100
T3+	between 100 and 150
T2	between 150 and 300
T1	between 300 and 750 PL
T0	between 750 and 2,000 PL
TS	between 2,000 and 5,000 PL
T exp	Greater than 5,000 PL **(PL = Poid Lourdes Heavy Weight)

Table A.41: Slow Lane Traffic Characterization

Note: When traffic is T1 or T0, it is advisable to use a modified binder to guarantee a fast rise in cohesion and a high viscosity to ensure optimum wetting of the gravel. Another alternative would be the implementation of a double seal coat instead of a single one.

Aggregate Application Rate:

Gradation d/D	AAR (L/m^2)
4/6	6 - 7
6/10	8 – 9
10/14	11 - 13

Table A.42: Slow Lane French Aggregate Application Rate

$$\mathbf{AAR = 12\ L/m^2}$$

Binder application rate:

The asphalt emulsion application rate is shown in the table below and corresponds to:

- Homogeneous surface
- Smooth-textured
- Free from bleeding (traditional coated type, normally worn)
- Supporting traffic from 50 to 100 PL/d /direction (T3-).

Base Design		
Gradation d/D	Cutback BAR (kg/m^2)	EAR (kg/m^2)
4/6	1.05	1.30
6/10	1.35	1.75
10/14	1.60	2.15

Table A.43: Slow Lane French Emulsion Application Rate

$EAR = 2.15\ kg/m^2$

This application rate is subject to corrections meeting the specific site conditions.

Parameter		**Correction of Dosage (%)**
Traffic (HV/ln/day)	T0…… > 750	-15
	T1…… 300 – 750	***-12***
	T2…… 150 – 300	-8
	T3+…… 100 – 150	-5
	T3-…… 50 – 100	0
	T4…… 25 – 50	+5
	T5……< 25	+10
	No HV	+12
Environment	Very Sunny	-5
	Sunny	-2
	Normal	***0***
	Shady	+5
	Very Shady	+10

Profile		Flat & Straight	0
		Sloping & Straight	***-5***
		Flat & curvy	+2
		Sloping & Curvy	-2
Existing Texture	Very rough ..…….……..	MTD > 1.7	+18
	Rough.…..……..……..……..	MTD > 1.2	+12
	Not that rough ……..…..……..	MTD > 0.8	+6
	Smooth not bleeding ….…….…….	***MTD < 0.8***	***0***
	Tendency to bleed ……...……..	MTD < 0.8	-5
	Bleeding ……..…….	MTD < 0.8	-10
Porosity and Permeability		Permeable	+5
		Impermeable	***0***
Hardness or rigidity		***Not Punch-able***	***0***
		Punch-able	+7
Construction Time		April/May	0
		June/July/August	***0***
		Starting September	+5
Binder Category		Cutback with Mineral Oil	+3
		Modified Cutback	+1
		Cutback with vegetable oil	-3
		Emulsion @65%	+6
		Emulsion @69%	***0***
		Modified emulsion @69%	0
Gradation		***Normal (as guided)***	***0***
		Finer	-5
		Coarser	+5
Flakiness		***>15%***	***-4***
		<10%	+4
		Normal Range	0
Region		Hot	-4
		Moderate	***0***
		Cold	+4
Altitude		***< 500m***	***0***
		500 – 1000m	+2
		> 1000 m	+4

Cumulative dosage correction of -21%

$\text{EAR} = 2.15 - 0.21 \times 2{,}15$

$\mathbf{EAR = 1.70 kg/m^2}$

Fast/Passing Lane

Traffic Class	Average Annual Daily Truck Traffic AADTT
T5	between 0 and 25
T4	between 25 and 50
T3-	between 50 and 100
T3+	between 100 and 150
T2	between 150 and 300
T1	between 300 and 750 PL
T0	between 750 and 2,000 PL
TS	between 2,000 and 5,000 PL
T exp	Greater than 5,000 PL **(PL = Poid Lourdes Heavy Weight)

Table A.44: Fast Lane Traffic Characterization

For low traffic volumes, 6/10 aggregates are recommended, but 10/14 can be used in order not to vary the whole design across the lanes of the roadway.

Aggregate Application Rate:

Gradation d/D	AAR (L/m^2)
4/6	6 - 7
6/10	8 – 9
10/14	11 - 13

Table A.45: Fast Lane French Aggregate Application Rate

$$\mathbf{AAR = 12\ L/m^2}$$

Binder application rate:

The asphalt emulsion application rate is shown in the table below and corresponds to:

- Homogeneous surface

- Smooth-textured
- Free from bleeding (traditional coated type, normally worn)
- Supporting traffic from 50 to 100 PL/d /direction (T3-).

Base Design		
Gradation d/D	Cutback BAR (kg/m^2)	EAR (kg/m^2)
4/6	1.05	1.30
6/10	1.35	1.75
10/14	1.60	2.15

Table A.46: Fast Lane French Emulsion Application Rate

$\mathbf{EAR = 2.15\ kg/m^2}$

This application rate is subject to corrections meeting the specific site conditions.

Parameter		**Correction of Dosage (%)**
Traffic (HV/ln/day)	T0…… > 750	-15
	T1…… 300 – 750	-12
	T2…… 150 – 300	-8
	T3+…… 100 – 150	-5
	T3-…… 50 – 100	0
	T4…… 25 – 50	***+5***
	T5……< 25	+10
	No HV	+12
Environment	Very Sunny	-5
	Sunny	-2
	Normal	***0***
	Shady	+5
	Very Shady	+10
Profile	Flat & Straight	0
	Sloping & Straight	***-5***
	Flat & curvy	+2
	Sloping & Curvy	-2

Existing Texture	Very rough ..…….……....	MTD > 1.7	+18
	Rough…..……..……..……..	***MTD > 1.2***	***+12***
	Not that rough ……..…..……..	MTD > 0.8	+6
	Smooth not bleeding ……..……	MTD < 0.8	0
	Tendency to bleed ……...……..	MTD < 0.8	-5
	Bleeding ……..……	MTD < 0.8	-10
Porosity and Permeability		Permeable	+5
		Impermeable	***0***
Hardness or rigidity		***Not Punch-able***	***0***
		Punch-able	+7
Construction Time		April/May	0
		June/July/August	***0***
		Starting September	+5
Binder Category		Cutback with Mineral Oil	+3
		Modified Cutback	+1
		Cutback with vegetable oil	-3
		Emulsion @65%	+6
		Emulsion @69%	***0***
		Modified emulsion @69%	0
Gradation		***Normal (as guided)***	***0***
		Finer	-5
		Coarser	+5
Flakiness		***>15%***	***-4***
		<10%	+4
		Normal Range	0
Region		Hot	-4
		Moderate	***0***
		Cold	+4
Altitude		***< 500m***	***0***
		500 – 1000m	+2
		> 1000 m	+4

Cumulative dosage correction of +8%

$\text{EAR} = 2.15 + 0.08 \times 2{,}15$

$\mathbf{EAR = 2.32 kg/m^2}$

Shoulder

Traffic Class	Average Annual Daily Truck Traffic AADTT
T5	between 0 and 25
T4	between 25 and 50
T3-	between 50 and 100
T3+	between 100 and 150
T2	between 150 and 300
T1	between 300 and 750 PL
T0	between 750 and 2,000 PL
TS	between 2,000 and 5,000 PL
T exp	Greater than 5,000 PL **(PL = Poid Lourdes Heavy Weight)

Table A.47: Slow Lane Traffic Characterization

For very low traffic volumes, 6/10 aggregates are recommended, but 10/14 can be used in order not to vary the whole design across the lanes of the roadway. This alternative would end up being too expensive and a reconsideration of the design would be needed.

Aggregate Application Rate:

Gradation d/D	AAR (L/m^2)
4/6	6 - 7
6/10	8 – 9
10/14	11 - 13

Table A.48: Shoulder French Aggregate Application Rate

$$\mathbf{AAR = 12\ L/m^2}$$

Binder application rate:

The asphalt emulsion application rate is shown in the table below and corresponds to:

- Homogeneous surface
- Smooth-textured
- Free from bleeding (traditional coated type, normally worn)
- Supporting traffic from 50 to 100 PL/d /direction (T3-).

Base Design		
Gradation d/D	Cutback BAR (kg/m^2)	EAR (kg/m^2)
4/6	1.05	1.30
6/10	1.35	1.75
10/14	1.60	2.15

Table A.49: Shoulder French Emulsion Application Rate

$\mathbf{EAR = 2.15\ kg/m^2}$

This application rate is subject to corrections meeting the specific site conditions.

Parameter		**Correction of Dosage (%)**
Traffic (HV/ln/day)	T0…… > 750	-15
	T1…… 300 – 750	-12
	T2…… 150 – 300	-8
	T3+…… 100 – 150	-5
	T3-…… 50 – 100	0
	T4…… 25 – 50	+5
	T5……< 25	+10
	No HV	***+12***
Environment	Very Sunny	-5
	Sunny	-2
	Normal	***0***
	Shady	+5
	Very Shady	+10
Profile	Flat & Straight	0
	Sloping & Straight	***-5***
	Flat & curvy	+2
	Sloping & Curvy	-2

Existing Texture	***Very rough ……..……..…….... MTD > 1.7***	***+18***
	Rough……..……..…….. MTD > 1.2	+12
	Not that rough ……..……..…….. MTD > 0.8	+6
	Smooth not bleeding ……..……. MTD < 0.8	0
	Tendency to bleed ……...…….. MTD < 0.8	-5
	Bleeding ……..……. MTD < 0.8	-10
Porosity and Permeability	Permeable	+5
	Impermeable	***0***
Hardness or rigidity	***Not Punch-able***	***0***
	Punch-able	+7
Construction Time	April/May	0
	June/July/August	***0***
	Starting September	+5
Binder Category	Cutback with Mineral Oil	+3
	Modified Cutback	+1
	Cutback with vegetable oil	-3
	Emulsion @65%	+6
	Emulsion @69%	***0***
	Modified emulsion @69%	0
Gradation	***Normal (as guided)***	***0***
	Finer	-5
	Coarser	+5
Flakiness	***>15%***	***-4***
	<10%	+4
	Normal Range	0
Region	Hot	-4
	Moderate	***0***
	Cold	+4
Altitude	***< 500m***	***0***
	500 – 1000m	+2
	> 1000 m	+4

Cumulative dosage correction of +21%

$\text{EAR} = 2.15 + 0.21 \times 2{,}15$

$\mathbf{EAR = 2.60 kg/m^2}$

RESULTS

Slow Lane				
Design Method	**AAR**		**BAR**	
Hanson	66 m^2/m^3		1.20 L/m^2	
Kearby	116 m^2/m^3		1.04 L/m^2	
McLeod	78 m^2/m^3		1.13 L/m^2	
Modified Kearby	116 m^2/m^3		0.87 L/m^2	
Spanish	11.8 L/m^2	85 m^2/m^3	1.4 kg/m^2	[3]1.4 L/m^2
New Zealand	87 m^2/m^3		1.22 L/m^2	
Australian	105 m^2/m^3		1.00 L/m^2	
South African	91 m^2/m^3		1.08 L/m^2	
British	14 kg/m^2	[2]**114 m^2/m^3**	1.20 L/m^2	
French	12 L/m^2	83 m^2/m^3	[1,3]1.70 kg/m^2	1.17 L/m^2
Fast/Passing Lane				
Design Method	**AAR**		**BAR**	
Hanson	66 m^2/m^3		1.20 L/m^2	
Kearby	116 m^2/m^3		1.04 L/m^2	
McLeod	78 m^2/m^3		1.48 L/m^2	
Modified Kearby	116 m^2/m^3		1.19 L/m^2	
Spanish	11.8 L/m^2	85 m^2/m^3	1.4 kg/m^2	[3]1.4 L/m^2
New Zealand	87 m^2/m^3		1.47 L/m^2	
Australian	105 m^2/m^3		1.86 L/m^2	
South African	91 m^2/m^3		1.70 L/m^2	
British	14 kg/m^2	[2]**114 m^2/m^3**	1.40 L/m^2	
French	12 L/m^2	83 m^2/m^3	[1,3]2.32 kg/m^2	1.60 L/m^2
Shoulder				
Design Method	**AAR**		**BAR**	
Hanson	66 m^2/m^3		1.20 L/m^2	
Kearby	116 m^2/m^3		1.04 L/m^2	
McLeod	78 m^2/m^3		1.87 L/m^2	
Modified Kearby	116 m^2/m^3		1.47 L/m^2	
Spanish	11.8 L/m^2	85 m^2/m^3	1.4 kg/m^2	[3]1.4 L/m^2
New Zealand	87 m^2/m^3		1.87 L/m^2	
Australian	105 m^2/m^3		2.55 L/m^2	
South African	91 m^2/m^3		1.77 L/m^2	
British	14 kg/m^2	[2]**114 m^2/m^3**	1.5 L/m^2	
French	12 L/m^2	83 m^2/m^3	[1,3]2.60kg/m^2	1.79 L/m^2

[1] 69% Emulsion **[2] 1600 kg/m³ as a bulk unit weight** **[3] $\rho = 1.0$ tonne/m³**

Table A.50: Summary of Various AARs and BARs

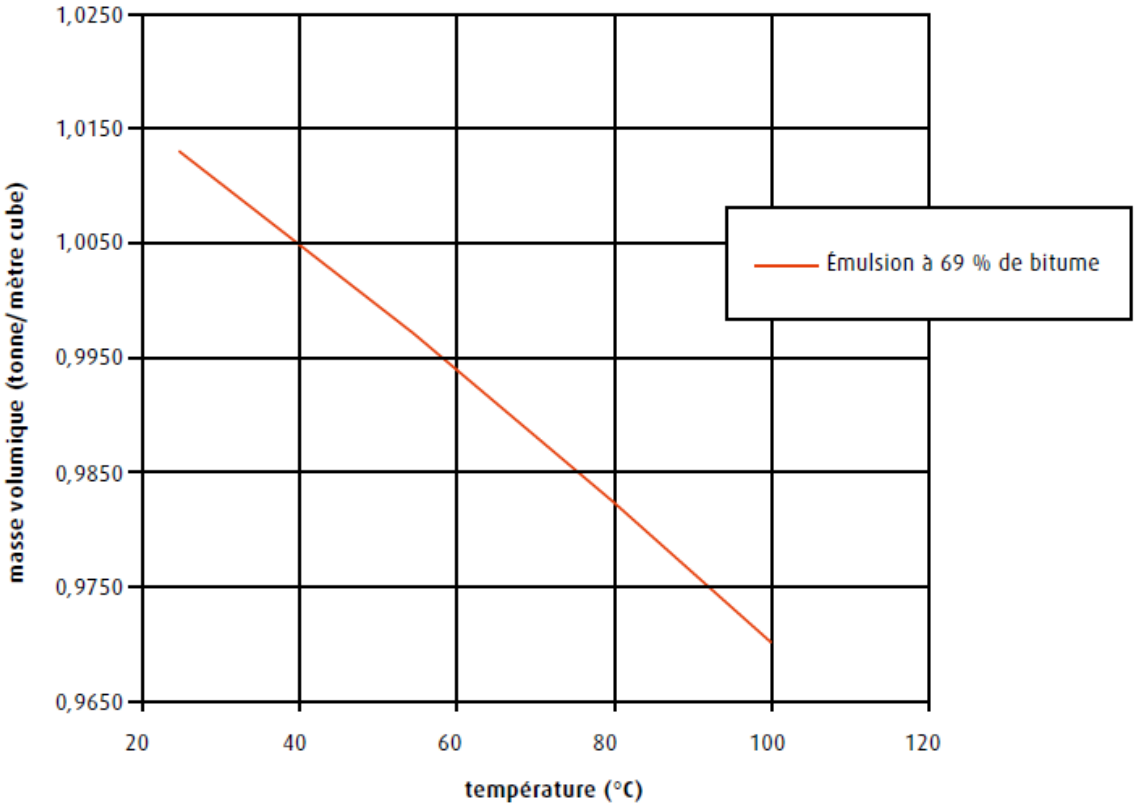

Figure A.25: Volumetric Mass of 69% Binder Emulsion vs. Temperature

For all means and purposes of this exercise, $\rho = 1.0\ \text{tonne}/\text{m}^3$ in reference to Figure A.25.

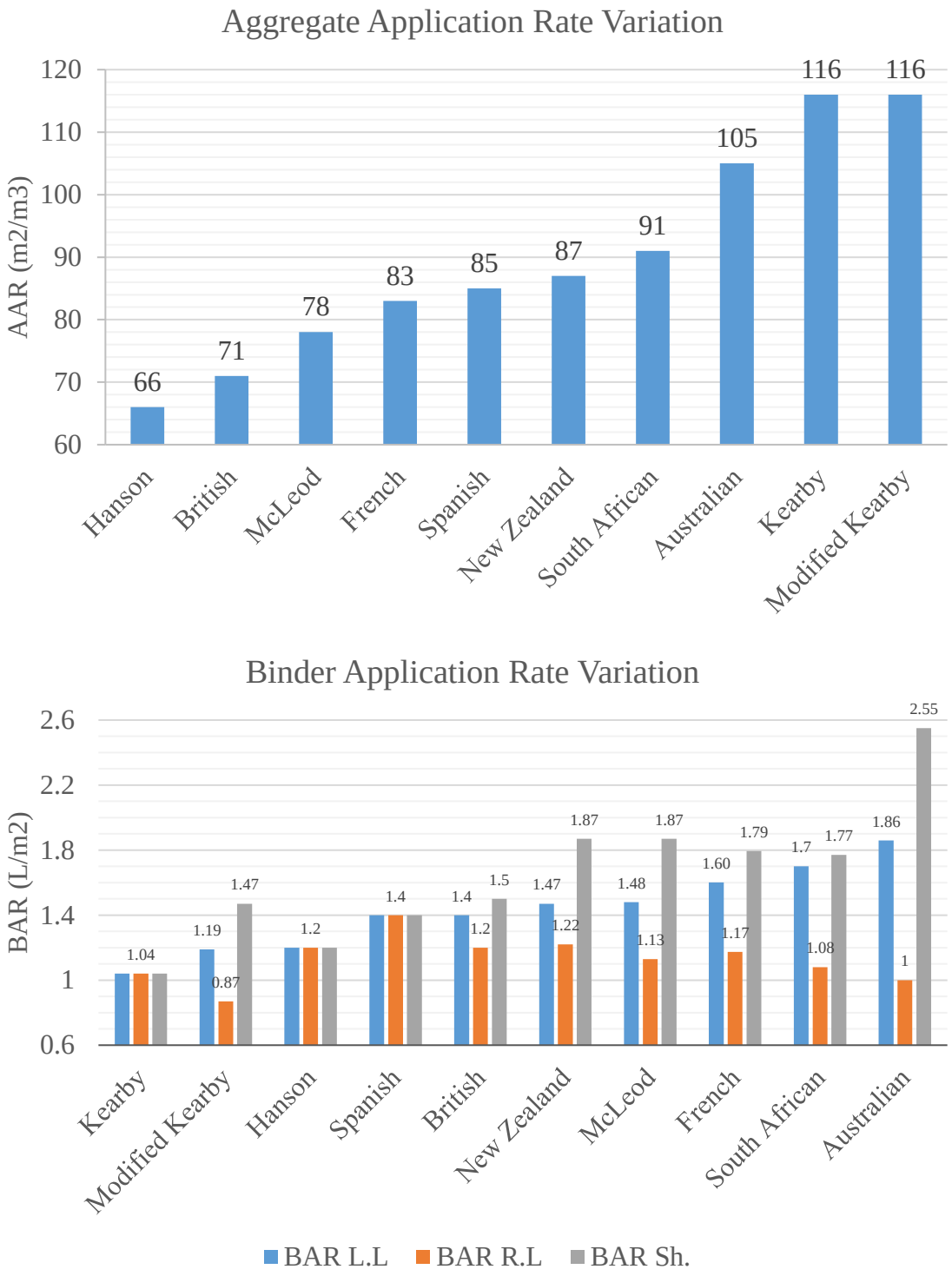

Figure A.26: Comparison of Different Design Method Dosages

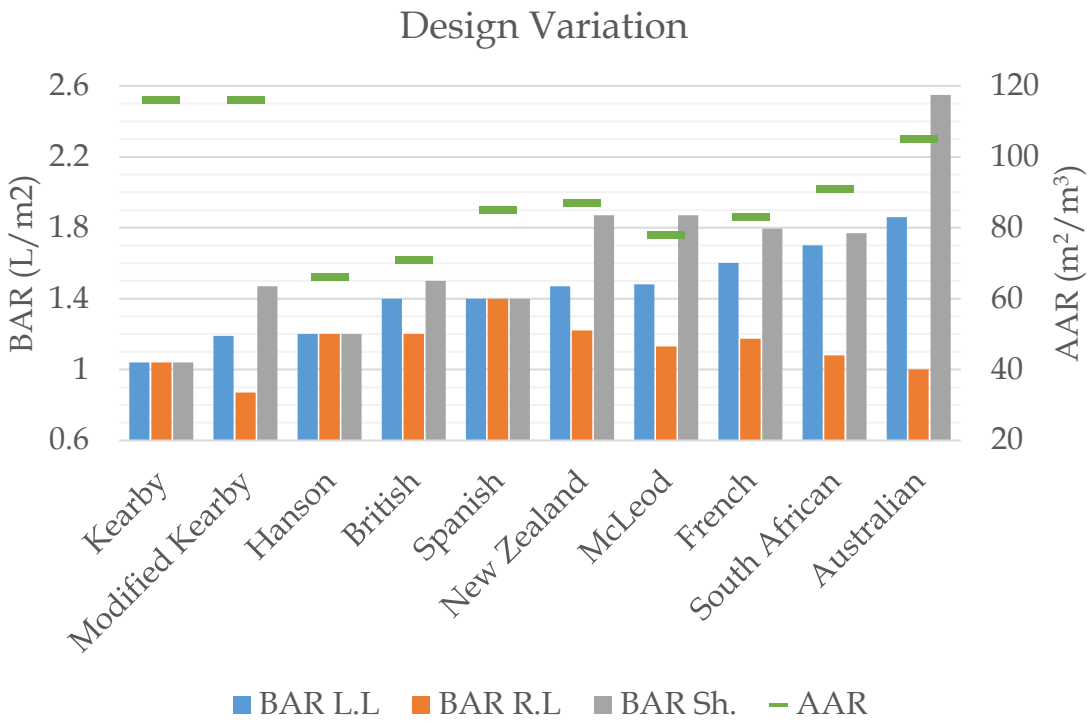

Figure A.26 Continued

As shown in the graphs of Figure A.26, different design methods recommend different aggregate and binder application rates. This widespread of designs is based on the inherent bias pertaining to assessing the existing site conditions and adopting different adjustment rates and factors. This makes the whole design process and assumptions questionable. Unfortunately, agencies end up having to rely on the site engineer's knowledge, common sense, and experiences in assessing the conditions on site and recommending adequate measures. In addition, the variability motivates researchers to investigate automated design methods that would quantify the site-specific conditions and eliminate the need for biased assessments. Lasers offer a high potential to quantify the surface at hand in a fast, objective, and reliable manner.

Bibliography

Adlinge, S., & Gupta, A. (2012). Pavement Deterioration and its Causes. *International Organization of Scientific Research Journal of Mechanical & Civil Engineering (IOSR-LMCE)*, 09-15.

AFNOR. (2007). *Surface Dressing Requirement European French Standard.* La Plaine Saini-Denis: Association Francaise de Normalisation (AFNOR).

AFNOR. (2009). *Tests for Mechanical and Physical Properties of Aggregates - Part 8: Determination of the Polished Stone Value.* Paris: Association Francaise de Normalisation.

AFNOR. (2010.1). *Road and Airfield Surface Characteristics - Test Methods - Part 1: Measurement of Pavement Surface Macrotexture Depth Using a Volumetric Patch Technique.* Paris: Association Francaise de Normalisation.

AFNOR. (2010.2). *Tests for Mechanical and Physical Properties of Aggregates - Part 2: Methods for the Determination of Resistance to Fragmentation.* Paris: Association Francaise de Normalisation.

AFNOR. (2011). *Tests for Mechanical and Physical Properties of Aggregates - Part 1: Determination of the Resistance to Wear (Micro-Deval).* Paris: Association Francaise de Normalisation.

Alderson, A. (2001). *Aggregate Packing and Its Effect on Sprayed Seal Design.* Sydney, Australia: Austroads Project Report TEPN 013.

Alderson, A. (2006). *Update of the Austroads Sprayed Seal Design Method.* Sydney, Australia: Austroads Incorporated Publication No. AP–T68/06.

Ali, H., & Mohammadafzali, M. (2014). *Asphalt Surface Treatment Practice In Southeastern United States.* Florida International University . Baton Rouge: Lousiana Transportation Research Center Southeast Transportation Consortium.

Ambarish, B. (2012). *Breaking and Curing Rates in Asphalt Emulsions.* Austin: The University of Texas at Austin.

Amsler, D. E., & Quinn, J. J. (1977). *Simplified Surface Texture Measurement Method.* Unpublished manuscript prepared for ASTM Subcommittee E17.23.

ASCE. (2017.1). *Infrastructure Report Card: A Comprehensive Assessment of America's Infrastructure.* Reston: The American Society of Civil Engineers.

ASCE. (2017.2). *Report Card for Texas' Infrastructure: Texas Section of the American Society of Civil Engineers.* Reston: The American Society of Civil Engineers.

ASTM. (2014). *ASTM C136 Standard Test Method for Sieve Analysis of Fine and Coarse Aggregates.* West Conshohocken: American Society of Testing and Material International.

ASTM. (2015.1). *ASTM E965 Standard Test Method for Measuring Pavement Macrotexture Depth Using a Volumetric Technique.* West Conshohocken: American Society of Testing and Material International.

ASTM. (2015.2). *ASTM E2157 Standard Test Method for Measuring Pavement Macrotexture Properties Using the Circular Track Meter.* West Conshohocken: American Society of Testing and Material International.

ASTM. (2018). *ASTM D6433 Standard Practice for Roads and Parking Lots Pavement Condition Index Sirveys.* West Conshohocken: American Society of Testing and Material International.

Austroads. (2010). *AG:PT/T251 – Ball Penetration Test.* Bituminous Surfacings Research Reference Group on behalf of Austroads.

Banerjee, A., Smit, A., & Prozzi, J. A. (2012). Modeling the Effect of Environmental Factors on Evaporative Water Loss in Asphalt Emulsions for Chip Seal Applications. *Construction and Building Materials, Elsevier, 27*(1), 158-164.

Bardesi, A., & Tomas, R. (2004). *Riegos con Gravilla.* Madrid, Spain: Asociacion Tecnica de Emulsiones Bituminosas.

Bateman, D. (2016). *Design Guide for Road Surface Dressing - Road Note 39 (Issue 7).* TRL Limited.

Beatty, T. L., Jackson, D. C., Dawood, D. A., Ford, R. A., Moulthrop, J. S., Taylor, G. D., . . . Webb, Z. L. (2002). *Pavement Preservation Technology in France, South*

Africa, and Australia. Alexandria: US Department of Transportation Federal Highway Administration.

Bland, M. (2001). *An Introduction to Medical Statistics.* Oxford7: Oxford University Press.

BSI. (2002.1). *Aggregates for Bituminous Mixtures and Surface Treatments for Roads, Airfields, and Other Trafficked Area. BS EN 13043.* London: British Standard Institution. Retrieved from http://shop.bsigroup.com/Navigate-by/Standards/

BSI. (2002.2). *Surface Dressing – Test Methods – Part 1: Rate of Spread and Accuracy of Spread of Binders and Chippings. BS EN 12272-1.* London: British Standards Institution.

BSI. (2004). *Sampling and Examination of Bituminous Mixtures for Roads and Other Paved Areas: Part 112, Method for the Use of Road Surface Hardness Probe. BS 598-112.* London: British Standard Institution.

BSI. (2009). *UK national guidance for the use of BS EN 13043 "Aggregates for bituminous mixtures and surface treatments for roads, airfields and other trafficked areas". PD 6682-2.* London: British Standards Institution.

BSI. (2013). *Bitumen and Bituminous Binders – Framework for Specifying Cationic Bituminous Emulsions. BS EN 13808.* London: British Standard Institution.

Caminos y Aeropuertos. (2011). *Ligantes y Conglomerantes.* Galicia, Spain: Escuela Técnica Superior de Ingenieros de Caminos, Canales y Puertos, Universidade da Coruña.

Cawley, B., & Gray, J. (2017). *Pavement Preservation: How.* Washington D.C.: U.S. Department of Transportation Federal Highway Administration.

Chamberlin, W. P., & Amsler, D. E. (1982). *Measuring Surface Texture by the Sand-Patch Method.* American Society for Testing and Materials.

Chen, B., Zhang, X., Yu, J., & Wang, Y. (2017). Impact of Contact Stress Distribution on Skid Resistance of Asphalt Pavements. *Journal of Construction and Building Materials, 17,* 330-339.

Chen, D., Lin, D., & Luo, H. (2003). Effectiveness of Preventative Maintenance Treatments Using Fourteen SPS-3 Sites in Texas. *American Society of Civil Engineers (ASCE) Journal of Performance of Construction Facilities, 17*(3), 136-143.

CISA. (2013). *Cybersecurity and Infrastructure Security Agency Transportation Systems Sector*. Retrieved January 2019, from Department of Homeland Security: https://www.dhs.gov/cisa/transportation-systems-sector

Cohen, Y., & Cohen, J. (2008). *Statistics and Data with R: An Applied Approach Through Examples.* John Wiley & Sons, Ltd.

COLTO. (1987). *Standard Specifications for Road and Bridge Works.* Pretoria: Department of Transport.

Daleiden, J., & Chen, D. (2005). Lessons Learned from the Long-term Pavement Performance Program and Several Recycled Section in Texas. *Transportation Research Record: Journal of the Transportation Research Board No. E-C078,* 70-84.

Edumine. (2018). *Professional Development and Training for Mining and the Geosciences*. Retrieved from EduMine: Average Specific Gravity of Various Rock Types

Einarsson, I. T. (2009). *Chip Seals Examination of Design and Construction in Two Countries.* Seattle: University of Washington.

Elmore, W., Solaimanian, M., McGennis, R., Phromson, C., & Kennedy, T. (1995). *Performance-Based Seal Coat Specifications.* Center for Transportation Research, The University of Texas at Austin. Austin: Texas Department of Transportation.

Epps, J. A., Gallaway, B. M., & Hughes, C. H. (1981). *Field Manual on Design and Construction of Seal Coats. Research Report No. 214-25.* College Station: Texas A&M Transportation Institute.

Epps, J., & Gallaway, B. (1972). *Synthetic Aggregate Seal Coats - Current Texas Highway Department Practices.* Austin: The Highway Departement in

Corporation with the U.S. Department of Transportation Federal Highway Administration.

Epps, J., Gallaway, B., & Brown, M. (1974). *Synthetic Aggregate Seal Coats.* Austin: The Highway Departement in Corporation with the U.S. Department of Transportation Federal Highway Administration.

Fugro. (2017). *Automatic Road Analyzer (ARAN)*. Retrieved 2018, from Roadware: https://www.fugro.com/our-services/asset-integrity/roadware

Geiger, D. (2005). *Pavement Preservation Definition.* Washington D.C.: Federal Highway Administration (FHWA).

Gransberg, D. (2010). *Microsurfacing: A Synthesis of Highway Practice.* Iowa State University , National Cooperative Highway Research Program. Washington D.C.: Transportation Research Board.

Gransberg, D. D., & James, D. B. (2005). *Chip Seal Best Practices.* Washington D.C.: NCHRP Synthesis 342, Transportation Research Board,.

Halil, S., Nicholas, F., & Patrick, L. (2008). *Validation of ODOT's Laser Macrotexture System.* Publication FHWA/OH-2008/12, Ohio Department of Transportation.

Hall, J. W., Smith, K. L., Wambold, J. C., Yager, T. J., & Rado, Z. (2009). *Guide for Pavement Friction* . Washington D.C.: National Cooperative Research Program.

Hanson, F. (1935). *Bituminous Surface Treatment of Rural Highways.* Wellington: New Zealand Society of Civil Engineers.

Hao, X., Sha, A., Sun, Z., Li, W., & Zhao, H. (2016). Evaluation and Comparison of Real-Time Laser and Electric Sand-Patch Pavement Texture-Depth Measurement Methods. *Journal of Transportation Engineering*, *142*(7). doi:10.1061/(ASCE)TE.1943-5436.0000842

Hayden, C. M. (1982). *Pavement Surface Characteristics and Materials ASTM Special Technical Publication 763.* Philadelphia: American Society for Testing and Materials.

Henault, J. W., & Jessica, B. (2011). *Characterizing the Macrotexture of Asphalt Pavement Designs in Connecticut.* Division of Research. Connecticut Department of Transportation.

Hicks, R., Seeds, S., & Peshkin, D. (2000). *Selecting a Preventive Maintenance Treatment for Flexible Pavements.* Washington D.C.: Research Report, Foundation of Pavement Preservation.

Hogervorst, D. (1974). *Some Properties of Crushed Stone for Road Surfaces.* Bulletin of the International Association of Engineering Geology - Bulletin de l'Association Internationale de Géologie de l'Ingénieur, 10, 59-64.

Holmgreen, R., Epps, J., Hughes, C., & Gallaway, B. (1985). *Field Evaluation of The Texas Seal Coat Design Method.* Austin: Research Report 297-1F, Texas Transportation Institute.

Holtrop, W. (2008). Sprayed Sealing Practice in Australia. *Road and Transport Research, 17*, 41-60.

Huang, Y. R., Copenhaver, T., Hempel, P., & Mikhail, M. (2013). *Development of Texture Measurement System Based on Continuous Profiles from Three-Dimensional Scanning System.* Washington D.C.: Transportation Research Record: Journal of the Transportation Research Board. doi:10.3141/2367-02

IDRRIM. (2017). *Enduits superficiels d'usure.* Paris: Institut des Routes, des Rues et des Infrastructures de Mobilité, Centre d'études et d'expertise sur les risques, l'environnement, la mobilité et l'aménagement.

Jones, W. (2015). Best Practices for Pavement Construction. *APAM 59th Annual Meeting.* Mount Pleasant: Asphalt Pavement Association of Michigan.

Kass, R., Eden, U., & Brown, E. (2014). *Analysis of Neural Data.* New York: Springer.

Kearby, J. P. (1953). *Tests and Theories on Penetration Surfaces.* Texas: Texas Highway Department.

Keyence. (2016). *Inline Profile Measurement - The World's Fastest at 64000 Profiles/sec.* Tasca: Keyence Corporation of America.

Khou Sid'Ahmed, O., Barreto, M., & Strelow, H. (2009). *Illustrated Glossary for Transport Statistics.* EUROSTAT, ITF, and UNECE.

Kim, R., & Adams, J. (2012). *Development of a New Chip Seal Mix Design Method.* North Carolina State University, Department of Civil, Construction, & Environmental Engineering. Raleigh: North Carolina Department of Transportation.

Kouchaki, S., Roshani, H., Prozzi, J. A., & Hernandez, J. B. (2017). Evaluation of Aggregates Surface Micro-Texture Using Spectral Analysis. *Journal of Construction and Building Materials, 156*, 944-955.

Kouchaki, S., Roshani, H., Prozzi, J., Cordoba, C., & Hernandez., J. (2018). Evaluation of a Line Laser Scanner to Improve the Measurement of Average Least Dimension in Chip Seal Design Methods. *Transportation Research Record: Journal of the Transportation.*

Kutay, M., Ozdemir, U., Hibner, D., Kumbargeri, Y., & Lanotte, M. (2016). *Development of an Acceptance Test for Chip Seal Projects.* Michigan State University, Department of Civil & Environmental Engineering. Lansing, Michigan: The Michigan Department of Transportation Report No. SPR-1649.

Lane, D. M. (2001). *Hyperstat.* Mason: Atomic Dog Publishing Inc.

Larsen, F. (1968). *Effect of Road Network on Economic Development.* Denmark's Technical University, Traffic Engineering and Town Planning. Lyngby: Institute for Highway Engineering.

Laser Technology Inc. (2019). *Professional Measurement Products*. Retrieved from Laser Technology Incorporation Measurably Superior: http://www.lasertech.com/Professional-Measurement-Products.aspx

Lawson, W., & Senadheera, S. (2009). Chip Seal Maintenance Solutions for Bleeding and Flushed Pavement Surfaces. *Journal of Transportation Research Record, Transportation Research Board of the National Academies*(2108), 61-68.

Lee, J., Shields, T., & Jun Ahn, H. (2011). *Performance Evaluation of Seal Coat Materials and Designs.* Indiana Department of Transportation and Purdue

University. West Lafayette, Indiana: Joint Transportation Research Program. doi:10.5703/1288284314619

Lee, M. (2017). *Seal Coat and Surface Treatment.* Texas Department of Transportation.

Lord, A., & Shuler, S. (2008). *An Analysis of Two Leading Chip Seal Design Methods.* Fort Collins, Colorado: Colorado State University.

Mahoney, J., Slater, M., Keifenheim, C., Uhlmeyer, J., Moomaw, T., & Willoughby, k. (2014). *WSDOT Chip Seals: Optimal Timing, Design And Construction Considerations* . Seattle: Washington State Transportation Center.

Major, N. (1993). *Investigation Into the High Incidence of Pavement Chip Loss.* Transit New Zealand Research Report No. 25. 71pp.

Martinez, W., Garcia, N., Smit, A., & Prozzi, J. A. (2017). *Life-Cycle Cost Analysis of Pavement Preservation Techniques in Texas.* Washington D.C.: 96th Annual Meeting of Transportation Research Board, January 8-12, 2017.

Martinez-Alonso, W., Prozzi, J., & Smit, A. (2017, August). Life-Cycle Cost Analysis of Pavement Preservation. *Master's Thesis*, 97. Austin, Texas: The University of Texas at Austin.

McLeod, N. (1969). A General Method of Design for Seal Coats and Surface Treatments. *The Association of Asphalt Paving Technologies.* Toronto, Canda: E.D. Etnyre & Co.

Meegoda, N. J., Hettiarachchi, C., Rowe, G., Bandara, N., & Sharrock, M. (2002). *Correlation of Surface Texture, Segregation, and Measurement of Air Voids.* Publication FHWA-NJ-2002-026, FHWA.

Merritt, D., Lyon, C., & Persaud, B. (2015). *Evaluation of Pavement Safety Performance.* McLean: U.S. Department of Transportation Federal Highway Administration Research, Development, and Technology Turner-Fairbank Highway Research Center.

Mouaket, I., Sinha, K., & White, T. (1992). *Guidelines for Management of Chip and Sand Seal Coating Activity in Indiana.* Washington D.C.: Transportation Research

Record: Journal of the Transportation Engineering Board, No. 1507, pp. 81-90, National Research Council.

Nemati, K. (2015). *Concrete Technology - Aggregates for Concrete.* Seattle: University of Washington.

Ong, G., Fwa, T., & Guo, J. (2005). *Modeling Hydroplaning and Effects of Pavement Micro-texture.* Washington D.C.: Transportation Research Record: Journal of the Transportation Research Board, 1905, 166-176.

Patrick, J. (1999). *Background to the Development of the Transit New Zealand performance-based Chipseal Specifications.* TNZ P/17 requirements. Opus Central Laboratories Report.

Peshkin, D., Smith, K., Wolters, A., Krstulovich, J., Moulthrop, J., & Alvarado, C. (2011). *Guidelines for the Preservation of High-Traffic-Volume Roadways.* Washington D.C.: SHRP 2 Report S2-R26-RR-2. Transportation Research Board.

Pierce, L., & Kebede, N. (2015). *Chip Seal Performance Measures - Best Practices.* Olympia, Washington: Washington State Department of Transportation: Office of Research & Library Services.

Prozzi, J. A., & Serigos, P. A. (2016). *Performance of Preventive Maintenance in Texas.* Waikiki, Hawaii: Civil Engineering Conference in the Asian Region CECAR7, August 30-September 2, 2016.

Queiroz, C., & Gautam, S. (1992). *Road Infrastructure and Economic Development: Some Diagnostic Indicators.* Infrastructure Operations Division and the Transport Division, Western Africa Department and Infrastructure and Urban Development Department. Washington D.C.: The World Bank.

Radhakrishnan, D. (2016, July 14). *Quantifying Quality: The Pavement Condition Index*. Retrieved from Citizen consumer and civic Action Group: https://www.cag.org.in/blogs/quantifying-quality-pavement-condition-index

Rahman, F., Islam, M. S., Musty, H., & Hossain, M. (2012). Aggregate retention in chip seal. *Transportation Research Record: Journal of the Transportation Research Board.*, 56-64.

Ravi, S. (2018). US Critical Infrastructure. *Clade X*, p. 6.

Roberts, C., & Nicholls, J. (2008). Design Guide for Road Surface Dressing. *Transportation Research Laboratories*, 64.

Roberts, F., Kandhal, P., Brown, E., Lee, D., & Kennedy, T. (1996). *Hot Mix Asphalt Materials, Mixture Design, and Construction.* Lanham, Maryland: National Asphalt Pavement Association Education Foundation.

Rodrigue, J.-P., & Notteboom, T. (2017). *Transportation and Economic Development.* New York: Routledge. ISBN 978-1138669574.

SABS. (1996). *Standardized Specification for Civil Engineering Construction (Standard Specification; 1200-M:1996).* Pretoria: South African Bureau of Standards.

SANRAL. (2007). *Technical Recommendation for Highay: Design and Construction of Surfacing Seals.* Pretoria, Republic of South Africa: The South African National Roads Agency Ltd.

Schlotzhauer, S. D. (2007). *Elementary Statistics Using JMP*. SAS Publishing.

Scott, J. (1986). Seal Coating Practice in Saskatchewen. *Transportation Research Record: Journal of the Transportation Research, TRB, National Research Council*(1096), 140-146.

Sengoz, B., Topal, A., & Tanyel, S. (2012). Comparison of Pavement Surface Texture Determination by Sand Patch Test and 3D Laser Scanning. *Journal of Periodica Polytechnica Civil Engineering*, 73-78.

Serigos, A., Smit, A., & Prozzi, J. (2014). Incorporating Surface Microtexture in the Prediction of Skid Resistance of Flexible Pavements. *Transportation Research Record: Journal of the Transportation Research Board*. doi:2457.105-113.10.3141/2457-11.

Serigos, P., Smit, A., & Prozzi, J. (2017). *Performance of Preventive Maintenance Treatments for Flexible Pavements in Texas.* The University of Texas at Austin. Austin: Center for Transportation Research.

Shuler, S. (1990). Chip Seals for High Traffic Pavements. *Transportation Research Record Journal of the Transportation Research Board, National Research Council*,(1259), 24-34.

Smith, R., & Beatty, C. (1999). *Microsurfacing Usage Guidelines.* Washington D.C.: Transportation Research Record: Journal of the Transportation Research Board.

TMH. (1984). *Special Methods for Testing Roads.* Pretoria: Department of Transport (Technical Methods for Highways; TMH6).

Tomkins, L., Horner, B., Lampley, J., & Shields, T. (2018, January). Chip Seal Breakout. *Slurry Systems Workshop*. Las Vegas, Nevada: International Slurry Surfacing Association Preserving Pavement.

Transit NZ. (2002). *Specification for Sealing Chip. TNZ M/6 Spec.* Wellington: Transit New Zealand.

Transit NZ, RCA, & Roading NZ. (2005). *Chipsealing in New Zealand.* Wellington: Transit New Zealand, Road Controlling Authorities & Roading New Zealand.

TRIP. (2016). *The Interstate Highway System Turns 60: Challenged to Its Ability to Continue to Save Lives, Time, and Money.* Washington D.C.: TRIP National Transportation Group.

TxDOT. (1997). *Survey of States: Preventive Maintenance Needs.* Survey Performed by Lead State Members on Pavement Preservation: Texas Department of Transportation.

TxDOT. (2004). *TEX-224-F Determining Flakiness Index.* Austin: Texas Department of Transportation.

TxDOT. (2014). *TEX-404-A Determining Unit Mass (Weight) of Aggregates.* Austin: Texas Department of Transportation.

TxDOT. (2017.1). *Roadway Inventory Annual Reports.* Texas Department of Transportation Data Management, Transportation Planning & Programming.

TxDOT. (2017.2). *Seal Coat and Surface Treatment Manual.* Maintenance Division. Austin: Texas Department of Transportation.

TxDOT. (2019). *Transportation Funding in Texas.* Texas Department of Transportation Division of Financial Management.

Universal Laser Systems Inc. (2018). *The Fundamentals of Laser Technology*. Retrieved from Universal Laser Systems: https://www.ulsinc.com/learn

US Corps of Engineers. (1997, June). Pavement Distress Identification Guide for Asphalt-Surfaced Roads and Parking Lots. *PAVER Asphalt Distress Manual*. Champaign, Illinois: US Army Construction Engineering Laboratories.

US DHS. (2015). *Transportation Systems Sector Cybersecurity Framework Implementation Guidance.* Washington D.C.: Implementation Guidance.

USDOT. (2016). *2015 Status of the Nation's Highways, Bridges, and Transit: Conditions and Performance.* Washington DC: U.S. Department of Transportation Federal Highway Administration Federal Transit Administration.

USDOT. (2017). *Preservation*. Retrieved 2019, from US Department of Transprotation Federal Highway Administration: https://www.fhwa.dot.gov/preservation/

Van, T., Gaj, S., Cawley, B., & Gray, J. (2017). *Pavement Preservation: When, Where, and How.* Washington D.C.: U.S. Department of Transportation Federal Highway Administration.

Viner, H., Abbott, P., Dunford, A., Dhillon, N., Parsley, L., & Read, C. (2006). *Surface Texture Measurement on Local Roads.* TRL Limited.

Viv, B., Liz, C., & Jonathan, B. (2004). *Statistical Review 9 One-way Analysis of Variance.* Brighton: BioMed Central Ltd. doi:10.1186/cc2836

Wang, D., Liu, P., Wang, H., Ueckermann, A., & Oeser., M. (2017). Modeling and testing of road surface aggregate wearing behavior. Journal of Construction and Building Materials. *131*, 129-137.

Wang, W., Yan, X., Huang, H., Chu, X., & Abdel, N. (2011). Design and Verification of a Laser Based Device for Pavement Macrotexture Measurement. *Journal of Elsevier, Transportation Part C, 19*, 682-694.

Wood, T., Janisch, D., & Gaillard, F. (2006). *Minnesota Seal Coat Handbook.* Maplewood: Minnesota Department of Transportation.

World Health Organization. (2017). *Road Traffic Injuries.* WHO.

Wu, Z., Groeger, J., Simpson, A., & Hicks, R. (2010). *Performance Evaluation of Various Rehabilitation and Preservation Treatment.* Washington D.C.: US Department of Transportation.

Yaacob, H., Hassan, N. A., & Hainin, M. R. (2014). Comparison of Sand Patch Test and Multi Laser Profiler in Pavement Surface Measurement. *Jurnal Teknologi, 70*(4), 103-106.

Yazgan, B., & Senadheera, S. (2003). *A New Testing Protocol for Seal Coat (Chip Seal) Material.* Lubbock: Texas Tech University.

Zhang, X., Liu, T., Liu, C., & Chen., Z. (2014). Research on Skid Resistance of Asphalt Pavement Based on Three-Dimensional Laser-Scanning Technology and Pressure-Sensitive Film. *Journal of Construction and Building Materials, 69,* 49-59.

Zheng, W., Groeger, J. L., Simpson, A. L., & Hicks, G. R. (2010). *Performance Evaluation of Various Rehabilitation and Preservation Treatments.* Washington D.C.: Federal Highway Administration.

Zoghi, M., Ebrahimpour, A., & Pothukutchi, V. (2010). *Performance Evaluation of Chip Seals in Idaho.* Pocatello, Idaho: Report No. FHWA-ID-10-190, Idaho Transportation Department.